



*LULEÅ UNIVERSITY  
OF TECHNOLOGY*

# **Thermal Crack Risk Estimation and Material Properties of Young Concrete**

Anders Hösthagen

**Luleå 2017  
Division of Structural and Fire Engineering  
Department of Civil, Environmental and Natural Resources Engineering  
Luleå University of Technology  
SE-97187 Luleå, Sweden**

Cover picture: Upper graphic; normalized elastic 3D calculation yielding restraint in a young concrete tunnel section. Bottom left; a modelled cross section of one of the tunnel walls. Bottom right; visualization of a calibration of the equivalent restraint method model to a local restraint method model.

## **Academic thesis**

For the Degree of Licentiate (Tech. Lic) in Structural Engineering, which by due of the Technical Faculty Board at Luleå University of Technology will be publicly defended in:

Room F1031, Luleå University of Technology  
Tuesday, October 10<sup>th</sup>, 2017, 10:00

Discussion leader: Dr. Mårten Larson, Metroselskabet I/S  
Principal supervisor: Prof. Jan-Erik Jonasson, Luleå University of Technology  
Assistant supervisors: Prof. Mats Emborg, Luleå University of Technology  
Adj. prof. Hans Hedlund, Luleå University of Technology  
Dr. Marin Nilsson, Luleå University of Technology



## **PREFACE**

The research within this licentiate thesis started 2014, and was carried out at the Department of civil, environmental and natural resources engineering at the division of structural and fire engineering of Luleå University of Technology in Sweden. The financially supported by Swedish Transport Administration and Development Fund of the Swedish Construction Industry, SBUF, is much appreciated.

My earnest gratitude goes to my principle supervisor Professor Jan-Erik Jonasson for his mediated knowledge, always giving me of his time and his kind support. Gratitude is also given my assistant supervisors, Professor Mats Emborg, Dr. Martin Nilsson and Adj. prof. Hans Hedlund for their support and constructive comments throughout this work.

Mr. Kjell Wallin and tekn Dr. Carsten Vogt have given me knowledgeable input to this work and deserves heartfelt thanks.

Without the love, support and caring from my parents, my academic career would never have started, and I will always be grateful.

I feel a cordial gratitude towards my wife Johanna and my children Signe and Assar for unconditional love and great support.

*Anders Hösthagen*

*Enköping, September 2017*

## ABSTRACT

This thesis presents how to establish a theoretical model to predict risk of thermal cracking in young concrete when cast on ground or an arbitrary construction. The crack risk in young concrete is determined in two steps: 1) calculation of temperature distribution within newly cast concrete and adjacent structure; 2) calculation of stresses caused by thermal and moisture (due to self-desiccation, if drying shrinkage not included) changes in the analyzed structure. If the stress reaches the tensile strength of the young concrete, one or several cracks will occur.

The main focus of this work is how to establish a theoretical model denoted *Equivalent Restraint Method* model, ERM, and the correlation between ERM models and empirical experiences. A key factor in these kind of calculations is how to model the restraint from any adjacent construction part or adjoining restraining block of any type.

The building of a road tunnel and a railway tunnel has been studied to collect temperature measurements and crack patterns from the first object, and temperature and thermal dilation measurements from the second object, respectively. These measurements and observed cracks were compared to the theoretical calculations to determine the level of agreement between empirical and theoretical results.

Furthermore, this work describes how to obtain a set of *fully tested material parameters* at CompLAB (test laboratory at Luleå University of Technology, LTU) suitable to be incorporated into the calculation software used. It is of great importance that the obtained material parameters describe the thermal and mechanical properties of the young concrete accurately, in order to perform reliable crack risk calculations. Therefore, analysis was performed that show how a variation in the evaluated laboratory tests will affect the obtained parameters and what effects it has on calculated thermal stresses.

*Keywords: Thermal cracking risk, young concrete, Equivalent Restraint Method, strength development, heat of hydration, creep, shrinkage, thermal dilation, modeling, field observations.*

# TABLE OF CONTENT

PREFACE .....	v
ABSTRACT .....	vi
TABLE OF CONTENT .....	vii
1. INTRODUCTION.....	1
1.1. General background .....	1
1.2. Objectives and research questions.....	2
1.3. Limitations.....	3
1.4. Outline of the thesis.....	3
1.5. Appended papers .....	4
2. REASONS TO RESTRICT THERMAL CRAKING AT EARLY AGES .....	7
3. THERMAL CRACKS IN YOUNG CONCRETE AND SIMPLIFIED METHODS OF CRACK RISK ESTIMATIONS .....	9
3.1. Definition of thermal cracks at an early age.....	9
3.2. Later through cracks formation - details .....	11
3.3. Early age crack risk analysis .....	13
3.4. Temperature development yielding crack risk .....	16
3.4.1. Crack risk analyses for typical structures.....	16
3.4.2. Estimation of later through crack risks based on temperature and basic shrinkage development .....	16
4. METHODS FOR COMPUTERIZED CALCULATIONS OF STRUCTURAL STRESS .....	21
4.1. Overview of stress calculations .....	21
4.2. Out-of-Plane stress calculations .....	22
5. RESTRAINT ESTIMATION.....	25
5.1. Definition of restraint .....	25
5.2. Factors yielding restraint.....	28
5.3. Methods of restraint estimation .....	29
5.4. Typical restraint situations .....	31

5.4.1. Uni-axial restraint.....	32
5.4.2. Non-resilient boundary.....	32
5.4.3. Partly resilient boundary .....	33
5.4.4. Partly resilient boundary – End slip .....	34
5.4.5. Partly resilient boundary - Rotation .....	34
5.4.6. Partly resilient boundary - Piles .....	36
6. EQUIVALENT RESTRAINT METHOD, ERM.....	38
6.1. Background and outline of the ERM.....	38
6.2. Volume deformation in the FEM calculations .....	39
6.3. 3D FEM restraint calculation .....	39
6.4. Calculations of stresses without measures on site .....	41
6.5. Calibration of the ERM model .....	42
6.6. Application of the ERM model .....	43
6.6.1. Interpretation of the resulting stress/strain ratios using ERM .....	43
6.6.2. Simulating measures on site using ERM and LRM .....	44
6.7. Results when comparing ERM models to empirical measurements .....	45
7. EVALUATION OF MATERIAL PROPERTIES FOR YOUNG CONCRETE.....	46
7.1. Introduction .....	46
7.2. Method .....	47
7.2.1. Strength growth .....	47
7.2.2. Heat of hydration.....	49
7.2.3. Basic shrinkage and free thermal dilation .....	50
7.2.4. Basic creep tests .....	51
7.2.5. Stresses in concrete at full restraint.....	52
7.3. Results .....	53
8. CONCLUSIONS .....	55
8.1. Overall observations.....	55
8.1.1. The Equivalent Restraint Method (ERM) .....	55
8.1.2. Material properties of young concrete.....	55
8.2. Answer to research questions .....	56
8.3. Future research .....	57
References .....	59





# 1. INTRODUCTION

## 1.1. General background

Restrained movements within young concrete during the construction phase, caused by thermal dilation, basic shrinkage and drying shrinkage, is a major reason for early age cracking, see e.g. ACI Committee 207 (2002), Emborg and Bernander (1994), Mihashi and Leite (2004), Kianousha, Acarcanb and Ziari (2008), Cusson and Repette (2000). Any adjoining structure or a restraining entity (such as rock, subgrade) bonded to the young concrete increase the risk of cracking since the restraint becomes higher, see e.g. Nilsson (2003) and Gasch (2016). A cracked concrete may lead to increased permeability which exposes the reinforcement bars often leading to corrosion. Furthermore, harmful liquids or gases may penetrate into the concrete, which may cause damage either to the concrete itself or materials behind the concrete. These effects have a negative impact on the durability, maintenance and the environment around the structure. Therefore, it is of importance to understand the factors which influencing cracking risk and establish reliable calculation models.

Several factors need to be taken into account at crack risk estimations; mechanical behavior, temperature changes, moisture changes and restraint. The drying shrinkage is always affecting the surfaces exposed to air, and it might be relevant for the deformation of the total young concrete bodies for thin structures. Fortunately, for most civil engineering structures the “typical thickness” is in the size of order of about 0.5 m or more, where drying shrinkage is of minor importance. Besides, for vertical structures, like common wall type structures, the maximum surface stresses occur within 1 to 2 days after casting, when the vertical formwork still is left on place. This excludes the effect of drying shrinkage for these types of structure concerning early surface cracking. So, for a majority of civil engineering structures the simplification of not taking drying shrinkage into account can be regarded as an acceptable approximation. On the other hand, for the case of topping of horizontal surface with rather thin layers, drying shrinkage might be the most interesting case to study, however this is not analyzed here. The effect of basic shrinkage is generally accounted for in the material parameters which serves as an input to the material model within most calculation model.

If the predicted stress level is higher than accepted, measures to avoid thermal cracking due to temperature changes, like cooling pipes or heating cables, could be introduced within most

calculation models, see for instance Bosnjak (1999), Rostásy (1998) and Emborg (1998). In Sweden, pre-calculations to analyze the risk of cracking during the heating and cooling phases are needed to establish possible measures against thermal cracking for most civil engineering structures. Often several calculations are needed at the prediction of eventual measures and to establish working instructions of how to avoid early cracking on site. Variations of environmental conditions as well as material choices and different measures should thus be made, and yet the analyzing technique has to be cost-effective. In general, full 3D FE calculations for both the thermal and structural calculations for hardening concrete, are time-consuming and the available software are often expensive, which invites the use of more cost-efficient, and often simplified, calculation models.

When using simplified models, the structural situation usually can be described with respect to the possibilities to counteract non-elastic deformations. This can, point-by-point, be described by a local restraint factor ( $\gamma_R$ ) between 0 and 1 in the newly cast concrete, where 0 means totally free situation (moves freely, giving no stresses) and 1 means fully counteraction of the non-elastic deformation (no external deformation leading to fully, 100 %, restraint). The local restraint factors are typically determined from counteraction of the restraint situation for the studied section including young concrete and the adjacent structure when analyzing the so called “out of plane stresses”, see e.g. JCI Committee (1992) and Nilsson (2003). These structural restraint conditions are usually described as axial restraint and rotational restraint around different axes.

In every simplified model, an estimation of the restraint is needed, which could be a hard task at more complex situations. Furthermore, simplified models often lack the possibility to model arbitrary measures influencing the thermal development to diminish the thermal dilation yielding stresses. Within this thesis, a new way of describing the restraint situation, called ERM = Equivalent Restraint Method, for an arbitrary spatial structure is presented and discussed. Hereby, both on site measures using cooling pipes in the newly cast concrete as well as using heating cables in the existing adjacent concrete structure can be analyzed for rather complex structural situations, see further Chapter 6.

## 1.2. Objectives and research questions

Main objectives of the research performed are:

- To present the background and analyse the conditions applying the Equivalent Restraint Method.
- Examine the importance of different test procedures to establish material parameters aimed for estimation of early age crack risks in concrete.

Research questions within this work are addressed as;

RQ1: Which structures can be simulated using the ERM when estimating early age crack risks?

RQ2: Which measures on site can be treated using the ERM when estimating early age crack risks?

RQ3: How important is each individual laboratory test to create material properties for operational analyses of crack risks?

### **1.3. Limitations**

Since thermal crack risk estimations at early ages is a very wide research field, the work presented in this thesis was restricted by several limitations as follows:

As a natural process at the development of the Equivalent Restraint Method, calibration to full scale situation is one task. However, due to limited resources, only one typical case has been studied. In future research, other situations will be studied with the method (as mentioned in Chapter 8)

At the study of the importance of each individual laboratory test, only the effect of an alternation of the individual parameters in an evaluated parameter set was studied.

Effect of drying shrinkage, one important reason for stress occurrence at early ages, has not been studied in this work. As mentioned in the text, drying shrinkage shouldn't be neglected in stress analyses for thinner structures. However, as this study is mainly focussed on more massive structures, the drying effects can be excluded without any larger inaccuracy of end results.

### **1.4. Outline of the thesis**

This thesis consists of eight chapters, and their contents are briefly described below;

*Chapter 1* introduces the subject matter.

*Chapter 2* discusses damage types caused at early age thermal cracking.

*Chapter 3* gives an overview of the denotation thermal cracks, and illustrative examples of simplified crack risk estimations.

*Chapter 4* discusses computerized methods of stress calculations.

*Chapter 5* provides an overview of methods of restraint estimations.

*Chapter 6* describes the ERM which is an integrated method to determine the restraint with 3D elastic calculations and perform stress/strain analysis with the Compensation Line Method.

*Chapter 7* discusses the process of evaluation of material properties for young hardening concrete.

*Chapter 8* provides the most prominent results of the research of the ERM and the evaluation of material properties for young concrete, answers to the research questions and suggestions for future works within this field of research.

## 1.5. Appended papers

### Paper I

*“Simplified Methods for Crack Risk Analyses of Early Age Concrete - Part 1: Development of Equivalent Restraint Method”*, Al-Gburi M, Jonasson J-E, Nilsson M, Hedlund H & **Hösthagen A**, Published in Nordic Concrete Research, Publication no. 46, 2012, pp. 17-37.

In *Paper I* the Equivalent Restraint Method is introduced.

### Paper II

*“Thermal Crack Risk Estimations of Concrete Tunnel Segments - Equivalent Restraint Method Correlated to Empirical Observations.”*, **Hösthagen A**, Jonasson J-E, Emborg M, Hedlund H, Wallin K, Stelmarczyk M, Published in Nordic Concrete Research, Publication no. 49, 2014, pp. 127-143.

In *Paper II* and *III* the ERM is analyzed by comparing predictions of through cracking to empirical observations.

### Paper III

*“Thermal Crack Risk Estimations of Concrete Walls – Temperature and Strain Measurements Correlated to the Equivalent Restraint Method.”*, **Hösthagen A**, Jonasson J-E, Emborg M, Nilsson M, to be published.

### Paper IV

*“Evaluation of Material Properties for Young Concrete.”*, **Hösthagen A**, Jonasson J-E, Emborg M, Nilsson M, to be published.

Here it is shown how material parameters suitable for the ERM are obtained through laboratory tests.

Paper V

*“Thermal Crack Risk of Concrete Structures – Evaluation of Theoretical Models for Tunnels and Bridges.”*, Nilimaa J, Emborg M, **Hösthagen A**, to be published.

In this paper, a study of crack risk estimation for a typical case, where pre-calculations to estimate the crack risk at Gamla Uppsala, Sweden, were carried out by ERM, and a validation of the estimation is performed.



## 2. REASONS TO RESTRICT THERMAL CRAKING AT EARLY AGES

From a functional point of view, damage mechanisms in reinforced concrete structures concerning cracking are dependent on the crack widths and the type of damage attack. Thus, restrictions can be found in building codes ranging from an allowable maximum width ( $w^{\max}$ ) of 0.05 mm (almost crack free) to 0.5 mm and sometimes 1.0 mm.

In Sweden, there are requirements in the design process regarding the maximum crack width at severe environmentally conditions. These requirements are valid for the “general” design situations in the serviceability limit state analyses, with respect to risk of cracking caused by volume changes due to early temperature development and basic shrinkage. The philosophy in the national regulations is to plan for a “crack free situation”. In case of early cracking, the situation enters into an evaluation whether to take repair actions or not.

The types of damage connected to thermal cracks at early ages in reinforced concrete bodies can be divided into the following groups (simplifications based on Betonghandbok (1994)):

- Appearance of the concrete surface
- Lowering at the bearing capacity of the structure
- Corrosion of reinforcement bars
- Degradation mechanisms of concrete
- Throughflow of gases and liquids

The groups are not totally independent, but they represent the damage types usually discussed in the literature.

1. *Appearance of the concrete surface.* One important cause of bad appearance is when visible repair of cracks shows the injected cracks in sharp contrast to the general concrete surface. Another sharp and non-wanted appearance might be a consequence of throughflow of water, see item 5 below.
2. *Lowering of the bearing capacity of the structure.* Cracking causing collapse rather shortly after construction of a structure is not included here, as when this happens there usually is a fatal mistake made either in the design process or in the performance on site. But, if the bearing capacity are lowered due to progressive durability attack, and if no repair is performed in due time, the consequence might be a partial or total collapse of the structure in question.

3. *Corrosion of reinforcement bars.* In severe environmental conditions, cracks in concrete might strongly lower the corrosion initiation time, i.e. the time period when the reinforcement bars start to corrode. This initiation period is regarded as the design life-time in advance, which means that the cracking and crack widths are significantly important with respect to corrosion. In the regulations, this is controlled by restrictions of the calculated stress ratios with respect to early thermal cracking depending mainly on the exposure classes for the situation in question. In addition, there are also restrictions in the codes with respect to mix design parameters for different environmental situations.
4. *Degradation mechanisms of concrete.* The most important durability attacks in Sweden are i) frost attack, ii) corrosion of reinforcement and iii) chemical attack. The mechanisms are completely different; i) a frost attack with respect to cracking is more severe for rather large crack widths (> about 0.5 mm) than for “crack-free” concrete, and is usually not the decisive condition with respect to cracking; ii) the degradation with respect to corrosion usually means that the concrete cover of reinforcement is spalled by the pressure from the corrosion products, and iii) chemical attacks usually mean that “aggressive” liquids (e.g. sea water, sulphate-water, acidic water) dissolve the paste gradually and thereby makes the concrete weaker by time.
5. The *throughflow of gases and liquids* are significant already for rather small crack widths in the size of order of 0.1 mm. The flow of gases within through crack might be dangerous for people if the construction is a shelter in war, even if the concrete as is not destroyed. However, the flow of low lime water may significantly dissolve the paste, and this is a well-known issue to be regularly controlled and repaired, if necessary, in concrete dams and constructions with similar conditions of one side water pressure. The phenomenon is usually called leaching, and the final result might be observed visually as white coloured "work of arts" on the downstream side.

### 3. THERMAL CRACKS IN YOUNG CONCRETE AND SIMPLIFIED METHODS OF CRACK RISK ESTIMATIONS

#### 3.1. Definition of thermal cracks at an early age

The subject of cracking is a comprehensive task, and there exists no generally accepted standard definition of early age concrete cracks. Several mechanisms may contribute to risk of cracking at fresh and hardening concrete such as thermal movements, drying shrinkage, basic shrinkage, evaporation and settling due to gravity forces within the material. This work focuses on the most dominant mechanisms, thermal movement including effects of heat of hydration and basic shrinkage, present in all type of newly cast structures. Cracks originating from these volume changes are usually denoted “thermal cracks at early ages”, where “early age” generally covers the time period from casting until the newly cast concrete body is in thermal equilibrium with the surroundings including the adjacent structures.

In Sweden, there are requirements in the design process to take care of the maximum crack width at severe environmentally conditions for the “general” design situations in the serviceability limit state analyses. However, with respect to risk of cracking caused by volume changes due to early temperature development and basic shrinkage, the philosophy in the national regulations is to plan for a “crack free situation”. In case of early cracking despite this occurs, the situation enters into a discussion whether to take repair actions or not.

In a general structure, there exist no unified scientific definition of type of thermal cracks at early ages. But, for a “typical engineering structure”, where the newly cast concrete body can be described by two larger spatial dimensions, and one significant smaller third dimension, here named “thickness”, two groups of cracks can be significantly defined as:

- *Early surface cracks*
- *Later through cracks*

These two definitions of early age cracking are very informative to use for the discussion around how to analyse and distinguish between the most common cracks in typical engineering structures, like slabs, walls, bridges, tunnels, towers, columns, pillars etc. As a rough estimation, at least two thirds of all civil engineering structures are covered by the above mentioned typical structure.

For general discussions concerning early age cracking, it is practical to introduce two time periods with respect to the thermal development in the newly cast concrete body by:

- *Thermal expansion phase*
- *Thermal contraction phase*

The thermal expansion phase includes the time from casting as long as the average temperature is rising, and the contraction phase includes the cooling period thereafter. Based on these definitions, the main type of cracks can be clearly described as:

- a) *Early surface cracks* arise during the expansion phase, where a typical time after casting is in the size of order of one to two days. For thicker concrete bodies, the time of the expansion phase might be significantly longer.

The mechanism behind the formation of surface cracks is that the interior of the concrete construction is getting warmer than the surface, as the surface is cooled down by the surroundings. Hence, the interior is more prone to expand than the surface. Thus, at this stage, the force equilibrium over the thickness causes tensile stresses at the surface and compression in the interior. If this surface stress is larger than the momentary tensile strength, early surface cracks will arise, see Figure 1, where the typical behaviour of the surface stress development is shown schematically described by the curve denoted  $\sigma_s$ .

The stress development shown is representative for a freely cast construction, i.e. no restraint from any adjoining construction parts or subgrade, or an undisturbed part of the construction. As the rate of the temperature gradient slows down and decreases, the tensile stresses decrease and usually shifts to compression, which is a consequence of changed material properties in a hydrating concrete body.

Furthermore, as cracks forming in the heating phase normally tend to “close” in the cooling phase, the effects of these cracks on static capacity, function and durability can be a subject to discussion. The term close means that the concrete transforms from a tensile to a compression stress state, and probably due to “interlocking” still there are open slits from the concrete surface into some depth of the concrete. These open slits may still act as channels to transport harmful gases and liquids into the concrete, i.e. even at later ages the concrete may be regarded as “cracked” from a phenomenological point of view. Besides, surface cracks can also initiate through cracks, which would not develop otherwise. Hence, crack risks concerning early surface cracks are in the regulations considered equally harmful as later through cracks with respect to the ratio of tensile stress to the momentary tensile strength.

- b) *Later through cracks* are related to the average volume decrease due to both temperature drop and more or less homogenous basic shrinkage during the critical contraction phase, see Figure 2. Typically, through cracks generate over the entire cross section as a result of restraint from the adjacent existing structural concrete or subgrade. Depending on dimensions and other prevailing conditions, the cracks may appear weeks, months and in extreme cases even years after a section has been poured. The critical time period for later through cracks starts from the point of “zero stress” shortly after the temperature maximum in Figure 2, and continues until cracking appears or to the maximum tensile stress to tensile strength ratio is reached. In chapter 3.2, a more detailed description of later through cracks is presented.

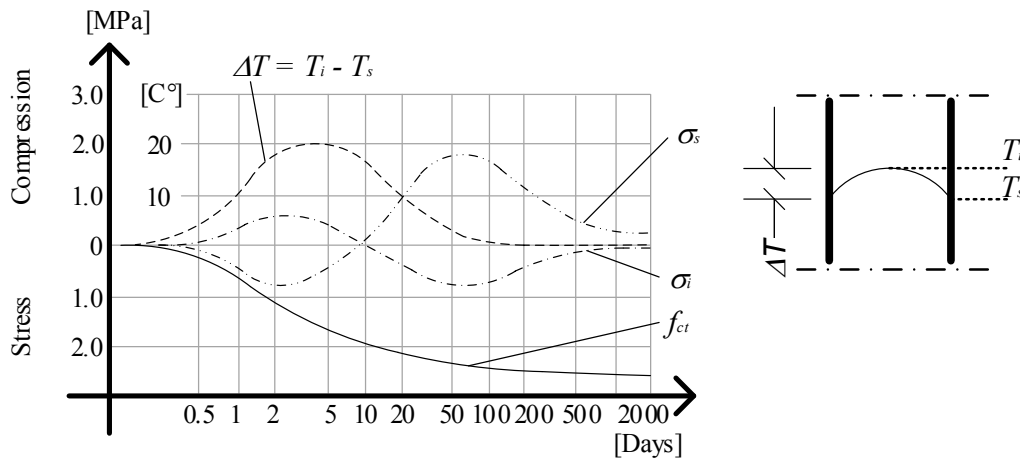


Figure 1. Schematic demonstration of the stress development at the surface and the interior of a concrete construction, and the development of surface tensile strength. Stress development showed is representative for a freely cast construction or an undisturbed (i.e. no cooling or heating) part of a construction.  $T_s$  and  $T_i$  is the surface and interior temperature,  $\sigma_s$  and  $\sigma_i$  is the surface and interior stress and  $f_{ct}$  is the surface tensile strength. (From Bernander, (1998), slightly modified.)

Cracks formed in the cooling phase tend to remain open permanently. Therefore, through cracks are often considered as being more critical than surface cracks, impairing appearance and durability. It is sometimes argued that functional requirements for avoidance of through cracking in the contraction phase should be stricter than for surface cracking originating in the expansion phase, but in the present regulations the level of accepted crack risks are mainly dependent on the environmental conditions covered by exposure classes for all types of early thermal cracking.

### 3.2. Later through cracks formation - details

Figure 2 shows the principle of how later through cracks are formed at the occasion of full restraint. Here the loading is regarded as the average temperature contraction over the cross section as well as the basic shrinkage. In total, the loading of the newly cast concrete is considered as a formal homogenous contraction during the critical contraction phase. This situation is only valid with respect to assessment of risk of later through cracks.

The initial condition is showed in Figure 2.a where the concrete has just been poured in the form work and the hydration has not yet started. At each end of the structure, the concrete is cast to a non-resilient material, i.e. full restraint is given along the length axis of the concrete body. Figure 2.b, as the hydration starts the temperature increases and the concrete body expands in every direction. Since full restraint is present along the length axis the thermal dilation is hindered which compresses the concrete. The young concrete has at this stage low strength and the compression yields both elastic and plastic deformations.

As the concrete reaches its maximum temperature it starts to cool off, see Figure 2.c. The compression is decreasing due to negative thermal dilation and basic shrinkage until it reaches a stress-free state sometime after the temperature peak. Thereafter the stress inside the concrete

increases, and if it exceeds the tensile strength, later through cracks appear, Figure 2.d. If the tensile strength is not reached, the relaxation of the concrete is beginning to be prominent. The effects of the relaxation become more significant over time, which decreases the tensional stresses until some residual stress level, see Figure 2.e.

The formation of cracking in concrete is fundamentally a balance between tensile strength and tensile stress. Several factors influence the strength and stress, see Figure 3, where it is clearly illustrated that the restraint situation plays a significant role for the stress and thereby for the formation of later through cracks.

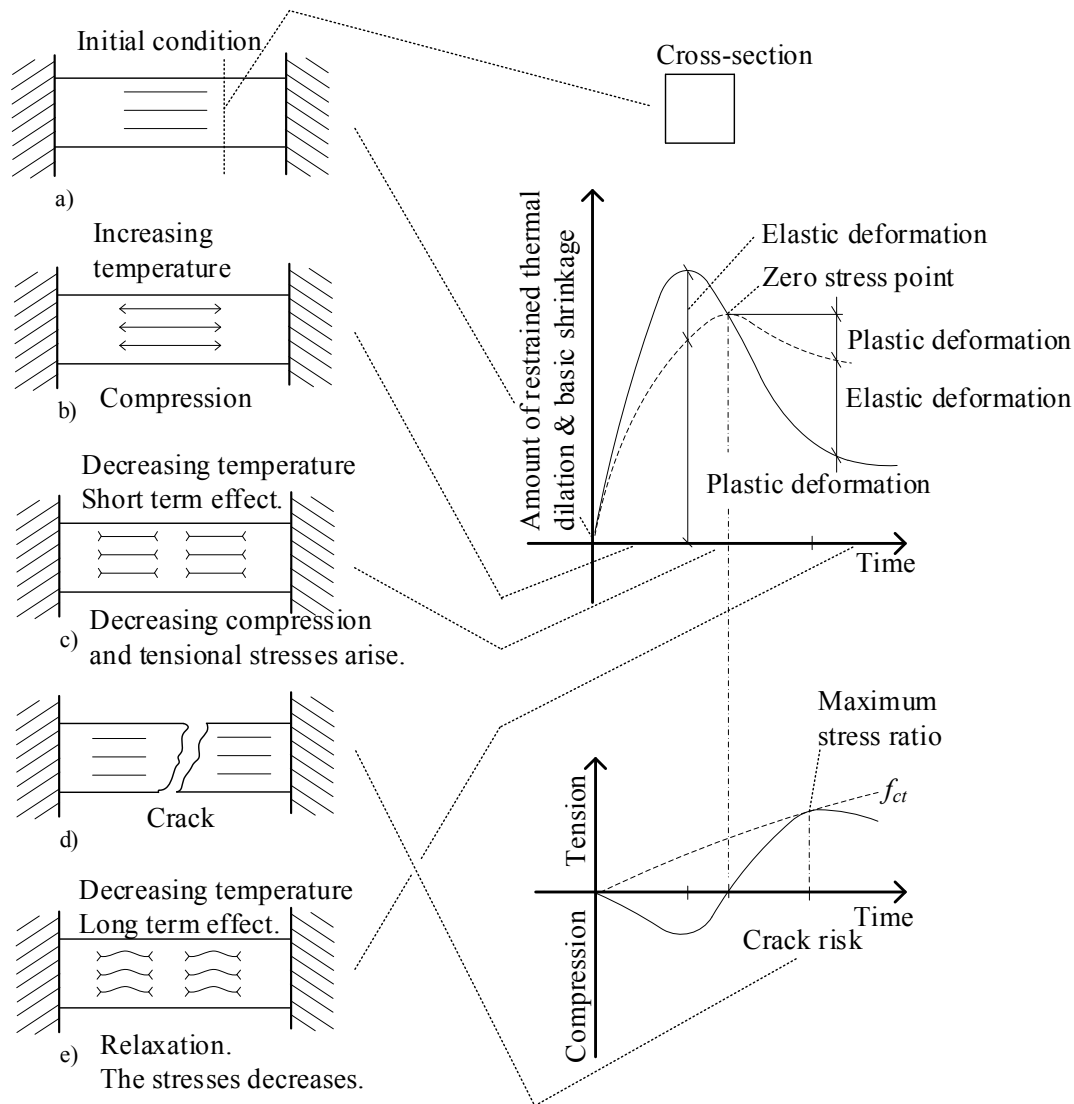


Figure 2. Mechanism of possible appearance of through cracks at full restraint at occasion of thermal dilation and basic shrinkage. (From Löfqvist (1946) and Betonghandbok (1994) slightly modified.)

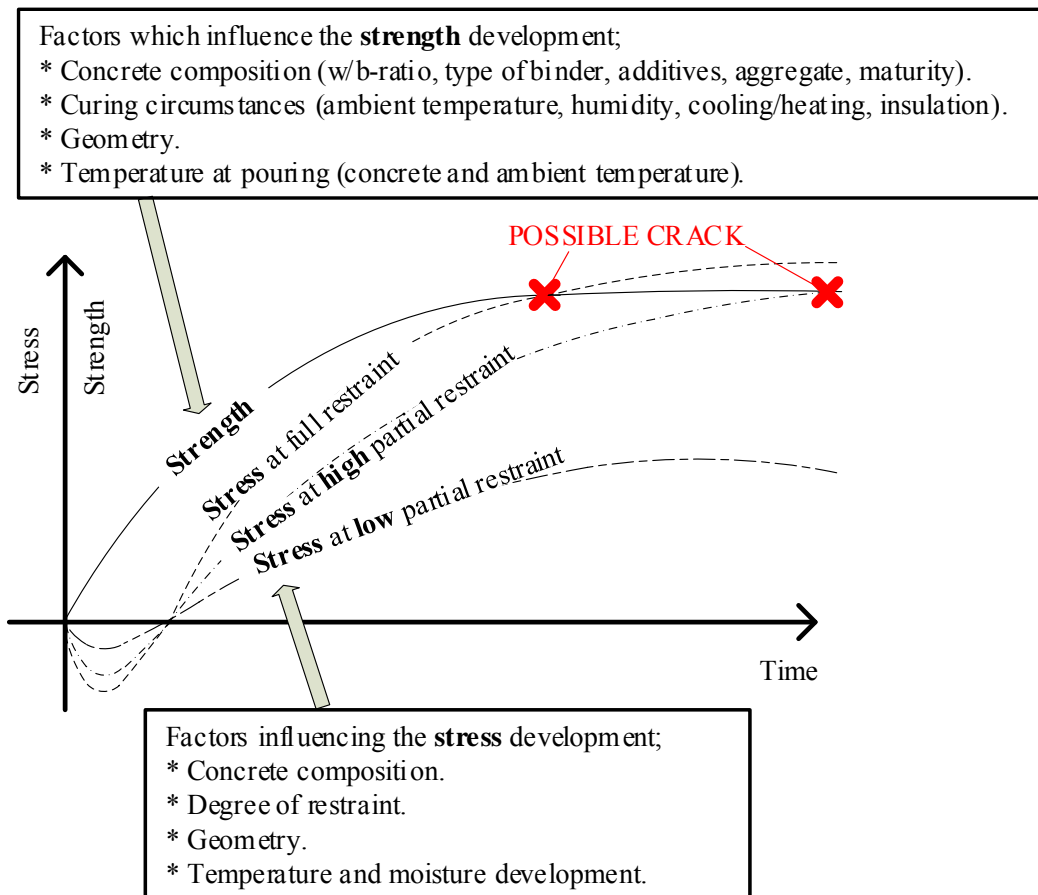


Figure 3. Factors which influence the stress and strength development in a hardening concrete element at full or partial restraint. (From Nilsson M (2003) slightly modified.)

### 3.3. Early age crack risk analysis

The process of how to estimate the early age crack risks within newly cast concrete structures, due to the early temperature development caused by hydration and the resulting thermal dilation and basic shrinkage, may be subdivided into five steps:

1. *General conditions.* General conditions need to be determined; dimensions of the ingoing parts of the analysed structure, material properties, environmental properties and any possible measure to avoid cracking
2. *Temperature development and basic shrinkage.* The temperature development and the basic shrinkage are determined by either calculations or tabular values. Calculations of temperatures for early age concrete are rather easy to perform, as long as the basic shrinkage is regarded to be independent of the temperature development, and several computer programs with such models exist. In these cases, an approximate model estimating basic shrinkage based on the so-called maturity concept is usually applied. Coupled models treating temperature and basic shrinkage simultaneously are still to be verified, although several non-linear effects have indicated in testing, see for instance Bjøntegaard (1999) and Orosz (2017). A discussion of crack risk analyses based on temperature development and basic shrinkage are given in Section 3.4.

3. *Restraint.* The restraint situation is obvious in some cases, e.g. when a whole structure, the new concrete body including possible adjacent existing structures, is analysed for the condition of total force equilibrium from static point of view. This might for the analysed structure be described as “free to deform”.  
In other cases, a very small new concrete body might be statically connected to very large or very stiff adjacent structures, where the restraint might be estimated to be very high, and approximately approaching total or 100 % restraint, which for the new concrete body can be described as “totally hindered to deform”.  
In intermediate situations, where the analysed structure (new concrete and adjacent structures) is somewhere between free and totally hindered to deform, there might be a need to calculate the restraint situation prior to calculations of the development of stresses, see Chapter 5 for information on how the restraint may be estimated.
4. *Structural stress calculations.* Calculations of stress development is performed, i.e. the maximal representative tensile stress is compared to the compressive strength. More detailed discussion concerning stress analysis is given in Chapter 4.
5. *Estimation of crack risk.* The stress ratios are compared to accepted levels, which in the national regulations (e. g. Swedish AMA Anläggning 13 (2014)) are given as the lowest safety value,  $S$ , strongly dependent on the exposure class and other conditions for the structure in question.

Figure 4 shows a simplified sketch of the principal procedure for estimation of crack risk.

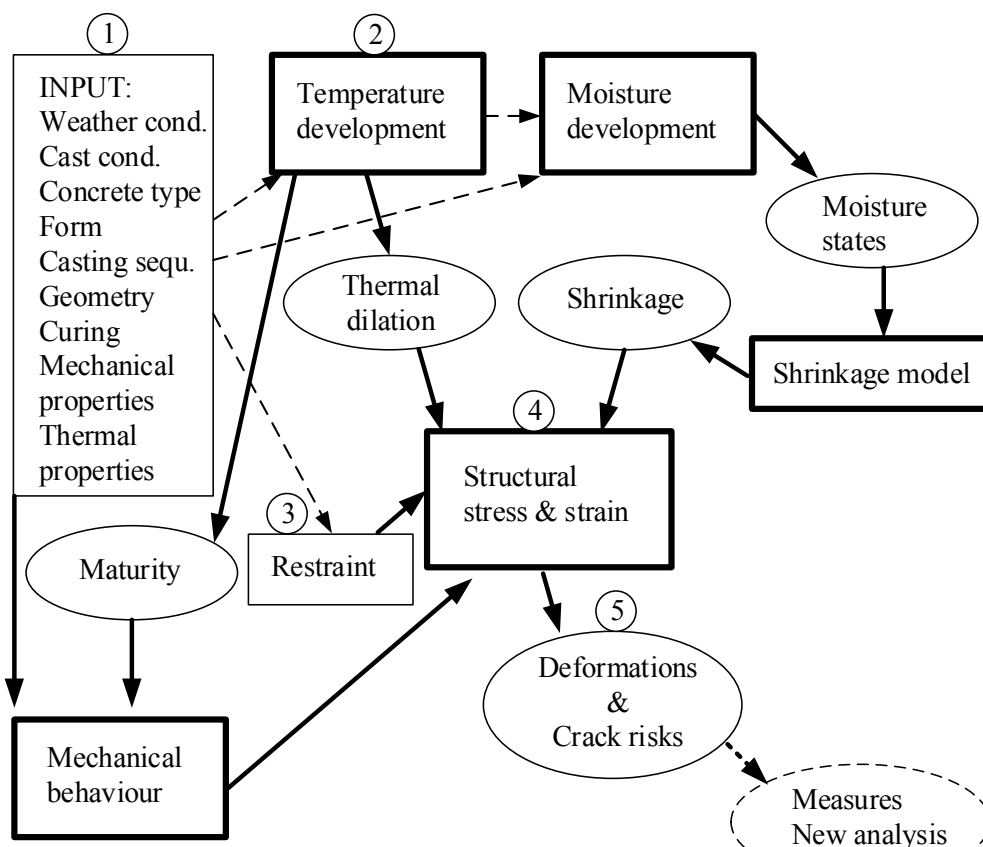


Figure 4. Schematic process of how to perform crack risk analysis. Numbers refers to the five steps of thermal crack risk estimation mentioned in the text. Thin boxes indicate input values or possible calculations. Thick boxes indicate possible calculations. Ovals indicate results of a calculation. (From Emborg and Bernander (1994), modified.)

From the value of lowest safety value  $S$  the maximum allowable stress level,  $\xi$ , is for a uniaxial stress state defined by

$$\xi = \frac{1}{S} = \frac{\sigma_{\max}(t_{\max})}{f_{ct}(t_{\max})} \quad (1)$$

where

- $\sigma_{\max}(t_{\max})$  = design tensile stress in the newly cast concrete body, Pa
- $t_{\max}$  = time reaching the design tensile situation, s
- $f_{ct}(t_{\max})$  = tensile strength at the position and time reaching  $\sigma_{\max}$ , Pa

The design tensile situation may also be represented by a strain level,  $\eta$ , which for a uniaxial formulation is expressed by

$$\eta = \frac{\varepsilon_{cm}(t_{\max})}{\varepsilon_{ct}^{ref}(t_{\max})} \quad (2)$$

where

- $\varepsilon_{cm}$  = stress related tensile strain in the concrete material, -
- $\varepsilon_{ct}^{ref}$  = stress related “reference” strain, calculated as

$$\varepsilon_{ct}^{ref} = \frac{f_{ct}(t_{\max})}{E_{c,eff}(t_{\max})} \quad (3)$$

where

- $E_{c,eff}$  = modulus of elasticity including creep effects, Pa

In a general 3D formulation of stresses and strains corresponding formulations might be very complicated, but for the uniaxial formulation shown here, the stress level and the strain level are related through the “working curve”, see ConTeSt Pro (2008), used in the calculation, i.e. the relation between stress and stress related strain. Two situations are commonly used in different existing computer models:

- linear stress–strain curve
  - nonlinear stress–strain curve
- a) Using a *linear stress–strain curve* means that i) the stress level and the strain level are identical, and ii) the stress and strain level are larger than unity,  $> 1$ , at very high loadings, or that the safety value,  $S$ , is lower than unity,  $< 1$ , which formally represents a cracked situation. When using this approach when  $S < 1$ , the subsequent analysis usually means that effects of measures on site, change of concrete mix or similar actions are introduced until the allowable value of  $S > 1$  is reached.
  - b) Using a *non-linear stress–strain curve* means that the stress never can exceed the tensile strength, which means that i) the stress level and the strain level may not be the same, especially at high loading situations, and ii) the calculated stress level never can exceed unity,  $\xi \leq 1$ , but the calculated strain level larger than unity,  $\eta > 1$ , may occur for high loading situations. When the calculated stress and/or strain levels are larger than allowable values, the subsequent analyses are quite similar as for the use of a linear working curve.

If the non-linear formulation has a linear curve starting from origin of the working-curve, the stress and strain level are identical, until the non-linear part is reached.

### 3.4. Temperature development yielding crack risk

#### 3.4.1. Crack risk analyses for typical structures

As mentioned above for typical structures two type of crack are defined:

- Early surface cracks
- Later through cracks

Analyses concerning *early surface crack risks* can easily be performed for a self-balancing situation analysing any section in parallel with the thickness of the structure as shown in Figure 1, where the external restraint is zero, i.e. far enough from the structural joint to an adjoining structure, if any. As a help tool, calculated crack risks concerning early surface crack risks without any methods on site for common structures of walls and slabs on ground are presented in diagrams in Method 2 in Emborg et al (1997). The denotation “Method 2” refers to the national regulations using pre-calculated results. Only referring to these diagrams, about 90 per cent of common typical engineering structures can be shown to fulfil the demanded safety value without any measures on site. The remaining amount of structures can easily be analyzed by computer calculations. However, one comment should be made regarding the diagrams within Emborg et al (1997). The undelaying calculations was based on concrete with cement binder that not exists any more. Also, no variations regarding consistence class has been done. Thus, the diagrams cannot be considered as totally accurate for self-compacting concrete. The given statements in this paragraph of text end the discussions concerning analysis concerning early surface crack risks in this thesis.

Results from analyses concerning *later through crack risks* without measures on site are also presented in Emborg et al (1997) for a number of typical engineering structures of the type “wall cast on existing concrete slabs founded on frictional materials”, i.e. structures like tunnels, integral bridges, actual wall-on-slab etc. Now the situation is reversed, as only about five per cent of the structures concerning through cracking can be shown in the hand book diagrams, that the demanded safety value can be fulfilled without any measures on site. In practice, almost all structures concerning later through crack risks have to be analysed individually by calculations. Therefore, in the subsequent text in this thesis concerning crack risks only matters concerning through cracking are considered.

#### 3.4.2. Estimation of later through crack risks based on temperature and basic shrinkage development

When the position and direction of the design stress as well as and the restraint value are identified, the estimation of the through crack risk described as stress ratio can be formulated as

$$\xi = \frac{(\Delta\varepsilon_{sh} + \Delta T_c \cdot \alpha_c) \cdot E_{c,eff}(t_{max})}{f_{ct}(t_{max})} \cdot \gamma_R \quad (4)$$

where

$\Delta\varepsilon_{sh}$	= basic shrinkage from zero-point stress, see Figure 2, to the maximum stress ratio, -
$\Delta T_c$	= temperature difference from zero-point stress to the maximum stress ratio, °C
$\alpha_c$	= thermal dilation coefficient for the concrete, °C <sup>-1</sup>
$\gamma_R$	= restraint value in the design position {0,1}, -

The corresponding formulation as strain ratio, here approximated to be as simple as possible, may be

$$\eta = \frac{(\Delta\varepsilon_{sh} + \Delta T_c \cdot \alpha_c) \cdot \varphi_{load} \cdot \gamma_R}{\varepsilon_{ct}(t_{max})} \quad (5)$$

where

$\varphi_{load}$	= loading factor (< 1) taking care of reduction in stress related strains due to creep/relaxation effects from zero stress point to the maximum strain ratio, -
$\varepsilon_{ct}(t_{max})$	= strain at cracking at the time of maximum strain, -

Note that  $\varepsilon_{ct}(t_{max})$  in Eq. 5 is not the same as  $\varepsilon_{ct}^{ref}(t_{max})$  in Eqs. 2 and 3. The latter is calculated using the tensile strength, whereas  $\varepsilon_{ct}(t_{max})$  in Eq. 5 represents the actual strain at fracture/cracking. This means that the strain ratio according to Eq. 2 might exceed unity ( $\eta > 1$ ) without cracking, but the strain ratio equals unity in Eq. 5 means cracking.

Both Eqs. 4 and 5 may be used as manual methods. The resulting stress or strain levels are probably in the right size of order, and might act as a relevant base for early discussions of what materials to choose and what actions to be taken when planning for a crack free situation.

The most important difference between Eq. 4 and Eq. 5 is that both  $E_{c,eff}(t_{max})$  and  $f_{ct}(t_{max})$  in Eq. 4 are strongly time dependent, but both  $\varphi_{load}$  and  $\varepsilon_{ct}$  may for quick calculations, according to Larson (2003), be approximated as constants by setting

$$\varphi_{load} \approx 0.7 \quad (6)$$

and tensile fracture strain at short-term loading can be expressed as, see for example Löfqvist (1946) and Hilleborg (2009)

$$\varepsilon_{ct} \approx 100 \cdot 10^{-6} \quad (7)$$

Furthermore, for quick estimations the thermal dilation may be approximated as

$$\alpha_c \approx 10 \cdot 10^{-6} \text{ °C}^{-1} \quad (8)$$

The value of  $\varepsilon_{ct}$  in Eq. 7 corresponds to formation of tensile cracks for a temperature drop of about 10°C at short-time loading and the situation of full restraint ( $\gamma_R = 1$ ).

There are two alternative ways of modelling the creep/relaxation effect in Eq. 5: either using Eqs. 6 and 7 or using  $\varphi_{load} = 1$  and  $\varepsilon_{ct} \approx 140 \cdot 10^{-6}$  ( $\approx (100/0.7) \cdot 10^{-6}$ ) representing the tensile fracture strain condition, corresponding to a temperature drop of about 14°C, at long-term loading from zero stress point to the maximum strain ratio at full restraint.

Now, using Eq. 5 with respect to approximations in Eqs. 6-8, the situation for a quick estimation of risk of through cracking is reduced to determine  $\Delta\varepsilon_{sh}$ ,  $\Delta T_c$  and  $\gamma_R$  for a certain situation, and finally compare the estimated strain ratio with the allowable strain ratio as the inverse of the needed safety value,  $S$ .

Simplified manual formulas can be based on the principles shown here either as stress related or strain related analyses for general purposes, see further Larson (2000 and 2003).

From the discussion above it is evident that the *temperature development* is one of the key factors estimating crack risks, and we have to consider the temperature in the newly cast element as well as the interaction with the environment and adjacent structures. The most important areas to take into account are, see also Figure 4

- thermal properties of the concrete (heat of hydration, maturity function etc.).
- mix design parameters (type and content of binder, type and amount of admixtures)
- geometry and dimensions of the structure being cast and adjoining structures.
- environmental conditions (ambient air temperature, temperature of adjoining structures and sub-grade, wind velocity, solar radiation).
- conditions at pouring (placing temperature, formwork etc).
- measures on site (Time of formwork removal, heat insulation, cooling, use of heating cables etc.).

One further step for quick estimation of risks of through cracking for the typical structure wall-on-slab was the development of the Excel spread sheet CRAX1 (which is an abbreviation for Crack Risk Analysis using the eXcel spread sheet number 1, (CRAX1, 2003)). The temperature key values are presented in diagrams taking into account all areas listed above.

Based on this information CRAX1 calculates  $\Delta\varepsilon_{sh}$ ,  $\Delta T_c$  and  $\gamma_R$ , i.e. all what is needed to use a modified formulation of Eq. 5, see Eq. 9 and Figure 5.

$$\eta = (\Delta\varepsilon_{sh} + c_{1,W} \cdot \alpha_c \cdot (T_{cast} - T_{ambient}) + c_{2,W} \cdot \alpha_c \cdot (T_{max} - T_{cast}) - c_{3,C} \cdot \alpha_c \cdot (T_{max} - T_{cool}) - c_{3,H} \cdot \alpha_c \cdot (T_{heat} - T_{ambient})) \cdot \frac{\varphi_{load}}{\varepsilon_{ct}(t_{max})} \cdot \gamma_R \cdot \begin{cases} c_{4,W} \\ c_{4,C} \\ c_{4,H} \end{cases} \quad (9)$$

where

- $T_{cast}$  = concrete casting temperature (in the formwork after treatment on site), °C  
 $T_{ambient}$  = average temperature of the ambient air, °C  
 $T_{max}$  = peak temperature in the newly cast concrete at the position of the design value, averaged over the wall thickness, °C  
 $T_{cool}$  = the temperature in the circulating cooling water, °C  
 $T_{heat}$  = the average temperature in the heated adjacent slab, °C  
 $c_{i,j}$  = correction factors calibrated from comparisons (by “manual regression”) with a lot of computer calculations both on temperatures and crack risks.-

- index  $i$  = {  
 1 reflects the initial situation at setting of the newly cast concrete body  
 2 reflects "natural" temperature rise situation of the newly cast concrete  
 3 reflects the situation using measures (cooling or heating) on site  
 4 reflects different non-linear effects on final strain ratios
- index  $j$  = {  
 $W$  reflects the situation without measures on site  
 $C$  reflects the situation using cooling pipes  
 $H$  reflects the situation using heating cables

The restraint distribution along the height of the structure,  $y$ , for the typical case wall-on-slab founded on frictional material,  $\gamma_R(y)$ , is in CRAX1 calculated according to the method presented in Section 5.1, developed in Nilsson (2003).

With respect to the temperature differences presented in Eq. 9, the following temperature definitions can be stated:

- 1) Initial temperature difference =  $T_{cast} - T_{ambient}$   
 2) Hydration heat effect =  $T_{max} - T_{cast}$   
 3) Cooling of young concrete =  $T_{max} - T_{cool}$   
 4) Heating of adjacent structure =  $T_{heat} - T_{ambient}$

These temperature differences can also be described in the following way:

- 1) = "Built in" difference at casting causing tensile stresses  
 1) + 2) = "Natural" difference causing tensile stresses without any measures on site  
 1) + 2) - 3) = Difference causing tensile stresses after cooling of the newly cast structure  
 1) + 2) - 4) = Difference causing tensile stresses after initial heating of adjacent structure

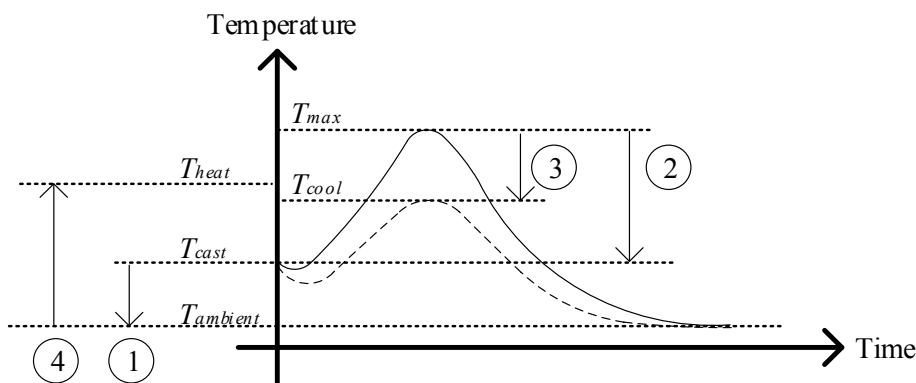


Figure 5. Illustration of the temperature differences used in Eq. 9.



## 4. METHODS FOR COMPUTERIZED CALCULATIONS OF STRUCTURAL STRESS

### 4.1. Overview of stress calculations

In general, any casting of concrete a structure can be analyzed with respect to early stresses by the most common numerical method in structural design, 3D FEM (three-dimensional Finite Element Method), calculating 1) temperature developments, 2) moisture fields and 3) resulting stresses with 3D elements. However, such calculations are both time-consuming and the available software are often costly at purchase and time consuming to use. This motivates the need of different more cost- and time-effective calculation models for every day design purposes.

The main focus in this study is to analyze the simplified method ERM (Equivalent Restraint Method), which is a new application of the CLM (Compensated Line Method), first introduced in Japan in the middle of the 1980's (mentioned in JCI Committee Report, 1992), further developed in Sweden (Emborg, 1989), and today widely used on the Swedish market by the computer program ConTeSt Pro (2008). Since the ERM implies "Out of Plane" calculations for the crack risk analyses, a detailed explanation of the method "Out of Plane" stress calculation is given in Section 4.2.

The finite element method is often utilized in conventional structural analysis for the modelling of both pure linear elastic behavior and non-linear behavior owing to plasticity, cracking, buckling and hydration heat development. It is therefore also possible to make use of FEM-programs for the analysis of thermal stresses in young concrete. The main advantage is that complex geometry and boundary conditions can be studied.

However, considerable additional knowledge of the different material properties of young concrete then has to be established. For example, it is essential to observe that whenever 2D- or 3D- analysis is contemplated, one must be aware of that the visco-elastic properties observed using 1-dimensional testing equipment may not be directly suitable to be transformed into 2D (or 3D) situations.

This is mainly due to the many ways in which shear deformation may contribute to the total deformation in different states of stress. Creep deformations under isotropic stress conditions

are certainly not the same as those in states of markedly un-isotropic stress. For instance, in cases where the two (three) principal stresses are of the same magnitude and have the same sign shear deformation is zero, whereas if at least two of the principal stresses have *opposite* signs, a case with pure shear deformation arises.

## 4.2. Out-of-Plane stress calculations

In Out-of-Plane stress calculations of the stress state is formally uni-axial, analogous with the wide spread engineering beam and simplified plate theories, and three subdivisions can be identified:

1. *Point-by-Point Calculations, PPC.*
2. *Compensation Line Method, CLM.*
3. *Compensation Plane Method, CPM.*

### *PPC. Point-by-Point Calculations*

In the PPC, a point or a system of points within a structure are analyzed. To perform stress calculations four steps are acquired; a), a decisive location in the structure is identified, i.e. where the highest crack risk is expected. b) The degree of restraint is estimated for a single point, c) the temperature development is calculated, and thereafter, d) a stress calculation is performed.

A PPC can be performed using point-wise formulations like the formulations shown in chapter 3 or other simplified methods, see for instance Larson (2000 and 2003). There is also a possibility using computerized compensated line or compensated plane methods neglecting the structural rotations and using axial restraint values valid for the analyzed point.

### *CLM. Bending of a straight plane – 1D*

The Compensation Line Method approximates a structure sectioned in finite laminar sections, see Figure 6, and calculations are performed similar to the engineering beam theory i.e. the model assumes that the cross section remains plane at bending. The method prerequisite that a uniaxial stress field can be applied i.e. that the eigenstresses feature a dominant direction. Furthermore, the temperature and moisture state have to be averaged in direction of the rotation axis, i.e. the temperature and the moisture field formally only vary with the height of the “beam”, see direction  $y$  in Figure 6. The section where equilibrium regarding strain distribution is obtained, is called the Compensation Line. The effect of longitudinal translation and bending of the beam is modelled by localize the Compensation Line and apply force and momentum equilibrium in the longitudinal direction of the beam, see e.g. Emborg (1989):

$$\int \sigma \cdot dA = 0 \quad (\text{normal force}) \quad (10)$$

$$\int \sigma_z \cdot z_k \cdot dA = 0 \quad (\text{bending moment in one direction}) \quad (11)$$

where

- $\sigma$  = thermal and shrinkage normal stress, Pa
- $z_k$  = distance to neutral layer, m
- $dA$  = area of an incremental layer of the beam, m<sup>2</sup>

Adjoining structures may be modeled as finite layers of the beam, assuming full bound between the layers. An alternative to incorporate adjoining structures is to model the restraint as an external factor, which make the above integrals to differentiate from zero.

The method is applicable to determine both the risk of through and surface cracking.

*CPM. Bending of a straight plane – 2D*

The Compensation Plane Method utilizes the same assumptions as the CLM with the difference that the beam is allowed to bend in the orthogonal direction also, and a plane is formed where equilibrium is fulfilled regarding force and bending in the two directions, i.e. the Compensation Plane. Hence, three equations of equilibrium are set up for the plane surface in relation to the centroid of the section. If no restraint from adjoining constructions is present, it is possible to calculate the internal stress for each section by localizing the plane yielding the integrals to equal zero:

$$\int \sigma \cdot dA = 0 \quad (\text{normal force}) \quad (12)$$

$$\int \sigma_z \cdot z \cdot dA = 0 \quad (\text{bending moment in } x \text{ direction}) \quad (13)$$

$$\int \sigma_y \cdot z \cdot dA = 0 \quad (\text{bending moment in } y \text{ direction}) \quad (14)$$

The ERM performs stress and strain ratio analyses using CPM.

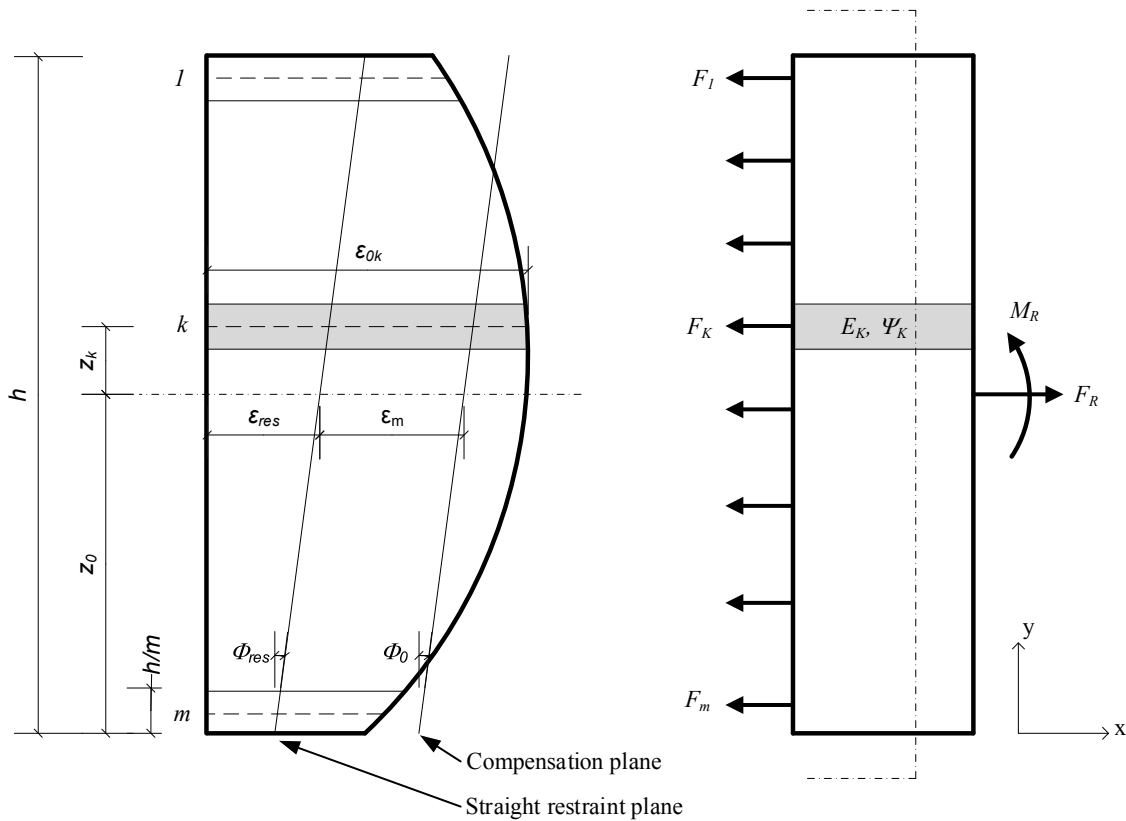


Figure 6. Sectioning of a structure in  $m$  finite laminar sections with the individual thickness,  $h/m$ , and mechanical material properties,  $E_k$  (elastic modulus) and  $\psi_k$  (creep coefficient) for section  $k$ . The translation strain for the whole structure is defined as  $\epsilon_{res}$  and  $\Phi_{res}$  defines the degree of bending for the structure.  $z_k$  is the distance to the neutral layer,  $M_R$  and  $F_R$  is the momentum and axial force in the cross section. (From Onken and Rostásy (1995), slightly modified.)



## 5. RESTRAINT ESTIMATION

The *restraint* is affected by the general structural configuration such as, dimensions, stiffness of adjoining structures, the degree of bonding to the same, ground friction and the conditions under which the element is being poured (casting sequences, construction joints, weather conditions etc.). Experience from calculations, where the restraint has been varied verifies its paramount effect not only on the level of stress but also on stress development, for instance, whether the concrete will be in tension or compression at a certain point in time after casting.

### 5.1. Definition of restraint

The degree of restraint,  $\gamma_R$ , can be defined as the possibility of the concrete to deform. The free deformation may have different origins, such as thermal dilation and deformations due to different moisture related deformations. If the young concrete is free to move, there is no restraint ( $\gamma_R = 0\%$ ), and if the young concrete is not allowed to move at all, it experiences full (or total) restraint ( $\gamma_R = 1 = 100\%$ ). Situations where full restraint may occur are, for example, when a concrete structure is cast between two inflexible entities.

The restraint in the axis of the structural joint is decisive for crack formation perpendicular to the axis. The restraint factor,  $\gamma_R$ , in newly cast concrete, can formally be expressed by, see Al-Gburi (2015):

$$\gamma_R = \frac{\sigma_{ui}}{\sigma_{full}} = \frac{\sigma_{ui}}{-\zeta \cdot E_{28} \cdot \Delta\varepsilon^0} \quad (15)$$

where

- $\sigma_{ui}$  = resulting FEM stress in the young concrete in direction  $i$ , Pa
- $\sigma_{full}$  = stress at full restraint in the examined point, Pa
- $\Delta\varepsilon^0$  = differential free deformation, in this case contraction ( $\Delta\varepsilon^0 < 0$ ) in relation to a stress-free state, of the examined point, -
- $E_{28}$  = modulus of elasticity at 28 days, Pa
- $\zeta$  = maturity factor for the present elastic modulus in relation to the modulus at 28 days, -

The differential free deformation can be caused by different free deformations within the newly cast concrete or different deformations between the newly cast concrete and the adjoining structures or a combination of both.

Sometimes, in older literature, there has been attempts to distinguish between so called “internal” and “external” restraint whether the differential deformation is inside the newly cast concrete or caused as a difference to adjacent structures. However, according to the opinion of Swedish researchers and specialists, such definitions are confusing as they only can be valid for certain special structural cases. In more generalized computational methods (like the FE analyses) encompassing adjacent restraining structures as well as subgrades, *all* early age stresses are actually internal stresses with respect to the total construction analyzed. Hence, the terms “external and internal restraints” do *not* appear to be a rational basis for a general classifying of early age cracks in concrete.

On the other hand, the term external restraint is relevant describing the counteracting forces applied to a total cross section or a whole structure, see further the text below concerning external translation and external rotational restraint. The denotation could sometimes also be convenient for pedagogical reasons explaining the complicated matter of occurrence of load-independent stresses.

A semi-analytical method for determination of the restraint suitable for CLM and CLP and valid for cases where a concrete member is cast upon a restraining member is presented in Nilsson (2003), where all listed factors in Section 5.2 may be taken into account.

The method starts formulating the strain in a point of a *reference cross section* with the assumption of “full structural contact without gliding in the joint area between the new concrete and the adjoining structure body” (modelled by  $\delta_{slip} \equiv 1$ ), and that “plane sections remain plane” (modelled by  $\delta_{res} \equiv 1$ ), see Eq. 17 and further on for more general structures. The resulting deformations, see Figure 7, can be described by one translational strain,  $\varepsilon_0^t$ , and two rotational based strain components,  $\varepsilon_0^{ry}(z)$  and  $\varepsilon_0^{rz}(y)$ , reflecting rotation around  $y$ -axis and  $z$ -axis, respectively. For a studied point ( $y, z, x = \text{constant}$ ), the resulting stress in the  $x$ -direction,  $\sigma_x$ , is expressed by (based on expressions in Nilsson (2003))

$$\sigma_x(y, z, x = \text{constant}) = \zeta \cdot E_{28} \cdot (-\Delta\varepsilon^0 + \varepsilon_0^t + \varepsilon_0^{ry}(z) + \varepsilon_0^{rz}(y)) \quad (16)$$

where

index  $_0$  = reflects the situation of compatibility conditions based on “plane sections remains plane”.

The reference restraint situation is valid for a *sufficient long construction*, where  $\delta_{slip} = \delta_{res} \equiv 1$  according to Figures 9 and 11, and when combining Eqs. 15 and 16 the restraint value can be described by

$$\gamma_{R,0}^{ref}(y, z, x = \text{constant}) = \frac{-\Delta\varepsilon^0 + \varepsilon_0^t + \varepsilon_0^{ry} \cdot (z) + \varepsilon_0^{rz} \cdot (y)}{-\Delta\varepsilon^0} \quad (17)$$

where

$\gamma_{R,0}^{ref}$  = restraint in a point ( $y, z$ ) of a self-balanced section at a prechosen length coordinate ( $x = \text{constant}$ ) for the reference situation with  $\delta_{slip} = \delta_{res} \equiv 1$ .

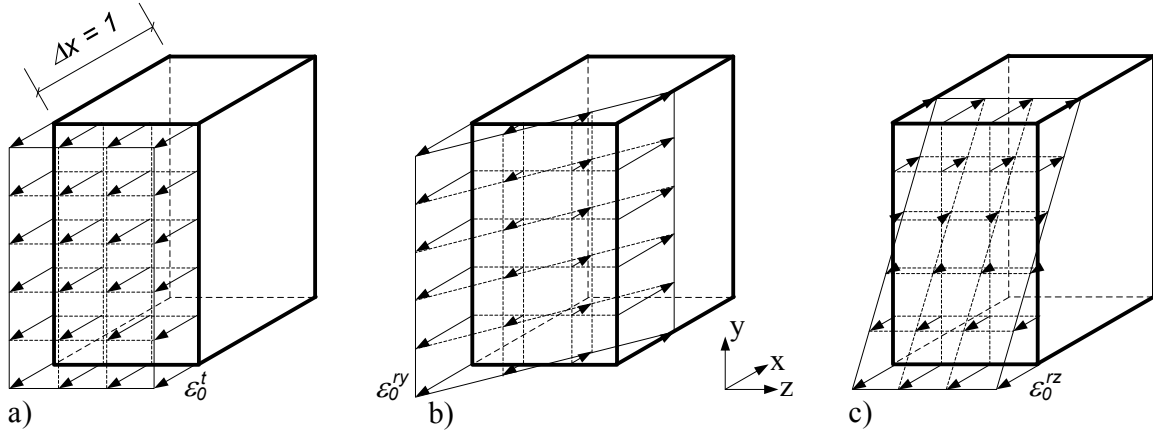


Figure 7. Possible deformation for a cross-section: a) translation, b) rotation around y-axis and c) rotation around z-axis. Figure from ConTeSt Pro (2008), slightly changed.

For a cross-section consisting of real structures, where resilience due to slip in the construction joint ( $\delta_{slip} \leq 1$ ) and non-linear effects due to limited length/height-ratios ( $\delta_{res}(y) \leq 1$ ) occur, the restraint coefficient for a *self-balanced structure*,  $\gamma_{R,0}$ , can be expressed as in Nilsson (2003)

$$\gamma_{R,0}(y, z, x = \text{constant}) = \frac{-\delta_{slip} \cdot \delta_{res}(y) \cdot \Delta \varepsilon^0 + \varepsilon_0^t + \varepsilon_0^{ry}(z) + \varepsilon_0^{rz}(y)}{-\Delta \varepsilon^0} \quad (18)$$

which can be transformed into a start restraint value reduced with respect to one translational and two rotational deformations expressed by as in Nilsson (2003)

$$\gamma_{R,0}(y, z, x = \text{constant}) = \delta_{slip} \cdot \delta_{res}(y) - \gamma_R^t - \gamma_R^{ry}(z) - \gamma_R^{rz}(y) \quad (19)$$

More detailed information concerning  $\delta_{slip}$  and  $\delta_{res}$  are given in Section 5.4 and Nilsson (2003).

The situation for a self-balanced structure can be defined by external structural restraint factors  $\equiv 0$  for each possible deformation in question by

$$\text{Self-balancing structure} \begin{cases} \gamma_{RT} = 0 & \text{for translational restraint for the whole section} \\ \gamma_{RR,y} = 0 & \text{for total rotational restraint around z - axis for the whole section} \\ \gamma_{RR,z} = 0 & \text{for total rotational restraint around y - axis for the whole section} \end{cases}$$

Full restraint means that these structural restraint factors  $\equiv 1$ , and partial structural restraint means that these factors are within the range  $\{0,1\}$ .

So, for a situation with respect to arbitrary structural restraints for each possible deformation Eq. 19 is generalized to

$$\gamma_R(y, z, x = \text{constant}) = \delta_{slip} \cdot \delta_{res}(y) - (1 - \gamma_{RT}) \cdot \gamma_R^t - (1 - \gamma_{RR,y}) \cdot \gamma_R^{ry}(z) - (1 - \gamma_{RR,z}) \cdot \gamma_R^{rz}(y) \quad (20)$$

where

$\gamma_R$  = restraint in a point  $(y, z)$  of a cross-section for a prechosen length coordinate  $(x = \text{constant})$ , -

These restraint factors apply to every point in the whole cross-section, where  $\gamma_R^t$ ,  $\gamma_R^{ry}(z)$ ,  $\gamma_R^{rz}(y)$  determine the local restraint at each individual point. The local restraint may for instance be affected by an uneven maturity, temperature and/or moist distribution over the analyzed plane, yielding a non-homogenous restraint profile.

## 5.2. Factors yielding restraint

Due to several factors, the true degree of restraint in different locations of a newly cast concrete structure often is hard to determine. Factors that influence the degree of restraint,  $\gamma_R$ , may be:

- a) *Resilience of the young concrete.* The length to height ratio,  $L/H$ -ratio, of the newly cast concrete is often influencing the restraint to a high degree, see e.g. Emborg (1998) and Nilsson (2003). The restraint decreases in perpendicular direction from the casting joint, and the magnitude of the restraint is determined by the  $L/H$ -ratio.
- b) *Slip in the casting joint.* Laboratory tests, see Nilsson (2000), as well as field documentation proves that the phenomena exists. The reason is explained as micro cracks arising in the casting joint at the longitudinal edges of the construction, and propagates to the centre of the casting joint (Bernander, 1998). This “slip” phenomenon decreases the restraint from the adjoining structure and is influenced by the construction length. The slip is considerable diminished in case of high amount of reinforcement through the joint.
- c) *Geometry of adjoining structure.* The degree of restraint heritage from an adjoining structure is primarily dependant on the joint area, relative dimensions and modulus of elasticity between the newly casted section and the adjoining structure, see Al-Gburi, M. (2015). In case of piles in the adjoining structure, the restraint may increase, see Nilsson (2000).
- d) *Temperature gradients in the young concrete.* In cooled areas (using cooling pipes) within the newly cast concrete and areas near an adjoining structure where a significant heat flow may occur, the restraint in the closest uncooled areas is increased to some degree. The reason is the difference in movements of the cooled and not cooled areas. For example; if a wall is cooled near the casting joint to a base slab, the uncooled area is expanded more at the temperature peak of the young concrete. At the cooling phase of the hydrated concrete, the concrete is contracting. Due to the difference in elongation between cooled and not cooled areas together with the restraint from the base slab, the uncooled area experiences a higher degree of restraint compared to a non-cooled case.
- e) *Contraction or elongation of the adjoining structure.* If the adjoining structure is deformed before the newly cast concrete has reached the ambient temperature, the degree of restraint is changed.  
Depending on the relative direction of the deformation for the adjoin structure versus the thermal dilation of the newly cast concrete, the restraint is either decreased or increased. For example; if an adjoining structure is heated before a cast until the cooling phase of the young concrete, the thermal dilation of the adjoining structure follows the thermal dilation of the young concrete, which decreases the restraint.
- f) *Resilience of the ground.* If the system of young concrete and adjoining structure is located on ground, the flexibility and stiffness of the ground may influence the restraint, see Nilsson (2000). Any friction between the concrete structure the foundation also contributes to the restraint.

### 5.3. Methods of restraint estimation

- *Equations reflecting uniaxial deformations.* It is very simple to derive an equation describing the restraint within a structure for a uniform uniaxial stress case, i.e. a pure axially loaded member. This may be valid where the rotation around the horizontal axes are fully hindered ( $\gamma_{RR,y} = \gamma_{RR,z} = 1$  and  $\gamma_{RT} < 1$ , see Eq. 20). Consider a system where a concrete element with symmetric section is cast with full bound on top of an adjoining structure, see Figure 8a. Now, if the adjacent structure is large enough, a uni-axial restraint situation will occur. The interaction between the two blocks in Figure 8 may be derived as follows

$$\sigma_1 = E_1 \cdot \varepsilon_R \quad (21)$$

and

$$\sigma_1 = \frac{F_1}{A_1} \quad (22)$$

where

$\varepsilon_R$	= restrained deformation causing stresses in block 1, Figure 8b, -
$E_1$	= elasticity modulus in block 1, Pa
$F_1$	= force in block 1, N
$A_1$	= section area in block 1, m <sup>2</sup>

Combining Eqs. 21 and 22 gives the force in a restrained block at homogenous deformation:

$$F_1 = \varepsilon_R \cdot E_1 \cdot A_1 \quad (23)$$

If the free deformation,  $\varepsilon_{free}$ , is normalized to 1, see Figure 8c, then  $\varepsilon_R$  is defined as the restraint value,  $\gamma_R$ . Consider the system of the two blocks with full bound in the joint between block 1 and block 2, the force in each block is described as

$$F_1 = \gamma_R \cdot E_1 \cdot A_1 \quad (24)$$

and

$$F_2 = (1 - \gamma_R) \cdot E_2 \cdot A_2 \quad (25)$$

where

$A_2$	= area of block 2, m <sup>2</sup>
$E_2$	= elasticity modulus of block 2, Pa

The force in the blocks are equal,  $F_1 = F_2$ , yielding

$$\gamma_R = \frac{1}{1 + \frac{A_1 \cdot E_1}{A_2 \cdot E_2}} \quad (26)$$

Eq. 26 has been applied calculating restraint stresses since long, and can be found in for instance ACI Committee 207 (2002).

When we have situations where a rather small body of new concrete is cast with a structural joint connected to a much larger body, e.g. repair casting of new side beams to an existing concrete bridge, casting on well cleaned bedrock, wall cast at the edge of a base slab and the slab is significantly wide etc., Eq. 26 may be applicable as an engineering model calculating thermal stresses in the newly cast concrete,  $A_1$ . The main technical issue is how to establish the area of the block 2,  $A_2$ , as an “equivalent part” of the real adjacent structure. The restraint from the adjacent structure may be estimated in several ways like;

- *Tables*. Tables where restraint values are presented for some typical construction situations may be used to more or less accurately estimate the restraint at certain positions, see e.g. Nilsson (2003).
- *Artificial Neural Network (ANN)*. The restraint is estimated by the aid of a programmed spread sheet. The spread sheet performs an interpolation from the results of a parametric variation, for some typical construction situations, see e.g. CraX1 (2003) and Al-Gburi (2015).
- *Finite Element Method (FEM)*. The restraint may be estimated by normalized elastic calculation made by commercial available FE programs such as ABAQUS, DIANA, ATHENA, COMSOL Multiphysics, HACON, B4Cast and 4C-Temp&Stress. In Section 6.3 a demonstration of how to normalize the elastic calculations to yield restraint is given.

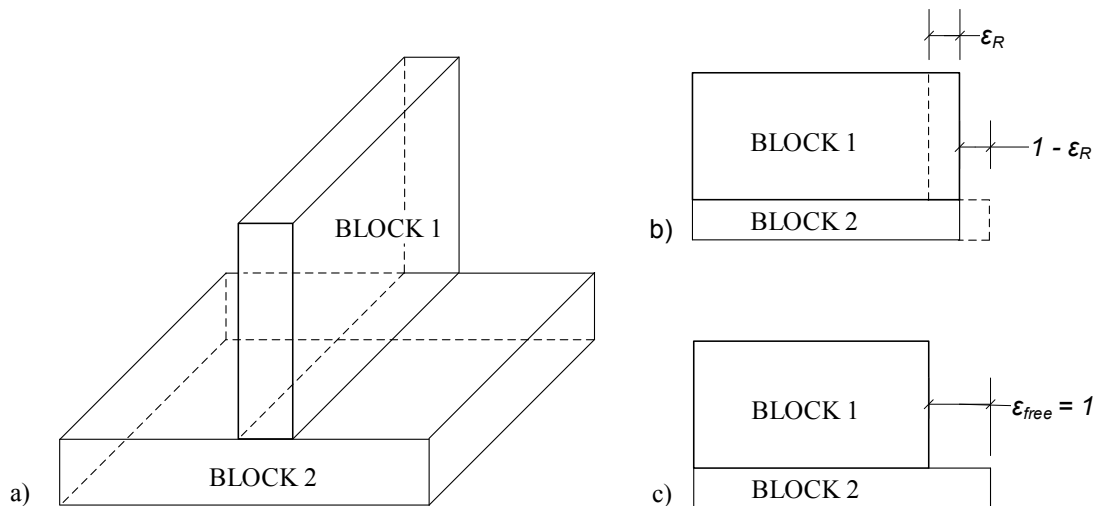
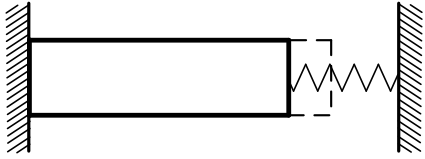
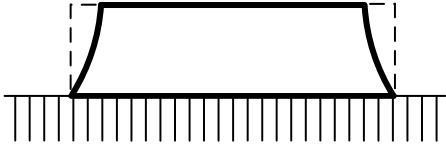
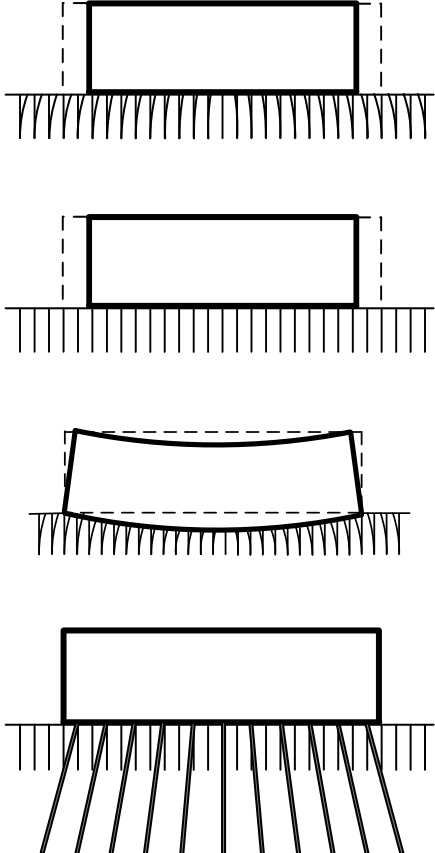


Figure 8. Illustration of a uni-axial restrained system containing two blocks, where block 1 is homogeneously contracting. The only factor contributing to the stress development is the differential deformation between the two blocks. a) = combined structure of two blocks, b) = full restraint along the joint between the two blocks, and c) = no restraint along the joint between the two blocks.

## 5.4. Typical restraint situations

In this section, common typical restraint situations are demonstrated, see Table 1 (slightly changed from Nilsson et al, 2015). The table declare the restraint situation and provides a sketch for each typical situation. In the subsequent sections, each typical situation is described and suggestions regarding estimation of the degree of restraint is given.

Table 1. Common typical restraint situations, from Nilsson et al (2015)

<p>1. Uni-axial restraint (Section 5.4.1)</p>	
<p>2. Non-resilient boundary (Section 5.4.2)</p>	
<p>3. Partly resilient boundary</p> <p>3.1. Translation (deformed foundation) (Section 5.4.3)</p> <p>3.2. Slide/Slip (in interface to foundation) (Section 5.4.4)</p> <p>3.3. Rotation (deformation in the foundation) (Section 5.4.5)</p> <p>3.4. Piles (Section 5.4.6)</p>	

### 5.4.1. Uni-axial restraint

The uni-axial restraint situation is defined with a restraint in only one direction, the restraint in all other directions are negligible. The situation can be visualized as a rod restraint, where the restraining material in one end may be resilient, see Figure 9 (slightly changed from Nilsson et al, 2015).

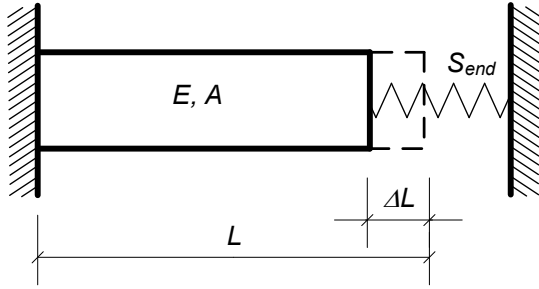


Figure 9. Illustration of a restrained rod from Nilsson et al (2015).

A similar derivation as for Eq. 26 can be performed to express the uni-axial restraint,  $\gamma_R$ , with a dependency of the end-stiffness,  $S_{end}$ , as showed for instance in Nilsson et al (2015)

$$\gamma_R = \frac{1}{1 + \frac{E \cdot A}{L} \cdot \frac{1}{S_{end}}} \quad (27)$$

where

$E = E_{c,eff}(t)$  = the effective modulus of elasticity in the young concrete, Pa

$A$  = the cross-section of the rod,  $m^2$

$L$  = length of the rod, m

$S_{end}$  = uniaxial end-stiffness of the possible resilient material, N/m

The described restraint situation could be applied to one dimensional restraint situations as well as for long sections of walls or slabs (roughly over 20 m), see e.g. Nilsson (2003).

### 5.4.2. Non-resilient boundary

A non-resilient boundary condition could be considered if the construction is cast on a totally stiff foundation, where the concrete closest to the boundary have no possibility to move, i.e.  $\delta_{slip} = 1$  and  $\gamma_R^0 = 1$ . This implies that the properties of the foundation become of no interest. In practice, non-resilient boundaries are rare, but for instance, at certain castings toward crack-free bedrock this restraint situation may appear.

The degree of restraint in the concrete body is solely dependent on the distance from the joint, yielding

$$\gamma_R = \delta_{res} \quad (28)$$

Figure 10 displays the relation between  $\delta_{res}$  and distance to the joint,  $y/H$ , for several  $L/H$  - ratios.

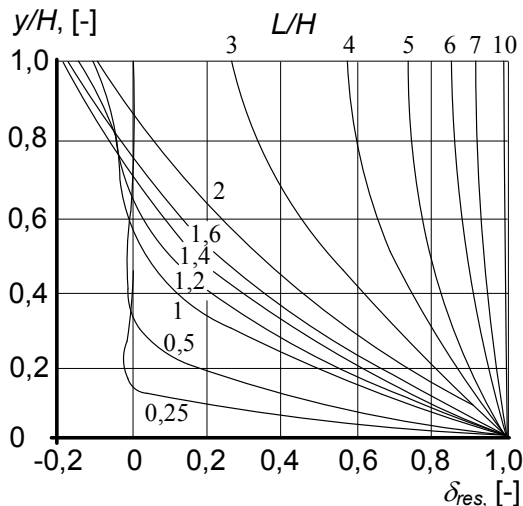


Figure 10. Relation between  $\delta_{res}$  and distance to the joint,  $y/H$ , for several  $L/H$ -ratios, Emborg (1989) and Nilsson (2003).

### 5.4.3. Partly resilient boundary

A partly resilient boundary with respect to translation implies a foundation of homogenous material which is resilient to some degree.

Depending on the type of foundation, different approaches to estimate the translation restraint is taken. The most common partly restraining foundations are gravel, rock or mature concrete. As for the cases of gravel (or similar friction yielding material) and rock the restraint can be estimated with the assumption of an elastic half space, e.g. Bernander (2001). However, structures cast upon gravel, or similar ground materials, can be cast up to 40 m long with negligible translational restraint. For the situation with a rock foundation, extensive examination of the rock is needed to obtain a valid modulus of elasticity. In many cases such examination is not practical, instead the translation restraint,  $\gamma_{RT}$ , is estimated to 60 – 80 %, depending on the degree of cracks and the roughness of the surface.

For situations where young concrete is cast upon mature concrete, three typical situations could be distinguished, see Figure 11. Here the joint between young and mature concrete is considered as a partly resilient boundary, but the boundary between the mature concrete and the foundation may also influence the translational restraint:

- The boundary between the mature concrete and the foundation is non-resilient.
- The boundary between the mature concrete and the foundation is partly resilient.
- The foundation gives no restraint.

At a 2D or 3D stress/strain analysis each member is modeled, where the translational restraint,  $\gamma_{RT}$ , from the foundation is proportional to the sizes of each member, modulus of elasticity and interface properties between the foundation and mature concrete.

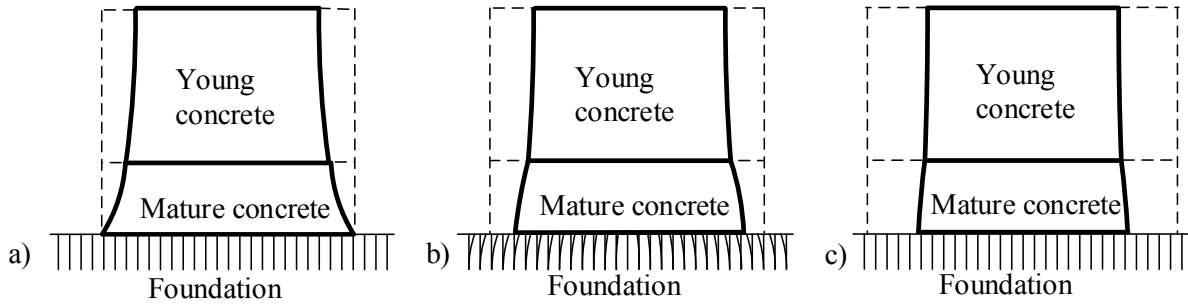


Figure 11. Young concrete casted upon mature concrete (partly resilient boundary) with a) a non-resilient foundation, b) partly resilient foundation and c) no restraint from foundation

#### 5.4.4. Partly resilient boundary – End slip

End slip in the joint between young and mature concrete,  $\delta_{slip}$ , may decrease the translation restraint. No theoretical model has been derived concerning  $\delta_{slip}$ , but diagrams based on empirical observations in Emborg et al (1997) and laboratory tests in Nilsson (2000) has been implemented in the computer model ConTeSt Pro (2008), see Figure 12.

#### 5.4.5. Partly resilient boundary - Rotation

A partly resilient boundary with respect to rotation can be considered for a slab or a beam on homogenous elastic material, where the analysed structure is at all times in contact with the foundation. The rotational restraint  $\gamma_{RR}$  in Figure 13 has been derived in Nilsson (2000) and presented as a function of the so-called elastic length,  $L_e$ , expressed by

$$L_e = \sqrt[4]{\frac{\kappa}{K_j} \cdot 2 \cdot E_{slab} \cdot I_{trans,z}} = \sqrt[4]{\frac{2}{W \cdot c} \cdot 2 \cdot E_{slab} \cdot I_{trans,z}} \quad (29)$$

and

$$c \approx 1.3 \cdot \frac{E_{found}}{H} \cdot \left( \frac{E_{found}}{E_{slab}} \right)^{1/3} \quad (30)$$

where

- $\kappa$  = shape factor, -
- $K_j$  = compression modulus, Pa
- $E_{slab}$  = modulus of elasticity for the young concrete at studied time, Pa
- $I_{trans,z}$  = transformed second moment of inertia of the cross section for bending around  $z$ -axis,  $m^4$
- $E_{found}$  = modulus of elasticity of the foundation, Pa
- $L$  = length of the slab/beam, see Figure 13, m
- $W$  = width of the slab/beam, see Figure 13, m
- $H$  = height of the slab/beam, see Figure 13, m
- $c$  = modulus of foundation,  $N/m^3$

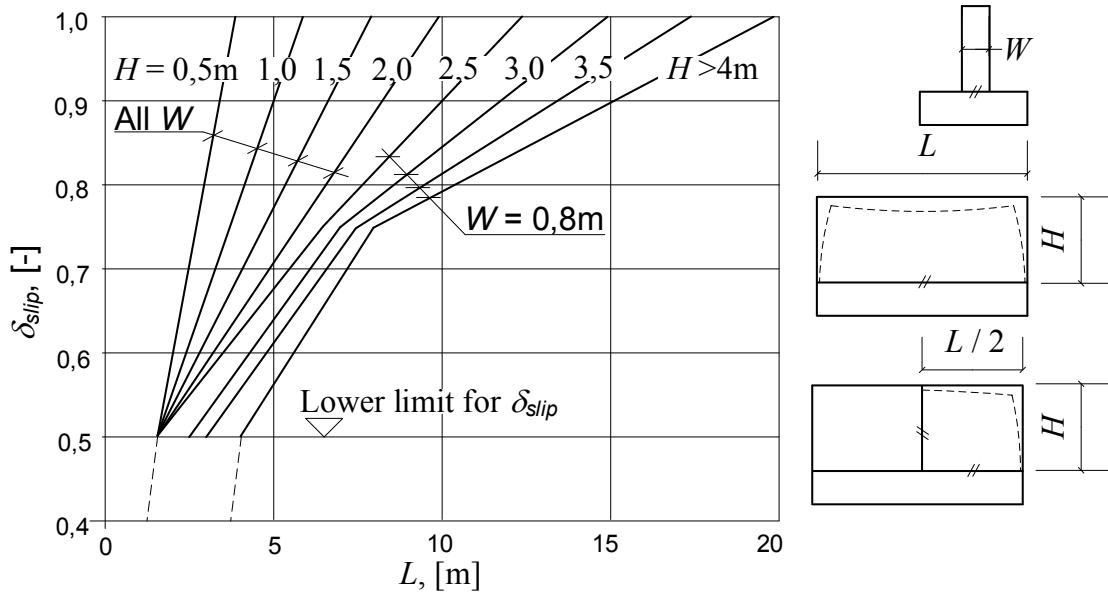


Figure 12.  $\delta_{slip}$  as a function of construction length, height and width of the newly cast construction member. (Figure from ConTeSt Pro (2008) and Nilsson (2000).)

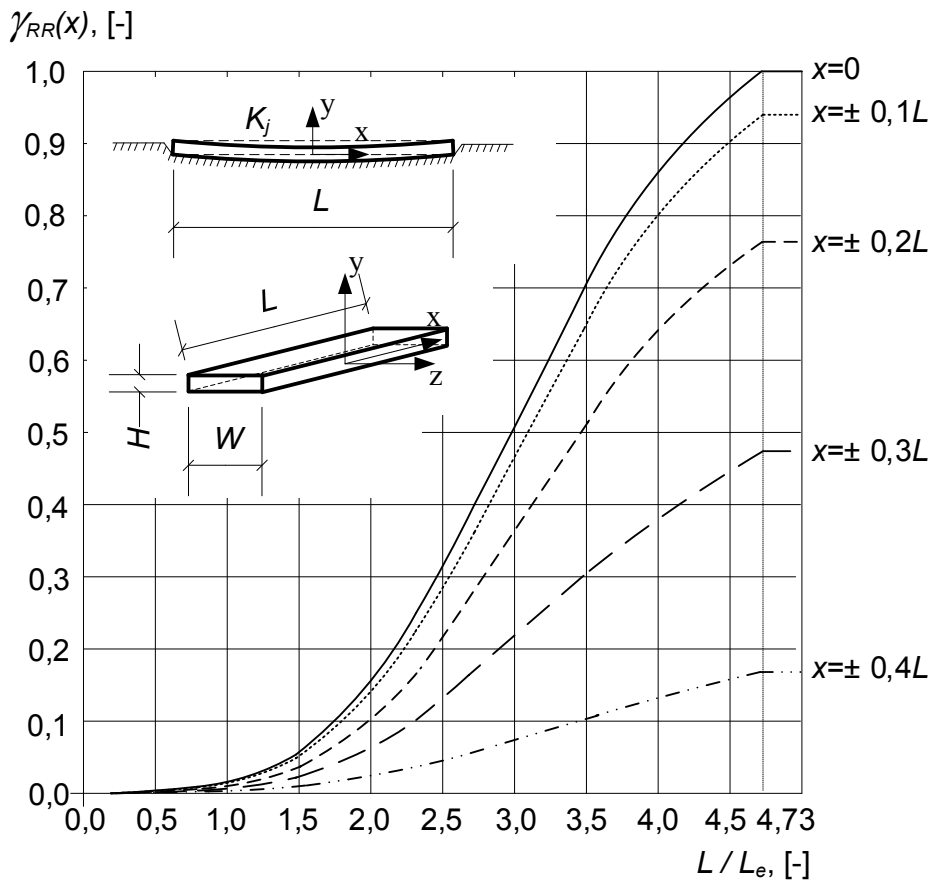


Figure 13. Beam on an elastic foundation. (Figure from Nilsson (2000), slightly modified.)

Table 2. Shape factor,  $\kappa$ , as a function of the width/length-ratio,  $W/L$ , see Löfling (1993).

$W/L$	0.2	0.4	0.6	0.8	1.0
$\kappa$	0.94	0.83	0.75	0.69	0.65

Table 3. Modulus of compression,  $K_j$ , for different types of foundation materials, see Bernander (1993) and Nilsson (2003).

Type of soil and compaction	$K_j$ , MPa
Clay, soft	0.5 - 2
Clay, semi-solid	1 - 3
Clay, sandy and silty	2 - 5
Sand, soft	3 - 10
Sand, medium dense to dense	10 - 60
Gravel, medium dense to dense	10 - 60

For a majority of cases, where the construction part is cast upon a partly resilient foundation, the rotational restraint is negligible. Only at “long” structures the restraint may be significant due to an increased  $L/L_e$ -ratio (Nilsson, 2000).

#### 5.4.6. Partly resilient boundary - Piles

For slabs and walls-on-slab founded on homogenous material such as clay or soil, may both the transitional ( $\gamma_{RT}$ ) and rotational ( $\gamma_{RR}$ ) restraint for the structure may, from an engineering point of view, be neglected if the length of the structure is not very long. This assumption follows the same reasoning as in section 5.4.5. Using piles may increase both the translational and rotational restraint, see Eqs. 30 and 31 (Nilsson et al, 2015).

$$\gamma_{RT} = \frac{1}{1 + \frac{E_{slab} \cdot A_{slab} \cdot L_p}{n_\alpha \cdot E_p \cdot A_p \cdot L \cdot \sin^2 \alpha}} \quad (30)$$

where

- $A_{slab}$  = cross section of the slab, m<sup>2</sup>
- $L$  = length of slab, m
- $n_\alpha$  = number of inclining piles, -
- $\alpha$  = inclination of piles, -
- $E_p$  = elastic modulus of the piles, Pa
- $A_p$  = cross section area of one pile, m<sup>2</sup>
- $L_p$  = length of the piles, m

For the rotational restraint, the original derivation in Nilsson (2000) was performed for a slab on elastic homogenous foundation, and for equally spread piles under the slab/beam, the contact area is adjusted with respect to the total area of the piles (Nilsson et al, 2015). This ends up in the following expressions

$$\gamma_{RR}(x=0) = 1 - \frac{2 \cdot \left( \cos \frac{L_{slab}}{2L_e} \cdot \sinh \frac{L_{slab}}{2L_e} + \sin \frac{L_{slab}}{2L_e} \cdot \cosh \frac{L_{slab}}{2L_e} \right)}{\sin \frac{L_{slab}}{L_e} + \sinh \frac{L_{slab}}{L_e}} \quad (31)$$

$$L_e = \sqrt[4]{\frac{4}{W \cdot c_p} \cdot E_{slab} \cdot I_{trans,z}} \quad (32)$$

$$c_p \approx 1.3 \cdot \frac{n \cdot A_p}{A_{slab}} \frac{E_p}{H} \cdot \left( \frac{n \cdot A_p}{A_{slab}} \cdot \frac{E_p}{E_{slab}} \right)^{1/3} \quad (33)$$

where

$c_p$  = modulus of foundation for the piles, N/m<sup>3</sup>  
 $n$  = total number of piles, -

An overview of the situation for a slab with piles is found in Figure 14.

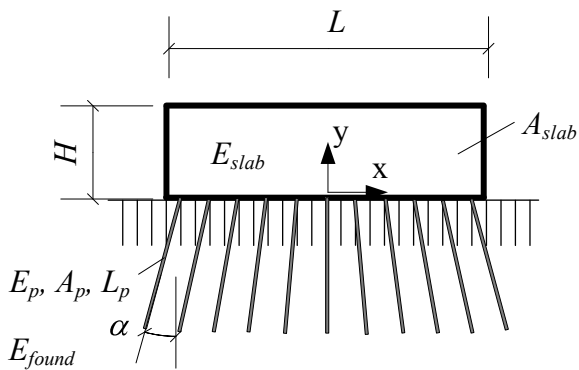


Figure 14. Concrete with piles cast upon a foundation consisting of a homogenous material (e.g. clay or soil). Figure from Nilsson et al (2015), slightly modified.

## 6. EQUIVALENT RESTRAINT METHOD, ERM

### 6.1. Background and outline of the ERM

As mentioned earlier, out-of-plane calculation methods (when applicable) give the opportunity to perform a set of at estimation of crack risk estimations, needed when a lot of alternatives have to be analyzed to find an acceptable solution. The idea of ERM is to simulate a more complicated situation with an equivalent out-of-plane construction. The main condition is that the ERM model have to be equivalent with respect to restraint within the young concrete body. Thus, consequences of measures like heating, cooling, and insulation etc. can now be analyzed by the ERM model.

The development of the ERM is given in Paper 1, and the method consists of the following three steps;

- a) Elastic 3D FEM calculation is used to yield the restraint situation of the cross section of the young concrete body.
- b) The stress averaged over the thickness of the young concrete is determined by the LRM model using the restraint from a). The stress is determined for a number of positions to be able to establish a tensile stress distribution including the maximum stress ratio. Either the stress ratio or the strain ratio is calculated in this step.
- c) To establish the ERM a representative structure, including the young concrete body and a part of the adjoining structure, is chosen. The representative model can apply CLM and CPM models, and the available restraint parameters (mainly  $\gamma_{RT}$  and  $\gamma_{RR,i}$ , but also  $\delta_{slip}$  and  $\delta_{res}$  may be used, see definitions in Chapter 5) are “calibrated” until acceptable agreement is achieved for the stress/strain ratios from LRM within the tensile part of the young concrete body.

Now an ERM model able to analyse the risk of through cracks is established, to which arbitrary temperature altering measures (such as cooling pipes, heating cables etc.) can be applied.

Within this work, the Abaqus software has been used to estimate the restraint in step a). LRM in step b) is repeated calculations of the stress in one point, i.e. for different prechosen positions from the construction joint, and any existing out-of-plane model can be applied point-by-point using repeated calculations. Here, the ConTeSt software has been used to perform stress/strain development analysis in both step b) and c), as it is the same material models applying LRM and calibrating ERM.

## 6.2. Volume deformation in the FEM calculations

The free movements in the young concrete, thermal dilation and basic shrinkage, is the driving forces for possible causes of early age thermal cracking. The restraint in the young concrete body is the counter-action to these deformations from the adjoining structures. When calculating the restraint, the shape of the actual free movements during the contraction phase have to be simulated, and for a young concrete body of uniform thickness the free deformations may be approximated by a constant volume decrease, although thermal cooling to the air at the top and to the adjacent structure at the bottom usually exist. Also, the basic shrinkage may be approximated to be constant and homogenous within the young concrete body. This approach of a homogenous block to simulate contraction for uniform thicknesses has been established since long, see for instance Olofsson (1999).

If we have any other situation for the young concrete body, like non-uniform insulation and/or variable thickness, the volume decrease of the concrete body can from a theoretical point of view not be simulated by a constant value valid all over the body. However, there is no restrictions concerning the shapes of the adjacent structures in the FEM calculations, as they are not supposed to have any non-elastic deformation.

## 6.3. 3D FEM restraint calculation

Most commercial available 3D FEM analysis tools can be used to perform elastic calculations rather easily. Some computer programs can apply non-elastic strains, but it is more common to apply a temperature difference, and then the non-elastic strain is calculated as thermal dilation, see Eq. 34.

$$\varepsilon^0 = \alpha \cdot \Delta T \quad (34)$$

where

$$\begin{aligned} \varepsilon^0 &= \text{free deformation in the young concrete body, -} \\ \alpha_T &= \text{thermal dilation coefficient, } ^\circ\text{C}^{-1} \\ \Delta T &= \text{temperature difference in the young concrete body, } ^\circ\text{C} \end{aligned}$$

The implementation of the temperature change varies from software to software and is left to the interested reader to examine.

When applying the non-elastic deformation  $\varepsilon^0$  on the young concrete body, the restraint,  $\gamma_R$ , is described by (compare Eq. 15)

$$\gamma_R = \frac{\sigma_{ii}}{(-\varepsilon^0 \cdot E_c)} \quad (35)$$

where

$$E_c = \text{elastic modulus in the young concrete, Pa}$$

When the adjacent structure consists of mature concrete using the same concrete mix as in the newly cast body, it can be applied in the FEM model to be  $1/0.93 \approx 1.075$  times the modulus of the young concrete, where the value 0.93 was found to be a representative ratio between the elastic modulus in the young concrete during the contraction phase and the modulus of the mature concrete (Larson, 2003). When the adjacent structure consists of other material, the actual modulus in question should be used.

Theoretically it is irrelevant what non-elastic deformation to choose, but it is practical preferable to use the following condition

$$\left| -\varepsilon^0 \cdot E_c \right| \equiv 1 \quad (36)$$

which gives

$$\gamma_R = \sigma_{ui} \quad (37)$$

Using basic SI-units for all properties in the FEM calculation, the resulting stresses (formally in Pa) directly corresponds to the desired restraint values, and usually a built-in postprocessor can be directly employed to visualize, gather and evaluate the decisive situation concerning the restraint values in the young concrete body.

The first step when all restraint values exist is to search for the position of the highest restraint in parallel with the construction joint between the young concrete body and the adjoining structure. From that point, we follow the whole cross-section in the young concrete perpendicular to the construction joint. Two typical situations may happen

- a) Maximum restraint at the middle in the thickness direction
- b) Maximum restraint at one of the surfaces in the thickness direction

*Typical case a)* occurs when the geometry is symmetric around a line perpendicular to the joint for the analyzed cross-section or when the rotational restraint around this line for other reasons are very high. For case a), the restraint from the FEM calculation is somewhat higher at the middle part in the thickness direction than at the surfaces. A representative restraint causing through cracking is employed by the average restraint over the thickness. This technique is equated with the technique using the beam theory for stress analysis, see for instance the use of the computer program TEMPSTRE-N (Emborg, 1990) or the use of CLM in ConTeSt Pro (ConTeSt, 2008), as the restraint values in these models are only depending on the distance from the structural joint between the young concrete and the adjacent structure.

*Typical case b)* occurs when the total structure is more or less asymmetric around a line perpendicular to the joint for the analyzed cross-section, i.e. we have a situation influenced by some rotation around this line. Case b) is easily identified where the decisive restraint value is highest at one of the surfaces, and consequently, the representative restraint is chosen to be the highest surface value.

The end result from the 3D analyses is a restraint curve within the young concrete body, from the joint between the new concrete and the adjacent structure through the whole young concrete body. One example of an estimated restraint curve is presented in Figure 15, which illustrates the 2<sup>nd</sup> casting of a wall-on-slab, which is the fourth casting in the following sequence: 1) 1<sup>st</sup> slab, 2) 1<sup>st</sup> wall, 3) 2<sup>nd</sup> slab, and 4) 2<sup>nd</sup> wall. Two structural casting joints exist for this fourth work step, a vertical joint at the left end of the 2<sup>nd</sup> wall and a horizontal joint at the bottom of the new concrete. This means that two restraint curves have to be established

- 1) Along a vertical line perpendicular to the bottom joint, where it is a risk of formation of vertical cracks, see the decisive line marked with red color in Figure 15. The resulting restraints curve is valid for calculation of stresses in the horizontal direction.
- 2) Along a horizontal line perpendicular to the joint at the left side, where it is a risk of formation of horizontal cracks. The resulting restraints curve is valid for calculation of stresses in the vertical direction. This situation is not illustrated in Figure 15.

#### 6.4. Calculations of stresses without measures on site

From the restraint curve the horizontal stress ratios or strain ratios are calculated using LRM for the case without any measures, and here CLM is applied pointwise using ConTeSt Pro. The resulting strain ratios are illustrated with cross marks in Figure 16. The restraint value is highest at the construction joint, but the maximum stress or strain ratio has a maximum about 1m above the joint. The reason is that the existing slab cools down the lower of the newly cast wall, and the resulting stress or strain ratios are always a result of the free deformation (temperature and shrinkage) multiplied with the restraint, see Eqs. 4 and 5.

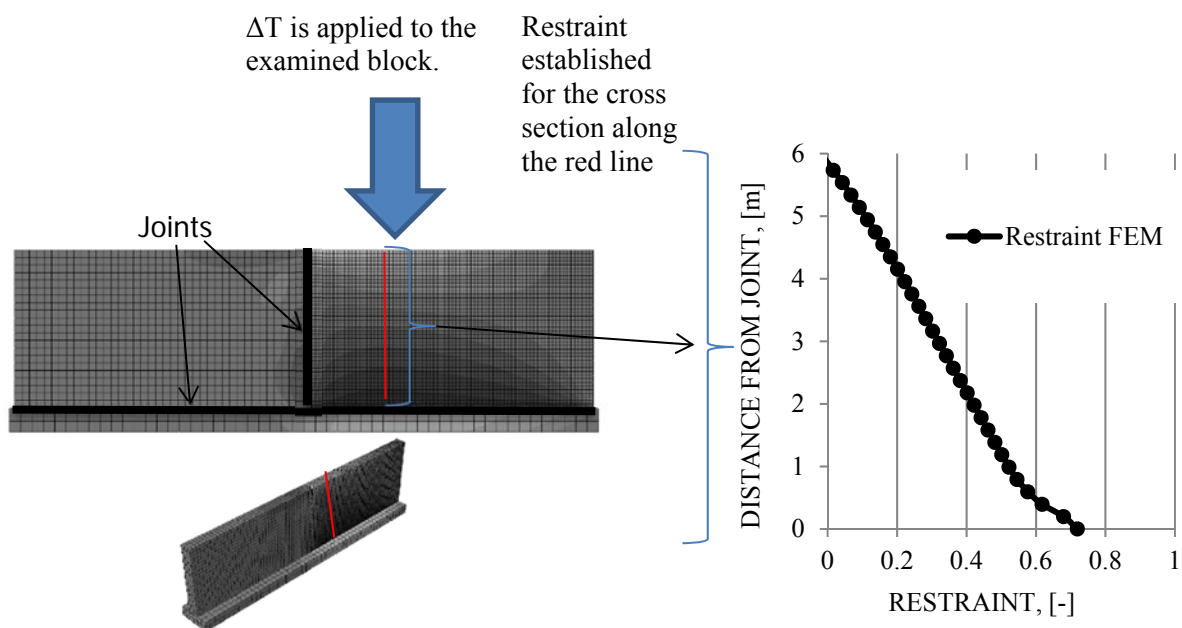


Figure 15. Restraint profile established from a 3D FEM calculation valid for calculations of stresses in the horizontal direction when casting the 2<sup>nd</sup> part of the wall

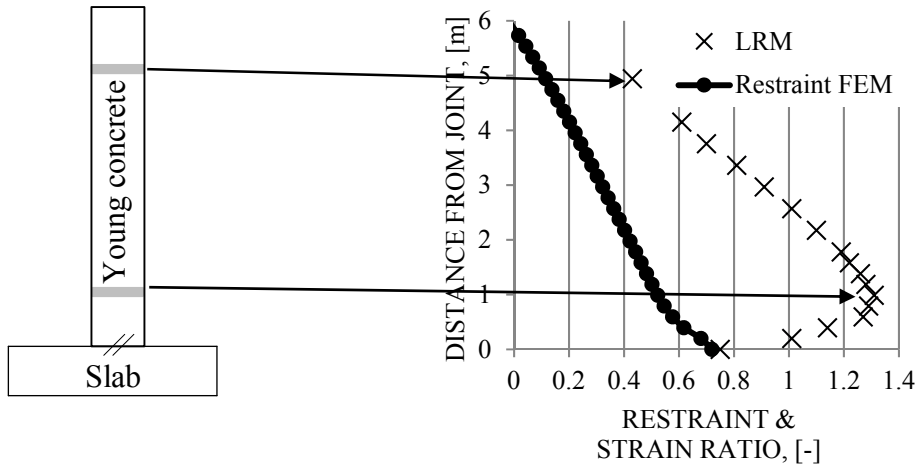


Figure 16. Calculating of horizontal stresses in a wall using LRM

## 6.5. Calibration of the ERM model

To convert the real structure to an ERM model starts with the choice of the spatial dimensions for a cross section at the decisive position for one type of cracking, here that means a continuation based on Figure 16. The most common way of creating an equivalent model is to maintain the real shape of the young concrete section and to create a “representative” part of the all adjoining structure creating a structure that is easy to calculate with existing “out of plane” computer programs. The situation in Figure 17 is already a structure that can be analyzed as the typical case wall-on-slab, and, and we might in this case maintain the shape and size of the slab as it is.

An approximate guideline is that for larger adjacent structures the size of the adjacent structure might be chosen to be in the size of order balancing the transitional restraint in the point for the maximum stress or strain determined by LRM, expressed, see Eq. 26, by

$$A_{adj} \approx \frac{\gamma_R(\sigma_{\max})}{1 - \gamma_R(\sigma_{\max})} \cdot \frac{E_c}{E_{adj}} \cdot A_c \quad (38)$$

where

- $A_{adj}$  = area of the adjacent structure aimed for the ERM model, m<sup>2</sup>
- $\gamma_R(\sigma_{\max})$  = restraint from the FEM calculation at the position of the maximum stress/strain in the young concrete determined by LRM, see Figure 16, -
- $A_c$  = area of the young concrete, m<sup>2</sup>
- $E_{adj}$  = elastic modulus in the adjacent structure, Pa

In paper 1 a simplified application of Eq. 38 is used for the 2<sup>nd</sup> and following casting sequences of a pillar, based on  $\gamma_R(\sigma_{\max}) \approx 0.5$  and  $E_{adj} \approx E_c$ , which ends up in  $A_{adj} \approx A_c$  for the typical structure wall-on-wall.

The calibration of the ERM parameters is now performed for the ERM structure which involves adjustments using one or several possible restraint parameters ( $\gamma_{RT}$ ,  $\gamma_{RR,i}$  and  $\delta_{res}$  and  $\delta_{slip}$ ) for the ERM structure until acceptable agreement is achieved within the decisive part,

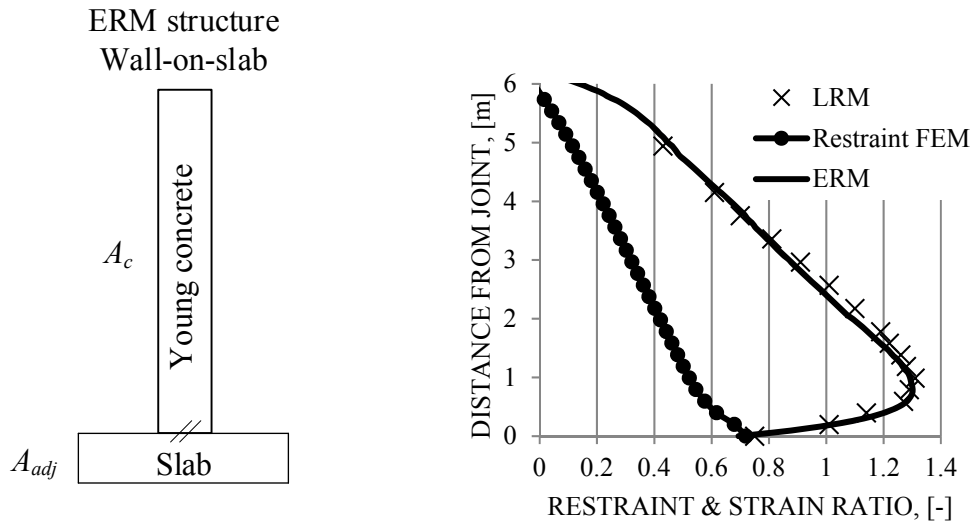


Figure 17. Establishing an ERM model by acceptable fitting with respect to calculated strain ratios.

i.e. the main part of the tensile stress/strain ratios from LRM in the young concrete. Based on the LRM values shown in Figure 16, the ERM result is presented by the solid line in Figure 17. This calibration may be done with CLM using ConTeSt Pro, as such very fast calculations are to prefer, if a number of combinations of adjustments have to be checked. Only one rotation is adapted in the ERM model ( $\gamma_{RR,i}$  around a horizontal axis in Figure 17), and the rotation around the perpendicular axis is zero ( $\gamma_{RR,j} \equiv 1$ ), where index  $j$  here represents rotation around a vertical axis. An easy and safe way to ensure no rotation around axis  $j$  is to construct a symmetric structure in the ERM model, which “automatically” fulfill the required rotational condition.

The possibility to use several restraint adjustment parameters may be needed at calibration of the ERM model, as the shape of the LRM results can be influenced by a rather complex 3D system of adjacent structures.

## 6.6. Application of the ERM model

### 6.6.1. Interpretation of the resulting stress/strain ratios using ERM

The application of ERM can either use CLM or CPM models, which both are fast and easy to use. If we use CPM we usually have to take care of variable stresses over the thickness of the young concrete at the position and time of maximum stress/strain ratio, see Figure 18.

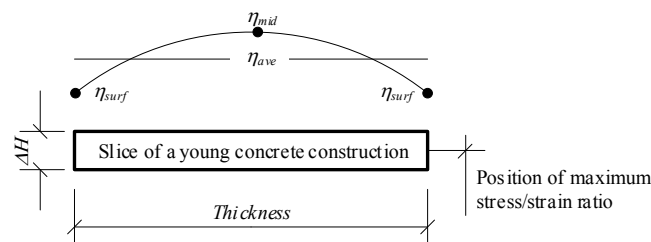


Figure 18. Strain ratio variation over the thickness of the young concrete at the position of maximum strain ratio for estimation of risks of through cracking.

If we have the situation illustrated in Figure 18, i.e. the stress/strain ratios are lower at the surfaces than in the middle of the young concrete body, we have to calculate the average value to compare with the allowable stress/strain ratios in the codes. The reason is that the lower stresses at the surfaces are stabilizing the inner part with higher stresses, which means that only micro cracks can occur inside the concrete even if the maximum stress is approaching the tensile strength. When also the surface stresses are approaching the tensile strength, the situation will be unstable and a macro crack will be formed, i.e. a through crack is created. These stability conditions might be analysed by fracture mechanics, but such analyses are complicated and are not performed here. By using the technique of averaging measured temperatures and calculations applying Eq. 5, Larson (2000), has shown that the average strain ratio reaching unity ( $\eta_{ave} \rightarrow 1$ ) can be employed as significant fracture criteria. The restraint values in Larson (2000) were created using elastic 3D FEM calculations.

If we have a resulting situation applying ERM with the highest strain ratio at the surface, the surface value should be used estimating the crack risk ( $\eta_{surf}$  decisive). The reason might be that a non-symmetric temperature field is created for some reason.

Finally, if we use CLM applying the ERM model, the values from such a calculation always result in average stress/strain ratios. Therefore, it is preferable to use CPM when applying ERM.

### 6.6.2. Simulating measures on site using ERM and LRM

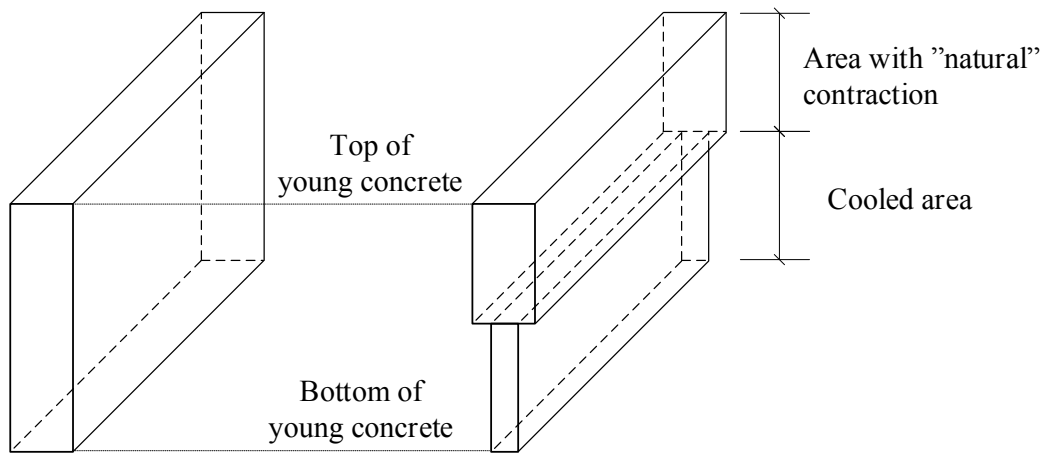
Since ERM is a systematic created structural system capable of reflecting the real situation in the young concrete, not only the “natural” situation without measures on site can be analysed, but also the most common measures

- Cooling of the young concrete by water.
- Heating of the adjacent structure.

These measures can easily be analysed applying ERM in the same way as for direct typical cases as 1<sup>st</sup> casting of a wall-on-slab with. But, using LRM we have the following situation

- Cooling of the young concrete by water may be analysed in some cases with LRM.
- Heating cannot be applied with LRM.

One consequence using cooling and LRM is that the cooling of the young concrete affects the contraction in the young concrete, and the cooling of the whole concrete body is no longer homogenous, see Figure 19. When LRM are used with temperatures from cooling, the result is more or less wrong, as the “natural” restraint is obtained from the 3D FEM calculation is no longer valid from theoretical point of view. Despite this fact, sometimes cooling and LRM may be approximately correct, see paper 1, but here no systematic investigation concerning this has been performed.



a) "natural" contraction

b) less swelling and contraction in the cooled area

Figure 19. Schematic sketch showing differences in contraction of young concrete due to a) "natural" reasons and b) influence of cooling.

### 6.6.3. Non-homogenous contraction in the young concrete

When we have a situation in the young concrete with variable thickness a homogenous contraction is not valid estimating restraints by elastic 3D FEM calculations, as the temperature in the young concrete is dependent on the thickness. This situation is interesting for a number of structures, and it might be possible to apply variable contraction in the young concrete body in the elastic 3D FEM calculations, but such investigations are not done within this work.

## 6.7. Results when comparing ERM models to empirical measurements

In Paper 2 and 3 it is examined how the ERM corresponds to field measurements.

It is thus demonstrated how the ERM corresponds to empirical experiences. As the main focus within the work is on the restraint modelling it was chosen to study a wall and roof segments in a tunnel project. Crack documentations and temperature measurements from castings were compared with results from ERM analyses. It was observed a good correlation between the thermal crack prediction by the ERM and the observations at field.

Paper 3 demonstrates how the ERM corresponds to field experiences. The method in Paper 3 is improved compared to Paper 2. The improvements were; 1) Thermal dilation was measured. 2) The concrete was tested and evaluated. 3) The temperature was measured in the direct vicinity of the construction with the placement of the temperature gauges well documented. The result of the work is that the ERM model described the observed field temperatures and strains with a very good precision, which implies that the restraint is well estimated for this typical case.

In paper 5, it is shown that all analyzed structures where the post-calculated tensile stress exceeds 70% of the tensile strength is cracked within the first weeks.

## 7. EVALUATION OF MATERIAL PROPERTIES FOR YOUNG CONCRETE

### 7.1. Introduction

The risk of early thermal cracking in concrete is a complex subject, and analyses of crack risks have been performed for a long time, especially when constructing massive concrete structures, like dams, and structures submerged in water. For example, one very well documented project with complex measures to counteract early thermal cracking is the construction of the Hoover dam in US during the 1930's (see Arizona Leisure: available at <http://www.arizona-leisure.com/hover-dam-building.html>). The technique of taking measures against thermal cracking has been applied and evolved since this pioneering project. Important historical and recent research in the area has thus been performed at various universities, institutes and companies.

Nowadays, with the aid of computers and customized software, stress and strain analysis at early ages can be calculated in several ways thus making it possible to analyse the risk of cracking within a construction. Hence, thermal and mechanical properties for the young and aging concrete have to be known, and the design of laboratory tests achieving the needed properties depend on how the concrete behaviour is modelled in the software.

For the models developed at Lulea University of Technology, the tests needed can be divided into the following property areas: *strength development*, *heat of hydration*, *basic shrinkage*, *thermal dilation*, *basic creep* and *stress at full restraint*. The evaluation of these tests provides a parameter set of thermal and mechanical properties necessary to perform crack risk calculations for the young concrete. The quality of the evaluation depends on the accuracy of the measurements performed and the thoroughness at parameter determination. Therefore, it is of great importance to investigate the sensitivity of the evaluation on the final crack risk estimation for each test. From above, the following questions can be defined: what influence does each parameter have on the final crack risk estimation and which one has the major influence?

## 7.2. Method

The method comprises a) description of the tests performed to specimens of a concrete mix, b) examination of the evaluation process of the numerical data from the tests and c) analyses of the stress calculations performed with the parameters evaluated.

The overall philosophy when testing young concrete according to the areas above is that it shall cover what is needed to make estimations of 1) strength growth at variable temperatures, 2) temperature development from heat of hydration, 3) free deformations at variable temperature, taking basic shrinkage into account, 4) growth of elastic modulus and the creep behaviour and 5) stresses at restrained conditions.

The first two tests to be performed and evaluated are the *strength development* and the *heat of hydration* tests. From the evaluation of these tests a temperature reference curve (for a 0.7 m wall) is established. This curve is used at the tests of the *basic shrinkage* and *thermal dilation (free deformation)*. Beside the temperature reference curve, the expression of equivalent time of maturity is established which is also needed in the evaluation of the *basic creep* tests (i. e. creep at moisture sealed conditions). The *thermal dilation tests* are executed in two ways a) by letting a moist sealed concrete specimen freely expand and contract due to hydration, performed simultaneously with the basic shrinkage and b) *stress at full restraint*, consisting of specimen undergoing thermal development at full restraint, yielding the stress development.

### 7.2.1. Strength growth

The main purpose of this test procedure is to establish the reference strength growth, see Eq. 39 (e.g. Fjellström, 2013), and the temperature rate factor, see Eq. 41 (e.g. Jonasson, 1994), usually denoted “maturity function” in international literature. The reference strength curve is defined for the following conditions in Eq. 40:  $\beta_T = 1$  ( $T = 20^\circ\text{C}$  in Eq. 41),  $\beta_A = 1$  (no additional adjustments due to admixtures) and  $\Delta t_e^0 = 0$  (the equivalent time is zero at time of casting). The latter two adjustments are normally set to the reference conditions for the first time a recipe is tested, and if we later test the same recipe and only change the type and/or the amount of admixtures, the effects on hydration rate, retardation and/or acceleration, might be modelled only adjusting  $\beta_A \neq 1$  and/or  $\Delta t_e^0 \neq 0$ . The reference strength growth is defined for three stages, see Fjellström (2013), by Eq. 39. The three stages are

Stage 1: fresh concrete ( $0 \leq t_e < t_S$ )

Stage 2: between initial and final setting ( $t_S \leq t_e < t_A$ )

Stage 3: hardening concrete ( $t_e \geq t_A$ )

$$f_{cc}^{ref} = \begin{cases} 0 & \text{for } 0 \leq t_e < t_S \\ \left( \frac{t_e - t_S}{t_A - t_S} \right)^{n_A} \cdot f_A & \text{for } t_S \leq t_e < t_A \\ \exp \left( s \cdot \left( 1 - \left( \frac{672 - t^*}{t_e - t^*} \right)^{n_{cc,28}} \right) \right) \cdot f_{cc,28} & \text{for } t_e \geq t_A \end{cases} \quad (39)$$

The expression for stage 3 in Eq. 39 is based on a formula in EN 1992-1-1:2004 (Euro Code 2), and modified to fulfill the condition  $f_{cc}^{ref}(t_A) = f_A$ , and  $t^*$  is calculated by

$$t^* = \frac{672 - \delta_c \cdot t_A}{1 - \delta_c} \quad (40)$$

with

$$\delta_c = \left( 1 - \frac{1}{s} \cdot \ln \frac{f_A}{f_{cc,28}} \right)^{1/n_{cc,28}}$$

where

- $t^*$  = is calculated by Eq. 40, but has no physical meaning, h
- $t_e$  = equivalent time calculated by Eq. 41, h
- $t_S$  = equivalent time at initial setting, where the concrete starts to transform from a “liquid” to a “solid” state, h
- $t_A$  = equivalent time at final setting, where the concrete surface no longer can be troweled, modelled by the time when the strength reaches  $f_A$ , h
- $f_A$  = concrete strength at final setting, usually chosen to be the strength level 0.5 MPa, Pa
- $s$  = parameter influencing the curve shape in time of the hardening concrete, -
- $n_{cc,28}$  = parameter influencing the curve shape in time of the hardening concrete, -
- $f_{cc,28}$  = 28 days strength of the concrete, Pa

Equivalent time of maturity,  $t_e$ , is defined in Jonasson (1994) by the expression

$$t_e = \beta_\Delta \cdot \int_0^t \beta_T \cdot dt + \Delta t_e^0 \quad (41)$$

where

- $\beta_\Delta$  = possible adjustment parameter due to admixture changes, normally  $\beta_\Delta = 1$ , -
- $\Delta t_e^0$  = possible adjustment parameter due to admixture changes, normally  $\Delta t_e^0 = 0$ , h
- $\beta_T$  = temperature dependent maturity function expressed by Eq. 42 (see, Jonasson, 1984), -

$$\beta_T = \exp\left(\Theta_{ref} \cdot \left(\frac{30}{T+10}\right)^{\kappa_3} \cdot \left(\frac{1}{293} - \frac{1}{T+273}\right)\right) \quad (42)$$

where

- $T$  = concrete temperature, °C  
 $\Theta_{ref}$  = reference maturity parameter, formally activation energy divided by general universal gas constant, determined from strength growth tested at variable temperatures, K  
 $\kappa_3$  = parameter reflecting the variation of the activation energy by temperature, determined from strength growth tested at variable temperatures, -

### 7.2.2. Heat of hydration

The release of heat at hydration of cement may be determined from semi adiabatic calorimetric measurements, a technique established already in the 1950's, see e.g. Rastrup (1954). Example of a semi-adiabatic laboratory set-up used at Luleå University of Technology is shown in Figure 20a.

The released heat energy by cement weight at a certain time,  $q_{cem}(t)$ , can be evaluated from measured temperatures in a semi-adiabatic equipment (Fjellström, 2013) described by

$$q_{cem}(t) = \frac{\rho_c \cdot c_c}{C} \cdot \left( \eta \cdot (T_c(t) - T_{air}) + a \cdot \int_0^t (T_c(t) - T_{air}) \cdot dt \right) \quad (43)$$

where

- $q_{cem}$  = heat energy by cement weight, J/kg  
 $\rho_c$  = concrete density, kg/m<sup>3</sup>  
 $c_c$  = heat capacity by weight of concrete, J/kg °C  
 $C$  = cement content, kg/m<sup>3</sup>  
 $\eta$  = correction factor with respect to heat stored in the test set-up, values for  $\eta$ , see Fjellström (2013), -  
 $T_c(t)$  = measured temperature in the concrete specimen, °C  
 $T_{air}$  = ambient temperature, °C  
 $a$  = cooling factor, 1/s

In heat calculations, the generated heat per concrete volume,  $Q_h(t)$ , is of interest. An outline of the equations describing the heat of hydration within the software is given below, see Jonasson (1984). The generated heat per volume and time unit is

$$Q_h(t) = \frac{dq_{cem}(t)}{dt} \cdot C \quad (44)$$

where

$Q_h$  = generated heat per concrete volume, W/m<sup>3</sup>

The evaluated heat energy development using Eq. 43 can be approximated for computer calculations with the following formula, see Jonasson (1984),

$$q_{cem}(t) = \exp\left[-\left(\ln\left(1 + \frac{t_e}{t_1}\right)\right)^{-\kappa_1}\right] \cdot q_u \quad (45)$$

where

$q_u$  = total heat energy by cement weight, formally after infinite time, J/kg

$\kappa_1$  = free model parameter to get the acceptable fit with the test data, -

$t_1$  = free model parameter to get the acceptable fit with the test data, s

### 7.2.3. Basic shrinkage and free thermal dilation

From tests of free deformations for hydrating concrete, the deformation has to be split into thermal dilation and basic shrinkage, i.e. shrinkage at moisture sealed conditions, formally expressed by

$$\varepsilon_{free} = \varepsilon_T + \varepsilon_{sh}^0 \quad (46)$$

where

$\varepsilon_{free}$  = measured combined free deformation, -

$\varepsilon_T$  = thermal dilation, -

$\varepsilon_{sh}^0$  = basic shrinkage, -

Two type of free deformation tests are performed. One specimen is stored at about 20°C, and one specimen is placed in temperate water. The regulation of the temperate water simulates a temperature development in a real structure.

The thermal dilation is expresses by

$$\varepsilon_T = \alpha_T \cdot \Delta T_c(t) \quad (47)$$

where

$\alpha_T$  = thermal dilation coefficient, to be determined in the evaluation procedure, °C<sup>-1</sup>

$\Delta T_c(t)$  = measured temperature change in the concrete, °C

The basic shrinkage is, according to Hedlund (2000), expressed by

$$\varepsilon_{sh}^0 = \beta_{s0}(t_e) \cdot \varepsilon_{su} = \exp\left[-\left(\frac{t_{sh}}{t_e - t_S}\right)^{\eta_{sh}}\right] \cdot \varepsilon_{su} \quad (48)$$

$\varepsilon_{su}$  = reference ultimate shrinkage, to be determined in the evaluation procedure, -

$t_S$  = time of initial setting, end of stage 1 in Eq. 39, s

- $t_{sh}$  = time parameter affecting the shrinkage development, to be determined in the evaluation procedure, s
- $\eta_{sh}$  = parameter affecting the shrinkage development, to be determined in the evaluation procedure, s

#### 7.2.4. Basic creep tests

The basic creep evaluation is based on the theory described in Bažant and Wu (1974), and in Jonasson (1977) a subroutine is described which purpose is to transform measured creep data into relaxation values. The basic creep function for aging concrete used at LTU today is described in Larson (2003) by the means of the so called linear logarithmic model for concrete creep. For test set-up, see Figure 20 b.

The total compliance is the sum of one elastic part and one creep part (Linear Logarithmic Model), see Larson (2003), yielding

$$J(\Delta t_{load}, t_0) = \frac{1}{E(t_0)} + \begin{cases} a_1(t_0) \cdot \log\left(\frac{\Delta t_{load}}{\Delta t_0}\right) & \text{for } \Delta t_0 \leq \Delta t_{load} < \Delta t_1 \\ a_1(t_0) \cdot \log\left(\frac{\Delta t_1}{\Delta t_0}\right) + a_2(t_0) \cdot \log\left(\frac{\Delta t_{load}}{\Delta t_1}\right) & \text{for } \Delta t_{load} \geq \Delta t_1 \end{cases} \quad (49)$$

where

- $t_0$  = time of loading, d
- $t$  = time after mixing, d
- $E(t_0)$  = elastic modulus for load duration =  $\Delta t_0$ , Pa
- $\Delta t_0$  = “elastic” load duration, d
- $\Delta t_1$  = breakpoint in creep behaviour, d
- $\Delta t_{load}$  = time span after loading,  $t-t_0$ , d
- $a_1(t_0)$  = 1<sup>st</sup> “logarithmic” creep rate,  $\text{Pa}^{-12} / \log(\Delta t_{load})$
- $a_2(t_0)$  = 2<sup>nd</sup> “logarithmic” creep rate,  $\text{Pa}^{-12} / \log(\Delta t_{load})$

When a solution is found for the system of Linear Logarithmic Model, it is used as input to the program RELAX, see Jonasson and Westman (1999). RELAX transforms the creep values to relaxation values which are parameters to a series of parallel Maxwell elements describing the viscoelastic behaviour of the concrete. This is done by solving the function for relaxation modulus  $R(t, t_0)$ , from a compliance function  $J(t, t_0)$  see Bažant and Wu (1974).

### 7.2.5. Stresses in concrete at full restraint

With a temperature load corresponding to the mean temperature of a 700 mm thick wall, the stress at full restraint is measured. The free strain is hindered by the apparatus and an applied force is used to regulate the external strain to zero, see e.g. Westman (1999). The key feature of the test is to make the concrete specimen to undergo tensile strength failure. For test set-up, see Figure 20 c.

The tensile strength of the concrete,  $f_{ct}$ , is related to the compressive strength as follows

$$f_{ct} = \left( \frac{f_{cc}}{f_{cc}^{ref}} \right)^{\beta_1} \cdot f_{ct}^{ref} \quad (50)$$

where

$f_{cc}$  = compression strength, Pa-

$\beta_1$  = connection parameter tensile-compression strength according to Eurocode 1992-1-1, -

$f_{cc}^{ref}$  = reference compressive strength, Pa

$f_{ct}^{ref}$  = reference tensile strength, Pa

Calculations during the evaluation of the results from the stress rig can formally take place at a single point inside the concrete specimen, because it is considered to have a homogeneous state over its cross-section. To consider strain induced deformations, the so-called Picket effect, the strain dependent on temperature and moist related strains may be adjusted by introduction of adjustment factors,  $\rho_T$  and  $\rho_\varphi$ .

From the situation of cracking in the stress rig, the parameter  $f_{ct}^{ref}$  is determined. To complete a full set of material parameters,  $\alpha_{ct}$  (limit for start of non-linear stress-strain behaviour),  $\rho_T$  and  $\rho_\varphi$  are regarded as additional free model parameter to get an acceptable fit with the test data, if needed.

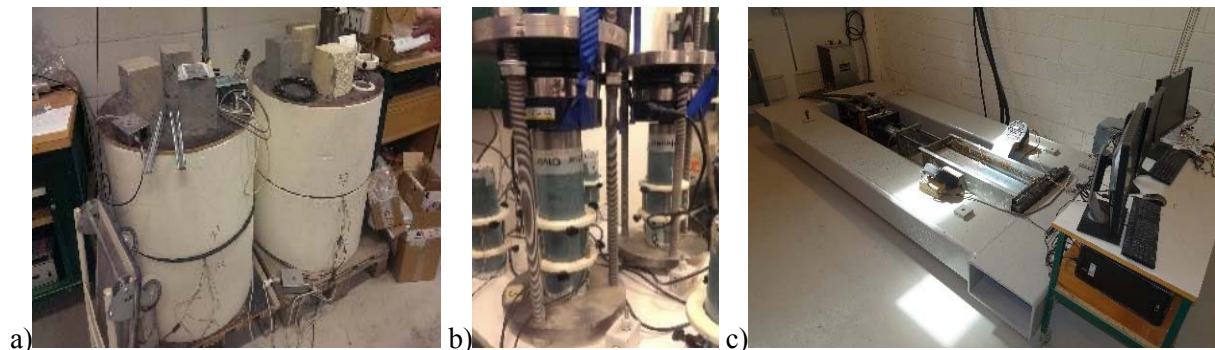


Figure 20. Set-ups for: a) Two semi-adiabatic tests. b) Basic shrinkage tests. c) Stress at full restraint.

### 7.3. Results

From the analyse of the stress calculation performed with the parameters evaluated, some observations can be made (see also Paper 4).

A slight change in ingoing parameters of the *maturity function* and *reference strength development* has a negligible effect on the calculated strain. For the test of *heat of hydration*, a decreased temperature by 0.5°C of the air surrounding the test equipment effect the calculated strain by 1 percentage. At the evaluation of *basic shrinkage* and *free thermal dilation*, the calculated strain is only slightly affected by a deviated estimation of the initial concrete temperature by 1°C. The *basic creep* evaluation exhibits a high sensitivity on the calculated strain.

An overall conclusion is that the fitting at evaluation of the *stress development at full restraint* tests more or less nullifies the effects of any deviation in the evaluation of the other tests.



## 8. CONCLUSIONS

### 8.1. Overall observations

#### 8.1.1. The Equivalent Restraint Method (ERM)

In general, ERM has been shown to be functional as a quick analyse method for rather complex structures, where typically cumbersome 3D calculations otherwise should be needed. This is important making possible the everyday work estimating actions for the large amount of situations needed concerning weather conditions, choices of materials, choice of measures on site, etc.

The first step using 3D FEM calculations to determine the restraint within the young concrete is the same as when applying the Local Restraint Method (LRM). At the development of a ERM model, a structure including both young concrete and an equivalent part of the adjacent body is created, which means that both cooling of young concrete as well as heating of the adjacent body can be analysed in a rational way. From a theoretical point of view, such measures on site cannot be performed with LRM, although cooling might be treated approximately in some cases.

#### 8.1.2. Material properties of young concrete

Five different types of laboratory tests for young concrete are performed at LTU denoted:

1. *strength development*
2. *heat of hydration* and
3. *stress at full restraint.*
4. *basic creep*
5. *basic shrinkage and thermal dilation (total free deformation)*

Stress at full restraint, can be considered as the most important test, where only the resulting stress in relation to the growth of the tensile strength can be used as a direct measure indicating the sensitivity to formation of early age cracks for the recipe in question.

The measured stresses are the end result combining all the other tested areas. Thus. if the models used are “theoretically” correct and no “unknown” phenomenon occurs, the calculated stress should coincide with the measured stress without any extra adjustments. As hydrating concrete is very complex phenomenon as such and new type of binders and supplementary materials are introduced to the market gradually, it is more likely that additional adjustments and/or development of new models are needed more frequently in the future.

But, for small changes of the mix design materials and proportions, only the first three laboratory test types can be applied, and basic creep and free deformations can be based on earlier experience. This simplifies and speeds up the test procedure. On the other hand, the three first test types have to be used every time a new recipe is investigated when mapping data for crack risk analyses

## 8.2. Answer to research questions

RQ1: Which structures can be simulated using the ERM when estimating early age crack risks?

- One restriction in the presented ERM version is that the basis for restraint calculation without measures is that a homogenous contraction of the young concrete body has been employed. The homogenous contraction simulates the situation during the decisive time period (from zero stress point until maximum stress ratio occurs) concerning estimation of risks for through cracking. This is acceptably met if the young concrete body has a constant thickness.
- The analysed structures have had limited rotation around an axis perpendicular to the thickness direction, as the total concrete structure has been symmetric, like sequential casting of horizontal tunnels, sequential castings of vertical pillars, etc. The ERM approximation of these structures is to take into account only the rotation around an axis in parallel with the thickness direction, as the effect of the limited rotation is included in the restraint values from the 3D FEM calculations.

RQ2: Which measures on site can be treated using the ERM when estimating early age crack risks?

Any traditional action on site (cooling of the young concrete, heating of the adjacent structure, insulation wherever needed) can be analysed. The ERM is based on equilibrium conditions for a structure consisting of a young concrete body and an adjoining structure, simulating the restraint situation within the young concrete without measures. Since the restraint from the adjoining structure is represented by a restraining block, any temperature altering measure may be applied to the model.

RQ3: How important is each individual laboratory test to create material properties for operational analyses of crack risks?

Out of the five performed tests, three are of significant importance, when it comes to provide an operational parameter set. These tests are the test of *strength development*, *heat of hydration* and *stress at full restraint*. As long as reliable measurements and a reasonable evaluation of these measurements can be provided there is room for errors in the measurements and evaluation for the remaining two tests; *basic shrinkage and free thermal dilation* and *basic creep*. If one or both of these tests are unreliable in one way or another, the corresponding parameter values can be estimated based on previous experiences.

### 8.3. Future research

To examine the limits using ERM, further research is needed, and some interesting examples are the following topics:

- Study asymmetric or irregular cross-sections of the young concrete, where no longer a homogenous contraction is valid for analyses of through cracking without measures.
- Analyse structures including rotation in two directions causing non-symmetric restraint over the thickness of the young concrete.
- Study of more typical cases are needed to examine the versatility of the method.
- Quantify the benefits using ERM instead of full 3D (2D on some cases) FEM. What is the increase of costs when using FEM? Are the material models in commercial FE program more unreliable and what are the possible effects on final result?

Further examination of the importance of each individual laboratory test at the evaluation of material properties could be valuable if further precision is desired at operational analyses of crack risks.



## References

- Al-Gburi M, “Restraint Effects in Early Age Concrete Structures”, Doctoral Thesis, Luleå University of Technology, Luleå 2015.
- AMA Anläggning 13, “Allmän material- och arbetsbeskrivning för anläggningsarbeten AMA Anläggning 13”, Svensk byggtjänst, 2014. (In Swedish).
- ACI Committee 207, “Effect of Restraint, Volume Change, and Reinforcement on Cracking of Massive Concrete,” ACI Committee 207.ACI207.2R-95. Reapproved 2002, 26 pp.
- Arizona Leisure, “Construction History of Hoover Dam – A Brief Overview of Hoover Dam Construction,” *Webpage*, Available at: <http://www.arizona-leisure.com/hoover-dam-building.html>.
- Bazant Z P, Wu S T, “Rate-type creep law for aging concrete based on Maxwell-Chain”, *Materials and Structures (RILEM, Paris)*, Vol 7. No. 37, 1974.
- Bernander S, “Practical Measurement to Avoiding Early Age Thermal Cracking in Concrete Structures. Prevention of Thermal Cracking in Concrete at Early Ages”, Ed. by R. Springenschmid. London, England, E & FNSpon, RILEM Report 15, 1998, pp.255-315.
- Bernander S, “Analysis of Deformations in an Elastic Halfspace due to Horizontal Loading,” Göteborg, Sweden: Con-Geo AB. Notes and calculations with diagrams. 2001, pp. 47.
- Bernander S, “Balk på elastiskt underlag åverkad av ändmomentet  $M_1$  (Beam on Resilient Ground Loaded by Bending End Moments  $M_1$ )”. Göteborg, Sweden: ConGeo AB. Notes and calculations with diagrams, 1993. (In Swedish).
- Betonghandbok “Material och Arbetsutförande” (Concrete Handbook – Material and Workmanship). Svensk Byggtjänst, 2<sup>nd</sup> Ed, 1994, pp 1128 and 837 (In Swedish)
- Bjøntegaard Ø, “Thermal Dilation and Autogenous Deformation as Driving Forces to Self-Induced Stresses in High Performance Concrete”, Doctoral Thesis, Division of Structural Engineering, Norwegian University of Science and Technology, 2000, 256 pp.
- Bosnjak D, “Self-Induced Cracking Problems in Hardening Concrete Structures”, Doctoral Thesis, Division of Structural Engineering, Norwegian University of Science and Technology, 1999:121, 171 pp.
- ConTeSt Pro, “User’s Manual - Program for Temperature and Stress Calculations in Concrete”, Developed by JEJMS Concrete AB in co-operation with Lulea University of Technology, Cementa AB and Peab AB. Lulea, Sweden, 2008, 197 pp.
- CraX1, “Temperatursprickor i betongkonstruktioner – handbok med diagram för sprickriskbedömning inklusive åtgärder för några vanliga typfall. Luleå: Luleå tekniska universitet, Teknisk Rapport 2001:14, Revised 2003, ISSN 1402-1536.
- Cusson D, Repette W, “Early-Age Cracking in Reconstructed Concrete Bridge Barrier Walls,” *ACI Materials Journal*, 97(4), July/August, 2000, pp. 438-446.
- DIANA FEA BV: “DIANA – Displacement Analyser,” *Software*, 2017, homepage: <https://dianafea.com/content/DIANA1>

- Emborg M, "Thermal Stresses in Concrete Structures at Early Ages", Doctoral Thesis, Dept. of Civil, Environmental and Natural Resources Engineering, Luleå University of Technology, Luleå, Sweden, 1989:73 D, 1990, 285 pp.
- Emborg M, "Development of Mechanical Behavior at Early Age", Ed. by R. Springenschmid. London, England, E & FNSpon, RILEM Report 15, 1998, pp. 76-148.
- Emborg M, Bernander S, "Assessment of the Risk of Thermal Cracking in Hardening Concrete," *Journal of Structural Engineering*, ASCE, Vol.120, No 10, October 1994. pp. 2893-2912.
- Emborg M, Bernander S, Ekefors K, Groth P, Hedlund H, "Temperatursprickor i betongkonstruktioner – Beräkningsmetoder för hydratationsspänningar och diagram för några vanliga typfall". Luleå: Luleå tekniska universitet. Teknisk rapport 1997:02. 100pp. ISSN 1402-1536. (In Swedish).
- Fjellström P, "Measurement and Modelling of Young Concrete Properties", Licentiate Thesis, Dept. of Civil, Environmental and Natural Resources Engineering, Luleå University of Technology, Luleå, Sweden 2013, 200 pp.
- Gasch, T, "Concrete as a multi-physical material with applications to hydro power facilities", Licentiate Thesis, KTH Royal Institute of Technology, 2016.
- Hedlund H, "Hardening Concrete – Measurements and Evaluation of Non-Elastic Deformation and Associated Restraint Stresses", Doctoral Thesis, Dept. of Civil, Environmental and Natural Resources Engineering, Luleå University of Technology, Luleå, Sweden 2000.
- Hilleborg A, "Concrete Hand Book, Materials Ch 13", Edition 2, Svensk Byggtjänst and Cementa AB, Sweden, 2009. (In Swedish)
- Hösthagen A, Jonasson J-E, Emborg M, Hedlund H, Wallin K, Stelmarczyk M, "Thermal Crack Risk Estimations of Concrete Tunnel Segments – Equivalent Restraint Method Correlated to Empirical Observations", *Nordic Concrete Research* No. 49, 2014/1.
- JCI, "A Proposal of a Method of Calculating Crack Width due to Thermal Stress," Tokyo, Japan: Japan Concrete Institute, Committee on Thermal Stress of Massive Concrete Structures, JCI Committee Report.1992, 106 pp.
- Jonasson J-E, "Computer Program for Non-linear Analyses of Concrete in View of Shrinkage, Creep and Temperature", *Fo/Research Bulletin*, No. 7:77, Swedish Cement and Concrete Research Institute, Stockholm 1977 (In Swedish).
- Jonasson J-E, "Slipform Construction – Calculations for Assessing Protection against Early Freezing. *Fo/Research Bulletin*, No. 4:84, Swedish Cement and Concrete Research Institute, Stockholm, 1984.
- Jonasson J-E, "Modelling of Temperature, Moisture and Stresses in Young Concrete", Doctoral Thesis, Dept. of Civil, Environmental and Natural Resources Engineering, Luleå University of Technology, Luleå 1994, 242 pp.
- Jonasson J-E, Westman G, "Conversion of Creep Data to Relaxation Data by the Program RELAX", IPACS Document, TG 3.2/1, Dept. of Civil, Environmental and Natural Resources Engineering, Luleå University of Technology, Luleå 2001.
- JSCE, "English Version of Standard Specification for Concrete Structures 2007", Japan Society of Civil Engineer, JSCE, December 2010, 503pp.
- Kianousha M R, Acarcamb M, Ziari A, "Behavior of base restrained reinforced concrete walls under volumetric change", *Engineering Structures*, 30, 2008, pp.1526–1534.
- Larson M, "Estimation of Crack Risk in Early Age Concrete – Simplified Methods for Practical Use", Licentiate Thesis, Dept. of Civil, Environmental and Natural Resources Engineering, Luleå University of Technology, Luleå 2000, 156 pp.

- Larson M, "Thermal Crack Estimation in Early Age Concrete – Models and Methods for Practical Application", Doctoral Thesis, Dept. of Civil, Environmental and Natural Resources Engineering, Luleå University of Technology, Luleå 2003, 203 pp.
- Löfving P, "Bestämning av jords hållfasthets- och deformationsegenskaper (Determination of the strength and deformation properties for ground)". Borlänge: Vägverket, Publication 1993:6, 30pp. (In Swedish).
- Löfquist B, "Temperatureffekter i hårdnande betong (Temperature Effects in Hardening Concrete)", Doctoral Thesis, Chalmers tekniska högskola, Stockholm 1946, Pp. 195. (In Swedish).
- Mihashi H, Leite J P, "State of The Art Report on Control of Cracking in Early Age Concrete," *Advanced Concrete Technology*, 2004, pp.141–154.
- Nilsson M, "Thermal Cracking of Young Concrete – Partial Coefficients, Restraint Effects and Influence of Casting Joints", Licentiate Thesis, Dept. of Civil, Environmental and Natural Resources Engineering, Luleå University of Technology, Luleå 2000. pp.267.
- Nilsson M, "Restraint Factors and Partial Coefficients for Crack Risk Analyses of Early Age Concrete Structures", Doctoral Thesis, Division of Structural Engineering, Luleå University of Technology, Luleå 2003, 170 pp.
- Olofsson J, "3D Structural Analyses of Crack Risk in Hardening Concrete Structures Verification of Three Steps Method", Luleå University of Technology, Division of Structural Engineering, IPACS Report, 1999, pp.52.
- Onken P, Rostásy F S, "A Practical Planning Tool for the Simulation of Thermal Stresses and the Prediction of Early Thermal Cracks in Massive Concrete Structures", Ed. by R. Springenschmid. London, England, E & FNSpon, RILEM Proceedings 25, 1995
- Orosz K, "Early Age Autogenous Deformation and Cracking of Cementitious Materials – Implications on Strengthening of Concrete Structures", Doctoral Thesis, Dept. of Civil, Environmental and Natural Resources Engineering, Luleå University of Technology, Luleå, Sweden 2017.
- Rastrup E, "Heat of Hydration in Concrete", *Magazine of Concrete Research*, Vol. 6, No. 17, September 1954.
- Rostásy F S, Tanabe T, Laube, M, "Assessment of External Restraint. In: Prevention of Thermal Cracking in Concrete at Early Ages", Ed. by R. Springenschmid. London, England, E & FNSpon, RILEM Report 15, 1998, pp. 149-177.
- Westman G, "Concrete Creep and Thermal Stresses – New Creep Models and Their Effects on Stress Developments", Doctoral Thesis, Dept. of Civil, Environmental and Natural Resources Engineering, Luleå University of Technology, Luleå, Sweden 1999.

***Doctoral and Licentiate theses*****Structural and Fire Engineering  
Luleå University of Technology****Doctoral theses**

1980 Ulf Arne Girhammar: *Dynamic fail-safe behaviour of steel structures*. Doctoral Thesis 1980:060D. 309 pp.

1983 Kent Gylltoft: *Fracture mechanics models for fatigue in concrete structures*. Doctoral Thesis 1983:25D. 210 pp.

1985 Thomas Olofsson: *Mathematical modelling of jointed rock masses*. Doctoral Thesis 1985:42D. 143 pp. (In collaboration with the Division of Rock Mechanics).

1988 Lennart Fransson: *Thermal ice pressure on structures in ice covers*. Doctoral Thesis 1988:67D. 161 pp.

1989 Mats Emborg: *Thermal stresses in concrete structures at early ages*. Doctoral Thesis 1989:73D. 285 pp.

1993 Lars Stehn: *Tensile fracture of ice. Test methods and fracture mechanics analysis*. Doctoral Thesis 1993:129D, September 1993. 136 pp.

1994 Björn Täljsten: *Plate bonding. Strengthening of existing concrete structures with epoxy bonded plates of steel or fibre reinforced plastics*. Doctoral Thesis 1994:152D, August 1994. 283 pp.

1994 Jan-Erik Jonasson: *Modelling of temperature, moisture and stresses in young concrete*. Doctoral Thesis 1994:153D, August 1994. 227 pp.

1995 Ulf Ohlsson: *Fracture mechanics analysis of concrete structures*. Doctoral Thesis 1995:179D, December 1995. 98 pp.

1998 Keivan Noghabai: *Effect of tension softening on the performance of concrete structures*. Doctoral Thesis 1998:21, August 1998. 150 pp.

1999 Gustaf Westman: *Concrete creep and thermal stresses. New creep models and their effects on stress development*. Doctoral Thesis 1999:10, May 1999. 301 pp.

1999 Henrik Gabrielsson: *Ductility in high performance concrete structures. An experimental investigation and a theoretical study of prestressed hollow core slabs and prestressed cylindrical pole elements*. Doctoral Thesis 1999:15, May 1999. 283 pp.

2000 Patrik Groth: *Fibre reinforced concrete – Fracture mechanics methods applied on self-compacting concrete and energetically modified binders*. Doctoral Thesis 2000:04, January 2000. 214 pp. ISBN 978-91-85685-00-4.

2000 Hans Hedlund: *Hardening concrete. Measurements and evaluation of non-elastic deformation and associated restraint stresses*. Doctoral Thesis 2000:25, December 2000. 394 pp. ISBN 91-89580-00-1.

2003 Anders Carolin: *Carbon fibre reinforced polymers for strengthening of structural members*. Doctoral Thesis 2003:18, June 2003. 190 pp. ISBN 91-89580-04-4.

2003 Martin Nilsson: *Restraint factors and partial coefficients for crack risk analyses of early age concrete structures*. Doctoral Thesis 2003:19, June 2003. 170 pp. ISBN: 91-89580-05-2.

2003 Mårten Larson: *Thermal crack estimation in early age concrete – Models and methods for practical application*. Doctoral Thesis 2003:20, June 2003. 190 pp. ISBN 91-86580-06-0.

2005 Erik Nordström: *Durability of sprayed concrete. Steel fibre corrosion in cracks*. Doctoral Thesis 2005:02, January 2005. 151 pp. ISBN 978-91-85685-01-1.

2006 Rogier Jongeling: *A process model for work-flow management in construction. Combined use of location-based scheduling and 4D CAD*. Doctoral Thesis 2006:47, October 2006. 191 pp. ISBN 978-91-85685-02-8.

2006 Jonas Carlswärd: *Shrinkage cracking of steel fibre reinforced self compacting concrete overlays – Test methods and theoretical modelling*. Doctoral Thesis 2006:55, December 2006. 250 pp. ISBN 978-91-85685-04-2.

2006 Håkan Thun: *Assessment of fatigue resistance and strength in existing concrete structures*. Doctoral Thesis 2006:65, December 2006. 169 pp. ISBN 978-91-85685- 03-5.

2007 Lundqvist Joakim: *Numerical analysis of concrete elements strengthened with carbon fiber reinforced polymers*. Doctoral Thesis 2007:07, March 2007. 50 pp. ISBN 978-91-85685-06-6.

2007 Arvid Hejll: *Civil structural health monitoring – Strategies, methods and applications*. Doctoral Thesis 2007:10, March 2007. 189 pp. ISBN 978-91-85685-08-0.

2007 Stefan Woksepp: *Virtual reality in construction: Tools, methods and processes*. Doctoral Thesis 2007:49, November 2007. 191 pp. ISBN 978-91-85685-09-7.

2007 Romuald Rwamamara: *Planning the healthy construction workplace through risk assessment and design methods*. Doctoral Thesis 2007:74, November 2007. 179 pp. ISBN 978-91-85685-11-0.

2008 Björnär Sand: *Nonlinear finite element simulations of ice forces on offshore structures*. Doctoral Thesis 2008:39, September 2008. 241 pp.

2008 Bengt Toolanen: *Lean contracting: relational contracting influenced by lean thinking*. Doctoral Thesis 2008:41, October 2008. 190 pp.

- 2008 Sofia Utsi: *Performance based concrete mix-design: Aggregate and micro mortar optimization applied on self-compacting concrete containing fly ash*. Doctoral Thesis 2008:49, November 2008. 190 pp.
- 2009 Markus Bergström: *Assessment of existing concrete bridges: Bending stiffness as a performance indicator*. Doctoral Thesis, March 2009. 241 pp. ISBN 978-91-86233-11-2.
- 2009 Tobias Larsson: *Fatigue assessment of riveted bridges*. Doctoral Thesis, March 2009. 165 pp. ISBN 978-91-86233-13-6.
- 2009 Thomas Blanksvärd: *Strengthening of concrete structures by the use of mineral based composites: System and design models for flexure and shear*. Doctoral Thesis, April 2009. 156 pp. ISBN 978-91-86233-23-5.
- 2011 Anders Bennitz: *Externally unbonded post-tensioned CFRP tendons – A system solution*. Doctoral Thesis, February 2011. 68 pp. ISBN 978-91-7439-206-7.
- 2011 Gabriel Sas: *FRP shear strengthening of reinforced concrete beams*. Doctoral Thesis, April 2011. 97 pp. ISBN 978-91-7439-239-5.
- 2011 Peter Simonsson: *Buildability of concrete structures: processes, methods and material*. Doctoral Thesis, April 2011. 64 pp. ISBN 978-91-7439-243-2.
- 2011 Stig Bernander: *Progressive landslides in long natural slopes. Formation, potential extension and configuration of finished slides in strain-softening soils*. Doctoral Thesis, May 2011, rev. August 2011 and April 2012. 250 pp. ISBN 978-91-7439-238-8. (In collaboration with the Division of Soil Mechanics and Foundation Engineering).
- 2012 Arto Puurula: *Load carrying capacity of a strengthened reinforced concrete bridge: non-linear finite element modeling of a test to failure. Assessment of train load capacity of a two span railway trough bridge in Örnsköldsvik strengthened with bars of carbon fibre reinforced polymers (CFRP)*. Doctoral Thesis, May 2012. 100 pp. ISBN 978-91-7439-433-7.
- 2015 Mohammed Salih Mohammed Mahal: *Fatigue behaviour of RC beams strengthened with CFRP, Analytical and experimental investigations*. Doctoral Thesis, March 2015. 138 pp. ISBN 978-91-7583-234-0.
- 2015 Jonny Nilimaa: *Concrete bridges: Improved load capacity*. Doctoral Thesis, June 2015. 180 pp. ISBN 978-91-7583-344-6.
- 2015 Tarek Edrees Saaed: *Structural control and identification of civil engineering structures*. Doctoral Thesis, June 2015. 314 pp. ISBN 978-91-7583-241-8.
- 2015 Majid Al-Gburi: *Restraint effect in early age concrete structures*. Doctoral Thesis, September 2015. 190 pp. ISBN 978-91-7583-374-3.
- 2017 Cosmin Popescu: *CFRP strengthening of cut-out openings in concrete walls – Analysis and laboratory tests*. Doctoral Thesis, February 2017. 159 pp. ISSN 1402-1544.

## Licentiate theses

1984 Lennart Fransson: *Bärförmåga hos ett flytande istäcke. Beräkningsmodeller och experimentella studier av naturlig is och av is förstärkt med armering*. Licentiate Thesis 1984:012L. 137 pp. (In Swedish).

1985 Mats Emborg: *Temperature stresses in massive concrete structures. Viscoelastic models and laboratory tests*. Licentiate Thesis 1985:011L, May 1985. rev. November 1985. 163 pp.

1987 Christer Hjalmarsson: *Effektbehov i bostadshus. Experimentell bestämning av effektbehov i små- och flerbostadshus*. Licentiate Thesis 1987:009L, October 1987. 72 pp. (In Swedish).

1990 Björn Täljsten: *Förstärkning av betongkonstruktioner genom pålimning av stålplåtar*. Licentiate Thesis 1990:06L, May 1990. 205 pp. (In Swedish).

1990 Ulf Ohlsson: *Fracture mechanics studies of concrete structures*. Licentiate Thesis 1990:07L, May 1990. 66 pp.

1990 Lars Stehn: *Fracture toughness of sea ice. Development of a test system based on chevron notched specimens*. Licentiate Thesis 1990:11L, September 1990. 88 pp.

1992 Per Anders Daerga: *Some experimental fracture mechanics studies in mode I of concrete and wood*. Licentiate Thesis 1992:12L, April 1992, rev. June 1992. 81 pp.

1993 Henrik Gabrielsson: *Shear capacity of beams of reinforced high performance concrete*. Licentiate Thesis 1993:21L, May 1993. 109 pp.

1995 Keivan Noghabai: *Splitting of concrete in the anchoring zone of deformed bars. A fracture mechanics approach to bond*. Licentiate Thesis 1995:26L, May 1995. 123 pp.

1995 Gustaf Westman: *Thermal cracking in high performance concrete. Viscoelastic models and laboratory tests*. Licentiate Thesis 1995:27L, May 1995. 125 pp.

1995 Katarina Ekerfors: *Mognadsutveckling i ung betong. Temperaturkänslighet, hållfasthet och värmeutveckling*. Licentiate Thesis 1995:34L, October 1995. 137 pp. (In Swedish).

1996 Patrik Groth: *Cracking in concrete. Crack prevention with air-cooling and crack distribution with steel fibre reinforcement*. Licentiate Thesis 1996:37L, October 1996. 128 pp.

1996 Hans Hedlund: *Stresses in high performance concrete due to temperature and moisture variations at early ages*. Licentiate Thesis 1996:38L, October 1996. 240 pp.

2000 Mårten Larson: *Estimation of crack risk in early age concrete. Simplified methods for practical use*. Licentiate Thesis 2000:10, April 2000. 170 pp.

- 2000 Stig Bernander: *Progressive landslides in long natural slopes. Formation, potential extension and configuration of finished slides in strain-softening soils.* Licentiate Thesis 2000:16, May 2000. 137 pp. (In collaboration with the Division of Soil Mechanics and Foundation Engineering).
- 2000 Martin Nilsson: *Thermal cracking of young concrete. Partial coefficients, restraint effects and influences of casting joints.* Licentiate Thesis 2000:27, October 2000. 267 pp.
- 2000 Erik Nordström: *Steel fibre corrosion in cracks. Durability of sprayed concrete.* Licentiate Thesis 2000:49, December 2000. 103 pp.
- 2001 Anders Carolin: *Strengthening of concrete structures with CFRP – Shear strengthening and full-scale applications.* Licentiate thesis 2001:01, June 2001. 120 pp. ISBN 91-89580-01-X.
- 2001 Håkan Thun: *Evaluation of concrete structures. Strength development and fatigue capacity.* Licentiate Thesis 2001:25, June 2001. 164 pp. ISBN 91-89580-08-2.
- 2002 Patrice Godonue: *Preliminary design and analysis of pedestrian FRP bridge deck.* Licentiate Thesis 2002:18. 203 pp.
- 2002 Jonas Carlswård: *Steel fibre reinforced concrete toppings exposed to shrinkage and temperature deformations.* Licentiate Thesis 2002:33, August 2002. 112 pp.
- 2003 Sofia Utsi: *Self-compacting concrete – Properties of fresh and hardening concrete for civil engineering applications.* Licentiate Thesis 2003:19, June 2003. 185 pp.
- 2003 Anders Rönneblad: *Product models for concrete structures – Standards, applications and implementations.* Licentiate Thesis 2003:22, June 2003. 104 pp.
- 2003 Håkan Nordin: *Strengthening of concrete structures with pre-stressed CFRP.* Licentiate Thesis 2003:25, June 2003. 125 pp.
- 2004 Arto Puurula: *Assessment of prestressed concrete bridges loaded in combined shear, torsion and bending.* Licentiate Thesis 2004:43, November 2004. 212 pp.
- 2004 Arvid Hejll: *Structural health monitoring of bridges. Monitor, assess and retrofit.* Licentiate Thesis 2004:46, November 2004. 128 pp.
- 2005 Ola Enochsson: *CFRP strengthening of concrete slabs, with and without openings. Experiment, analysis, design and field application.* Licentiate Thesis 2005:87, November 2005. 154 pp.
- 2006 Markus Bergström: *Life cycle behaviour of concrete structures – Laboratory test and probabilistic evaluation.* Licentiate Thesis 2006:59, December 2006. 173 pp. ISBN 978-91-85685-05-9.
- 2007 Thomas Blanksvärd: *Strengthening of concrete structures by mineral based composites.* Licentiate Thesis 2007:15, March 2007. 300 pp. ISBN 978-91-85685-07-3.

- 2008 Peter Simonsson: *Industrial bridge construction with cast in place concrete: New production methods and lean construction philosophies*. Licentiate Thesis 2008:17, May 2008. 164 pp. ISBN 978-91-85685-12-7.
- 2008 Anders Stenlund: *Load carrying capacity of bridges: Three case studies of bridges in northern Sweden where probabilistic methods have been used to study effects of monitoring and strengthening*. Licentiate Thesis 2008:18, May 2008. 306 pp. ISBN 978-91-85685-13-4.
- 2008 Anders Bennitz: *Mechanical anchorage of prestressed CFRP tendons – Theory and tests*. Licentiate Thesis 2008:32, November 2008. 319 pp.
- 2008 Gabriel Sas: *FRP shear strengthening of RC beams and walls*. Licentiate Thesis 2008:39, December 2008. 107 pp.
- 2010 Tomas Sandström: *Durability of concrete hydropower structures when repaired with concrete overlays*. Licentiate Thesis, February 2010. 179 pp. ISBN 978-91-7439-074-2.
- 2013 Johan Larsson: *Mapping the concept of industrialized bridge construction: Potentials and obstacles*. Licentiate Thesis, January 2013. 66 pp. ISBN 978-91-7439-543-3.
- 2013 Jonny Nilimaa: *Upgrading concrete bridges: Post-tensioning for higher loads*. Licentiate Thesis, January 2013. 300 pp. ISBN 978-91-7439-546-4.
- 2013 Katalin Orosz: *Tensile behaviour of mineral-based composites*. Licentiate Thesis, May 2013. 92 pp. ISBN 978-91-7439-663-8.
- 2013 Peter Fjellström: *Measurement and modelling of young concrete properties*. Licentiate Thesis, May 2013. 121 pp. ISBN 978-91-7439-644-7.
- 2014 Majid Al-Gburi: *Restraint in structures with young concrete: Tools and estimations for practical use*. Licentiate Thesis, September 2014. 106 pp. ISBN 978-91-7439-977-6.
- 2014 Niklas Bagge: *Assessment of Concrete Bridges Models and Tests for Refined Capacity Estimates*. Licentiate Thesis, November 2014. 132 pp. ISBN 978-91-7583-163-3.
- 2014 Tarek Edrees Saaed: *Structural identification of civil engineering structures*. Licentiate Thesis, November 2014. 135 pp. ISBN 978-91-7583-053-7.
- 2015 Cosmin Popescu: *FRP strengthening of concrete walls with openings*. Licentiate Thesis, December 2015. 134 pp. ISBN 978-91-7583-453-5.
- 2016 Faez Sayahi: *Plastic shrinkage cracking in concrete*. Licentiate Thesis, October 2016. 146 pp. ISBN 978-91-7583-678-2.
- 2017 Yahya Ghasemi: *Aggregates in concrete mix design*. Licentiate Thesis, Mars 2017. 60 pp. ISBN: 978-91-7583-801-4.



# **Paper I:**

## **Simplified Methods for Crack Risk Analyses of Early Age Concrete. Part 1: Development of Equivalent Restraint Method**

Al-Gburi M, Jonasson J-E, Nilsson M, Hedlund H & **Hösthagen A**, Published in Nordic Concrete Research, Publication no. 46, 2012, pp. 17-37.

# Simplified Methods for Crack Risk Analyses of Early Age Concrete

## Part 1: Development of Equivalent Restraint Method



Majid Al-Gburi  
M. Sc. Ph.D. Student  
Lulea University of Technology  
Dept. of Structural Engineering  
Email: majid.al-gburi@ltu.se



Dr. Jan –Erik Jonasson  
Professor  
Lulea University of Technology  
Dept. of Structural Engineering  
Email: jej@ltu.se



Dr. Martin Nilsson  
Lulea University of Technology  
Dept. of Structural Engineering  
Email: martin.c.nilsson@ltu.se



Dr. Hans Hedlund  
Adjunct professor  
Skanska Sverige AB  
and Lulea University of Technology  
Dept. of Structural Engineering  
Email: hans.hedlund@skanska.se



Anders Hösthagen  
M. Sc. Ph.D. Student  
Projektengagemang AB  
and Lulea University of Technology  
Dept. of Structural Engineering  
Email: anders.hosthagen@projektengagemang.se

### ABSTRACT

The present study deals with both the compensation plane method, CPM, and local restraint method, LRM, as alternative methods studying crack risks for early age concrete. It is shown that CPM can be used both for cooling and heating, but basic LRM cannot be applied to heating. This paper presents an improved equivalent restraint method, ERM, which easily can be applied both for usage of heating and cooling for general structures. Restraint curves are given for two different infrastructures, one founded on frictional materials and another on rock. Such curves might be directly applied in design using LRM and ERM.

**Key words:** Local restraint methods, compensation plane method, equivalent restraint method, crack risk, early age concrete.

## 1. BACKGROUND

Over the past few decades, a continuous progress in the research and understanding of the effect of the early mechanical and visco-elastic behavior of concrete has been presented, see e.g. [1], [2], [3], [4] and [5]. The main phenomenon causing early age cracking is volume change due to the variable moisture and temperature state in the concrete. With the use of high-performance concrete (low water cement ratio, high cement content) the volume changes increase because of the elevated heat of hydration and high autogenous shrinkage. Early-age thermal cracking is a result of the heat produced during hydration of the binder. Cracking originates either from different expansions (due to temperature gradients inside the young concrete during heating, which may result in surface cracking) or by restraint from the adjacent structure during the contraction phase, (the result of which may cause through cracking). For ordinary concrete structures, like tunnels, bridges, etc., surface cracking occurs within a few days, and through cracking occurs within a few weeks. Pre-calculation of stresses in young concrete is performed with the aim of analyzing the risk of these cracks occurring. If the crack risk is too high, actions are needed to prevent the cracking. Common actions on site are cooling of the young concrete and/or heating of the adjacent structure. Restraint from the adjoining structures is the main cause of through cracking. Unfortunately, for complex structures, it is an uncertain factor because it is hard to estimate [6].

The most general approach of modeling early age structures is 3D FEM analyses. This entails realistic modeling of young concrete and the bond between different parts of the structure. The method is very complex and therefore, in practice, it is replaced by different simplified methods, such as: the three-step engineering method, the compensation plane method, one-point calculation. These methods are described amongst others in [6], [7] and [8].

The focus of this study is devoted to establishing and applying restraint curves. To simplify crack risk calculations based on restraint curves, an improved method, denoted equivalent restraint method, is presented in the paper.

## 2. AIMS AND PURPOSE

The aims and purpose of this paper are to:

- Clarify the difference between the CPM (compensated plane method) and the LRM (local restraint method).
- Estimate and compare stresses using CPM and LRM for cases where the CPM conditions are fulfilled.
- Establish an engineering approach to crack risk analyses using local restraint curves for general structures and to be able to incorporate actions taken on site (heating/cooling).
- Analyze restraint situations for some typical infrastructures.

## 3. THE COMPENSATION PLANE METHOD

### 3.1 Classical Japanese method

The compensation plane method (CPM) was developed in 1985 as a calculation program that can be widely applied for thermal stress analyses of massive concrete structures, [9] and [10]. This method is based on the assumption of linear strain distribution, which is equivalent to the

statement that plane sections remain plane after deformations [11]. The cross-section is divided into discrete elements with individual temperature and level of maturity. The initial stress in the cross section is shown in the left part of figure 1. The sum of internally hindered stress, that is derived from the difference between the compensation plane and temperature distribution curve, is shown in the right part of figure 1. The externally restrained stresses are equivalent to the stresses caused by the forces, i.e. axial force  $N_R$ , and bending moment  $M_R$ , required to return the plane after deformation to the original restrained position, [9] and [10].  $N_R$  and  $M_R$  are given by the following equations using external restraining coefficients  $R_N$  and  $R_M$ , respectively.

$$N_R = R_N EA \bar{\epsilon} \quad (1)$$

$$M_R = R_M EI \bar{\varphi} \quad (2)$$

where  $E$ ,  $A$  and  $I$  are cross-section parameters;  $E$  is the Young's modulus;  $I$  is the moment of inertia;  $A$  is the cross-section area;  $\bar{\epsilon}$  is axial strain increment; and  $\bar{\varphi}$  is the gradient as curvature increment.

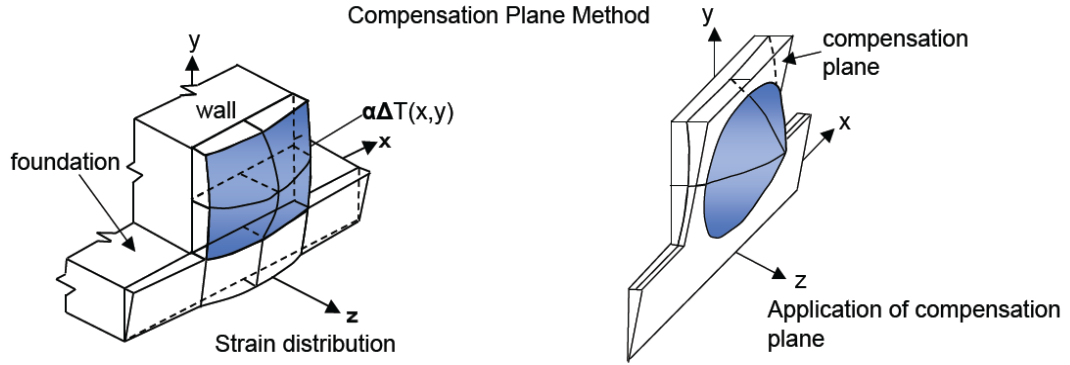


Figure 1 - Illustration of compensation plane method [10].

Different levels of maturity and stiffness can be taken care of in various parts of the cross-section, where the stress distribution is displayed and the compensation plane is considered [6]. The external restrained coefficients were derived from numerical calculation by the three-dimensional finite-element method. Finally, the initial stress  $\sigma(x, y)$  at a position with coordinates  $(x, y)$  is given by the following equation, [9] and [10].

$$\sigma(x, y) = E_i \{ \epsilon_0(x, y) - \bar{\epsilon} - \bar{\varphi}(y - y_g) \} + R_N E_i \bar{\epsilon} + R_M E_i \bar{\varphi}(y - y_g) \quad (3)$$

where  $E_i$  is the Young's modulus at position  $(x, y)$ ;  $\epsilon_0$  is the initial strain;  $y_g$  is center of gravity for the whole cross-section.

The advantage of CPM compared to full 3D early age analysis is clear, as the number of the unknowns is strongly reduced, [6] and [10]. If CPM is formulated in the simplest way, the number of unknowns is only 3: one translation and two curvatures. Besides, both computational time and time spent on the modeling and surveying of the results are largely decreased using CPM.

### 3.2 Non-plane section analyses

The classical compensation plane method, assumes that plane sections remain plane after deformation, which is only theoretically valid for high length to height ratios ( $L/H$ ),

approximately 5 or more (this is comparable to classical beam theory). However, in many real cases for thermal cracking, the length to height ratios is lower. In these cases, the assumption of plane sections is no longer valid. One way of taking this into account is to define restraint factors at different heights for various  $L/H$  ratios, see figure 2 from [12]. The restraint factors in figure 2 can be used directly in cases where we have a small volume of newly cast concrete on very large or very stiff foundations. For a finite foundation and pure translation, a multiplier,  $\delta_f$ , can be applied together with restraint factors [1] as:

$$\delta_f = 1/(1 + A_C E_C / A_F E_F) \quad (4)$$

where  $A_C$  and  $A_F$  are cross section areas of new concrete and old foundation respectively;  $E_C$  and  $E_F$  are modulus of elasticity for new concrete and old foundation.

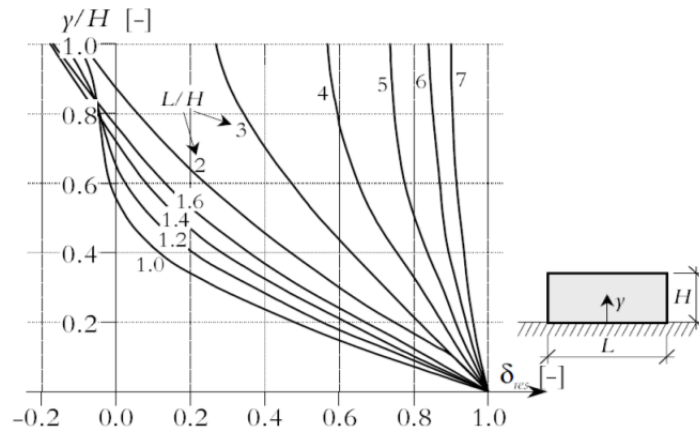


Figure 2 – Restraint factors for walls on stiff foundation [12].

Furthermore, for the case of massive concrete on rock, the effective restraining rock area  $A_F$  can be assumed to be  $2.5 A_C$  [1].

Implementation of the restraint factors to the compensated plane method has been performed in the following steps [2]:

- Reduction of the initial strains according to the restraint factors for the  $L/H$  ratio in question for fixed strains ( $R_N = R_M = 1$ ).
- Adding the axial deformation, if  $R_N < 1$ .
- Adding the rotational deformation, if  $R_M < 1$ .

One way of performing stress calculations in young concrete is to assume full adhesion in the joint between the newly cast concrete and the adjoining structure. Based on this assumption, an elastic calculation, where the wall is homogeneously contracting, will show results of maximum and minimum principal stresses like those shown in figure 3 from [13]. From the figure, it is seen that the principal stresses are, not unexpectedly, highest in the corner portion at the end of the construction joint (point A). However, generally speaking, cracking actually occurs as almost vertical cracks in the central part of the wall, see figure 3b. The overall conclusion from this discrepancy between theory and practice is that full adhesion cannot be present and slip failure occurs, initiating from the end of the joint (point A), see figure 4.

Assuming full adhesion is correspondingly too conservative, in particular for moderate structural lengths ( $L < 6\text{m}$ ) [13]. Usually macro cracks are not observed at the joint, which can

be interpreted as an occurrence of micro cracks at the end corner of the wall. This may be denoted joint "slip failure" or "micro cracking" at the end of the wall.

Based on the conclusions in [13], a slip factor has been introduced into the compensation plane method, [14], [15] and [16], see figure 5. The use of restraint factors together with slip factors for the compensation plane method, for a constant initial strain in the young concrete, is illustrated in figure 6 [14].

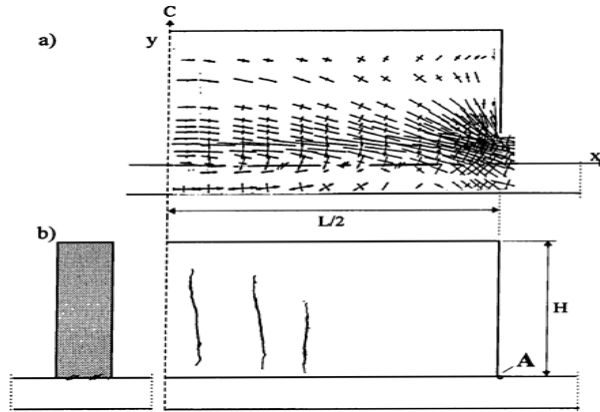


Figure 3 - Calculated maximum and minimum principle stresses for structure wall-on-slab using 2D elastic FEM [13].

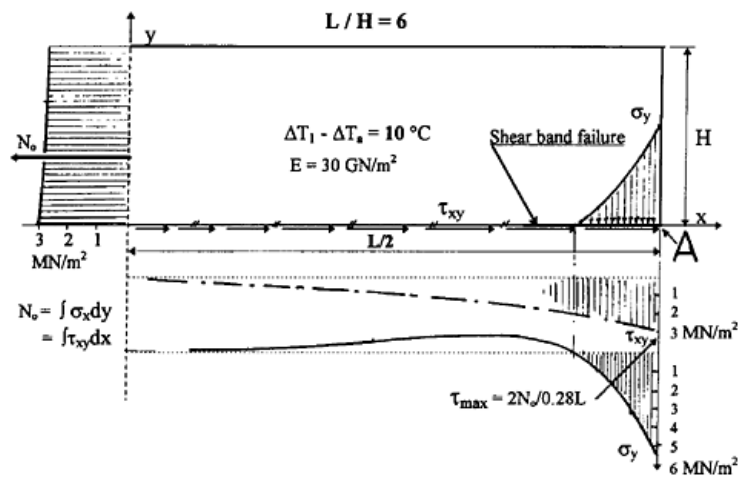
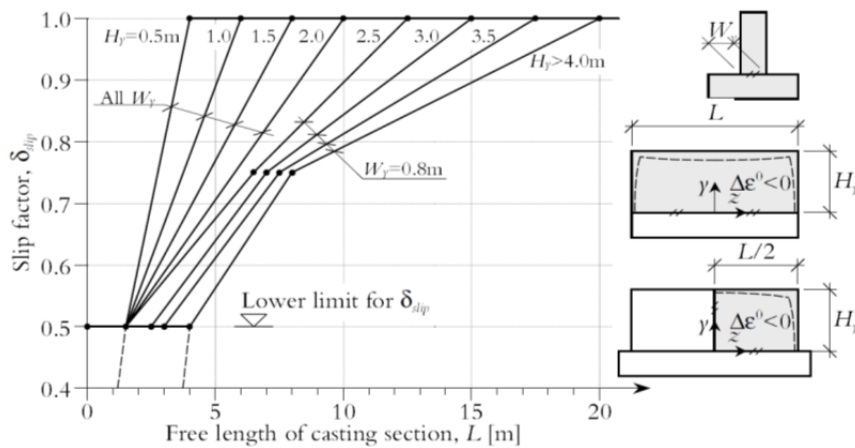
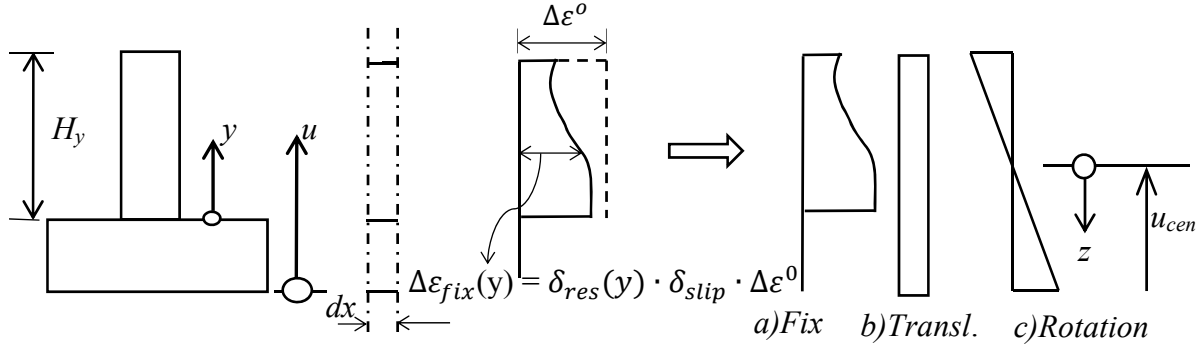


Figure 4 - Illustration of progressive joint failure starting at the end of the joint [13].



Figures 5 - Slip factor as function of free length ( $L$ ), height ( $H$ ) and width ( $W$ ) of the wall, [14], [15] and [16].



Figures 6 – Illustration of compensated plane method for non-plane section analyses [14].

The introduction of restraint factors in step “a)Fix” reducing the initial strain, see the term “ $\Delta\varepsilon_{fix}(y) = \delta_{res}(y) \cdot \delta_{slip} \cdot \Delta\varepsilon^0$ ” in figure 6, shows a simplified method to take into account a non-plane section (factor  $\delta_{res}(y)$ , see figure 2) and, if any, effects of local micro cracking ( $\delta_{slip}$ , see figure 5). An alternative approach may be to introduce the local restraint method together with, if any, the slip factor ( $\delta_{slip}$ ), see further chapter 4.

#### 4. THE LOCAL RESTRAINT METHOD

The method presented here is a point wise calculation denoted LRM (local restraint method). The LRM is primarily used for the evaluation of the restraint effect for a homogenous contraction in the newly cast concrete. If the new concrete is free to move, there will be no stresses in the concrete. But, if the young concrete is cast on an adjoining existing structure, stresses will arise in the concrete due to the restraining actions from the adjacent structure. The uniaxial restraint effect,  $R_i$ , is defined as:

$$R_i = \frac{\sigma_{ui}}{(-\Delta\varepsilon^0 E_C)} \quad (5)$$

where  $\sigma_{ui}$  = resulting stress from the elastic calculation, where  $i$  = a chosen direction in the concrete body;  $u$  = uniaxial coordinate in  $i$  direction;  $\Delta\varepsilon^0$  = the homogenous contraction in the concrete; and  $E_C$  = Young’s modulus in the early age concrete.

If the temperature caused by hydration of the new concrete is uniform, LRM is theoretically correct. In real cases, the temperature in young concrete is more or less non-uniform. Fortunately, in most civil engineering structures, the average temperature through the thickness (smallest dimension) is representing a homogenous contraction with respect to the risk of through cracking. So, for the purpose of stress calculations, LRM is probably a good engineering model provided no heating/cooling measures are taken on site. LRM might also be applicable for calculation of stresses when cooling is used, provided the changes in restraint caused from cooling can be neglected. Unfortunately the original LRM is not applicable in cases where heating is used because the structural balance between the concrete and the adjoining structure caused from heating give rise to a more complicated strain situation.

In this study, restraint curves are created by 3D elastic calculations using Eq. 5. For the cases presented here, the direction  $i$  is parallel with the direction of the joint, which is in agreement with the findings in Bernander [13], see figures 3 and 4. This simplification is the typical situation for many civil engineering structures like bridges, tunnels, harbors, etc. In more complicated cases the direction of maximum principal stress might be relevant, and the actual situation has to be evaluated by the user.

## 5. CRACK RISK ESTIMATIONS AT EARLY AGES

### 5.1 General background

The estimation of the risk of cracking of early age concrete structures can be based on five steps, [1], [8], [9], [13], [17], [18], [19], [20], [21] and [22]:

The first step: When no measures are taken on site, certain principle factors can be chosen to avoid or reduce the risk of thermal cracking at early ages. The most important principal factors are the choice of the structure with respect to dimensions and casting sequences as well as selection of mix design.

The second step: Estimation of thermal temperature development during the hydration phase. This can be done either by calculations or from measurements in real structures. From the temperature development, the strength growth is obtained. The temperature calculation also includes factors such as insulation, cooling and/or heating or other measures possible to perform on site.

The third step: Estimation of the structural interaction between the early age concrete and its surroundings. This can typically be done in two different ways: either starting with an estimation of the boundary conditions for a structure including early age concrete and adjoining structures. Alternatively this can be achieved by an estimation of restraint factors, such as LRM in chapter 4, for direct calculation of different positions in the early age concrete.

The fourth step: Structural calculations resulting in stresses and strains in the young concrete. These are usually presented as stress/strength or strain/ultimate-strain ratios as a function of time.

The final step: Comprises of crack risk design using partial coefficients - or crack safety factors – as design conditions in different codes and standards.

The present study shows the application of LRM to estimate the crack risk in concrete at early age, primarily aimed for the situation without measures taken on site. For cases using cooling pipes or heating cables, an additional method denoted ERM (equivalent restraint method) is evaluated in the paper.

### 5.2 Application of local restraint method

Application of the local restraint method can be performed in two different ways, either by using an equivalent material block simulating the actual restraint factor in any position in the young concrete, or by direct use of the restraint factor for the position in question within the new concrete. The former procedure may be used in most computer programs for fresh concrete, see for instance [15], [17], [23] and [24] and in the present study the latter procedure is applied with the ConTeSt program [15].

In this paper two cases for typical wall-on-slab structures are studied. Comparison are made between calculated strain ratios using compensation plane method (CPM) and local restraint method (LRM), see examples 1 and 2. The restraint curves in this study are calculated using a similar method to that presented in [16] using uniform contraction in the young concrete, and the Young's modulus is 7 percent lower than in the adjoining concrete [25].

### 5.2.1 Example 1

Three walls-on-slab structures with different casting situations are considered with the dimensions according to [23]. The cross-section of the wall was constant, with the width of the wall 0.4m, and the height of the wall 2.25m. Different restraint conditions for the wall are applied in the three situations, all with free translation and free bending of the total structures, as follows:

- Wall 1 cast on slab 1, casting length ( $L_{cast}$ ) = 6m.
- Wall 2 cast on slab 2, the wall cast against existing slab 2 and existing wall 1,  $L_{cast}$  = 6m.
- Wall 3 cast on slab 3,  $L_{cast}$  = 12m.

The free casting length,  $L_{free}$ , is defined as the length of a monolithic structure with two free ends. This means that  $L_{free} = L_{cast}$  for cases a and c. For the case b, we have to imagine a free monolithic length that is twice the real casting length, i.e.  $L_{free} = 2 \cdot L_{cast} = 12m$ . The denotation  $L$  has the meaning  $L_{free}$  in the subsequent figures and text. The restraint is calculated using Eq. 5, and the resulting distributions in the walls for cases a-c are shown in figure 7, where  $y$  is the vertical coordinate, and  $y = 2.5m$  at the joint between the slab and the wall. The figure shows that the distribution of restraint with height is approximately linear and roughly the same for all three cases. These restraints have been applied to both LRM and CPM for non-plane section analyses, and the maximum strain ratios are presented in table 1, where  $t$  is the time after casting.

Table (1), results CPM and LRM.

Case	Method	$y, m$	$t, h.$	Strain ratio, -
Case a	CPM	2.789	126	1.0500
	LRM	2.843	124	1.0143
	CPM-C	2.817	126	0.8051
	LRM-C	2.843	124	0.7363
Case b	CPM	2.873	116	0.9714
	LRM	2.843	130	1.0893
	CPM-C	2.873	116	0.9714
	LRM-C	2.843	130	1.0893
Case c	CPM	2.873	116	0.9714
	LRM	2.941	130	1.0369
	CPM-C	2.873	116	0.9714
	LRM-C	2.941	130	1.0369

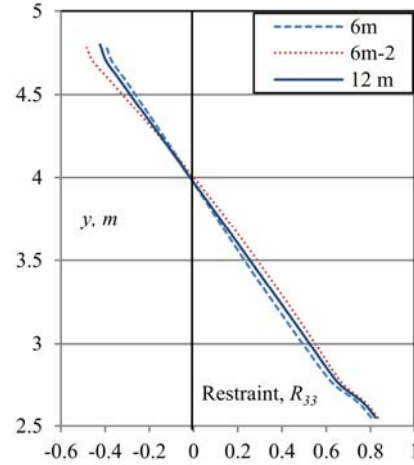


Figure 7 - Distribution of restraint with height in case a, b and c.

The denotation ‘-C’, see CPM-C and LRM-C, means that the slip factor according to figure 5 is taken into account. For the case a, the slip factor is 0.725, while in the other cases, b and c, there is no reduction due to slip effects, i.e. the slip factor is 1.0. The distributions of strain ratios at the time of maximum strain ratio are shown in figure 8. The strain ratio developments with time for the critical point are shown in figure 9. As can be seen in figure 8, the maximum strain ratios are approximately the same for case a using LRM and CPM, while the distribution in the wall is somewhat different. For cases b and c, the distribution is roughly the same, but the maximum strain ratio differs by about ten percent. These deviations might be dependent on the  $L/H$  ratio. In figure 9, it can be seen that the curve shapes for the strain ratio vs. time in the critical positions are very similar using LRM and CPM.

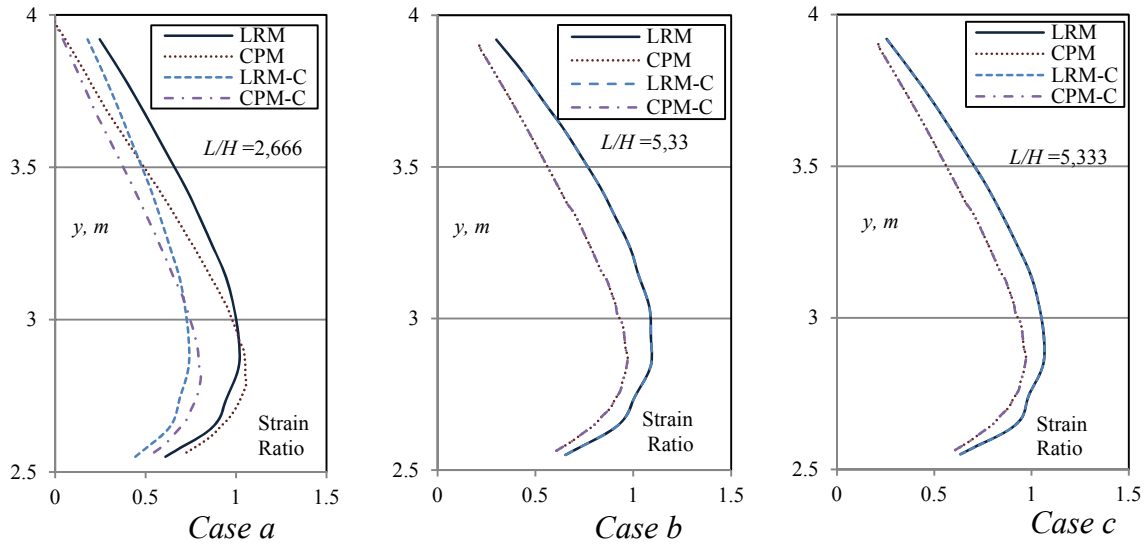


Figure 8 - Distribution of strain ratio with height at critical time using CPM and LRM.

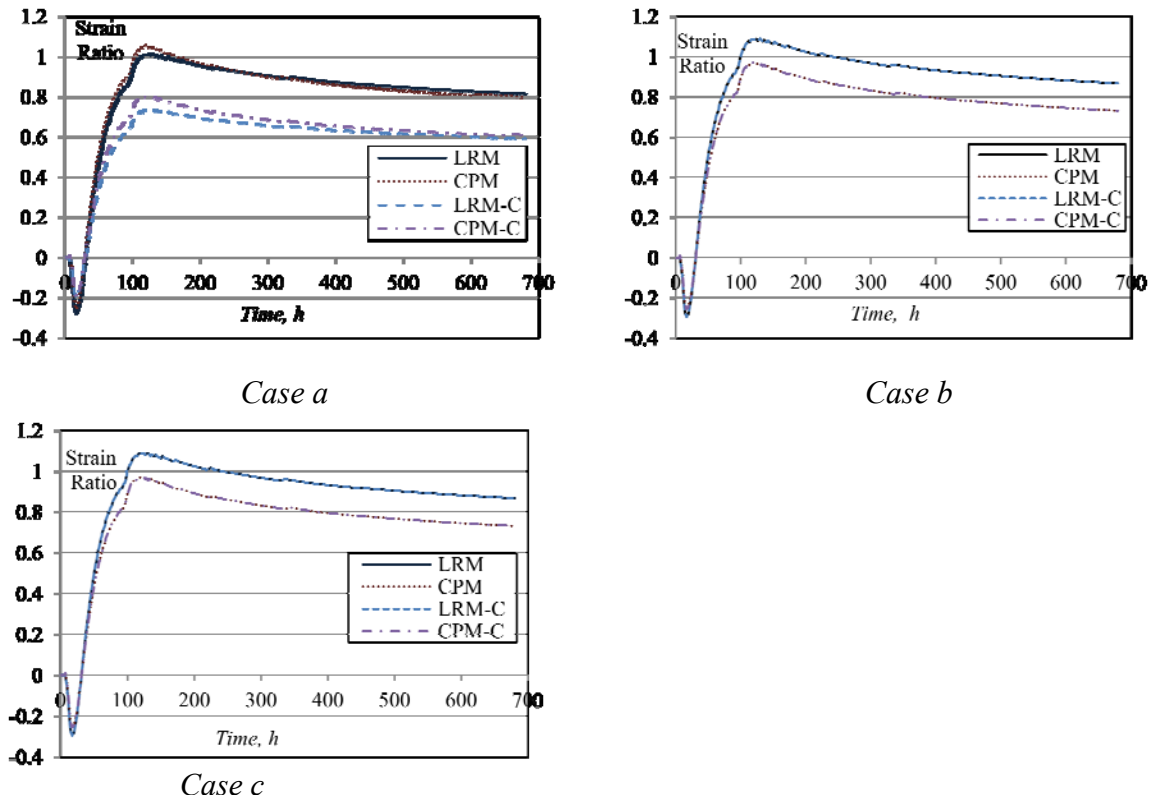


Figure 9 - Variation of strain ratio with time at the critical point in different casting situations, using CPM and LRM.

## 5.2.2 Example 2.

For a wall-on-slab structure, three walls with different length to height ratios are analyzed. The cross-section of the structure was constant; the width of the slab is 4m; the thickness of the slab is 1m; the width of the wall is 1m; the height of the wall is 4m; and the length of the wall is 5m ( $L/H$  1.25), 10m ( $L/H$  2.5), and 15m ( $L/H$  3.75), respectively. Different restraint conditions in

the walls occur, which is seen in figure 10. As can be seen from the figure the distribution is highly non-linear in the short wall,  $L=5\text{m}$ , while the distribution is approximately linear for  $L \geq 10\text{m}$ .

The maximum strain ratios for the LRM and CPM are presented in table 2. For  $L=5\text{m}$  and  $L=10\text{m}$  the resulting strain ratio using CPM is larger than that using LRM. However for  $L=15\text{m}$  the strain ratio using CPM is smaller than that using LRM. Considering the results from both table 1 and table 2, it seems that both LRM and CPM results in approximately the same maximum strain ratio for  $L/H$  in the region of about 2-4. As the restraint curves are constructed with a uniform contraction in the young concrete, the calculations presented here correspond to the “natural” situation, i.e. without measures taken on site.

Further, for short structures ( $L/H$  less than about 2) CPM yields higher strain ratios than LRM, but for longer structures ( $L/H$  greater than about 4) the opposite applies. According to figure 5, all cases in example 2 have slip factors less than 1, which also can be seen in figures 11-16.

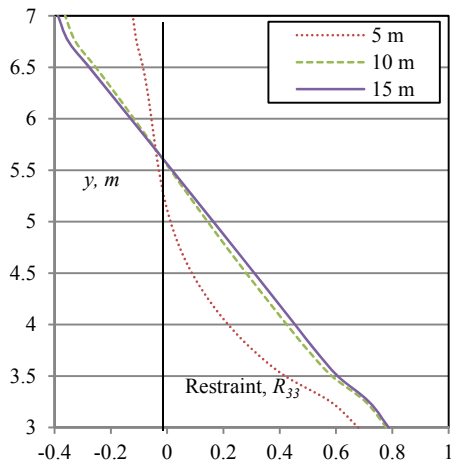


Figure 10 - Restraint variation with height for length 5, 10, and 15m.

Table 2 - Results CPM and LRM, example 2

Case	Method	$y, m$	$t, h$	Strain ratio, -
5m	CPM	3.325	272	1.3054
	LRM	3.25	272	1.0046
	CPM-C	3.325	272	0.7372
10 m	CPM	3.375	280	1.33
	LRM	3.5	272	1.2296
	CPM-C	3.375	280	1.0725
15 m	CPM	3.475	256	1.2428
	LRM	3.5	264	1.2719
	CPM-C	3.475	256	1.121
	LRM-C	3.5	264	1.157

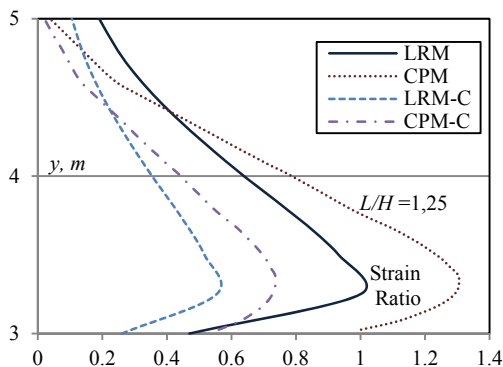


Figure 11 - Distribution of strain ratio with height at the critical time using CPM and LRM for 5m length.

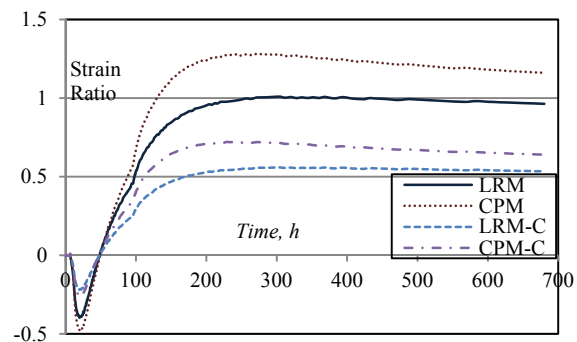


Figure 12 - Variation of strain ratio with time at the critical point for 5m length using CPM and LRM.

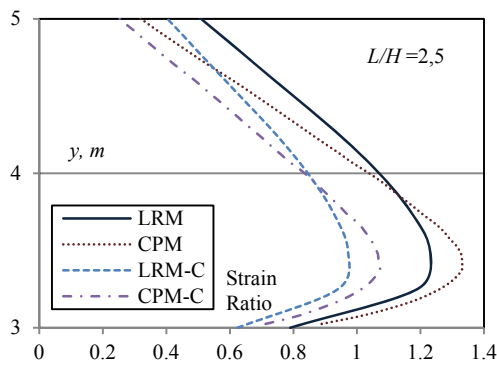


Figure 13 - Distribution of strain ratio with height, CPM and LRM using CPM and LRM for 10m

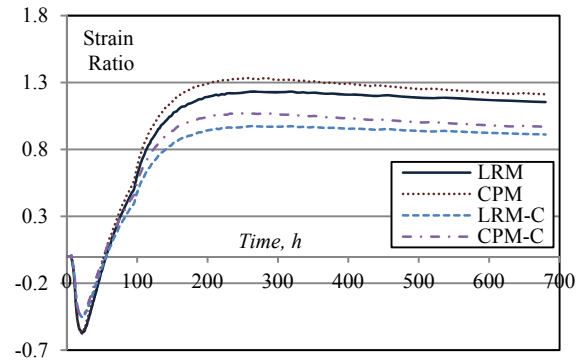


Figure 14 - Variation of strain ratio with time at the critical point using CPM and LRM for 10m

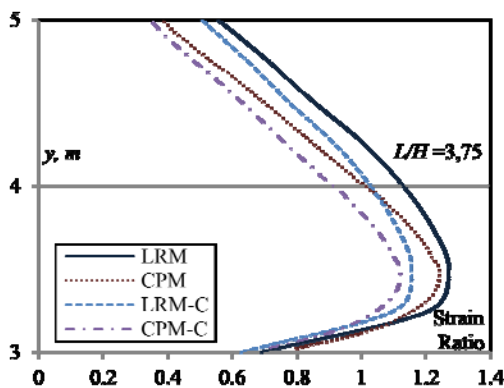


Figure 15 - Distribution of strain ratio with height, CPM and LRM for 15m length.

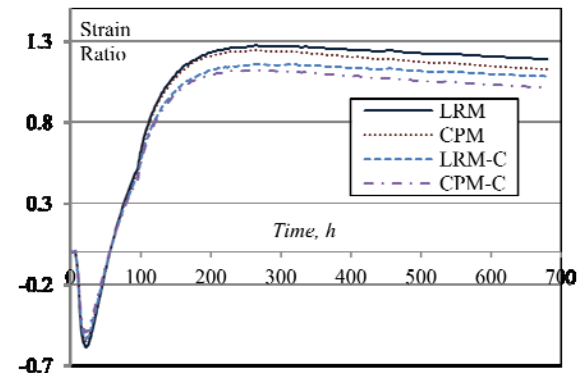


Figure 16 - Variation of strain ratio with time at the critical point using CPM and LRM for 15m.

From the results given in examples 1 and 2 one conclusion is that CPM and LRM are roughly the same for  $L/H \approx 2-4$ . This is very interesting since CPM and LRM are based on simplifications of different types. In CPM the non-plane sectional analyses are accounted for by the reduction of the load using restraint factors for walls on stiff foundations (figure 2). In LRM the same restraint factor is applied from the very beginning, i.e. from the time of casting. The "true" calculation results may be achieved by using a full 3D young concrete model, which is not possible in this project.

### 5.3 Development of equivalent restraint method ERM

The LRM can be used for analyzing the risk of through cracking when no measures are taken on site for situations where restraint curves have been established. The most common measures on site to reduce the crack risk are cooling of the newly cast concrete, [27] and [28], and heating of the adjacent structure [29]. CPM, when applicable, can be used for analysis and can accommodate both cooling and heating situations. As mentioned in chapter 4, basic LRM can only be used for cooling, if the estimated restraint is not changed significantly. In this chapter the outline for an equivalent restraint method (ERM) is established. The aim of this method is that it may be applied to both cooling and heating situations. The main steps to outline the ERM are:

- 1) Establish a stress or strain curve in the young concrete taking into account the restraining from the adjoining structure without measures (cooling/heating) by using LRM.
- 2) Choose relevant parts of the young concrete and adjoining structures to be used in CPM. In most cases this means the use of the same cross-section as in LRM and a part of the adjacent structures.
- 3) Create an equivalent restraint model, ERM, by the use of CPM matching the stress or strain curves in step 1 for the critical part of the young concrete by adjustments of boundary conditions for the chosen structure in step 2. This is performed by adjusting the parameters  $R_M$ ,  $R_N$ ,  $\delta_{res}$  in Figure 2 and  $\delta_{slip}$  in figure 5.
- 4) ERM from step 3 can be applied to both cooling and heating with relevant interaction between old and young concrete in a similar way as in basic CPM.

#### 5.4 Example on application of ERM

The ERM is applied here to the second and third casting of the hollow pillar in figure 17. The first casting sequence could also be applied to ERM as well as basic CPM using the typical wall-on-slab structure, but this is not shown here. The dimensions of the slab are  $1.7 \cdot 10\text{m}$  founded on frictional material. The outer dimension of the pillar is  $3.8\text{ m}$ ; the thickness of pillar walls is  $0.5\text{m}$ , and the height of each casting sequence of the pillar is  $5\text{m}$ .

Restraint curves from 3D calculations using Eq. 5 for homogeneous contraction in the new concrete are shown in Figure 18a for the first casting sequence of the pillar using different finite-element mesh from  $0.05 \cdot 0.05\text{m} - 0.5 \cdot 0.5\text{m}$ . Based on these results the restraint curves in figure 18b are calculated using the mesh  $0.25 \cdot 0.25\text{m}$ . As can be seen in the figure, the restraint curve is practically the same for sequences two and three, and the restraint for the first casting is somewhat higher.

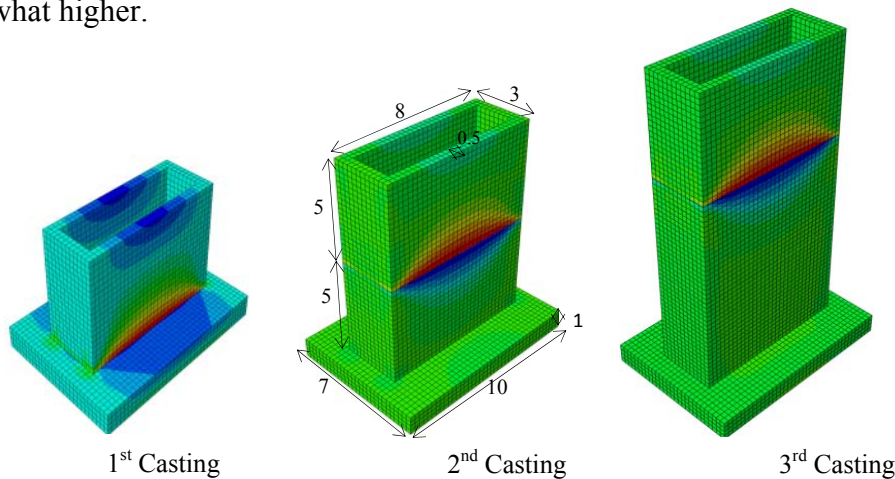


Figure 17 – Three casting sequence of a pillar.

The ERM is configured using CPM, where the new concrete and a chosen part of the adjacent old concrete is analyzed; see figure 19 for areas marked dark and light gray, respectively. For the ERM structure the boundary conditions are adjusted in such a way that the resulting stress-strain curve is in satisfactory agreement with the stress-strain ratios from LRM in the critical part of the young concrete, see LRM No measurement and EQM No measurement curves in figure 20. The construction of the ERM in figure 20 is created by the use of the ConTeSt program [15] with the following adjustments values:  $R_M = 0$ ,  $R_N = 0$ ,  $\delta_{res}$  for  $L=22\text{m}$ , and  $\delta_{slip}=0.95$ .

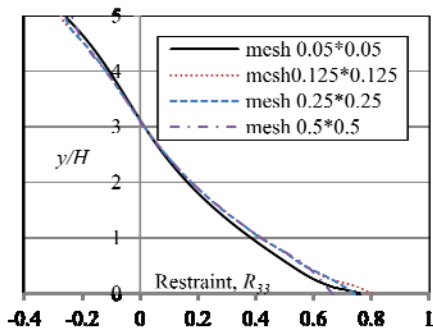


Figure 18a - Effect of mesh on restraint.

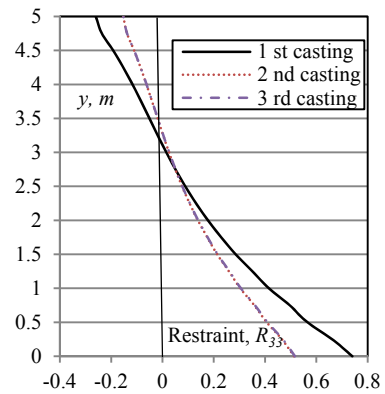


Figure 18b - Variation of restraint in three casting sequences of a pillar.

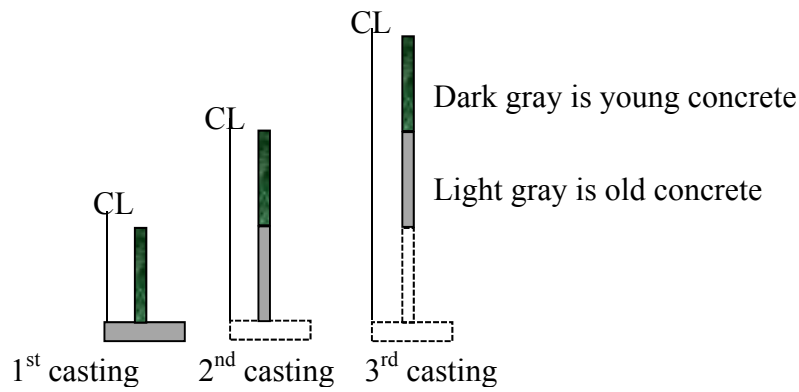


Figure 19 – Choice of equivalent models for three casting sequences of a pillar.

As can be seen in figure 20, the reduction of the strain ratio in the newly cast concrete can be estimated either by the LRM or the ERM for cooling in the young concrete or by the ERM when heating the adjacent structure before casting the new concrete .

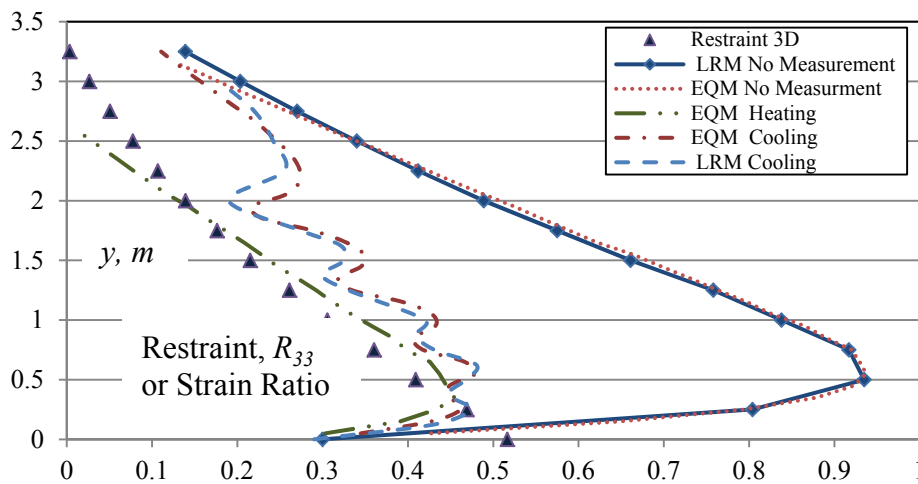


Figure 20 – Calibration of equivalent restraint method without measures, and effect of cooling pipes using LRM and ERM, and effect of heating using ERM.

## 6. RESTRAINT BY LRM FOR SOME COMMONLY USED INFRASTRUCTURES

### 6.1 General parameters

The restraint in the young concrete using Eq. 5 has been estimated in the 3D FEM calculations by the use of the following parameters:

- Elastic modulus in young concrete is 27.9 GPa.
- Elastic modulus in old (existing) concrete is 30 GPa.
- Poissons ratio in both young and old concrete is 0.2.
- Elastic modulus in rock is 20 GPa.
- Poissons ratio in rock is 0.35.

In the following, two specific infrastructures are used to show restraint curves for

- A double tunnel founded on frictional material
- A single tunnel founded on rock material

For the double tunnel the decisive restraints in different directions for consecutive casting sequences are calculated. For the single tunnel, the effect of different sizes of adjacent rock on the restraints in the length direction of the tunnel is presented.

### 6.2 Typical structure 1 - double tunnel founded on frictional material

The dimension and shape of the cross-section (in the  $xy$  plane) in the double tunnel is shown in figure 21. The length of each casting sequence is 15m (in the  $z$  direction).

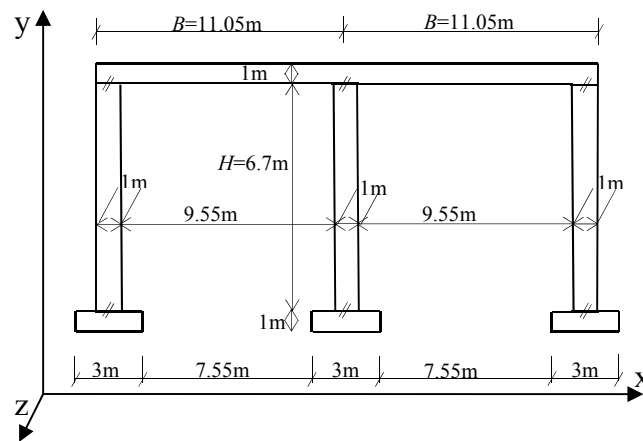


Figure 21- Cross-sectional dimensions of typical structure 1.

The restraint for typical structure 1 is estimated for three casting sequences for both the walls the roof, see figure 22. No restraint is estimated for the slabs as the dimensions are small and they are founded on frictional material. This means there is no significant risk of through cracking in the slabs.

All restraint curves are evaluated as uniaxial restraint parallel with the direction of the joint to the adjacent structure, see  $R_i$  in eq. 5. This means that for the walls  $R_{22}$  ( $R_y$ ) and  $R_{33}$  ( $R_z$ ) have been estimated depending on the direction of the restraining joint. For the roof the corresponding restraints are  $R_{11}$  ( $R_x$ ) and  $R_{33}$  ( $R_z$ ) respectively.

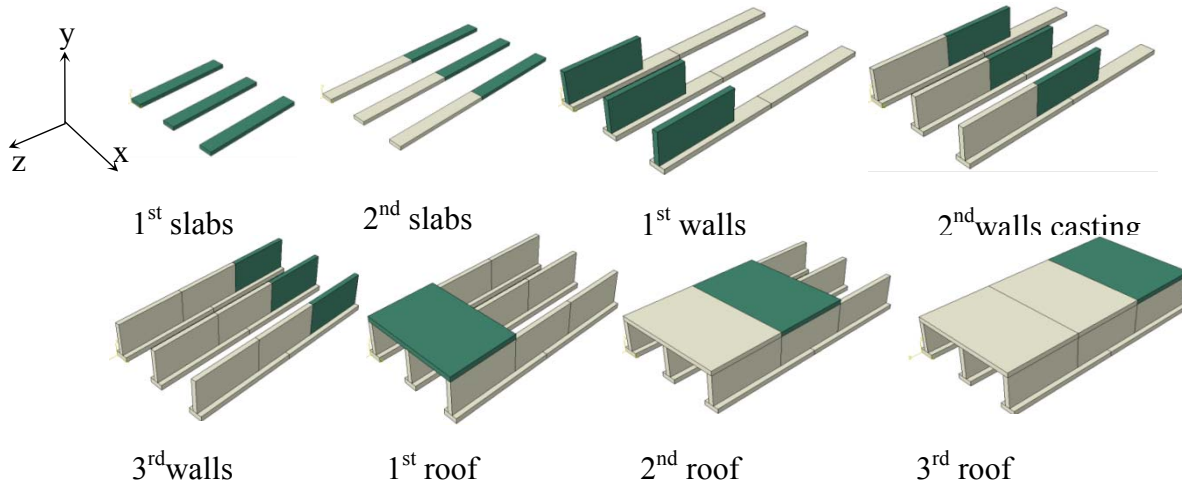


Figure 22 - Casting sequences for typical structure 1. Dark gray color means young concrete and light gray means old concrete.

The location of the maximum restraint in the horizontal joint between wall and slab for the 1<sup>st</sup> casting is at the middle of the joint, [13] and [16]. The resulting  $R_{33}$  in the critical point for typical structure 1 is shown in figure 23. For the 2<sup>nd</sup> and 3<sup>rd</sup> casting sequence of the wall, the critical point occurs at a distance of about  $0.2L$  from the joint, [21] and [25]. The evaluated critical results are shown in figure 23. As can be seen in the figure, the restraints for the 2<sup>nd</sup> and 3<sup>rd</sup> castings are roughly the same. In the tensile region, from  $y/H \approx 0.1$  to about  $0.6$ , the restraint for the 1<sup>st</sup> casting is somewhat lower than the restraints in the subsequent castings.

The location of the largest restraint in the vertical joint between wall and wall is about  $0.2H$  from the joint. The resulting  $R_{22}$  in the critical point is shown in figure 24. The critical part, as regards cracking, is the tensile restraint region, in this case from  $z/L = 0$  to about  $0.2$ . From figure 24 it is seen that the critical restraint is somewhat higher for the 3<sup>rd</sup> wall than in the 2<sup>nd</sup> wall casting.

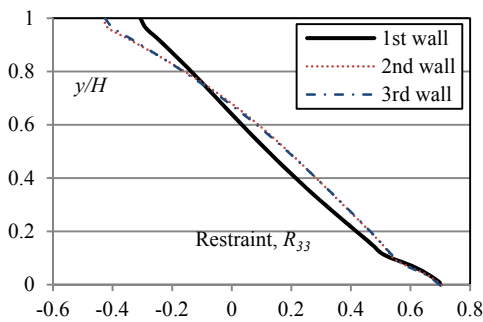


Figure 23- Restraint  $R_{33}$  in wall.

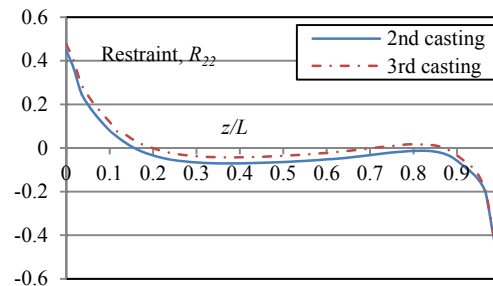


Figure 24 - Restraint  $R_{22}$  in wall.

For the 1<sup>st</sup> casting of the roof slab, the location of the largest restraint, as regards the horizontal joint between the roof and the wall, occurs in the middle of the roof in respect to the  $z$ -direction. The resulting  $R_{33}$  ( $R_z$ ) at the critical point is shown in figure 25. For the 2<sup>nd</sup> and 3<sup>rd</sup> castings of the wall, the critical point occurs near the outer walls at a distance of about  $0.2L$  from the free edge (in the  $z$ -direction). The resulting  $R_{33}$  ( $R_z$ ) for  $0.2L$  is shown in figure 25 and are denoted 2<sup>nd</sup> and 3<sup>rd</sup> roof. For the mid-section of the slab ( $0.5L$ ) the largest restraints,  $R_{33}$ , occur near the inner walls and are higher than the corresponding restraints at  $0.2L$  (compare the lines denoted 2<sup>nd</sup> and 3<sup>rd</sup> mid roof with those denoted 2<sup>nd</sup> and 3<sup>rd</sup> roof in figure 25). As can be seen in figure

25, the restraints in z-direction are different for all the casting sequences, and that the restraints are higher near the outer walls compared with the inner wall.

As regards the vertical joints between the different casting sequences of the roof, the location of the largest restraint occurs about  $0.2B$  from the inner wall. The resulting  $R_{11}$  ( $R_x$ ) at the critical point is shown in figure 26 for the 2<sup>nd</sup> and 3<sup>rd</sup> casting sequences. The rather small restraints for the 1<sup>st</sup> part of the roof are located at the position  $z/L = 0.5$  and originate from the horizontal joints between the roof and the walls. The tensile restraint region for the 2<sup>nd</sup> and 3<sup>rd</sup> castings are rather large, from joint and up to about  $0.7L$ , and the restraints are roughly the same.

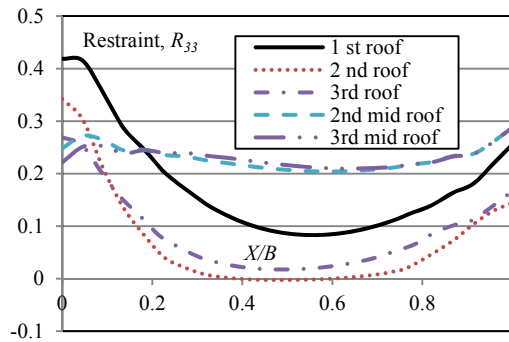


Figure 25 - Restraint  $R_{33}$  in the roofs.

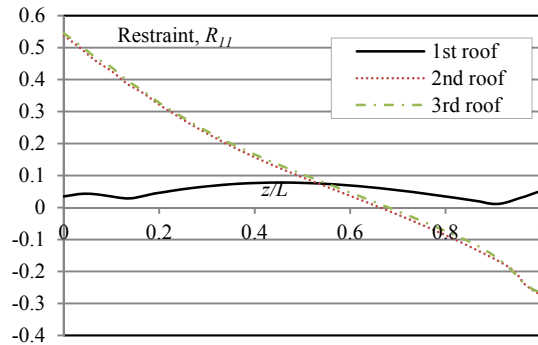


Figure 26 – Restraint  $R_{11}$  in the roofs.

### 6.3 Typical structure 2 - single tunnel founded on rock material

The shape of the cross-section (in the  $xy$  plane) for the single tunnel founded on rock and attached on two sides of the slabs (bottom and outer side), is shown in figure 27. Neither walls nor roof are connected to the rock. The length of each casting sequence is 17.5m (in the  $z$  direction). The restraint for typical structure 2 is estimated for two casting sequences for the slabs, walls and roof, see figure 28.

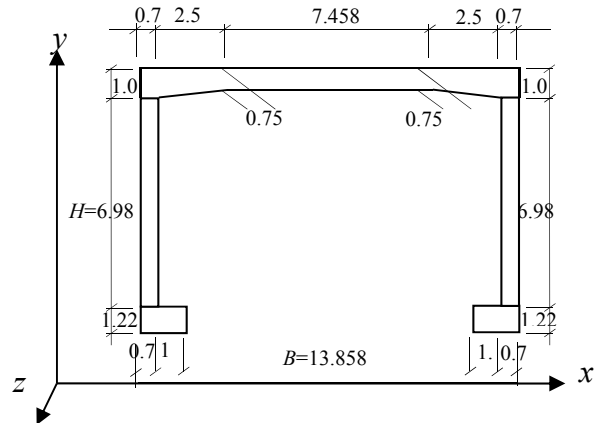


Figure 27- Cross-section of typical structure2.

All restraint curves are evaluated as  $R_{33}$  ( $R_z$ ) with respect to horizontal joints. The aim here is to evaluate the effect of rock dimensions on restraint in slabs, walls, and roof. The analyzed block of rock is shown in figure 29, where the side-length of the block,  $L_{Rock}$ , has been varied between 36 and 120m. The center  $yz$ -cross-section is the same for the rock block and the concrete structure.

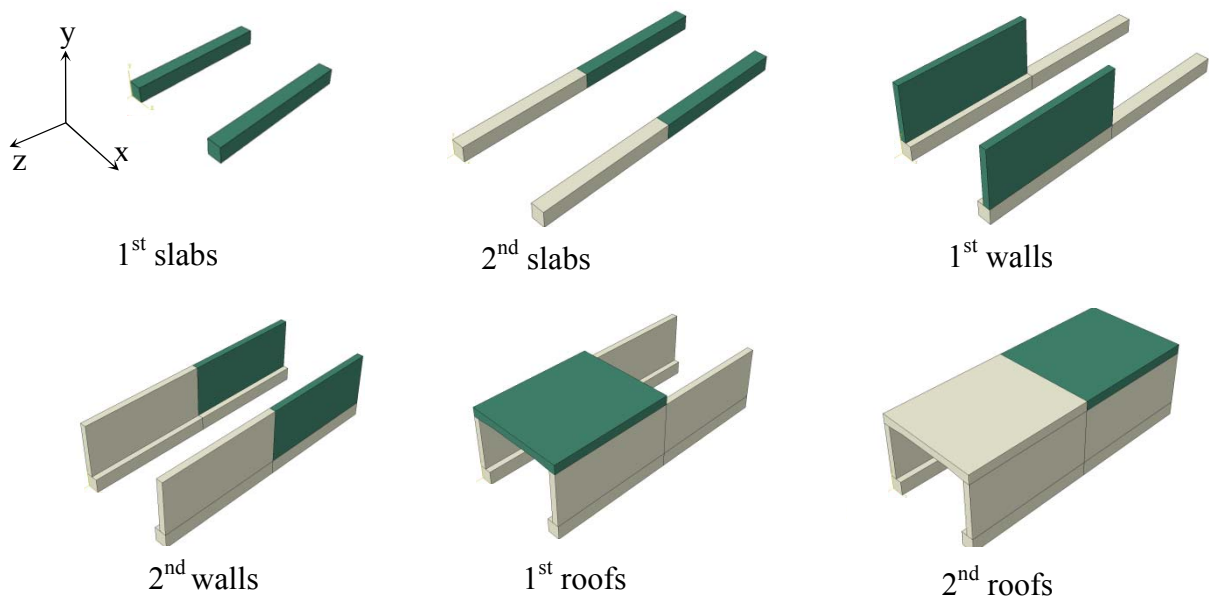


Figure 28 – Casting sequence of typical structure 2. Dark gray is young concrete, light gray is old.

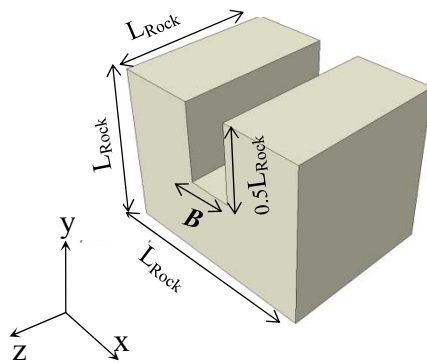


Figure 29 - Rock dimensions

For both the 1<sup>st</sup> and 2<sup>nd</sup> slab casting, the location of the largest  $R_{33}$  is in the middle of the slab. This result for the 1<sup>st</sup> slab is as expected, while this result for the 2<sup>nd</sup> slab is probably due to the effect of high restraint from the rock. As can be seen in figures 30 and 31, the restraint is higher in the 2<sup>nd</sup> slab, which probably originates from the horizontal joint between the slabs. The highest restraint is reached for rock blocks larger than 100m for the 1<sup>st</sup> slab casting, while for the 2<sup>nd</sup> slab casting it is already reached at  $L_{rock}$  equal to 50m.

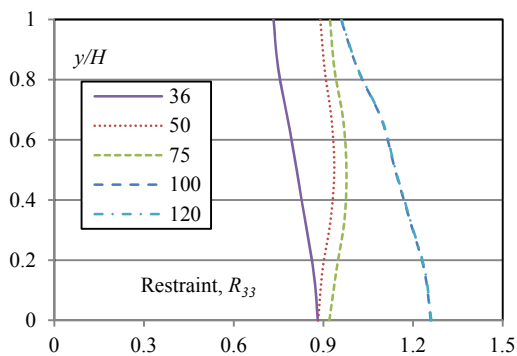


Figure 30 – Restraint  $R_{33}$  in 1<sup>st</sup> slab.

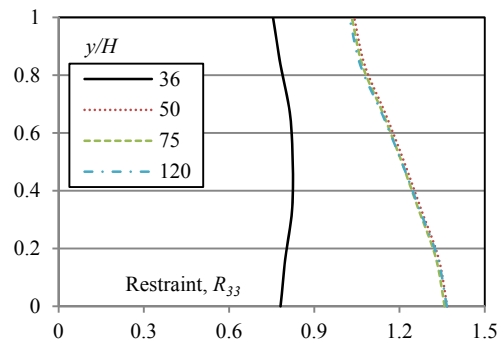


Figure 31 - Restraint  $R_{33}$  in 2<sup>nd</sup> slab.

The walls are not in contact with the rock at any position. The location of the largest restraint is in the middle of the wall for the 1<sup>st</sup> casting, and at about  $0.25L$  from joint for the 2<sup>nd</sup> wall casting. For both the 1<sup>st</sup> and 2<sup>nd</sup> roof casting the highest restraint effect is reached at a rock dimension of 50m, see figures 32 and 33. As can be seen in the figures, the restraint for the 1<sup>st</sup> roof casting is slightly lower than the 2<sup>nd</sup> roof casting.

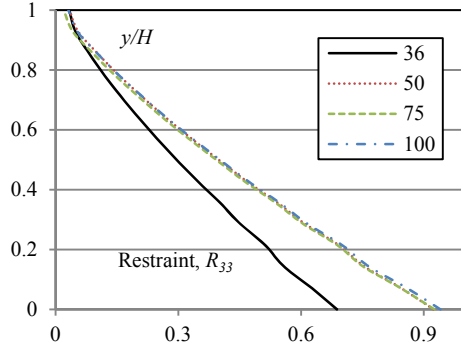


Figure 32 - Restraint  $R_{33}$  in 1<sup>st</sup> wall.

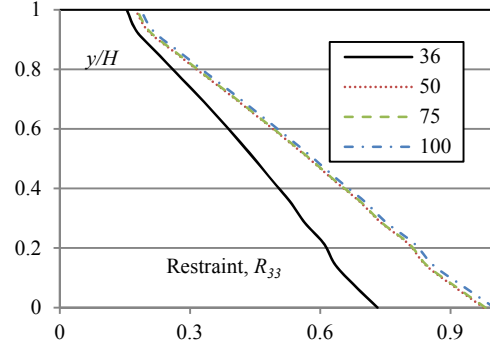


Figure 33 - Restraint  $R_{33}$  in 2<sup>nd</sup> wall.

For the 1<sup>st</sup> roof casting, the location of the largest restraint  $R_{33}$  is about  $0.66L$  from the free edge, while the location of largest  $R_{33}$  in the 2<sup>nd</sup> roof casting is about  $0.3L$  from the joint. The resulting  $R_{33}$  in the critical section is shown in figures 34 and 35. As can be seen from the figures, the highest restraint for both 1<sup>st</sup> and 2<sup>nd</sup> roof castings are reached at 50m. Figure 34 shows that the highest restraint is concentrated near the wall, while, on average, figure 35 shows somewhat higher restraint all over the roof in the critical section.

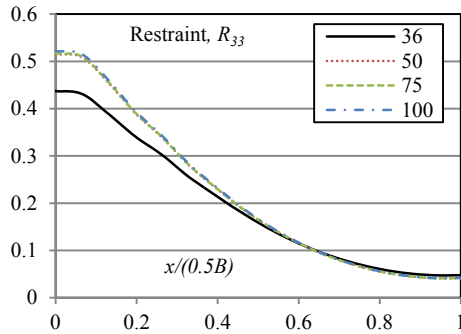


Figure 34 - Restraint  $R_{33}$  in 1<sup>st</sup> roof.

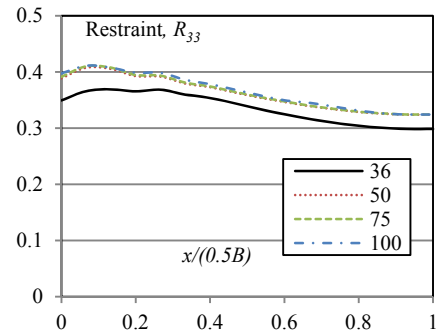


Figure 35 - Restraint  $R_{33}$  in 2<sup>nd</sup> roof.

The results for typical structures 1 and 2 might be applied directly in design (using LRM and ERM). It would be beneficial to study the effect of parameter variations to aid the implementation in practice.

Furthermore, it would be of interest to study other typical cases. In the second part [30] connected to this paper restraint factors for typical case wall-on-slab are presented in a simplified model using artificial neural network (ANN).

## 7. CONCLUSIONS

The CPM is primarily constructed to be used for structures with cross-sections simulated by axial deformation together with one or two rotations. This is not the case in more complicated structures, but LRM might be used in any type of structure at least as a basis for the estimation of risk for through cracking. Both CPM and LRM can be used when analyzing situations where no measures are taken on site. For walls-on-slabs CPM and LRM have shown to give resulting stresses for young concrete in the same order of size, especially for length to height ratios of about 2-4.

When CPM is applicable, measures taken on site, such as cooling and heating, are easy to examine, however when using basic LRM only cooling may be analyzed. In this paper an improved method, ERM (equivalent restraint method), has been developed. ERM is calibrated using LRM without measures, and it can easily be applied to accommodate both heating and cooling.

The restraint situations for two typical infrastructures are presented, and such restraint curves might be applied directly in design using LRM and ERM. For practical implementation it would be beneficial to perform further studies as regards the effects of parameter variation for a number of typical cases.

## 8. REFERENCES

1. ACI Committee 207, "Effect of Restraint, Volume Change, and Reinforcement on Cracking of Massive Concrete," ACI Committee 207.ACI207.2R-95. Reapproved 2002, 26 pp.
2. Emborg, M & Bernander, S., "Assessment of the Risk of Thermal Cracking in Hardening Concrete," *Journal of Structural Engineering*, ASCE, Vol.120, No 10, October 1994. pp. 2893-2912.
3. Mihashi, H., & Leite, J.P., "State of The Art Report on Control of Cracking in Early Age Concrete," *J. Advanced Concrete Technology*, 2004, 2 (2) pp. 141–154.
4. Kianousha, M.R., Acarcanb, M, Ziari, A., "Behavior of base restrained reinforced concrete walls under volumetric change," *Engineering Structures*, 30, 2008, pp.1526–1534.
5. Cusson, D. & Repette, W., "Early-Age Cracking in Reconstructed Concrete Bridge Barrier Walls," *ACI Materials Journal*, 97(4), July/August, 2000, pp. 438-446.
6. Bosnjak, D., "Self-Induced Cracking Problems in Hardening Concrete Structures," Department of Structural Engineering, Norwegian University of Science and Technology Doctoral Thesis 2000, 171 pp.
7. Rostásy, F S, Tanabe, T., Laube, M., "Assessment of External Restraint. In: Prevention of Thermal Cracking in Concrete at Early Ages," Ed. by Springenschmid. London, England: E& FNSpon. RILEM Report 15. State of- the Art Report by RILEM Technical Committee 119, prevention of Thermal Cracking in Concrete at Early Ages.1998, pp. 149-177.
8. Emborg, M., "Development of Mechanical Behavior at Early Age," Ed. by R. Springenschmid. London, England: E & FNSpon. RILEM Report 15. State of- the Art Report by RILEM Technical Committee 119, Prevention of Thermal Cracking in Concrete at EarlyAges.1998, pp. 77-148.
9. JSCE, "English Version of Standard Specification for Concrete Structures 2007," Japan Society of Civil Engineer, JSCE, December, 2010, 503 pp.

10. Sato, R., Shimomura, T., Maruyama, I., Nakarai, K., "Durability Mechanics of Concrete and Concrete Structures Re-Definition and a New Approach," Committee Reports of JCI, 8th International Conference on Creep, Shrinkage and Durability of Concrete and Concrete Structures (CONCREEP8), Ise-Shima, Japan, 2008.10.1.
11. JCI., "A Proposal of a Method of Calculating Crack Width due to Thermal Stress," Tokyo, Japan: Japan Concrete Institute, Committee on Thermal Stress of Massive Concrete Structures, JCI Committee Report.1992, 106 pp.
12. Emborg, M., "Thermal Stresses in Concrete at Early Ages," Doctoral Thesis, Division of Structural Engineering, Lulea University of Technology, 1989, 172 pp.
13. Bernander, S., "Practical Measurement to Avoiding Early Age Thermal Cracking in Concrete Structures," Prevention of Thermal Cracking in Concrete at Early Ages. Ed.by R. Springenschmid. London, England: E & FNSpon. RILEM Report 15. State of- the Art Report by RILEM Technical Committee 119, prevention of Thermal Cracking in Concrete at Early Ages.1998, pp. 255-315.
14. Jonasson, J.E., Wallin, K., Emborg, M., Gram, A., Saleh, I., Nilsson, M., Larsson, M., Hedlund, H., "Temperature Cracks in Concrete: Manual With Diagrams Sprick risk bedömning Including Measures for Some Common Scenarios," Part D and E., Technical report / Lulea University of Technology, 2001:14. Lulea: Lulea University of Technology, 2001, 110 pp. (in Swedish).
15. ConTeSt Pro., "User's Manual - Program for Temperature and Stress Calculations in Concrete," Developed by JEJMS Concrete AB in co-operation with Lulea University of Technology, Cements AB and Peab AB. Lulea, Sweden, 2003, 198 pp.
16. Nilsson, M., "Restraint Factors and Partial Coefficients for Crack Risk Analyses of Early Age Concrete Structures," Lulea, Sweden, Division of Structural Engineering, Lulea University of Technology. Doctoral Thesis 2003, 170 pp.
17. Olofsson, J., "3D Structural Analyses of Crack Risk In Hardening Concrete Structures Verification of Three Steps Method Methods," Lulea University of Technology, Division of Structural Engineering, IPACS Report, ISBN 91-89580-53-2, 1999, 52 pp.
18. Kheder, R., Al-Rawi, J., Al-Dhahi, K., "A Study of the Behavior of Volume Change Cracking in Base Restrained Concrete Walls," *Materials and Structures*, 27, 1994, pp. 383-392.
19. Klemczak, B., & Knoppik, A., "Early Age Thermal and Shrinkage Cracks in Concrete Structures Influence of Geometry and Dimensions of Structure," *Architecture Civil Engineer Environment*, the Silesian University of Technology, No.3, 2011, pp., 55-62.
20. Schiessl, P., Beckhaus, K., Schachinger, I., Rucker, P., "New Results on Early-Age Cracking Risk of Special Concrete," *Cement, Concrete and Aggregates*, Volume: 26, Issue Number: 2, 2004, ID CCA12304.
21. Bamforth, P. B., "Early Age Thermal Crack Control in Concrete," CIRIA 2007, Construction Industry Research and Information Association, London, CIRIA 2007, RP722 ISBN 978-8-86107-660-2, 112 pp.
22. Sule, M., & Van Breugel, K., "Cracking Behavior of Reinforced Concrete Subjected to Early-Age Shrinkage," *Materials and Structures*, Vol. 34, June 2001, pp., 284-292.
23. 4C-Temp & Stress for concrete - Description. (n.d.), Retrieved from Danish Technological Institute: <http://www.dti.dk/1265>.
24. B4cast ver. 3.0, User guide Available from ConTech Analysis ApS, program analyses <http://www.b4cast.com/default.htm>.
25. Larson, M., "Thermal Crack Estimation in Early Age Concrete Models and Methods for Practical Application," Lulea, Sweden, Division of Structural Engineering, Lulea University of Technology, Doctoral Thesis 2003.

26. Jonasson, J.E., Wallin, K., Nilsson, M., "Casting of Concrete Wall on Slabs, Study of Risk of Cracking Due to Temperature Changes during the Hardening Process," Lulea, Sweden, Division of Structural Engineering, Lulea University of Technology, 2009, 73 pp.
27. Emborg, M., & Bernander, S., "Avoiding of Early Age Thermal Cracking in Concrete Structures Predesign, Measures, Follow-Up," in "Thermal Cracking in Concrete at Early Ages," Proc. of the RILEM International Symposium, Edited by R. Springenschmid, E & FNSpon, London, 1994, pp. 409-416.
28. COIN Project report no 31, Bjøntegaard, O., "Basis for Practical Approaches to Stress Calculations and Crack Risk Estimation in Hardening Concrete Structures, State of the Art," (Norwegian Public Roads Administration), FA., 3, Technical performance, S.P., 3.1 Crack Free Concrete Structures, 2010, pp142.
29. Wallin, K., Emborg, M., Jonasson, J.E., "Heating Alternative to Cooling," Technical report, Lulea University of Technology, 1997:15. Lulea: Lulea University of Technology, 1997, 168 pp. (in Swedish).
30. Al-Gburi, M., Jonasson, J.E., Yousif, S., T., and Nilsson, M., "Simplified Methods for Crack Risk Analyses of Early Age Concrete Part 2: Restraint Factors for Typical Case Wall-on-Slab," aim to be published in the Nordic Concrete Research as this article part 1.



## **Paper II:**

### **Thermal Crack Risk Estimations of Concrete Tunnel Segments - Equivalent Restraint Method Correlated to Empirical Observations.**

**Hösthagen A**, Jonasson J-E, Emborg M, Hedlund H, Wallin K, Stelmarczyk M, Published in Nordic Concrete Research, Publication no. 49, 2014, pp. 127-143.

## Thermal Crack Risk Estimations of Concrete Tunnel Segments - Equivalent Restraint Method Correlated to Empirical Observations.



Anders Hösthagen, M.Sc. Ph.D. Student  
Projektengagemang AB & Lulea University of Technology (LTU)  
Div. Structural and Construction Engineering, SE-971 87 Luleå  
Email: anders.hosthagen@projektengagemang.se



Prof, Dr. Jan -Erik Jonasson  
Lulea University of Technology  
Div. Structural and Construction Engineering, LTU  
Email: jej@ltu.se



Prof, Dr. Mats Emborg  
Div. Structural and Construction Engineering, LTU &  
Betongindustri AB, Box 47312, SE-100 74 Stockholm  
Email: mats.emborg@ltu.se/mats.emborg@betongindustri.se



Adjunct prof, Dr. Hans Hedlund  
Skanska Sverige /Div. Structural and Construction Engineering, LTU  
Email: hans.hedlund@skanska.se/hans.hedlund@ltu.se



Kjell Wallin, Consulting Engineer  
Projektengagemang AB  
Email: kjell.wallin@projektengagemang.se



Marcin Stelmarczyk, M.Sc. CEO  
The Green Dragon Magic  
Email: marcin@greendragonmagic.com

### ABSTRACT

Avoiding thermal and moisture induced cracking in newly cast concrete structures implies large economical and technical benefits. Thus, it is of large interest to model one of the major influencing parameters correctly: the restraint. The present study deals with the correlation between numerical models and empirical observations regarding the restraint. The equivalent restraint method, ERM, is used which is established from calculations with the local restraint method, LRM. Casting of walls and roof in a tunnel construction is investigated. Correlation between models and empirical measurements is established in three steps: 1) the restraint situation is analyzed; 2) the calculated temperature developments are compared to empirical temperature measurements to calibrate the models; and 3) calculated strain ratios are compared with observed crack patterns. In general a good correlation is achieved.

**Key words:** Thermal and moisture cracking, early age concrete. local restraint method, equivalent restraint method, modelling

## 1. INTRODUCTION

The movements within newly cast concrete are inherited from temperature and moisture states and may cause cracking during the construction, see e.g. [1], [2], [3], [4] and [5]. For complex structures, such as bridges, tunnels, foundations and piers, comprehensive pre-calculations need to be performed in order to analyze the risk of cracking during heating phase and cooling phase. If high strains/stresses are predicted for any part of the structure, measures are needed to avoid cracking. Examples of measures are cooling of the young concrete, preheating of the adjoining construction and/or optimized concrete mix (alternative binders, lower cement content etc.). Such measures are described among others in [6], [7] and [8]. In the case of casting a section against an adjoining structure or a restraining entity (such as rock, subgrade), the restraint influencing on the newly cast concrete increases, and with high restraint the risk of cracking becomes higher, [1] and [9].

It is understood that to design the measures in a cost-effective fashion reliable predictions of restraint are crucial. However, it is known that the restraint usually is difficult to estimate correctly and therefore is an uncertain factor [6]. It is also known that models achievable to estimate the restraint and risk of cracking have different benefits and withdrawals. Here, the model called Equivalent Restraint Method, ERM [10], is used. Benefits of this method involve a possibility to extract the restraint analyzed by elastic 3D calculations and implement it into a compensated plane method for young concrete. These calculations are efficient from a time saving point of view compared with the use of a 3D viscoelastic-viscoplastic simulation for young concrete. Furthermore, the ERM makes it possible to analyze arbitrary measures/actions onsite in an easier way, such as cooling and/or heating.

This paper demonstrates the correlation between numerical models and empirical experiences specially regarding restraint modelling. By studying crack inventories and temperature measurements from a tunnel project and comparing to numerical models, conclusions regarding the correlation are made. The casting of wall and roof segments is investigated and to estimate the restraint situation Abaqus version 6.12 is used and the temperature and stress/strain ratio calculations are performed with ConTeSt version 5.0 [11].

## 2. AIMS AND OBJECTIVES

Besides evaluating the numerical model ERM (Equivalent Restraint Method) by correlating estimated crack risk to empirical observations of the resulting crack pattern the following aims and purposes of the present research are defined:

- To investigate the effect on the restraint when casting walls using a different casting order. The order of casting in a segmented wall is either as a series (Case 1 ) or casting a wall in between two completed walls (Case 2).
- To investigate the effect on the restraint when casting roof segments using different casting order. The order of casting the roof segments is either as a series (Case 3) or casting one segment in between two completed segments (Case 4).

### 3. THEORY

The Equivalent Restrain Method, ERM, is a method to analyze the risk of through cracking. ERM is a further development from the Local Restrain Method [10] and is an improved method to which arbitrary measures/actions against cracking can be applied. To the LRM only cooling is possible to model. Where the LRM is based on semi 2D analysis as a point wise calculation method the ERM is a semi 2D method where the restraint situation at every LRM step is combined into one ERM model by regression analysis. Since both LRM and ERM are based on linear line analysis they are denoted as semi 2D analysis methods. The establishment of the ERM is made in three steps;

The first step: *Estimation of the restraint situation.* By normalizing the restraint within young concrete according to:

$$|\alpha \cdot \Delta T \cdot 0.93 \cdot E_c| \equiv 1 \quad (1)$$

an elastic analysis shows the restraint situation for the young concrete. In Eq (1)  $\alpha$  is the heat expansion coefficient;  $\Delta T$  is the temperature change within the young concrete;  $E_c$  is the Youngs modulus for the mature, adjacent concrete; and 0.93 is a factor to convert the Youngs modulus from mature to young concrete. The system is set to be statically determined in order to simulate a self-balancing system. The maximum restraint for the axis of interest is searched and a 2D (position and restraint magnitude) restraint profile is exported into the second step.

The second step: *Calculation point wise stress/strain ratios with LRM.* The restraint profile given in the first step is used as input to the translation restraint parameter. Several files are created where the stress/strain ratio is calculated at different heights (or positions).

The third step: *Obtaining ERM by regression analysis with LRMs as a base.* A model is created where the translation and rotation restraint, resilience behaviour, construction length and restraining block design are varied to obtain a similar stress/strain ratio profile within the interesting span from the LRMs.

Using the same conditions (e. g. temperatures, measures/actions, material parameters) as for an empirical case into the model, post-calculations for the onsite crack risk can be made. Comparisons to observed crack patterns then tell whether or not the model gives reasonable results.

## 4. CALCULATIONS AND RESULTS

### 4.1 Geometries studied

Four different cases have been investigated. Two cases are dealing with casting wall segments in a tunnel construction (Case 1 and 2), and two cases with roof segment casting (Case 3 and 4). In Case 1 the end wall in a cast series is studied, see Figure 1. Case 2 handles the situation where the intermediate (second wall) is cast between two existing walls. The wall segments in Case 1 and 2 are parts of wall 1 in Figure 3. In Case 3 the end roof segment in a cast series is studied, see Figure 2, and in Case 4 the intermediate roof segment (second roof) is studied. Later in this paper the strain situation in the roof is compared to observed crack patterns. Since crack

patterns are only documented for the part of the roof between wall 1 and 2, see Figure 3, only this area is analyzed with the LRM and ERM.

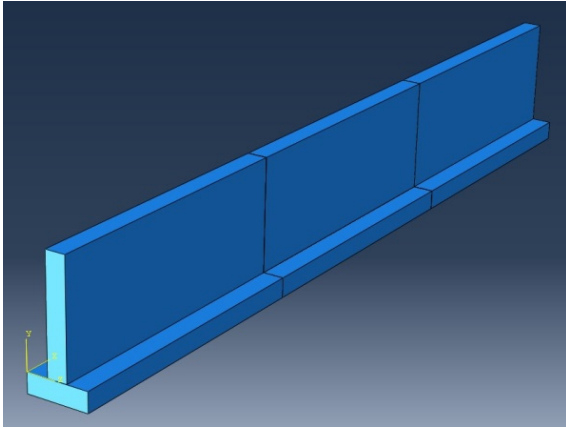


Figure 1 – Three casting sequences of typical case wall-on-slab. In Case 1, one of the end walls is the last casting, and in Case 2 the intermediate wall is the last casting.

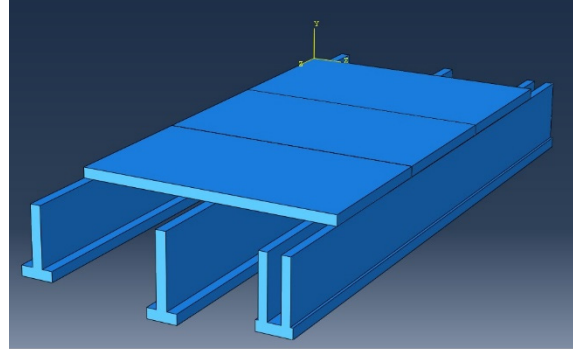


Figure 2 – Three casting sequences of roof segment. In Case 3, one of the end roof segments is the last casting, and in Case 4 the intermediate roof segment is the last casting.

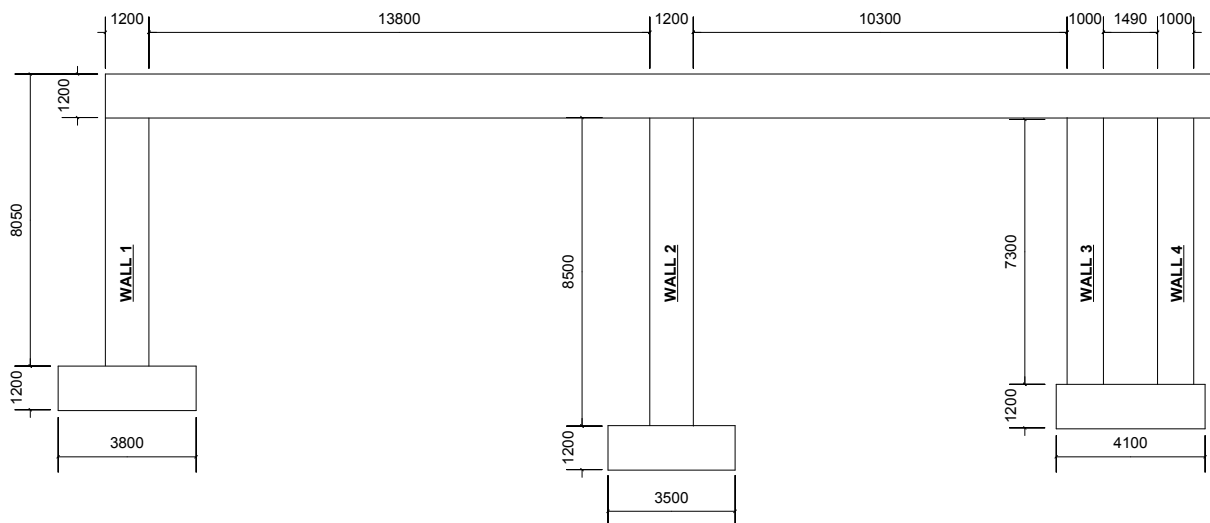


Figure 3 – Cross-section of studied tunnel geometries. Segments are 17.5 m long.

## 4.2 The first step, restraint estimation

### General parameters

The restraint in the young concrete has been estimated in the 3D FEM calculations by use of an elastic modulus in young and existing (old) concrete of 27.9 GPa and 30 GPa respectively and a Poisson's ratio 0.2 in both young and old concrete.

The restraint, defined as the degree of hindrance of movements in the concrete, is obtained by modelling the geometry with the Abaqus 6.12 software. The normalization according to Eq (1)

implies that elastic Abaqus calculations show the restraint situation for the young concrete, formally represented by the calculated stresses.

An area is searched for where a representative restraint situation occurring. Only looking for the maximum restraint could be misleading since it often occurs at beginning (“the ends”) of casting joints. At these positions the restraint profile along the axis of interest is another than the profile at other locations in the construction. A 2D (position and strain ratio magnitude) restraint profile is exported to be used in the second step as earlier described.

The boundary condition, which provides the system in a static state in space, can be set in several ways. The current boundary conditions for the wall castings are set by four points as shown in Figure 4 (here for Case 2). For Case 1 the same boundary conditions are used and the same principle is used for the Cases 3 and 4.

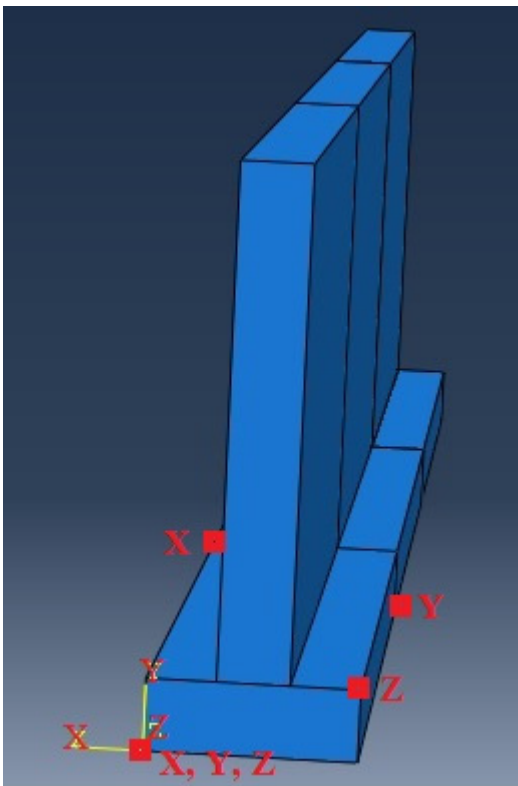


*Figure 4 – Location of the four boundary condition points and the axis along which the translation movement is locked to make the system statically determined.*

The restraint given by the calculations is the total restraint in all directions. In the result analysis of Abaqus it is possible to differentiate the restraint in any arbitrary direction.

#### *Restraint conditions for the walls*

The wall segments investigated in this paper are the segments in wall no 1 (Figure 1). For the wall the direction of interest regarding restraint is along the longitudinal direction (along the joint between the base slab and wall). The corresponding restraint for Cases 1 and 2 for elastic calculations when the newly cast concrete is contracting homogeneously is shown in Figures 5 and 6.

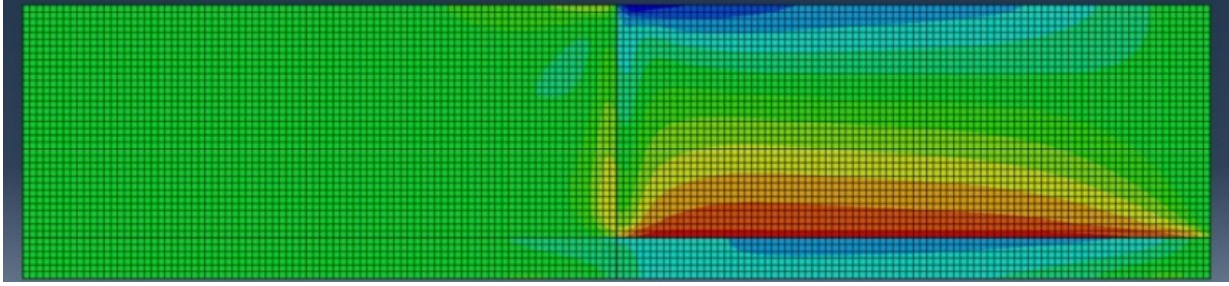


Figure 5 –Restraint values for Case 1 along the longitudinal direction of the tunnel. Maximum restraint is 0.76 and minimum is -0.64.

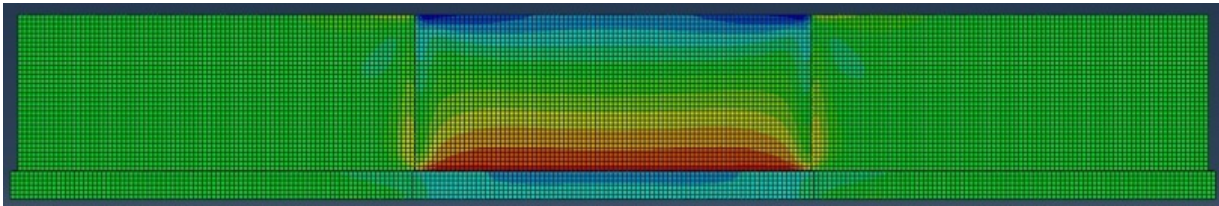


Figure 6 –Restraint values for Case 2 along the longitudinal direction of the tunnel. Maximum restraint is 0.76 and minimum is -0.64.

From the restraint analysis presented in Figures 5 and 6, it is seen that that the maximum value in the two cases are similar; 0.76. The main difference is that the distribution of the restraint in Case 2 displays a more extensive distribution of high restraint.

#### *Restraint conditions for the roof segments*

For the roof segments the directions of interest at restraint evaluation is along the axis parallel the joint to the wall and the casting joint to adjoining roof segment. The most significant restraint given by the walls origins from wall number 2 and the results are presented here. The corresponding restraints for Case 3 and 4 at elastic calculations are shown in Figures 7 - 9 where the newly cast concrete is contracting homogeneously.

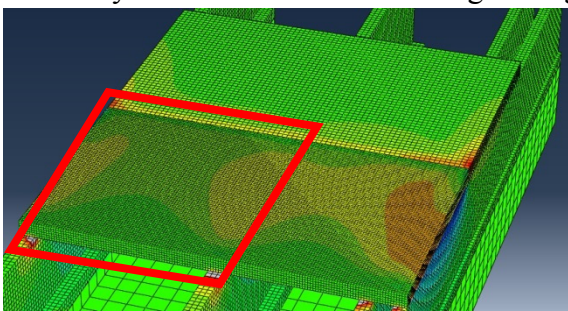


Figure 7 –Restraint values for Case 3 along the joints to the walls. Red square marks region studied. Maximum restraint is 1.00 and minimum is -0.84.

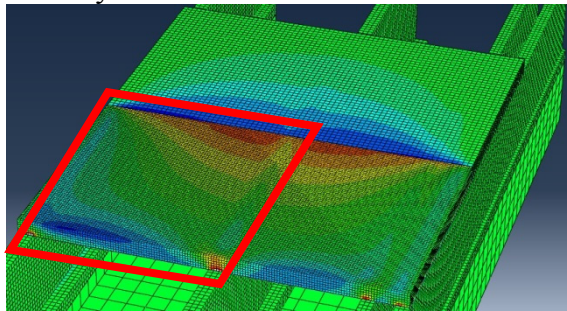
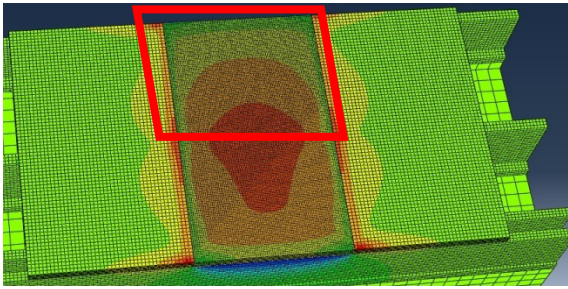
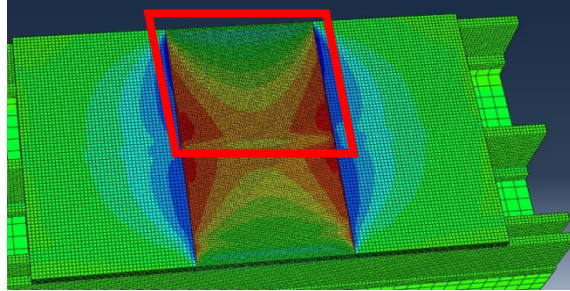


Figure 8 – Restraint values for Case 3 along the joint to the adjoining roof segment. Red square marks region studied. Maximum restraint is 1.00 and minimum is -0.58.



*Figure 9 –Restraint values for Case 4 along the joints to the walls. Red square marks region studied. Maximum restraint is 0.70 and minimum is -0.97.*



*Figure 10 –Restraint values for Case 4 along the joint to the adjoining roof segment. Red square marks. Maximum restraint is 0.85 and minimum is -0.60.*

### 4.3 The second and third step: development of LRM and ERM

#### *General parameters*

The stress/strain ratio of the young concrete has been estimated in the 2D FEM calculations by use of the following parameters:

- Concrete class: C35/45, w/C = 0.40 and C = 430 kg cement per m<sup>3</sup>.
- Wooden form, 21 mm. Heat conductivity 0.14 W/Km.
- Ambient air. Heat transfer coefficient 500 W/Km<sup>2</sup>. Wind speed 3 m/s.
- Initial temperatures, see Table 1.

The restraint conditions in the first step are imported into the LRM calculations by use of the correct restraint value point-by-point performing one calculation at each position. The calculated strain ratio for every LRM position is then plotted, see marks “X” in Figures 11 to 14. The strain ratio is defined by calculated strain divided by the strain at rapture. A regression analysis is performed to obtain the corresponding ERM by varying the translation and rotation restraint, resilience behaviour, construction length and restraining block dimension. For the LRM and ERM calculations the computer program ConTeSt 5.0 was used.

The parameter settings for the LRM calculations and the resulting parameter settings for the ERM when performing the analysis of the wall are shown in Table 1. In Figures 11 - 14 the regression analyses are presented for Cases 1 to 4 as well as the restraint profiles imported from the first step.

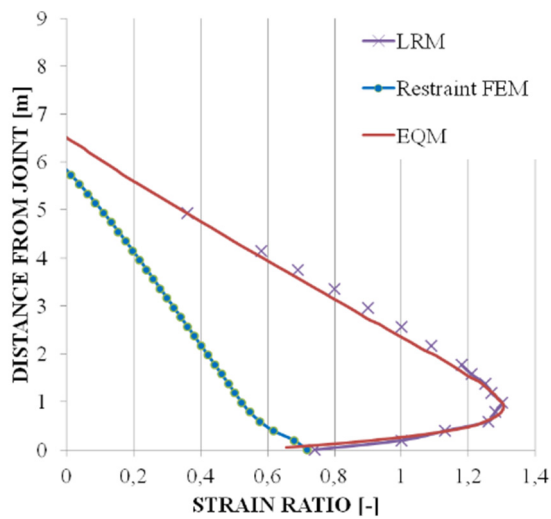


Figure 11 – Resulting ERM to resemble LRM strain ratios, Case 1.

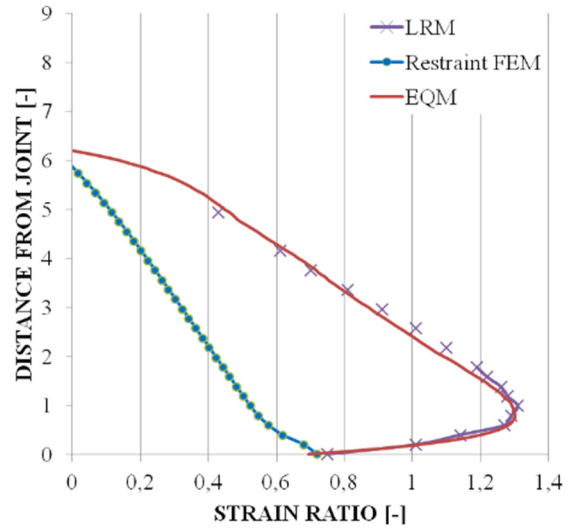


Figure 12 – Resulting ERM to resemble LRM strain ratios, Case 2.

Table 1 – Parameter settings for LRM and ERM, Cases 1- 4. Suffix after Case 3 and 4 refers to studied joint. Legend “Wall” determines the study of the joint between wall no 2 and the roof segment. “Roof” determines the study of the joint between mature roof and the newly cast roof segment.

	Tconcrete (°C)	Tair (°C)	Rotation restraint (%)	Translation restraint (%)	Resilience		Restraining block(s) (# (m x m))
					Structure length (m)	Reduction of L/H-ratio (-)	
<b>Case 1</b>							
LRMs	15	0	1	varies	-	-	-
ERM	15	0	0.1	0.15	35	Yes	1 (3.5 x 1.2)
<b>Case 2</b>							
LRMs	15	0	1	varies	-	-	-
ERM	15	0	0.3	0.17	40	Yes	1 (3.5 x 1.2)
<b>Case 3 - Wall</b>							
LRMs	25	15	1	varies	-	-	-
ERM	25	15	1	0	53	Yes	1 (2.6 x 1.2)
<b>Case 3 - Roof</b>							
LRMs	25	15	1	varies	-	-	-
ERM	25	15	1	0	53	Yes	1 (10.5 x 1.2)
<b>Case 4 - Wall</b>							
LRMs	25	15	1	varies	-	-	-
ERM	25	15	0.8	0	-	No	1 (6 x 1.2)
<b>Case 4 - Roof</b>							
LRMs	25	15	1	varies	-	-	-
ERM	25	15	1	0	65	Yes	1 (10.5 x 1.2)

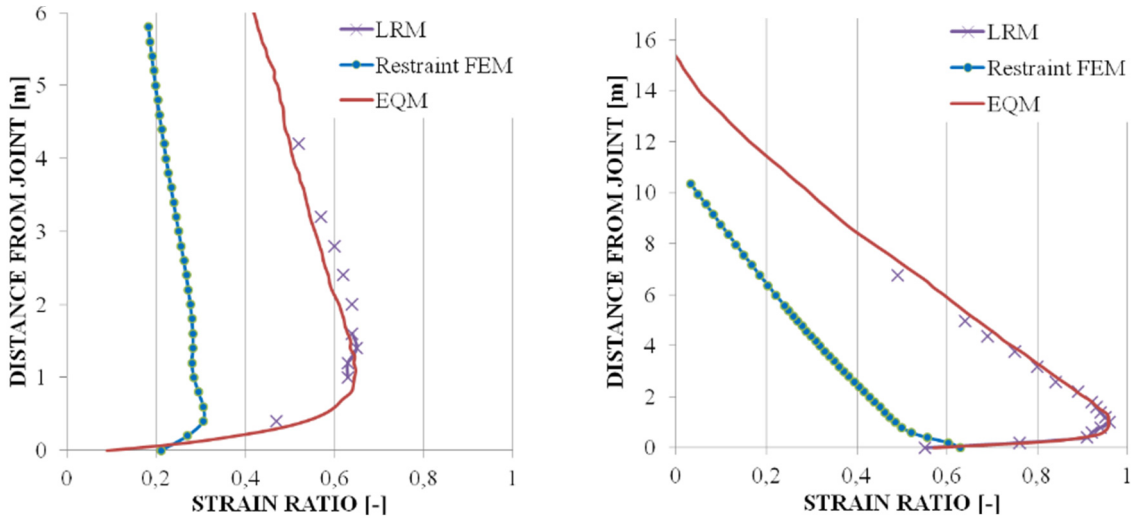


Figure 13 – Resulting ERMs to resemble the LRM strain ratios along the joints to adjoining wall (left) and roof (right) segments for Case 3.

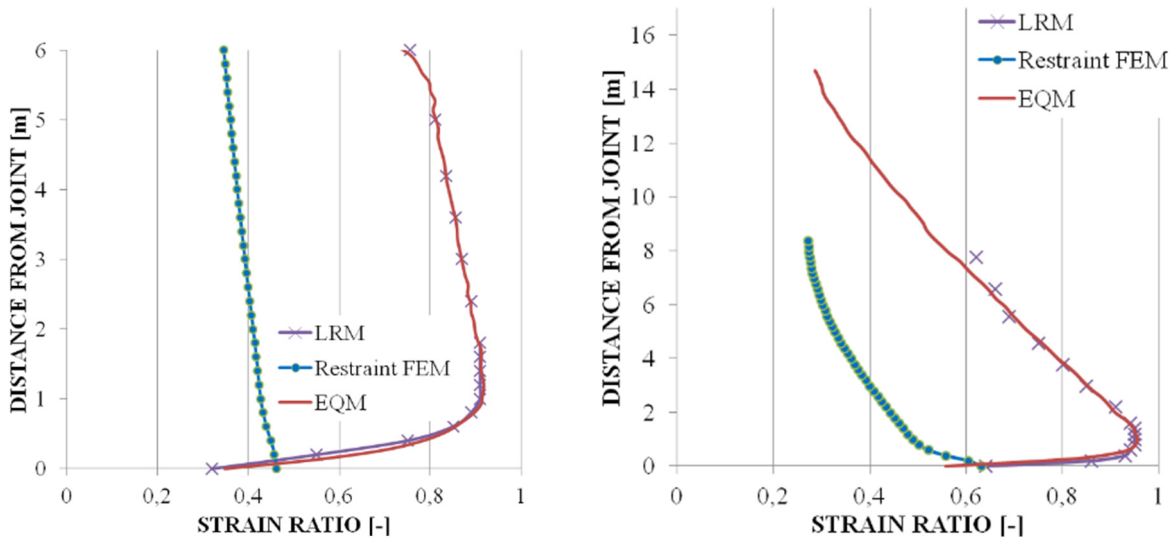


Figure 14 – Resulting ERMs to resemble the LRM strain ratios along the joints to adjoining wall (left) and roof (right) segments for Case 4.

#### 4.4 Observed crack pattern and post-calculation

Onsite temperature measurements were performed for most of the castings within the tunnel project. The measurements together with corresponding crack inventory were used to single out interesting parts of the construction to analyze. In the frame of this paper it is of interest to study the restraint situation in those parts of the construction which show one or just a few cracks. This is because it could be expected that the strain ratio is just around the threshold for the formation of cracks. With the aim of meeting the requirements of a crack free situation, cooling pipes in the walls were used onsite, see Figure 15. However, despite the cooling, cracks occurred in some cast sections. In the post-calculations, the same conditions (e. g. temperatures, measures, and material parameters) as for the specific empirical case was implied into the ERM.

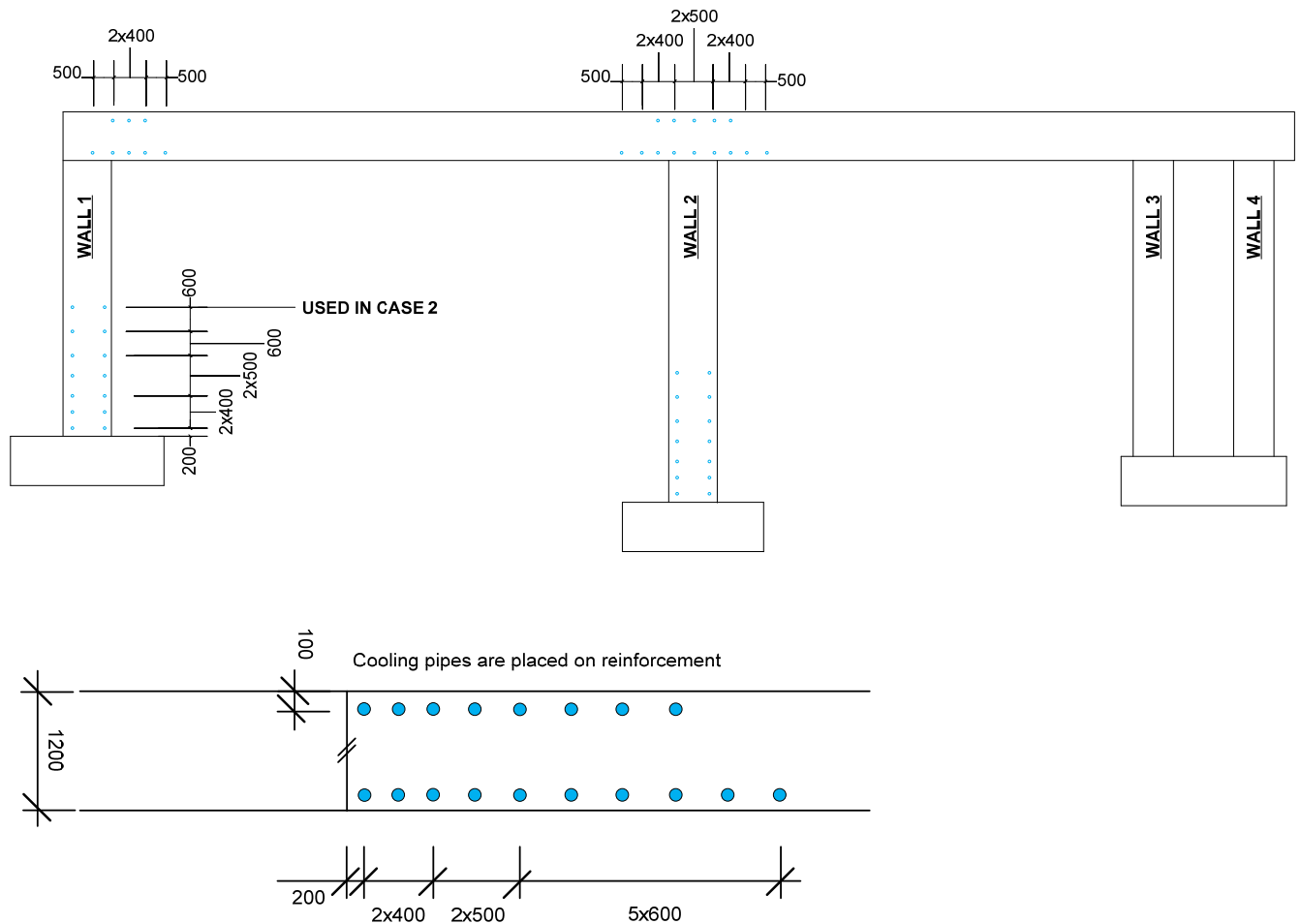


Figure 15 – Positions of used cooling pipes. The upper figure shows the cooling pipes above the joint to walls while the lower figure shows the cooling pipes to adjoining roof segment. Pipes over wall 3 and 4 are not shown.

### Observed crack patterns

For the construction parts investigated, observed cracks have been documented. The castings within the tunnel project have proceeded during more than 2 year's time and only sporadic crack inventories have been made. Case 4 have been checked for cracks two times and the others one time each. Figure 16 shows the documented cracks and when they were observed.

### Post-calculations

To perform the strain ratio post-calculations, simulations of the casting situation for the four cases are performed using the ERM with the existing cooling pipes and the registered environmental parameters. In Table 2 the following input parameters are listed: the initial concrete temperature, average ambient air temperature, form striking time, average cooling water temperature, and start and stop of cooling actions. The ambient air temperature and cooling water temperature are given as average values but indeed fluctuates over time. All parameters in Table 2 except form striking time are collected from onsite measurements. The form striking times are given by documentation since it could not be read from the measurements. To meet the measured temperature maximum in the cast concrete the heat

parameters within the software have been adjusted. All given times are counted from start of casting.

The resulting strain ratio profile as a function of strain ratio versus distance from joint, and the strain ratio at the position of the maximum strain ratio as a function of time is shown in Figures 17 - 20 for Cases 1 - 4 respectively. Start time of casting is set to 200 h in the calculations to make the system adjust itself before calculating the young concrete. Some figures show a slight discrepancy in maximum strain ratio between the two plotted graphs. This is due to the graph showing maximum strain ratio as a function of time is hand selected for a specific height.

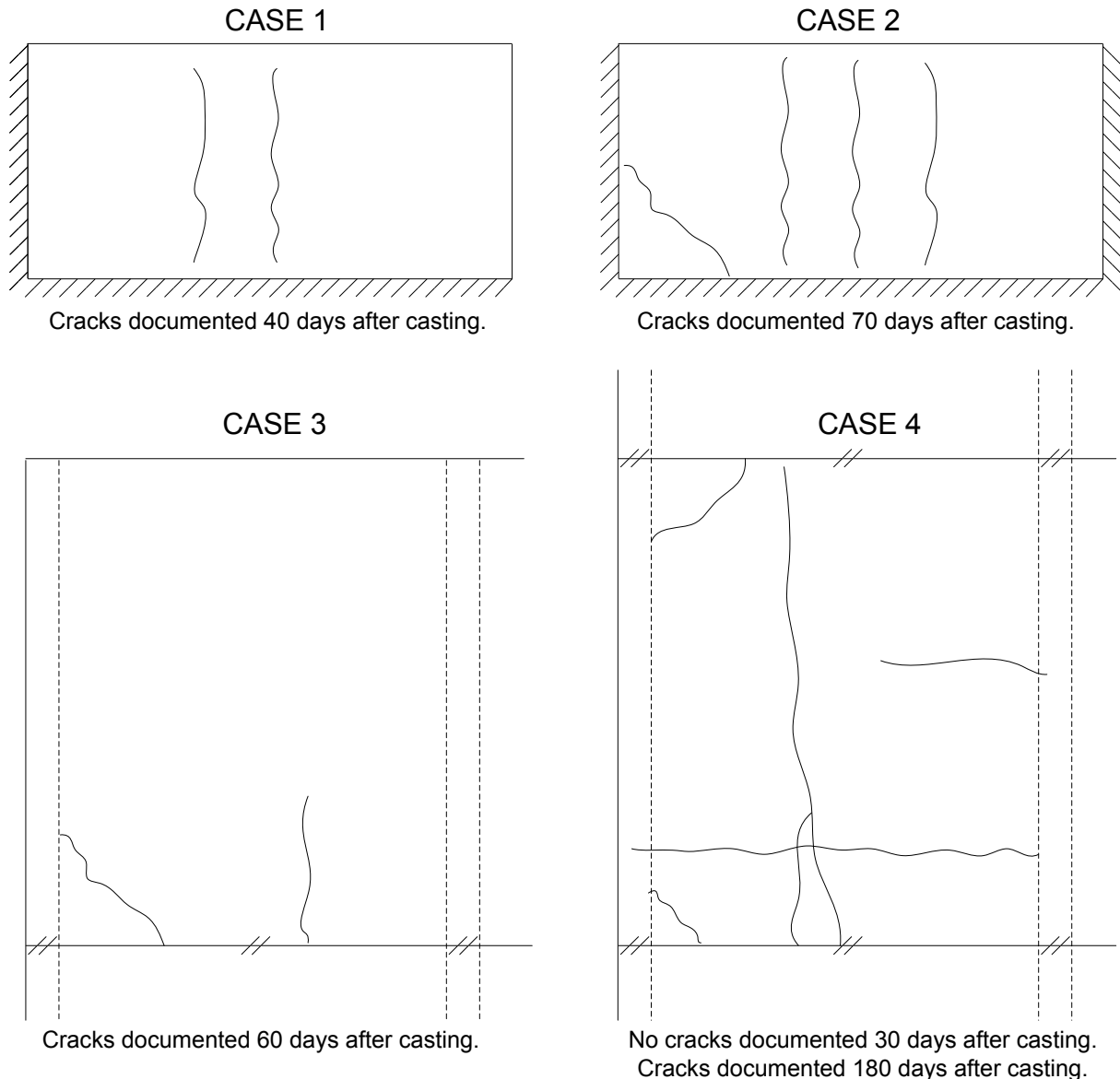


Figure 16 – Observed crack patterns and time of first observation for Cases 1 to 4. Crack widths are 0.1 mm or larger.

It can sometimes be hard to localize the exact height giving the maximum strain ratio. When looking at the figures it is important to bear in mind that follow up calculations of cracked situations states [12] that cracks were observed for estimated strain ratios of about 0.80 to 1.05.

In Figure 17 (Case 1) it is seen that the calculated strain ratio about 10 days (240 h) after time of casting reaches the maximum level of about 0.94, and that a high strain ratio remains for a rather long period of time. The conclusion is that the numerical modelling gives a clear indication that the wall is in danger of cracking during the current parameter set. The observed status of the construction part (see Figure 16) shows a moderate crack pattern suggesting that the strain within the construction is just enough to create cracks.

In Figure 18 (for Case 2) the maximal strain ratio is 0.91 that is reached about 12 days (288 h) after time of casting. As for Case 1 a high strain ratio remains for a significant time period after the strain ratio peak. The high strain ratio for an extended time period implies that the wall in Case 2 is in danger of getting cracked. By comparing the post-calculation to observed crack patterns, see Figure 16, it is plausible that the high strain inside the wall causes the construction to crack. Compared to the crack situation for Case 1 there is more cracks in Case 2. By looking at the restraint distribution in Figures 5 and 6 it is clear that Case 2 have a more extensive distribution of high restraint. This could be one explanation why more cracks were observed in Case 2 than in Case 1 for the studied tunnel construction. Another explanation is that the time of crack documentation, counted from start of casting, differs between the two cases. Whereas in Case 1 the crack inventory was done 40 days after casting but as late as 70 days for Case 2. This implies that the strain due to temperature gradients had a longer time to make effect. Hence, more cracks could appear.

In Figure 19 (for Case 3) the strain has been analyzed along the joint between the newly cast roof segment and the walls. The strain presented is in the roof segment over wall number 2. Moreover, the strain along the joint between the newly cast roof segment and the adjoining mature roof segment is presented. At the casting joint to the wall the maximal strain ratio is 0.70 and is reached about 14 days (336 h) after time of casting. At the joint between roof segments, the maximal strain ratio is 0.82 reached about 13 days (312 h) after time of casting. The strain ratio remains close to the maximum for an extended time period after it peaked. Even though the strain ratio is just around 0.80 for a short period of time cracks has been documented 60 days after casting, see Figure 16. A contributing factor when cracks are formed during a rather long period might be local changes in time of the environmental conditions like temperature, wind speed, and moisture states.

In Figure 20 the strain has been analyzed along the joint between the newly cast roof segment and the walls (for Case 4). The strain presented is in the roof segment over wall no. 2. Furthermore, also the strain along the joint between the newly cast roof segment and the adjoining mature roof segment is presented. For the joint to wall the maximal strain ratio is 0.80 which is reached about 15 days (360 h) after time of casting. The maximal strain ratio at the joint between roof segments is 0.84 which is reached about 15 days (360 h) after time of casting. For this casting the cooling failed; for some reason it started 30 h after start of casting and ended 6 h later and the temperature of the cooling water was about 28°C. In Figure 20 it is observed a significant region from the joint to the wall and outwards with high strain ratios, 0.75 – 0.80. Furthermore, it shows that 0.5 to 1 m away from the joint between roof segments the strain ratio exceeds 0.80. The maximum strain ratios more or less don't decrease at all for both cases, even 33 days (800 h) after casting. When looking at Figure 16 no cracks were visible 30 days after casting but had appeared 180 days after casting.

Table 2 – Environmental parameters for casting of Cases 1 to 4

	Tconcrete (°C)	Tair average (°C)	Form striking (h)	Cooling temp average (°C)	Cooling time	
					Start (h)	Stop (h)
Case 1	18	1	168	12	0	46
Case 2	16,5	4	288	9	0	34
Case 3	25	17	96	18	0	68
Case 4	25	20	240	28	30	36

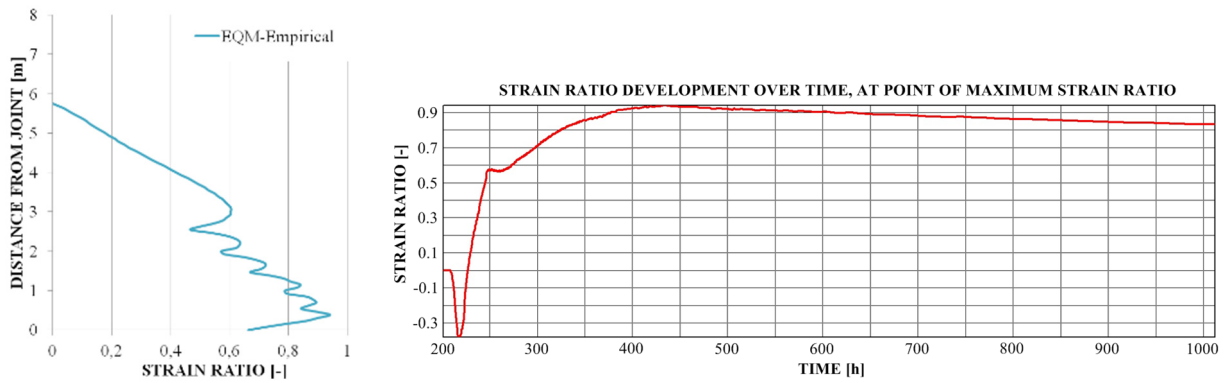


Figure 17 – Strain ratio profile at design position, and strain ratio versus time at position of maximum strain ratio for Case 1. Start time of casting is 200 h.

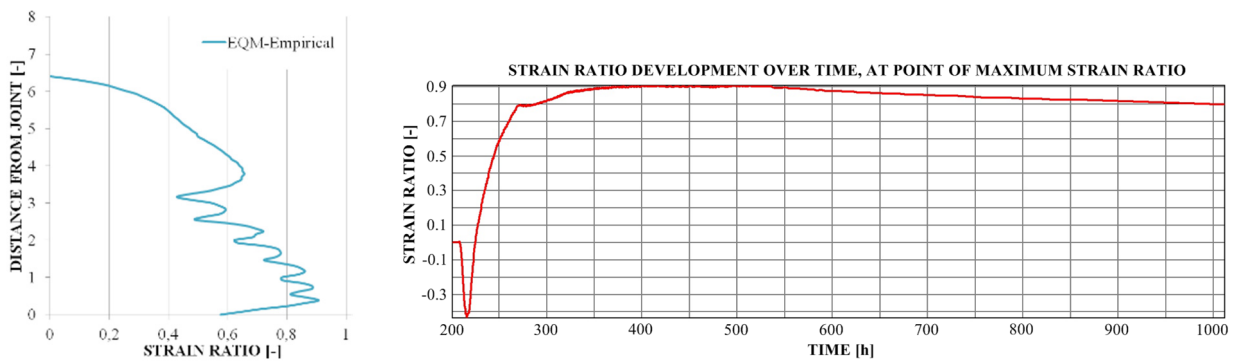


Figure 18 – Strain ratio profile at design position, and strain ratio versus time at position of maximum strain ratio for Case 2. Start time of casting is 200 h.

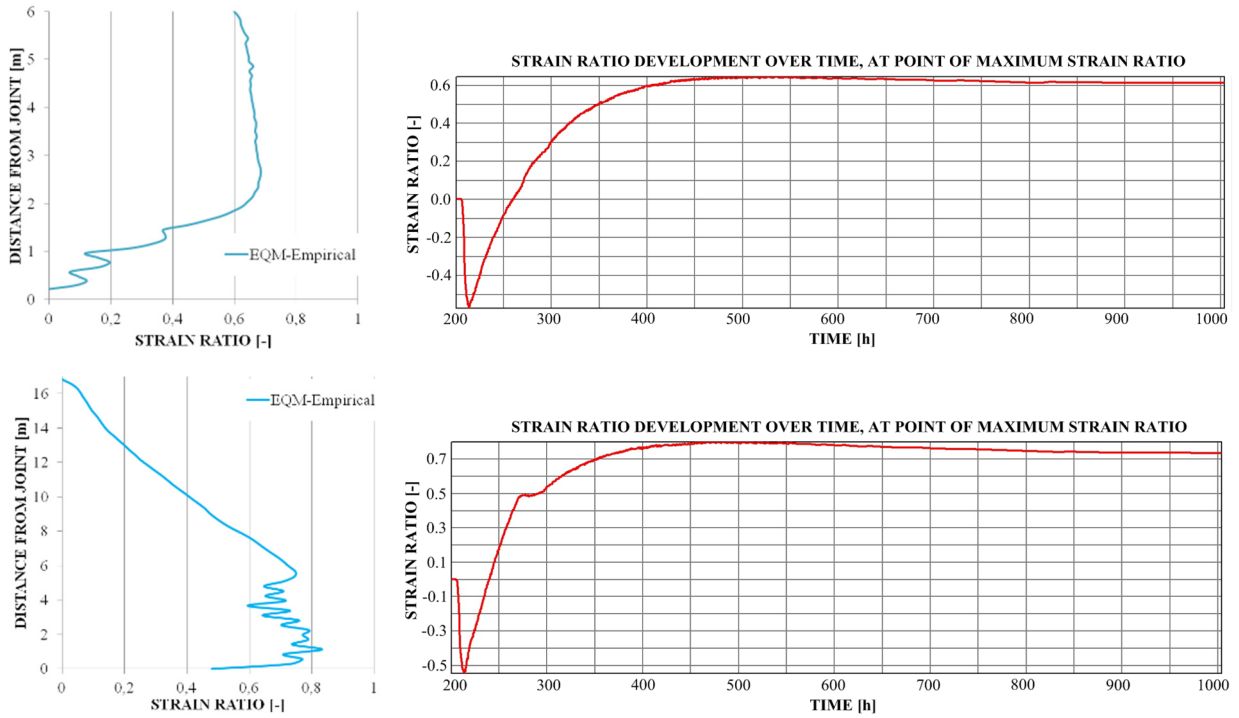


Figure 19 – Strain ratio profile at design position along the joints to adjoining wall (upper figure) and roof (lower figure) segments, and strain ratio versus time at position of maximum strain ratio for Case 3. Start time of casting is 200 h.

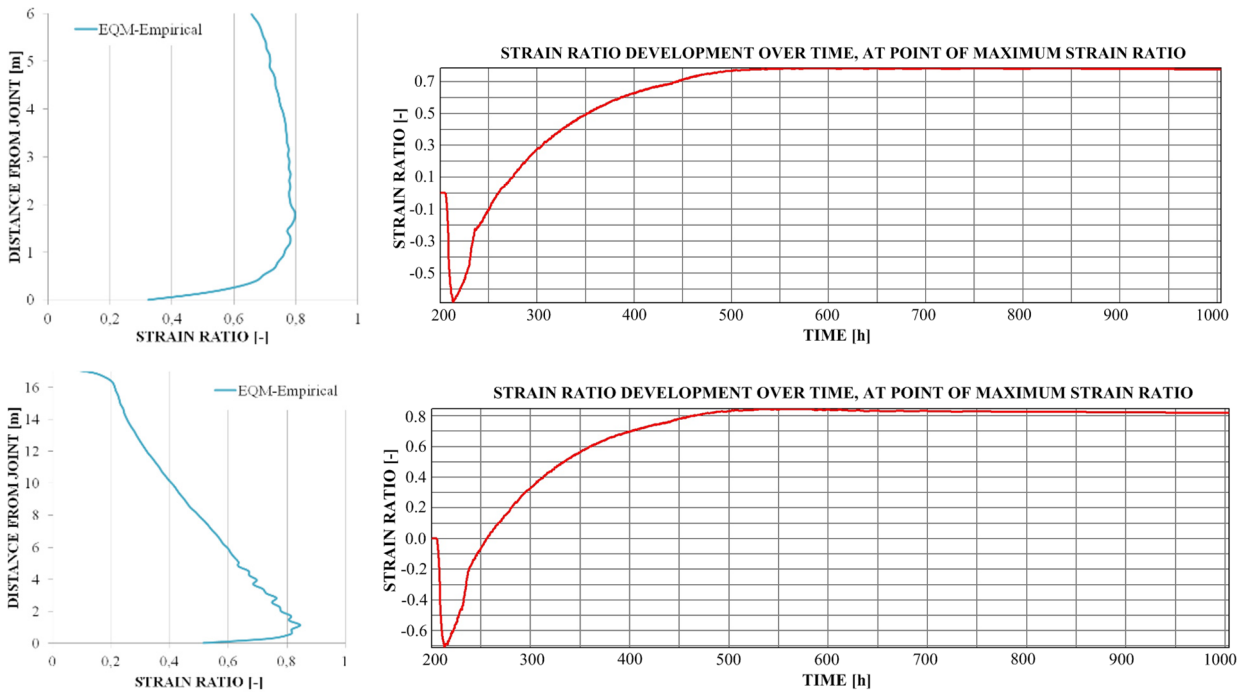


Figure 20 – Strain ratio profile at design position along the joints to adjoining wall (upper figure) and roof (lower figure) segments, and strain ratio versus time at position of maximum strain ratio for Case 4. Start time of casting is 200 h.

## 5. CONCLUSIONS

In the scope of this paper four typical casting situations were analyzed, two cases for wall segment castings (Cases 1 and 2) and two cases for roof segment castings (Cases 3 and 4). First a study of the restraint situation was performed. Secondly, the development of Equivalent Restraint Method was performed by subsequent regression analysis using ERM to resemble the Local Restraint Method calculations of strain ratio values. And finally, the developed ERMs were used to perform post-calculations for parts of a tunnel project representing Cases 1 to 4.

Regarding the objectives (Chapter 2) it can be concluded that analysis of the restraint in the wall segments (Cases 1 and 2) most likely explains why more cracks were observed casting intermediate wall than casting end walls, even though an extra pair of cooling pipes was added (see Figure 15). The effect of a more extensive restraint distribution, given by Abaqus, for Case 2, is not surprising. But that the magnitude is more or less the same as for Case 1 is interesting. When studying the observed crack patterns at these two cases, it is clear that for walls cast under the permissions of Case 2 more cracks are observed. An explanation could be that the total strain is larger than for Case 1. Added to this effect, there is slightly higher restraint above the point of maximum restraint in the construction for Case 2. Therefore a tendency of larger crack risk is present. For the studies of a cast end wall and a cast intermediate wall good correlations between the ERM and empirical observations were shown.

Furthermore, analysis of the restraint situation of the roof segments (Cases 3 and 4) shows an extended region of high strain ratio along the joint to the wall (upper part of Figures 19 and 20). The maximum strain ratio decreases slowly and as for Case 4 barely at all. This gives that a significant volume of the concrete is exposed to high strains under a long time. Along the joint to the adjoining roof segment the maximum strain ratio is just above 0.80. As for the joint to the wall, the maximum strain ratio decreases slowly, which strains that region for a long time and could therefore cause cracks. In Case 4 the cooling was poorly performed and the main reason why the strain ratio is not higher, especially when compared to Case 3, is favourable ambient temperature conditions and a long form striking time. If the form was stripped just after 4 days, as in Case 3, the roof segment most surely would show severe cracking within a day or two. For the studies of the roof segments an acceptable correlation between the ERM and empirical observations was shown.

The general conclusion from above is that a cast end wall experience a lower degree of total restraint compared to an intermediate cast wall. The same conclusion holds for roof castings when comparing restraint along the joint to the walls. The restraint inherited from adjoining roof segments is of the same magnitude for an end roof casting and an intermediate roof casting.

## 6. DISCUSSION

The work reported in this paper can be commented on as follows:

The onsite measurements that form the base of this paper, when it comes to correlate the ERM to empirical observations, are not as rigorous as hoped for. For example, systematic crack inventories with a short time span in-between would be beneficial to get a better view of when and where the cracks first start to appear.

There are more reasons that make the concrete crack than just movements caused by temperature development in the young concrete. For example the change of moisture gradients during time is one important factor which is not studied in the present ConTeSt calculations. The superposition of temperature strains and strain inherited from moisture gradients can be one factor that made the investigated concrete to crack.

To improve the comparison between the ERM model and empirical experience several parameters can be investigated further and calibrated. For example, the possible effect of self weight can be added to the Abaqus analysis on restraint. Furthermore, the temperature properties of the young concrete inside ConTeSt can be trimmed or updated.

To compare the post-calculations for these cases to each other could be misleading since the environmental parameters differ from each case. General assumptions such as differences in strain distributions can be done, but going into details should not be done. Comparisons of maximum strain ratios for the cases are therefore not valid due to the different parameter settings.

## REFERENCES

- 1.
2. Emborg, M & Bernander, S., "Assessment of the Risk of Thermal Cracking in Hardening Concrete," *Journal of Structural Engineering*, ASCE, Vol.120, No 10, October 1994. pp. 2893-2912.
3. Mihashi, H., & Leite, J.P., "State of The Art Report on Control of Cracking in Early Age Concrete," *J. Advanced Concrete Technology*, 2004, 2 (2) pp.141–154.
4. Kianousha, M.R., Acarcanb, M, Ziari, A., "Behavior of base restrained reinforced concrete walls under volumetric change," *Engineering Structures*, 30, 2008, pp.1526–1534.
5. Cusson, D. & Repette, W., "Early-Age Cracking in Reconstructed Concrete Bridge Barrier Walls," *ACI Materials Journal*, 97(4), July/August, 2000, pp. 438-446.
6. Bosnjak, D., "Self-Induced Cracking Problems in Hardening Concrete Structures," Department of Structural Engineering, Norwegian University of Science and Technology Doctoral Thesis 2000, 171 pp.
7. Rostásy, F S, Tanabe, T., Laube, M., "Assessment of External Restraint. In: Prevention of Thermal Cracking in Concrete at Early Ages," Ed. by Springenschmid. London, England: E& FNSpon. RILEM Report 15. State of- the Art Report by RILEM Technical Committee 119, prevention of Thermal Cracking in Concrete at Early Ages.1998, pp. 149-177.
8. Emborg, M., "Development of Mechanical Behavior at Early Age," Ed. by R. Springenschmid. London, England: E & FNSpon. RILEM Report 15. State of- the Art Report by RILEM Technical Committee 119, Prevention of Thermal Cracking in Concrete at EarlyAges.1998, pp. 77-148.
9. Nilsson, M., "Restraint Factors and Partial Coefficients for Crack Risk Analyses of Early Age Concrete Structures," Lulea, Sweden, Division of Structural Engineering, Lulea University of Technology. Doctoral Thesis 2003, 170 pp.
10. Al-Gburi M., Jonasson J-E., Nilsson M., Hedlund H. & Hösthagen A., "Simplified Methods for Crack Risk Analyses of Early Age Concrete - Part 1: Development of Equivalent Restraint Method", Nordic Concrete Research No. 46, 2012/2.

11. ConTeSt Pro., "User's Manual - Program for Temperature and Stress Calculations in Concrete", Developed by JEJMS Concrete AB in co-operation with Lulea University of Technology, Cementa AB and Peab AB. Lulea, Sweden, 2003, 198 pp.
12. Larson M., "Estimation of Crack Risks in Early Age Concrete – Simplified Methods for Practical Use", Licentiate Thesis 2000:10, Luleå University of Technology, Luleå. 2000.



## **Paper III:**

### **Thermal Crack Risk Estimations of Concrete Walls – Temperature and Strain Measurements Correlated to the Equivalent Restraint Method.**

**Hösthagen A**, Jonasson J-E, Emborg M, Nilsson M, to be published.

## Thermal Crack Risk Estimations of Concrete Walls – Temperature and Strain Measurements Correlated to the Equivalent Restraint Method



Anders Hösthagen, M.Sc. Ph.D. Student  
Betong & Stålteknik  
Anders.Hosthagen@bostek.se

Lulea University of Technology (LTU)  
Structural Engineering, SE-971 87 Luleå  
Anders.Hosthagen@ltu.se



Prof, Dr. Jan –Erik Jonasson  
Lulea University of Technology  
Structural Engineering, SE-971 87 Luleå  
Jan-Erik.Jonasson@ltu.se



Prof, Dr. Mats Emborg  
Betongindustri AB  
Box 47312, SE-100 74 Stockholm  
Mats.Emborg@betongindustri.se.

Lulea University of Technology  
Structural Engineering, SE-971 87 Luleå  
Mats.Emborg@ltu.se



Dr. Martin Nilsson  
Lulea University of Technology  
Structural Engineering, SE-971 87 Luleå  
martin.c.nilsson@ltu.se

## ABSTRACT

Self-induced non-elastic deformations in hardening concrete, caused by restrained volume changes due to thermal dilatation and moisture deformations, often leads to cracking. In thermal crack risk analyses, determination of the degree of restraint is vital. One model to estimate the restraint and calculate the thermal crack risk is the Equivalent Restraint Method, ERM. This method has previously been analysed but needs to be examined and validated further. Measurements of wall castings were performed and compared to calculations with ERM in order to establish a correlation to empirical observations. A satisfying correlation between theoretically estimated and measured time of through cracking was achieved. Based on this study and other, ERM is thus considered to work satisfyingly.

**Key words:** Thermal cracking, Early age concrete, Local restraint method, Equivalent restraint method, Modelling, Strain measurement, Field documentation.

## 1. INTRODUCTION

### 1.1 General

Restrained movements within young concrete during the construction phase, caused by thermal dilation and/or changing moist states, is a major reason for surface and through cracking, see e.g. [1] - [5]. Any adjoining structure or a restraining entity (such as rock, subgrade) bonded to the young concrete increase the risk of cracking since the restraint becomes higher, [1], [6] and [7].

Measures to avoid thermal cracking, like cooling pipes or heating cables, could be introduced within most calculation models if the strain level is predicted higher than approved, see [8] - [10]. One action to make the strain estimations more accurate, than using standard input parameters, is to test and evaluate the material properties of the concrete carefully. This process is described among others in [11].

To establish possible measures against thermal cracking, pre-calculations to analyse the risk of cracking during the heating and cooling phases are needed in Sweden for all civil engineering structures.

In [12], the importance to provide reliable predictions of the restraint is stated, when it comes to designing measures in a cost-effective way. This is especially true when it comes to cooling of repeated construction sections. The restraint is usually difficult to estimate and is therefore an uncertain factor [8]. One way to avoid the troubles of restraint estimations is to establish a complete 3D model with viscoelastic-viscoplastic behaviour of the young concrete. However, these kinds of models are cumbersome, time consuming at calculations and suitable software is often costly. At the restraint modelling, various methods can be used, from simple hand calculation methods [13], spreadsheet based methods [14], 1D and 2D FEM programs [15] to full 3D [16].

To simplify the restraint estimation for complex structural situations, the so called Local Restraint Method (LRM) [14] or the Equivalent Restraint Method (ERM) [14] may be used. In this work, the ERM is used. Benefits of this method involve a possibility to extract the restraint analysed by elastic 3D calculations and implement it into the Compensated Plane Method (2D FEM) for young concrete [17, 18, 19]. This is efficient from a time saving point of view compared to the use of a full 3D viscoelastic-viscoplastic simulation. Furthermore, the ERM makes it possible to analyse arbitrary measures/actions, such as cooling and/or heating.

The evaluation of how well the ERM corresponds to empirical experiences made in e.g. [12] was solely based on the correlation between theoretical and empirical temperatures along with the correlation between theoretical strain ratios and observed crack patterns for some typical cases. An important shortcoming in that analysis was that the time of the appeared cracks was not well documented, which lead to an obvious uncertainty in the evaluation. Despite this uncertainty, the results were considered rather satisfying.

This work provides a refined evaluation of the ERM compared to the evaluation made in [12]. What has been improved is that the model is enhanced with a set of fully tested parameters of the material properties and strain measurements was performed on a chosen typical full-scale cast. The strain measurements provide a good possibility for comparisons to calculated strains.

According to above, the objective is to evaluate the reliability of the estimated restraint obtained through the ERM. This is done by examine the correlation between the estimated risk of through cracking given by the model and field measurements.

## **2. METHOD**

### **2.1 General**

Within this work, a demonstration of the correlation between results from ERM and empirical experiences is performed. By studying temperature and strain measurements from the walls in a real tunnel project and comparing it to the ERM model counterpart, conclusions regarding the correlation are made. It is stated in [12] that several improvements could be done in case of further empirical studies aimed to evaluate the ERM. Within this work, the following improvements where performed; 1) thermal dilation is measured with strain gauges, 2) the concrete is tested and evaluated, 3) the temperature is measured in the direct vicinity of the construction with the placement of the temperature gauges well documented. With these improvements, the ERM model is further evaluated with the aim to see if the model can estimate through cracking in a satisfying way and validate the estimation of the restraint. To estimate the restraint situation, Abaqus version 6.13 is used and the temperature and induced stress/strain ratio calculations are performed with ConTeSt version 5.0 [15]. The strain measurements at site provided points of cracking within each of two examined walls, which made the comparisons between strain measurements and calculated strain ratios fairly easy.

The outline of the process of this work can be described as follows. First step; laboratory tests regarding material properties of the concrete. Second step; a theoretical model is developed (ERM) to analyse the temperature and strain development of the studied structure. Third step; onsite measurements of temperature and thermal dilation. Fourth step; onsite registered temperatures (of the ambient air, adjacent construction and fresh concrete when poured into form) is imported to the ERM, and measured and theoretical temperature developments is compared. Fifth step; calculations of stress and strain of examined sections for a comparison of measured and theoretical points of cracking. The prerequisite to perform the fifth step is that the tunnel walls cracks due to thermal dilatation. If they don't crack spontaneously, heating cables in the base slab can be activated to expand the slab to force cracks in the wall.

## 2.2 Tunnel segment and instrumentation

The typical case studied in this work is a railway tunnel segment, which consists of two walls and a roof cast as one monolith on a base slab. The base slab is cast, without piles, on top of a bed of gravel which insulates the system regarding restraint from any adhesive boundaries. Dimensions of the base slab, walls and roof are presented in Figure 1.

The figure also shows the position of the strain gauges inside the east and west walls. Totally four strain gauges was used, which consists of a cylindrical shell, a rod placed centrally in the shell and a Wheatstone bridge [23] attached to the rod to measure the strain. Two gauges was 2000 mm long with anchors at each end of the rod and mounted to transfer the thermal dilation to the rod. These gauges where mounted centric along the length of the walls and 800 mm up from the base slab. These gauges are denoted “main gauge” of which purpose is to measure the thermal dilation along the wall. Additional strain gauges, denoted “reference gauge”, were placed directly under and perpendicular to the main gauge to detect any drift in the instrumentation. One main and one reference gauge is showed in Figure 2.

Pre-calculations to estimate the maximum strain ratio (momentary strain through temporary developed maximum strain) in the walls revealed that the theoretical location of maximum strain is about 800 mm up from the base slab. Hence the main gauges were mounted in each wall at that location by adding extra reinforcement fixation bars attached to the present system of structured reinforcement. About 70 mm above the gauge a shelter, against poured concrete, was made by closely stacked reinforcement bars. The reference gauge was placed 650 mm from the base slab in the middle of the wall.

The measurement from the strain gauges was logged every 5 minutes as a median value of 300 recorded values. This procedure was chosen to limit the bulk of data and to smear out any temporary oddities that may occasionally occur for one or a few recorded values. The measured strain is the mean absolute strain over the length of the strain gauge.

Having a reliable picture of the temperature history of the studied construction parts are of superior importance when it comes to evaluate the correlation between measured and calculated temperatures and strains. The ideal would be to know the temperature at any given time at any spatial location for the studied objects. The equipment used at the study could simply not provide such an ideal state of information. Instead several temperature gauges were mounted at strategic places inside and outside the walls and in the base slab, see Figure 3. The figure shows the location of temperature gauges, where ten gauges were used to record the temperature in the base slab. Six gauges were placed in the walls; two close to the formwork surface at the height of the strain gauges, two close to the main strain gauges and two in the walls where the temperature gradient is expected to be one-dimensional, about 2 to 2,5 m up from the base slab. The ambient air was measured at two locations, outside of the base slab at the west side and likewise at the east side. Figure also shows the schematic placement of heating cables in the slab, which could be used to force the walls to crack if needed. A total of six cables were used with two lengths; 35 and 85 meters.

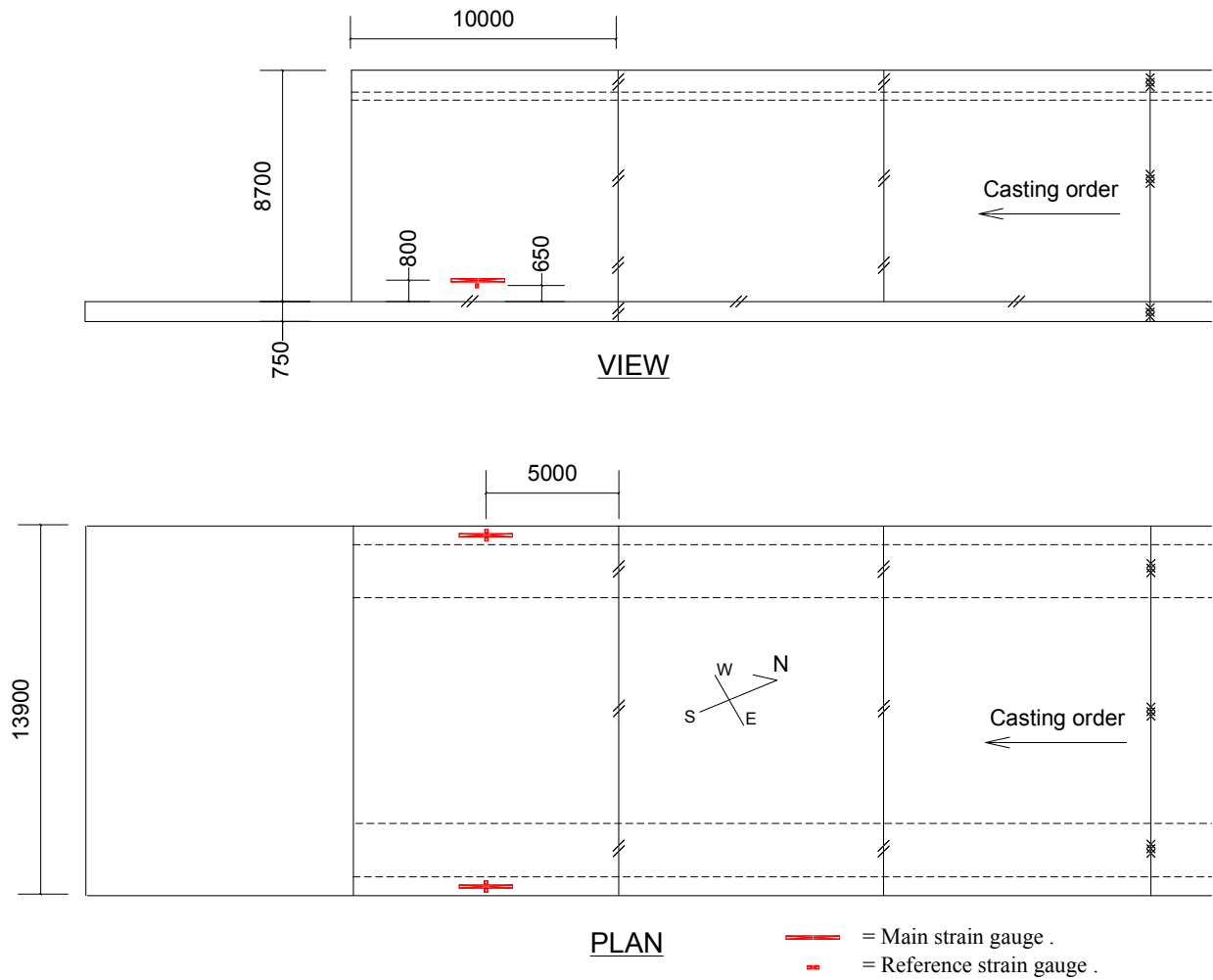


Figure 1 – Studied tunnel segment. Location of main and reference strain gauges.

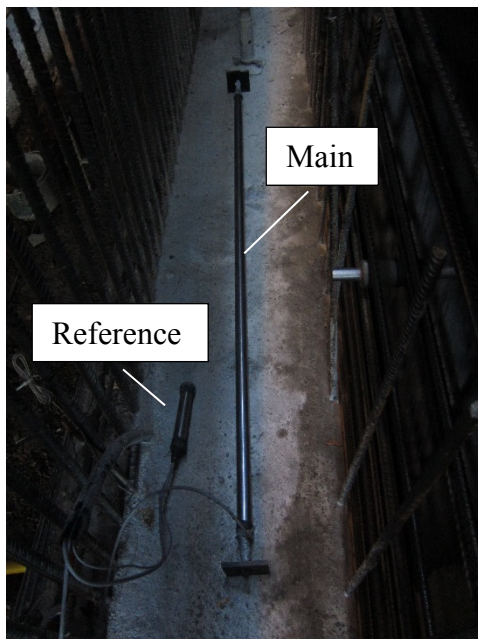


Figure 2 – Picture of one main and one reference strain gauge, before mounted into position.

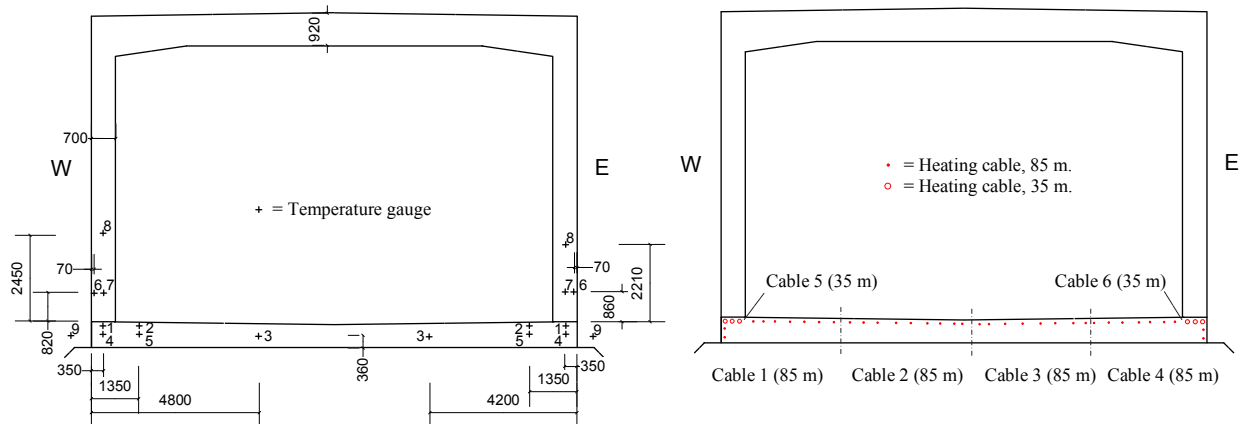


Figure 3 – Location of temperature gauges and sectioning of the heating cables.

### 2.3 Fully tested material parameters

Laboratory tests of used concrete was performed at LTU and evaluated to provide a set of material parameters suitable for the software ConTeSt. The following property areas of the concrete were tested; strength development, heat of hydration, basic shrinkage, thermal dilation, basic creep and stress at full restraint. The outcome gives a parameter collection suitable to be incorporated into the software ConTeSt in which the ERM model is created, see details in [11].

### 2.4 Restraint modelling and development of ERM model

The main purpose of the ERM is to provide a method to analyse the risk of through cracking, and can be modified to analyse the risk of surface cracking, see [20] where the principle of the method is described. The ERM is an improvement of the Local Restraint Method (LRM) [14] and is an improved method, into which arbitrary measures/actions against cracking can be applied. For example, it is not possible to perform crack risk analysis where heat cables are used as measure in LRM.

To create an ERM model several steps are required. The first step needed is an analysis of the restraint situation, which is made by a suitable 3D FEM software for elastic calculations, is performed yielding the stress development for the examined object. A certain temperature change is applied to the cast section of interest and stresses achieved are normalized to give the restraint situation for the young concrete, see [12]. The restraint in the young concrete has been estimated in the 3D FEM calculations by use of typical elastic modulus in young and existing (old) concrete of 27.9 GPa and 30 GPa respectively and a Poisson's ratio 0.2 of both the young and old concrete.

The second step is to localize a cross section in the 3D FEM where a representative restraint can be assumed for the actual analysed situation. In this case, the restraint profile at the middle of the wall is extracted to be imported into the LRM models.

The third step is to calculate the stress/strain ratio at different heights with the corresponding restraint at these heights given from the restraint profile.

The fourth step is to use the calculated stress/strain ratio at the different heights to construct a model where the transitional restraint comes from an adjacent block, and not from a factor take

from the restraint profile. So, from the LRM models a regression analysis were performed to obtain a similar stress/strain ratio profile for the ERM model as for the LRM models. In this work, the software

The LRM is built by several files where the stress/strain ratio is calculated at different heights, where the restraint profile given in the first step is used as input to the translational restraint at the corresponding heights. The final step is the erection of the actual ERM model. The model is created by regression analysis where the translation and rotation restraint, resilience behaviour, construction length and restraining block design are varied to obtain a similar stress/strain ratio profile as in the LRM model.

#### *General parameters used in 2D FEM (by ConTeSt)*

The stress/strain ratio of the young concrete has been estimated in the 2D FEM calculations by use of the following parameters:

- Concrete class: C30/37,  $w/C = 0.50$  and  $C = 365 \text{ kg/m}^3$ .
- Cement: CEM I 42,5 N MH/SR/LA (Anl ggningscement, by CEMENTA).
- Wooden form, 21 mm. Heat conductivity  $0.14 \text{ W/K m}$ .
- Ambient air. Heat transfer coefficient  $500 \text{ W/Km}^2$ . Wind speed  $2 \text{ m/s}$ .
- Initial concrete temperature is  $15^\circ\text{C}$  and the ambient air is  $5^\circ\text{C}$ .

## **2.5 Evaluation**

The ambient air temperature and the measured initial temperature of the young concrete are imported into the ERM model and thereafter the temperature development is calculated. If the temperature development not fully corresponds between the measured and theoretically achieved development (by ConTeSt), the maximum temperature is compared as a control point. Since the main mechanism behind the through cracking is the difference between the maximum temperature in the young concrete and the ambient temperature this control point is of great importance, see [???].

To measure strains inside a concrete construction is highly interesting when it comes to evaluate the correctness of theoretical models. To increase the relevancy of the measurements it is crucial to find a check point, or several, at where a comparison of the measurements and the calculations can be performed. In this work, the time of tensile failure is used. It is a distinct point if it could be accurately documented, and it is straight forward to equalize that point with the tensile strength.

Furthermore, the calculated strain ratio is a fictive value since ConTeSt does not calculate absolute strains. This makes a direct comparison between calculated strains and measured strains impossible. However, what can be done is a comparison of measured and calculated point of cracking. Hence, the comparison between a calculated strain ratio and measured strain serves as a very good control whether the model is reliable or not. If the comparison shows a good resemblance the estimation of the restraint should be satisfying.

Since the thermal dilation causes small movements of a structure, a magnitude of about  $1\text{-}200 \mu\text{m/m}$ , qualitative instruments are required to catch these movements as well as deformations when a crack occur.

### 3 RESULTS

#### 3.1 Material parameters

The concrete recipe and evaluated material parameters from laboratory testing can be found in Appendix A.

#### 3.3 Development of ERM model

The normalized elastic calculation and the location for the restraint profile are showed in Figure 4. In Figure 5 the restraint profile, calculated strain ratios for the LRM models and the strain ratio profile of the ERM model is shown.

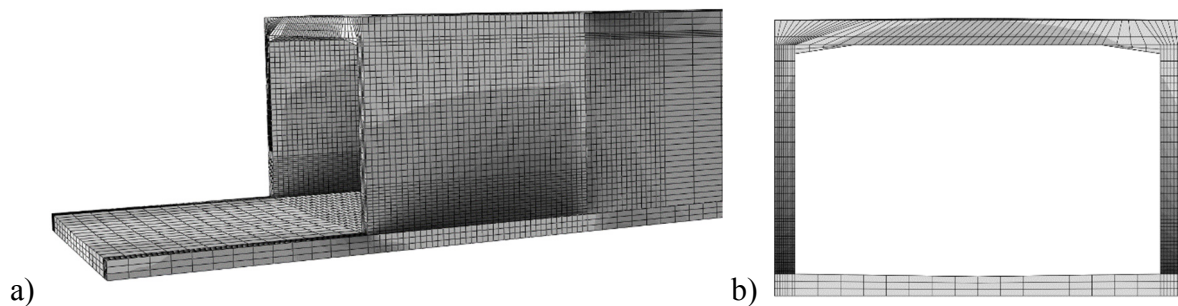


Figure 4 – Restraint, obtained by use of 3D FEM elastic calculation for a normalized temperature change. Maximum restraint is 0.72.  
 a) restraint along the longitudinal direction of the tunnel.  
 b) restraint at examined location (middle of the section).

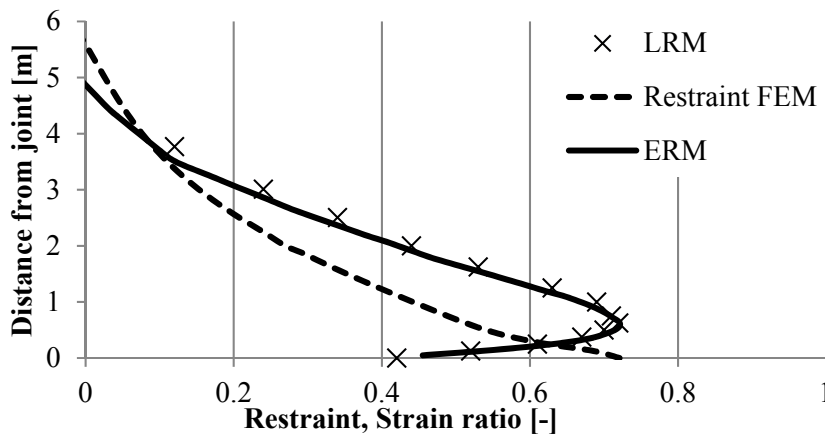


Figure 5 – Calculated restraint by FEM and resulting ERM to resemble LRM strain ratios.

#### 3.4 Temperatures

The measurements started 29 and 2 days prior the casting of west and east walls respectively. The casting of the base slab started 667 h (roughly 28 d) prior to the walls, and the time of wall cast is used as origo in all following figures.

The recorded ambient air temperature varies just slightly between the two gauges (standard variation of 0.5°C) but still two temperature profiles were created to simulate any effects of the small temperature differences between the both sides, see Figure 6. As the focus of this work lays at the correlation between the measured and calculated strain in the walls, the temperature history

inside the base slab is of minor importance as long as the recorded temperature corresponds to the calculated just before the wall castings.

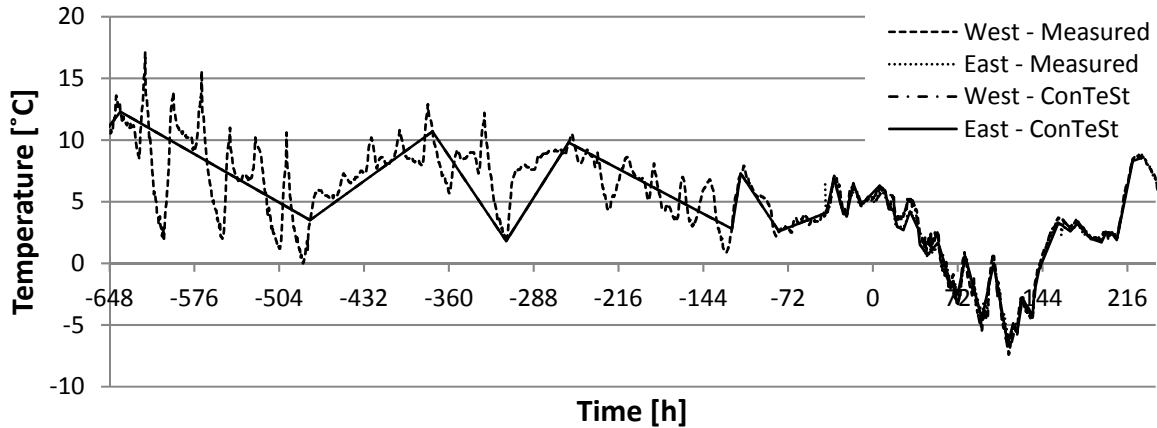


Figure 6 – Measured ambient air temperatures at east and west walls. Modelled ambient air temperatures is “West-ConTeSt” and “East-ConTeSt”.

A comparison between the measured temperatures and calculated of gauge 1 to 5 (all placed in the base slab) show a good correspondence, see Figures 7 to 9. The temperature condition at the start of the wall casting matched very well for all five gauges with a discrepancy ranging from  $0.01^{\circ}\text{C}$  to  $0.2^{\circ}\text{C}$ . After the time of removal of formwork, performed after 120 h, the discrepancy is larger and gauge 2 shows a maximum deviation of  $2.8^{\circ}\text{C}$ . However, gauges 3 and 5, who represent the average temperature in the base slab, show a maximum discrepancy of only  $1.2^{\circ}\text{C}$ . The increasing temperature after casting the wall at gauges 1 and 4 is due to the thermal conduction from the wall. Two observed patterns can be seen; firstly, all calculated maximum temperatures are  $1\text{-}2^{\circ}\text{C}$  lower than the measured maximums. Secondly, the measured and theoretical temperature development corresponds very well from some hours before casting the wall, until just after the time of removal of formwork. The ERM model seems to mimic the empirical temperature in a reliable way and a good description of the temperature state of the base slab at time of wall cast is achieved.

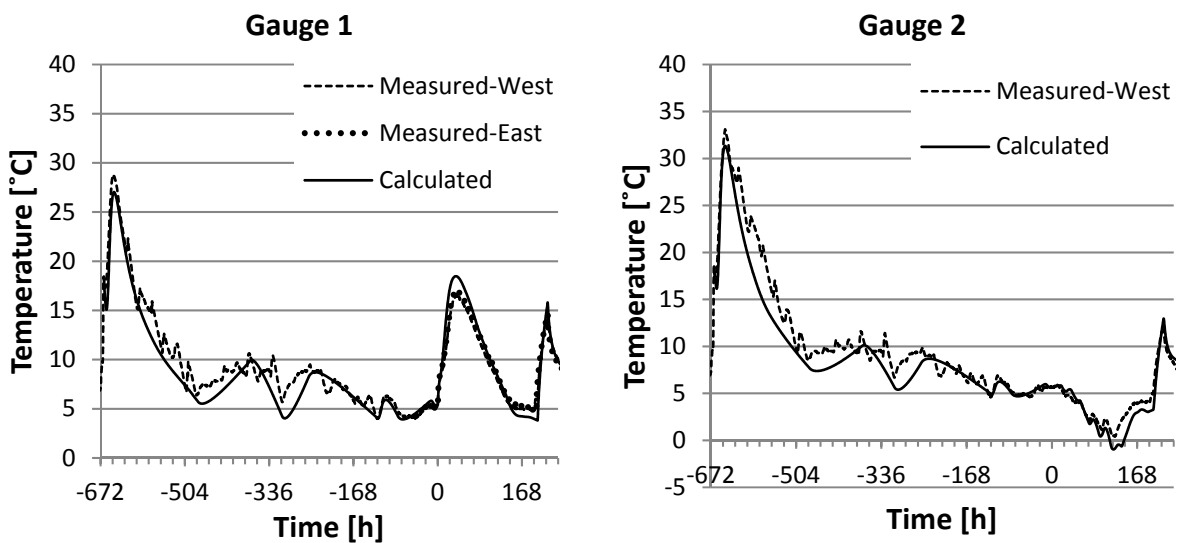


Figure 7 – Measured and calculated temperatures in the slab. Gauge no 2 at the east part of the base slab was damaged and is not showed.

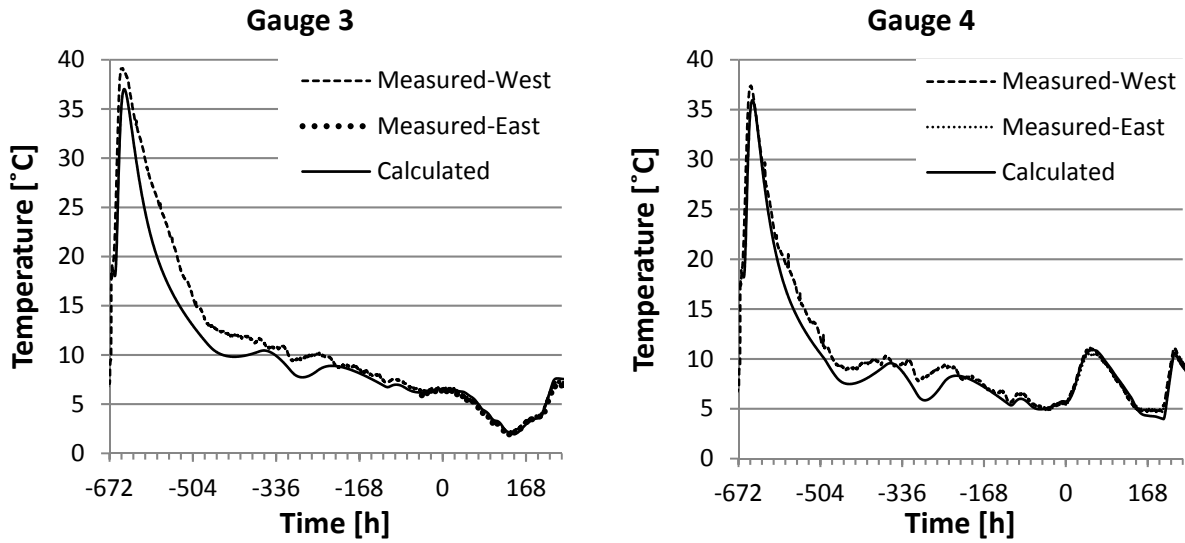


Figure 8 – Measured and calculated temperatures in the slab.

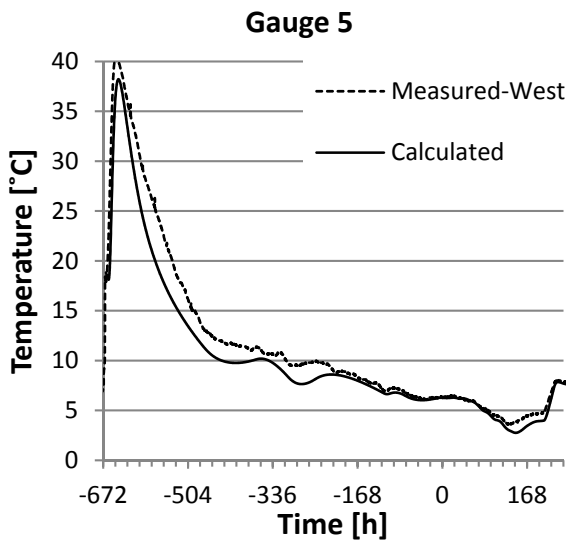


Figure 9 – Measured and calculated temperatures in the slab. The gauge at the east part of the base slab was damaged and is not showed.

Similar to the recorded and theoretical temperature developments of the base slab, the profiles for the walls correspond well to each other, see Figures 10 and 11 for the west and east walls. Gauge 8 should represent a part of the wall where only a temperature gradient across the thickness of the wall is present, hence that area should theoretically have adiabatic conditions in the other principal directions. At this location, the maximum achieved temperature differs only  $0.1^{\circ}\text{C}$  for the west wall  $0.5^{\circ}\text{C}$  for the east wall. Gauge 7 measures the temperature close to the strain gauge and the difference at maximum is  $2.8^{\circ}\text{C}$  for the west wall and  $1.3^{\circ}\text{C}$  for the east one. Gauge 6 is placed at the height of the strain gauge and 70 mm from the formwork, corresponding differences between calculations and recordings are  $1.2^{\circ}\text{C}$  for the west wall and  $0.4^{\circ}\text{C}$  for the east one. An overall tendency for all temperature profiles is that the calculated temperatures are lower (to a maximum of  $4.3^{\circ}\text{C}$  for gauge 6 in the east wall) compared to the recorded one after the temperature peaks until the point of tensile failure.

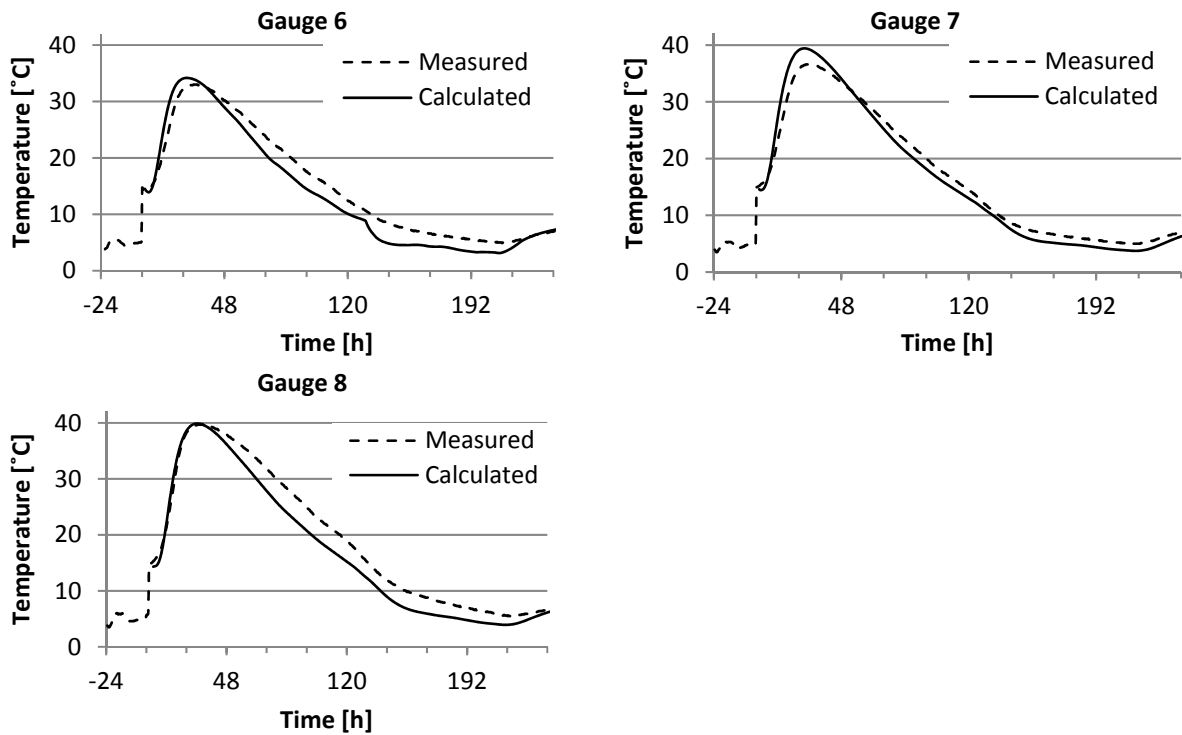


Figure 10 – Measured and calculated temperatures, for gauges 6 - 8, West wall.

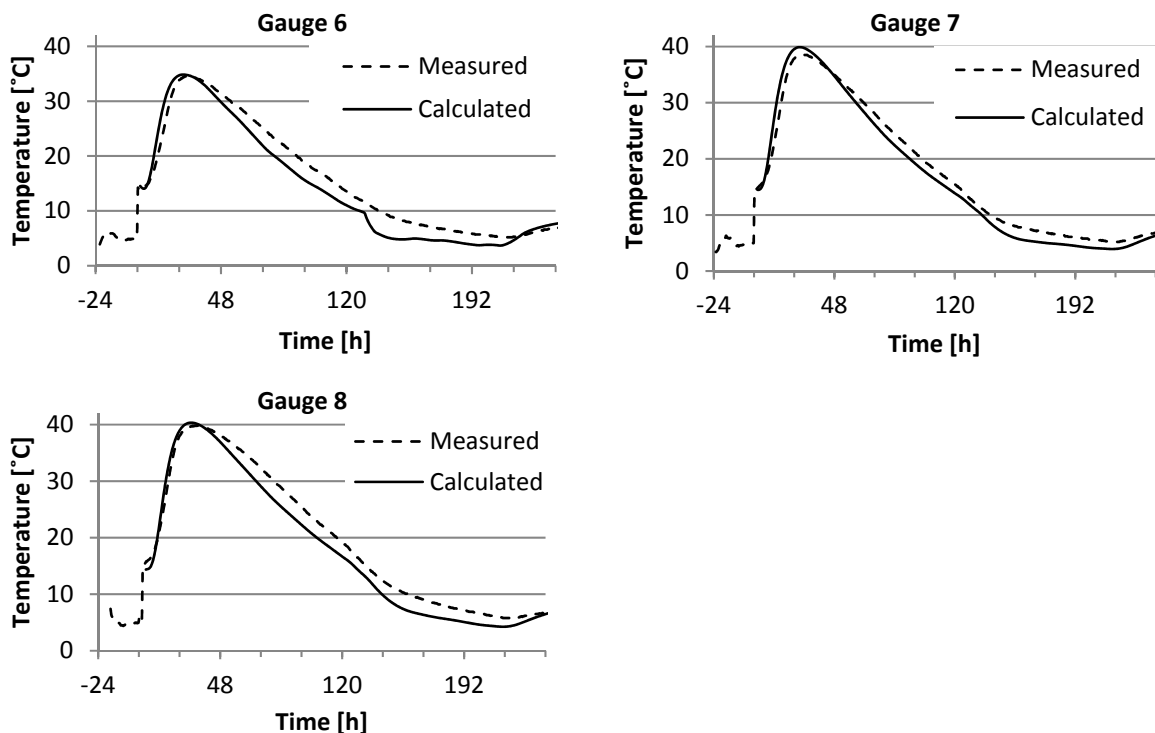


Figure 11 – Measured and calculated temperatures, for gauges 6 - 8, East wall.

### 3.5 Strains

#### Measured strains

In order to make sure that the free movement inside the concrete is measured, the raw data of the main gauges was calibrated to the corresponding data from each reference gauge. These gauges

are also used to detect a possibly drift in the system due to temperature variation in the cables or instruments. As can be noted in Figure 12, no significant drift is present from the reference gauge.

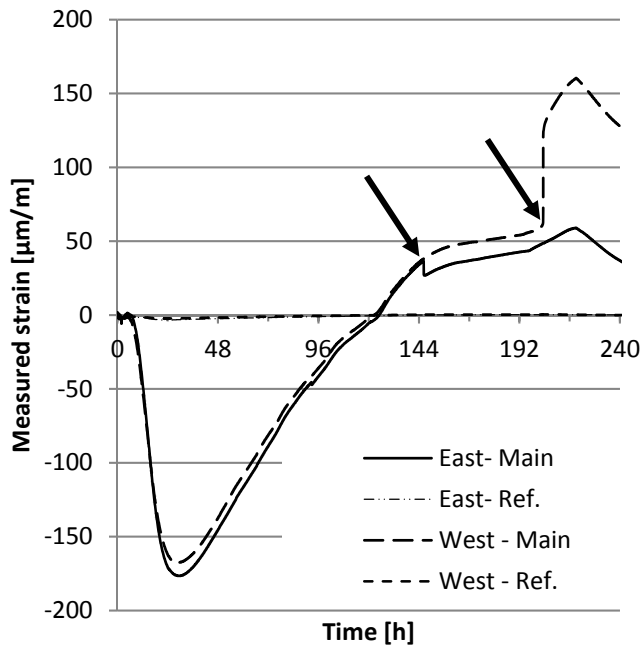


Figure 12 – Measured strain in the east and west walls. Arrows indicates point of cracking.

As seen in Figure 12 the east wall cracked spontaneously after 146 h, which is observed as a strain decrease. This is explained by the fact that a crack occurred between the strain gauge and the vertical joint to the adjacent wall. Thus, the crack unloads parts of the wall and a contraction is achieved; hence a sudden strain decrease is detected at the point of cracking. The west wall did not crack spontaneously and measures were taken to force it to crack. To increase the strain in the west wall, the heating cables in the base slab were thus activated to expand the slab. The time of activation, 199 h after wall casting, of the cables was documented and modelled in the ERM model. Additional to the heating cables a layer of 10 mm cellular plastic was placed above the concrete surface of the slab to keep the added heat in the slab. The slab torn the wall to tensile failure after 204 h. The crack propagated across the main strain gauge and an evident increase in measured strain was observed, see Figure 12.

#### Calculated strain ratios

The derived ERM model gave a theoretical strain ratio profile for the examined cross-sections of the walls. The calculated average strain ratio was compared to the measured strain, see Figure 13. The ERM model used measured, derived or estimated values for the ingoing parameters. The parameter used was the concrete and ambient air temperature, material parameters, wind speed, filling rate, material parameters, restraint and heat transfer coefficients.

To analyse the risk of cracking, an average was taken over an area (at the examined location in the construction) where the maximum strain ratio was calculated [21]. The area used as an average has a height that equals 15% of the wall width, and a width that equals the width of the wall.

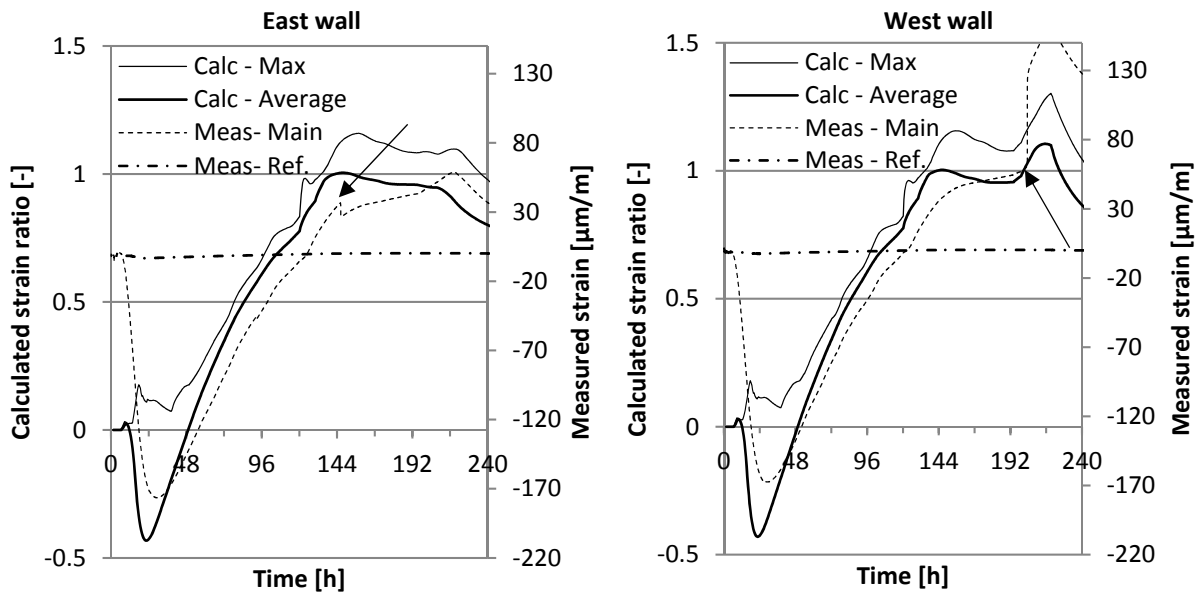


Figure 13 – Theoretical derived strain ratios in the east and west wall. Arrows indicates time of cracking.

In Figure 13 it is seen that the estimated time of cracking for the east wall is 146 h after casting. This is one hour and six minutes before the empirical obtained crack. The calculated average strain ratio at point of cracking is 1.01. The estimated time of cracking of the west wall is 203 h after casting, nearly two hours before the observed crack, see Figure 13. Already at 146 h after casting the calculated strain ratio shows a local maximum with magnitude 1.00, but no tensile strength failure was measured.

#### 4 SENSITIVITY OF MODEL PARAMETERS

One of the most significant issues when it comes to perform post-calculation is to mimic the measured counterpart, is the individual influence of a certain input parameter. Hence, sensitivity analyses for several input parameters of the ConTeSt software was performed to evaluate their impact on the calculated strain ratio. Thus, variations were made as follows: wind, initial concrete temperature, location of heating cables, model geometry, used temperature of ambient air and heat transfer coefficient of form work, see Table 1.

From the table, it is observed that a variation of the *wind* from 1 m/s to 9 m/s results in a maximum temperature decrease of 4.4°C and 6 percentages decrease of the strain ratio. These effects are more prominent at wind speed below 5 m/s. An increase or decrease from the *initial concrete temperature* with 1°C leads to an increase or decrease of the strain ratio with 3 percentages. The *location of the heating cables* does not have any effect on the strain ratio as long as the variation in height is less than 40 mm. A comparison between a *fully modelled cross section* and a *half modelled cross section* (see Figure 14). An insignificant difference was found and the fully modelled geometry is ought to be used only if the base slab is heated asymmetrically. The effect of how thorough the *temperature development of the ambient air* was modelled was tested by using three profiles; one profile with closely spaced temperature points, one with sparse spaced points and one with constant temperature, see figure 15. The conclusion is clear that it is of great importance to model the temperature development as thorough as possible. The *heat transfer coefficient* of the form work is built up by three parts within the ConTeSt software; thickness of the form, heat conductivity of the form and wind speed. The thickness was varied from 22 mm to 30 mm resulting in a heat transfer coefficient of 5.14 W/(m<sup>2</sup> K) and 3.97 W/(m<sup>2</sup> K) respectively.

The heat conductivity was set to 0.14 W/K m to mimic the property of wood, and the wind speed was constant 5 m/s. A difference of 8 percentages was obtained implying that this parameter is of palpable significance.

Table 1 – Sensitivity tests of input parameters in the ERM model. “var” indicates that the parameters are varying over time.

Tested parameter	T <sub>concrete</sub> [°C]	T <sub>air</sub> [°C]	Wind [m/s]	T <sub>max</sub> [°C]	Strain	Strain	Comment / Result
					ratio	average	
					Max		
					[-]	[-]	
<b>Wind</b>	15.5	var	1	44.6	1.18	1.06	Effect of wind
	15.5	var	3	43.7	1.17	1.04	change is more
	15.5	var	5	42.8	1.16	1.02	prominent for
	15.5	var	7	42.5	1.15	1.01	variations below
	15.5	var	9	42.2	1.15	1.00	5 m /s.
	14.5	var	5	41.9	1.12	0.99	
<b>T<sub>concrete</sub> (Concrete temperature at casting)</b>							$\Delta T = 1^\circ\text{C} \implies$
							0.03 in average strain ratio
<b>Location of heating cable</b>	15.5	var	5	43	1.15	1.02	50mm below surface
	15.5	var	5	42.8	1.16	1.02	70mm below surface
	15.5	var	5	42.7	1.16	1.02	90mm below surface
<b>Modelled geometry (Figure 14)</b>	15.5	6	5	43.5	1.04	0.92	Half
	15.5	6	5	43.5	1.03	0.92	Full
<b>Ambient temperature (Figure 15)</b>	15.5	var	5	42.8	1.16	1.02	Thorough
	15.5	var	5	42.4	1.19	1.05	Rough
	15.5	3	5	43.5	1.04	0.92	Constant
<b>Heat transfer coefficient, h, of form work</b>	15.5	6	5	43.5	1.04	0.92	$h = 5.14$
	15.5	6	5	44.2	1.11	1.00	$h = 3.97$

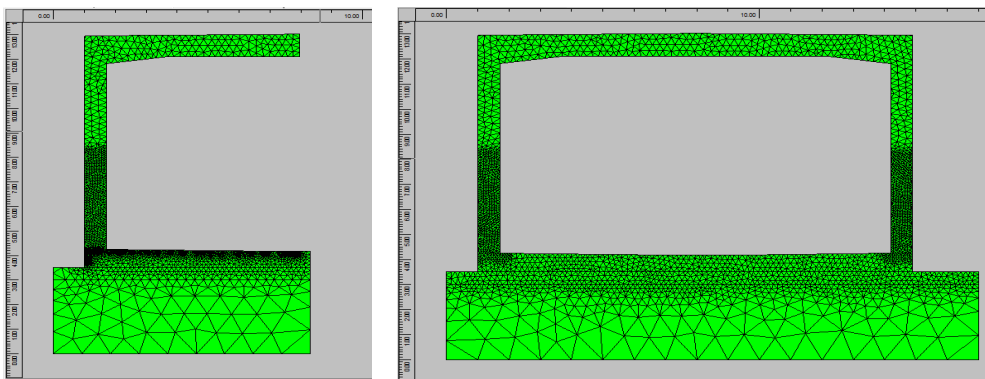


Figure 14– Two types of modelling; half and full cross section of the tunnel section.

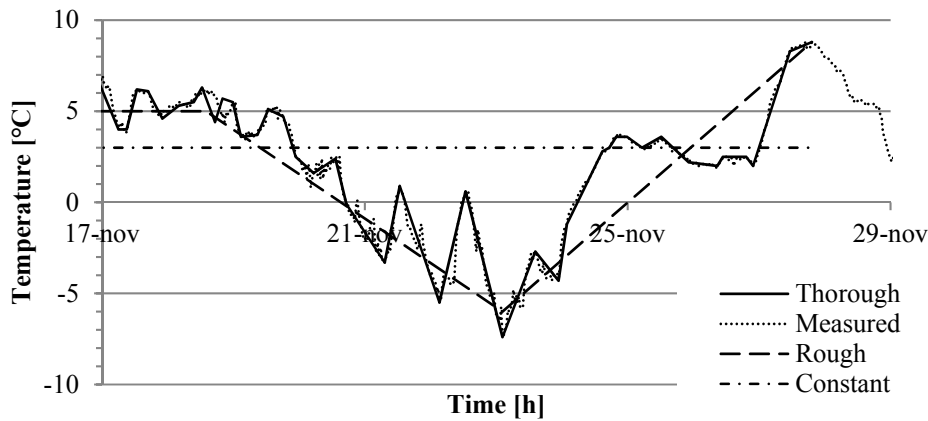


Figure 15 – Modelled temperature profiles of the measured ambient air, see Table 1.

## 5 CONCLUSIONS

In this work, the accuracy of modelling the restraint by use of Equivalent Restraint Method is demonstrated. Several laboratory tests were performed to the concrete used and an evaluation was performed to yield a set of parameters to the ERM model. Temperature and strain measurements were performed in field documentations, and final calculations with the ERM model were made to yield strain ratio development and time of cracking. The documented and calculated time of cracking were compared.

The measurements were performed at the casing of a section of a railway tunnel. The section consisted of a base slab, on that, two walls and a roof are cast as one monolith. This segment was cast to an adjacent, already completed, section. Eight heating cables were placed at the reinforcement of the base slab prior to the cast of the slab, to serve as a possibility to initiate cracking by expansion the slab.

Below main conclusions regarding the steps in the process stated in Section 3 are given, and at the end an overall conclusion is made.

### *Evaluation of material parameters*

A complete set of input material parameters was obtained from laboratory tests, see [22]. These parameters were tested in pilot calculations to evaluate how the set of parameters behaves compared to the standard parameters in the program. The concrete proved to give a higher maximum temperature with about 1–2 °C, compared to an already tested similar concrete to which ConTeSt provides a material parameter set.

### *Establishing the Equivalent Restraint Method Models*

The determination of the restraint situation for the ERM model was done in the same way as in [12]. The regression of the strain ratio for the LRM models to form the ERM model correspond well, and the model developed agreed to how it is proposed within the manual of ConTeSt [15] to model such a geometry and situation.

Regarding thermal parameters of the boundaries four major uncertainties can be pointed out; a representative initial temperature of the young concrete, the wind speed around the form, the heat conductivity of the form and the temperature profile outside and inside the walls. The initial temperature of the concrete should represent the thermal state when the concrete is poured. Since the casting proceeded several hours and several batches were used, a variation in temperature of the poured concrete is natural. Insufficient information regarding the pouring process and

limitations within the software made the choice for the initial concrete temperature to be the first recorded by a gauge located in the middle of the wall about 850 mm over the base slab. One should bear in mind that the temperature could vary in all directions around this gauge.

Furthermore, the wind around the wooden formwork play a significant role when it comes to cool the concrete. No gauge to measure the wind speed was used, but the wind profile over time varied a lot, both inside and outside the tunnel. The actual effect on the heat transfer coefficient is really hard to estimate even if the wind speed should have been recorded since several micro climates are present due to the sectioning in the formwork. The mentioned uncertainty of the wind condition combined with that no test of the heat conductivity of the form work was performed made the estimation of the heat transfer coefficient a questionable parameter. The argumentation about the uncertainties of the wind profile could also be considered valid for the temperature around the form work.

#### *Temperature comparisons*

A large agreement between the measured and calculated temperatures in the base slab and walls was desirable to verify whether or not the ERM model describes the field situation for the cast tunnel parts. For the base slab, the temperature condition at time of casting the walls were well predicted with the ERM model. The calculations for the two wall castings showed a nearly perfect resemblance. The maximum temperature measured by gauge 8 (where only a horizontal temperature gradient should be present) was closely predicted by the model. The calculated maximum at gauge 6 and 7 were higher than the corresponding measures. Gauge 7 showed the largest discrepancy, and one explanation to an overpredicted temperature could be that the thermal conductivity to the base slab is higher in reality due to the large amount of reinforcement bars. The reinforcement serves a thermal bridge if the parts outside the wall are cooler. Another explanation could be variances of the concrete temperature during the pouring process.

In general, the calculated temperatures showed a faster temperature decline than the recorded. This is possibly a result of a less fortunate estimated cooling factor,  $a$ , during the evaluation of material parameters. Another explanation could be that the wind speed was strong at the start of the cast and decreased after the temperature peak. The calculations use a constant wind speed throughout the whole calculation.

#### *Strain comparisons*

A remarkable good resemblance between the measured time of cracking and the calculated equivalent for both walls is demonstrated. The east wall cracked spontaneously about a day after removing the formwork. The maximum recorded strain is lower than the calculated depending on the fact that the crack appeared beside the strain gauge. Hence, the maximum strain at arbitrary location in the wall is not recorded. The established ERM model used the restraint situation at the middle of the wall, but the restraint at the location where the crack appeared is very similar. Even though the crack appeared beside the gauge, the ERM model manage to estimates the point of cracking just one hour earlier. The west wall needed the heating cables to expand the base slab increasing the strains to exceed the maximum strain before cracking. The calculated and measured point of cracking differed roughly two hours. An earlier local maximum of the strain ratio occurs in the calculation and the magnitude slightly exceeds the tensile strength. However, there is an uncertainty in many of the parameters used in the model and it is most possible that an over estimation of the strain ratio is present.

At the sensitivity analysis of some parameters is examined, and it is shown that a moderate variation of the heat transfer coefficient of the formwork changes the calculated strain ratio several percentages. Since it is cumbersome to test the heat transfer coefficient, it becomes as significant uncertainty factor in the performed calculations.

The overall conclusion is that the ERM model described the measured field temperatures and strains with a very good precision. Hence, the objective to evaluate the reliability of the restraint obtained by the ERM is fulfilled for the studied case.

## 6 DISCUSSION

To enhance the possibility to evaluate the correctness of the theoretical model further it is suggested that any field tests should be complemented with measurements of the wind speed. Moreover, tests of the heat transition coefficient of the form work is a good idea, to make the model more accurate.

Even though this work only compares the strain from two measurements with calculations, the typical situation of wall on slab is now declared to be well understood since reliable theoretical models are established to handle the restraint i.e. [6], [12], [14] and this work. The ERM has been applied to a variety of casting situations and therefore indeed seems to be well suited for crack risk estimations.

A suggestion to further validating the model, is to study other parts of a similar structure. An interesting study would be to investigate the area close to the construction joint between the two roof slabs. Experiences from the field prove that pre-calculations made to prevent thermal cracking for this structural case are less precise. If the ERM model could be compared to strain measurements of a roof to roof situation in a similar way as within this work, it would be of great importance to verify the method.

Several uncertain factors are present at this kind of studies; the wind (scaffolding, geometrical variations around the structure), initial concrete temperature, different temperature and wind condition inside and outside the tunnel, effect on the concrete temperature due to reinforcement bars, material parameters, pouring process (filling rate), moisture gradients, heat transfer coefficient of the formwork, adhesion at the joint between wall and base slab, mechanical deformations due to instabilities in the ground or external force caused by heavy machineries or nearby blasts. All these factors needed to be taken into consideration in one way or another. Even with this vast amount of parameter and parameter ranges the ERM model can describe the field situation with a satisfying precision. This implies that with the use of an ERM model together with suitable material parameters and reasonable values of the other input parameters reliable pre-calculations can be established to analyse the risk of through and surface cracking. From this analyse, suggestions of measures to decrease the risk can be made.

## 7 ACKNOWLEDGEMENTS

A sincere gratitude is given Gerard James for all work with the measurements of strain development. Others who contributed to this work and deserve to be acknowledged are Vilmer Andersson Vass for help during the measurements of the temperatures and Kjell Wallin for theoretically and practically orientated discussions.

The research has been supported by Swedish Contractors Fund for Research and Development, (SBUF).

## REFERENCES

1. ACI Committee 207: "Effect of Restraint, Volume Change, and Reinforcement on Cracking of Massive Concrete," *ACI Committee 207*, ACI207.2R-95, 2002, 26 pp.

2. Emborg M, Bernander S: "Assessment of the Risk of Thermal Cracking in Hardening Concrete," *Journal of Structural Engineering, ASCE*, Vol.120, No 10, October 1994. pp. 2893-2912.
3. Mihashi H, Leite J P: "State of The Art Report on Control of Cracking in Early Age Concrete," *J. Advanced Concrete Technology*, Vol. 2, No. 2, 2004, pp.141–154.
4. Kianousha M R, Acarcanb M, Ziari A: "Behavior of base restrained reinforced concrete walls under volumetric change," *Engineering Structures*, No. 30, 2008, pp.1526–1534.
5. Cusson D, Repette W: "Early-Age Cracking in Reconstructed Concrete Bridge Barrier Walls," *ACI Materials Journal*, Vol. 97, No. 4, July/August 2000, pp. 438-446.
6. Nilsson M: "Restraint Factors and Partial Coefficients for Crack Risk Analyses of Early Age Concrete Structures," *Doctoral Thesis*, Dept. of Civil, Environmental and Natural Resources Engineering, Luleå University of Technology, Luleå, Sweden, 2003, 170 pp.
7. Gasch T: "Concrete as a multi-physical material with applications to hydro power facilities", *Licentiate Thesis*, Dept. of Civil and Architectural Engineering, KTH Royal Institute of Technology, Stockholm, 2016, 144 pp.
8. Bosnjak D: "Self-Induced Cracking Problems in Hardening Concrete Structures," *Doctoral Thesis*, Dept. of Structural Engineering, Norwegian University of Science and Technology, 2000, 171 pp.
9. Rostásy F S, Tanabe T, Laube M: "Assessment of External Restraint," In: "Prevention of Thermal Cracking in Concrete at Early Ages," *RILEM Report*, No. 15, RILEM Technical Committee 119, 1998, pp. 149-177.
10. Emborg M: "Development of Mechanical Behavior at Early Age," In: "Prevention of Thermal Cracking in Concrete at Early Ages," *RILEM Report*, No. 15, RILEM Technical Committee 119, 1998, pp. 77-148.
11. Fjellström P: "Measurement and Modelling of Young Concrete Properties," *Licentiate Thesis*, Dept. of Civil, Environmental and Natural Resources Engineering, Luleå University of Technology, Luleå, Sweden, 2013, 200 pp.
12. Hösthagen A, Jonasson J-E, Emborg M, Hedlund H, Wallin K, Stelmarczyk M: "Thermal Crack Risk Estimations of Concrete Tunnel Segments – Equivalent Restraint Method Correlated to Empirical Observations," *Nordic Concrete Research*, No. 49, 2014, pp. 127-143.
13. Nilsson M: "Restraint Factors and Partial Coefficients for Crack Risk Analyses of Early Age Concrete Structures", *Doctoral Thesis*, Division of Structural Engineering, Lulea University of Technology, Lulea 2003, 170 pp.
14. Al-Gburi M: "Restraint Effects in Early Age Concrete Structures," *Doctoral Thesis*, Dept. of Civil, Environmental and Natural Resources Engineering, Luleå University of Technology, Luleå, Sweden, 2015, 201 pp.
15. JEJMS Concrete: "ConTeSt Pro – Users Manual - Program for Temperature and Stress Calculations in Concrete," *User's Manual*, Luleå, Sweden, April 2008, 198 pp.
16. DIANA FEA BV: "DIANA – Displacement Analyzer," *Software*, 2017, homepage: <https://dianafea.com/content/DIANA>
17. JSCE: "English Version of Standard Specification for Concrete Structures 2007", Japan Society of Civil Engineer, JSCE, December 2010, 503pp.
18. Sato R, Shimomura T, Maruyama I, Nakarai K: "Durability Mechanics of Concrete and Concrete Structures Re-Definition and a New Approach," *Proceedings*, 8<sup>th</sup> International Conference on Creep, Shrinkage and Durability of Concrete and Concrete Structures (CONCREEP8), Ise-Shima, Japan, 2008.
19. JCI: "A Proposal of a Method of Calculating Crack Width due to Thermal Stress," *JCI Committee Report*, Committee on Thermal Stress of Massive Concrete Structures, Japan Concrete Institute, Tokyo, Japan 1992, 106 pp.

20. Al-Gburi M, Jonasson J-E, Nilsson M, Hedlund H, Hösthagen A: "Simplified Methods for Crack Risk Analyses of Early Age Concrete - Part 1: Development of Equivalent Restraint Method," *Nordic Concrete Research*, No. 46, 2012, pp. 17-38.
21. Larson M: "Thermal Crack Estimation in Early Age Concrete – Models and Methods for Practical Application" *Doctoral Thesis*, Dept. of Civil, Environmental and Natural Resources Engineering, Luleå University of Technology, Luleå, Sweden, 2003:20, 190 pp.
22. Hösthagen A, Jonasson J-E, Emborg M, Nilsson M: "Evaluation of Material Properties for Young Concrete," to be published.
23. Moreton, D.N: "An Introduction to Measurements using Strain Gauges Karl Hoffmann", *Strain*, Vol 37:3, 2001, 127 pp.



## **Paper IV:**

### **Evaluation of Material Properties for Young Concrete.**

**Hösthagen A**, Jonasson J-E, Emborg M, Nilsson M, to be published.

## Evaluation of Material Properties for Young Concrete



Anders Høsthagen, M.Sc. Ph.D. Student  
Betong & Stålteknik  
Anders.Hosthagen@bostek.se  
and  
Luleå University of Technology  
Division of Structural and Fire Engineering  
SE-971 87 Luleå  
Anders.Hosthagen@ltu.se



Prof, Tech. Dr. Jan-Erik Jonasson  
Luleå University of Technology  
Division of Structural and Fire Engineering  
SE-971 87 Luleå  
Jan-Erik.Jonasson@ltu.se



Prof, Tech. Dr. Mats Emborg  
Betongindustri AB, Box 47312  
SE-100 74 Stockholm  
Mats.Emborg@betongindustri.se  
and  
Luleå University of Technology  
Division of Structural and Fire Engineering  
SE-971 87 Luleå  
Mats.Emborg@ltu.se



Tech. Dr. Martin Nilsson  
Luleå University of Technology  
Division of Structural and Fire Engineering  
SE-971 87 Luleå  
Martin.Nilsson@ltu.se

## ABSTRACT

Restrained volumetric changes in early age concrete may cause tensile strength failure, i.e. crack initiation and propagation. The volumetric changes are primarily induced by a change in thermal and moisture states, and it is of great importance to quantify the resulting stresses and strains that arise when the volumetric changes are restrained. Large economical and technical benefits are gained if measures to avoid cracking can be determined by calculations prior to casting. To perform such calculations, the following property areas of the concrete needs to be known; *strength development, heat of hydration, basic shrinkage, thermal dilation, basic creep and stress at full restraint.*

This work demonstrates how the concrete can be tested in a laboratory environment and how to evaluate the numerical data, thus yielding a parameter set that may be used during stress and strain development calculations. Furthermore, a brief investigation is performed on how sensitive the evaluation for each test is, with respect to crack risk estimation.

It is showed that the measured stress development from the stress development at full restraint test can be considered as a checkpoint for the total parameter set. The reason is that the calculated stress development, which is compared to the measured counterpart, is influenced by all evaluated parameters.

It is discussed that out of the performed tests, three are of significant importance when it comes to provide an operational parameter set for the calculations. These tests are the ones achieving strength development, heat of hydration and stress at full restraint.

**Key words:** Young concrete, material parameters, strength development, heat of hydration, basic creep, basic shrinkage, thermal dilation, modelling, stress at full restraint

## 1. INTRODUCTION

The risk of early thermal cracking in concrete is a complex subject indeed, and hence has been studied for a long time when constructing massive concrete structures. For example, one very well documented project with complex measures to counteract early thermal cracking is the construction of the Hoover dam in US during the 1930's, [1]. A sophisticated method of casting in blocks and ice water cooling of the concrete followed by injecting grout into the spaces between the blocks was used. This pioneering technique opened the door for performance of other major structures all over the world. The technique of taking measures against thermal cracking has been applied and evolved since this pioneering project. Important recent research in the area has thus been performed at various universities and projects such as LTU (Luleå University of Technology), NTNU (Norwegian University of Science and Technology), Braunschweig University of Technology, TMU (Technical University of Munich) and by the European Commission financed project IPACS (Improved Production of Advanced Concrete Structures) 1997-2001.

Nowadays, with the aid of computers and customized software, stress and strain analysis can be calculated in several ways for young concrete. During hardening these calculations make it possible to analyse the risk of cracking within a construction. In a high level of accuracy, a lot of thermal and mechanical properties for the young and aging concrete have to be known. The type of laboratory tests needed always depend on the way of how the concrete behaviour is modelled

in the software. For the models developed at LTU the tests needed are divided into the following property areas:

- *strength development*
- *heat of hydration*
- *basic shrinkage*
- *thermal dilation*
- *basic creep*
- *stress at full restraint*

The outcome of the evaluation of these tests provides a parameter set of thermal and mechanical properties necessary to perform crack risk calculations for the young concrete. Even if such a set of parameters is established it is not certain that it describes the behaviour of the young concrete in a reliable way. The quality of the evaluation namely depends on the accuracy of the measurements performed and the thoroughness during parameter determination. Therefore, it is of great importance to investigate the sensitivity of the evaluation for each test on the final crack risk estimation.

From above, the following research questions can be defined;

- Is it possible to estimate the accuracy of a specific test method?
- Is it possible to establish criteria of tolerances for each method, based on the influence at the final crack risk estimation?
- What influence does each parameter have on the final crack risk estimation, and which one has the most importance?
- Which improvements (if needed) can be made in the test set-ups and the evaluations?

## 2. AIMS, PURPOSES AND LIMITATIONS

To address the problem formulation above, aims and purposes can be formulated as:

- Presenting the models and equations used.
- Describing and discussing the steps at evaluation of the tests performed needed to describe a novel concrete.
- Analysing the consequences on the stress calculation when varying the fitting parameters at evaluation of the tests.

The above listed property areas are here described in accordance with the models used in the software ConTeSt [2], and all operative equations are presented. The focus is both on the evaluation of the tests and what the consequences are with respect to the calculation of stresses as a base for crack risk analyses.

The limitations of this work could be defined as:

- Only one collection of test set-ups, one collection of evaluation models and one software, ConTeSt, is singled out to the scope of this work. This approach is used to restrict the extent of this work, since there exist a variety of models describing each property area and several software (such as 4C, ABAQUS, ATENA, COMSOL Multiphysics, DIANA) that may perform equivalent analysis.
- Only one concrete mix is examined during the sensitivity evaluation.

### 3. METHOD

The method of this work comprises;

- A description of the tests performed to specimens of a concrete mix.
- An examination of the evaluation process of the numerical data from the tests.
- An analyse of the stress calculation performed with the parameters evaluated.

The overall philosophy when testing young concrete according to the test groups mentioned above is that it shall cover what is needed to make estimations of:

- Strength growth at variable temperatures.
- Concrete temperature taking heat of hydration into account.
- Free deformations (strains) at variable temperature, taking basic shrinkage into account.
- Growth of elastic modulus and the following creep behaviour.
- Stresses at restrained conditions.

Generally, it is well known that the most tested property of young concrete is the strength at 28 days using regulated hardening conditions. This is what is needed to characterize the strength class in most standards. For calculations and follow up situations also the strength development by time has to be known. To estimate temperatures together with calculations of strength is necessary in situations of planning actions on site, like how to avoid early freezing, how to meet demands of predetermined moisture hardening periods, how to fulfil different form stripping time – especially at winter conditions etc.

For stress calculations and estimations of risk of early cracking, all last three areas have to be clarified for a certain concrete mix. The stress development over time is tested for the average temperature of a 0.7 m thick wall at completely restrained conditions (100 % restraint). This situation is always the same, simulating the resulting stress for a “typical structure” that has been considered as a representative case for many civil engineering structures. One important consequence is that the test results (like early cracking, late cracking or no cracking for a certain maximum stress to strength level) are a direct measure of the tested concrete mix with respect to the sensibility of cracking. But, to get data for stress calculations also information concerning *free deformation*, *elasticity growth* and *creep* are needed.

The first two tests to be performed and evaluated are the *strength development* and the *heat of hydration* tests. From the evaluation of these tests a temperature reference curve (for the 0.7 m wall) is established. This curve is used at the tests of the *basic shrinkage* and *thermal dilation (free deformation)*. Beside the temperature reference curve, the expression of equivalent time of maturity is established which is also needed in the evaluation of the *basic creep* tests. The *thermal dilation tests* are executed in two ways; the first test is performed simultaneously with the basic shrinkage test by letting a moist sealed concrete specimen freely expand and contract due to hydration. The second thermal dilation test, i.e. *stress at full restraint*, consists of a cubic concrete specimen undergoing thermal dilation during full restraint, yielding the stress development.

A sensitivity demonstration is performed, where it is showed how an alternation of magnitude for some determined parameters effects the crack risk estimation.

## 4. BASIC THEORY – MAIN MATERIAL PROPERTIES

Below it is described how to obtain a set of fully tested material parameters for a young concrete mix. The test was performed at LTU. The evaluated parameters are suitable to be incorporated into the software ConTeSt. Since the laboratory tests and fundamental equations that describes the physical entities is arbitrary in the senses that other laboratories and software could use the tests and evaluation techniques and no previous article has covered the whole process, relevant excerpts of the theory are presented. Below the mix proportions of the examined concrete and an overview of the laboratory tests methods are given.

### 4.2 Strength development

Tests of how to determine the concrete strength development has been performed since early 1900 [4]. Both the temperature and the moisture effect the strength development. Since moisture so far is difficult to measure with sufficient precision the current evaluation models solely depend on temperature, see e.g. [5]- [10].

The main purpose of this test procedure is to establish the reference strength development function. From the performed tests, the first part to develop is the temperature dependent maturity function, thereafter the equivalent time of maturity. With these two functions, the reference strength development function can be established.

#### *Strength growth*

The compressive strength development,  $f_{cc}(t)$ , is examined by letting concrete specimens cure in water baths at different temperature conditions and the loading them compression to failure. The specimens are cast and cured in plastic forms with the dimension 100×100×100 mm. As soon as the concrete is poured into the forms and vibrated they are placed in temperate water baths for curing. At LTU normally four target curing temperatures for the water baths are used; 5°C, 20°C, 35°C and 50°C. The temperatures in the baths are logged for further use, see Eqs. 3 and 4. In this demonstration only curing at 20°C, 35°C and 50°C was done. The strength of the specimens cured at 20°C is tested at roughly 24, 32, 52, 120 and 672 hours after casting. At every test occasion three specimens are used. For the curing temperatures of 35°C and 50°C the strength tests are performed roughly at 8, 24, 32 and 52 hours after casting. The results from the strength tests at different curing temperature are used to determine the parameters for the equivalent time of maturity,  $t_e$ .

The compressive strength development at 20°C, without adjustment for the effects of high curing temperature, is referred to as the *reference strength development* and determined as; see e.g. [11]- [13] and Figure 3b. Three stages defined as

Stage 1: fresh concrete (  $0 \leq t_e < t_S$  )

Stage 2: between initial and final setting (  $t_S \leq t_e < t_A$  )

Stage 3: hardening concrete (  $t_e \geq t_A$  )

$$f_{cc}^{ref}(t_e) = \begin{cases} 0 & \text{for } 0 \leq t_e < t_S \\ \left( \frac{t_e - t_S}{t_A - t_S} \right)^{n_A} \cdot f_A & \text{for } t_S \leq t_e < t_A \\ \exp \left( s \cdot \left( 1 - \left( \frac{672 - t^*}{t_e - t^*} \right)^{n_{cc,28}} \right) \right) \cdot f_{cc,28} & \text{for } t_e \geq t_A \end{cases} \quad (1)$$

The expression for stage 3 in Eq. 1 is based on a formula in EN 1992-1-1:2004 (Euro Code 2), and modified to fulfil the condition  $f_{cc}^{ref}(t_A) = f_A$ , and  $t^*$  is calculated by

$$t^* = \frac{672 - \delta_c \cdot t_A}{1 - \delta_c} \quad (2)$$

with

$$\delta_c = \left( 1 - \frac{1}{s} \cdot \ln \frac{f_A}{f_{cc,28}} \right)^{1/n_{cc,28}}$$

where

- $t^*$  = is calculated by Eq. 2, but has no physical meaning [h]
- $t_e$  = equivalent time calculated by Eq. 3 [h]
- $t_S$  = equivalent time at initial setting, where the concrete starts to transform from a “liquid” to a “solid” state [h]
- $t_A$  = equivalent time at final setting, where the concrete surface no longer can be troweled, modelled by the time when the strength reaches  $f_A$  [h]
- $f_A$  = concrete strength at final setting, usually chosen to be the strength level 0.5 MPa
- $s$  = parameter influencing the curve shape in time for the hardening concrete [-]
- $n_{cc,28}$  = parameter influencing the curve shape in time for the hardening concrete [-]
- $f_{cc,28}$  = 28 days strength of the concrete [Pa]

The strength  $f_A$  [MPa] is calculated for when the equivalent time of maturity equals the time when trowelling is not possible any more,  $t_e$  [h], at the end of stage 2 in Eq. 1.

Equivalent time of maturity,  $t_e$ , is described in various literature, see e.g. [11] and [13].

$$t_e = \beta_\Delta \cdot \int_0^t \beta_T \cdot dt + \Delta t_e^0 \quad (3)$$

The parameters  $\beta_\Delta$  [-] and  $\Delta t_e^0$  [s] might be used when modelling effects of different admixtures. For a certain single evaluation, usually they are set to  $\beta_\Delta = 1$  and  $\Delta t_e^0 = 0$ .  $\beta_T$  is the temperature dependent maturity function given by [11], see also Figure 3a, as

$$\beta_T = \exp\left(\Theta \cdot \left[\frac{1}{293} - \frac{1}{T+273}\right]\right) \quad (4)$$

where

$\Theta$  is the thermal activation energy function described as

$$\Theta = \Theta_{ref} \cdot \left(\frac{30}{T+10}\right)^{\kappa_3} \quad (5)$$

with  $\Theta_{ref}$  [K] and  $\kappa_3$  [-] are maturity parameters, determined by measuring the compressive strength at different temperatures as described above.

By using the developed temperature dependant maturity function  $\beta_T$ , the real time is converted to equivalent time of maturity  $t_e$ . Both functions for  $t_e$  and  $\beta_T$  are determined by regression analyses.  $\beta_T$  describes the rate of the cement reaction in relation to the chosen reference temperature 20°C.

#### *Strength loss at elevated temperatures*

For some binders at some strength classes, it has been observed a loss of strength at higher curing temperatures, see e.g. [12]. This effect can be taken into consideration, and a model is presented in [12] and [13]. However, no further modelling of strength loss at higher temperatures is given here, meaning that  $f_{cc}(t_e) = f_{cc}^{ref}(t_e)$  in this paper.

### 4.3 Heat of hydration

The heat of hydration is, see e.g. Figure 5, determined by the evaluation of semi adiabatic calorimetric measurements, see e.g. [9]. In [12] a correction factor,  $\eta$ , was introduced to take the heat loss to the test set-up into account.

At present the semi-adiabatic test set-up at LTU consists of a cylindrical concrete sample cast in a metal bucket, a heating device and a cylindrical shaped cellular plastic unit. Two sizes of the cellular plastic unit are used simultaneously. To determine the heat of hydration and thermal properties, several processes can be applied, see e.g. [9], [12] and [14]. The total heat of hydration by cement weight at a certain time,  $q_{cem}$ , calculated from measured temperatures, using the semi-adiabatic calorimetric set-up, can be described by

$$q_{cem}(t) = \frac{\rho_c \cdot c_c}{C} \left( \eta \cdot (T_c(t) - T_{air}) + a \cdot \int_0^t (T_c(t) - T_{air}) \cdot dt \right) \quad (6)$$

where

- $q_{cem}$  = heat energy by cement weight [J/kg]
- $\rho_c$  = concrete density [kg/m<sup>3</sup>]
- $c_c$  = heat capacity by weight of concrete [J/kg °C]
- $C$  = cement content [kg/m<sup>3</sup>]
- $\eta$  = correction factor with respect to heat stored in the test set-up, values for  $\eta$ , see [12], -
- $T_c(t)$  = measured temperature in the concrete specimen [°C]

$T_{air}$  = ambient temperature [°C]  
 $a$  = cooling factor [1/s]

The cooling factor  $a$  determines the heat loss to the surroundings of the semi-adiabatic test set-up. This factor has been observed to vary between different tests and must be accurately documented for each single test, see [12].

In heat calculations the generated heat per concrete volume,  $Q_h$ , is of interest, see also [14], expressed by

$$Q_h(t) = \frac{dq_{cem}(t)}{dt} \cdot C \quad (7)$$

where

$Q_h$  = generated heat per concrete volume [W/m<sup>3</sup>]

The evaluated heat energy development using Eq. 6 can be approximated for computer calculations with the following formula

$$q_{cem}(t) = \exp\left(-\left(\ln\left(1 + \frac{t_e}{t_1}\right)\right)^{-\kappa_1}\right) \cdot q_u \quad (8)$$

where

$q_u$  = total heat energy by cement weight, formally after infinite time [J/kg]  
 $\kappa_1$  = free model parameter to get the acceptable fit with the test data [-]  
 $t_1$  = free model parameter to get the acceptable fit with the test data [s]

#### 4.4 Basic shrinkage and free thermal dilation

From tests of free deformations (unrestrained deformations at both about constant and variable temperature), the basic shrinkage (shrinkage at moisture sealed conditions) and the thermal dilation can be determined, see [15] and [16]. The temperature reference variation is usually calculated to for a 0.7 m wide wall, where the concrete temperature at casting as well as the ambient temperature is set to 20°C. The newly cast concrete is surrounded by a symmetric shelter described by a heat transfer coefficient of 4 [W/m<sup>2</sup>·K], simulating a common plywood form work. The resulting average temperature development may be regarded as a representative of a “real structure”.

The test set-up for examination of basic shrinkage and free thermal dilation consists of two concrete specimens cast in metal cylinders Ø80 mm [16]. After about 5-10 h the specimens are released from the metal form and strain gauges are mounted. Both specimens are sealed with plastic to avoid moisture loss to the surroundings. One specimen is placed in an environment with a temperature of roughly 20°C. The other is placed in a water bath where the temperature is regulated according to the calculated temperature development for the reference wall.

In the evaluating process, a determination of both the free thermal dilation and the basic shrinkage is performed. Basic shrinkage is referred to the volume change of the concrete due to chemically and physically consumed and bound water. Two evaluation procedures are used at LTU, described

in [17]. Here Method I is used and outlined below. In [16] an alternative method, Method II, is described and are used occasionally. The main difference between the two methods is that the basic shrinkage is described purely as a function of equivalent time in Method I and as a function of equivalent time and temperature in Method II.

The sealed concrete specimens undergo a volume change as a function of time, see Figure 6a. For the specimen stored at 20°C the main part of the volume change is due to basic shrinkage. The specimen placed in the temperate water, with the calculated reference temperature as the target curve, will undergo a volume change due to both free thermal dilation and basic shrinkage, see Figure 6b, formulated as

$$\varepsilon_{free} = \varepsilon_T + \varepsilon_{sh}^0 \quad (9)$$

where

$$\begin{aligned} \varepsilon_{free} &= \text{measured combined free strain, [-]} \\ \varepsilon_T &= \text{strain due to thermal dilation, [-]} \\ \varepsilon_{sh}^0 &= \text{strain due to basic shrinkage, [-]} \end{aligned}$$

The thermal dilation is expressed by

$$\varepsilon_T = \alpha_T \cdot \Delta T_c(t) \quad (10)$$

where

$$\begin{aligned} \alpha_T &= \text{thermal dilation coefficient, to be determined in the evaluation procedure, } ^\circ\text{C}^{-1} \\ \Delta T_c(t) &= \text{measured temperature change in the concrete, } ^\circ\text{C} \end{aligned}$$

The basic shrinkage is, according to Method I in [17] expresses by

$$\varepsilon_{sh}^0 = \beta_{s0}(t_e) \cdot \varepsilon_{su} = \exp\left(-\left(\frac{t_{sh}}{t_e - t_S}\right)^{\eta_{sh}}\right) \cdot \varepsilon_{su} \quad (11)$$

where

$$\begin{aligned} \varepsilon_{su} &= \text{reference ultimate shrinkage, to be determined in the evaluation procedure [-]} \\ t_S &= \text{time of initial setting, end of stage 1 in Eq. 1 [s]} \\ t_{sh} &= \text{time parameter affecting the shrinkage development, to be determined in the} \\ &\quad \text{evaluation procedure [s]} \\ \eta_{sh} &= \text{parameter affecting the shrinkage development, to be determined in the} \\ &\quad \text{evaluation procedure [s]} \end{aligned}$$

The development of basic shrinkage,  $\varepsilon_{sh}^0(t_e)$ , is determined by regression analysis by alternating the fitting parameters,  $\varepsilon_{su}$ ,  $t_{sh}$  and  $\eta_{sh}$ . The initial setting time,  $t_S$ , is already determined in the early described evaluation of the strength development analysis. The equivalent time,  $t_e$ , is calculated in accordance with Eq. 2.

#### 4.5 Basic creep tests

The basic creep evaluation is based on the theory described in [18] and [19], and in [20] a subroutine is described which purpose is to transform measured creep data into relaxation values. The basic creep function for aging concrete used at LTU today is described in [21] by the means of the so called linear logarithmic model for concrete creep.

Well known is that the concept of creep is defined as the deformation with respect to time that occurs for a concrete body with constant load (maintained in time), where a loading by maintained deformation yield to relaxation.

At LTU the creep is tested on eight cylindrical concrete specimens  $\varnothing 80$  [23]. All specimens are sealed to avoid moist exchange to the surroundings and therefore no drying shrinkage or drying creep is expected. Four specimens are mounted in mechanical test rigs and loaded to a prechosen value, that maintains in time. Two are loaded after about 5 days of curing and two after roughly 14 days (occasionally the load is applied after 28 days). The prechosen load level roughly 20 % of the compressive strength at the time of loading. This load is considered low enough to study linear creep, i.e. a creep defined where both the elastic strain and the creep is proportional to applied load. The sealed and loaded specimens undergo deformations due to *basic creep*. The remaining four specimens are used as references to deduct basic shrinkage from the loaded specimens. For more details of the laboratory set-up, see [12].

The total compliance,  $J$ , is the sum of one elastic part and one creep part

$$J(\Delta t_{load}, t_0) = \frac{1}{E(t_0)} + \Delta J(\Delta t_{load}, t_0) \quad (12)$$

where

$$\begin{aligned} t_0 &= \text{time at loading [d]} \\ \Delta t_{load} &= \text{time span after loading} = t - t_0 \text{ [d]} \\ t &= \text{time after mixing [d]} \end{aligned}$$

The elastic part of Eq. 12 is described by a modification of the model in Eurocode 1992-1-1

$$E(t_0) = \frac{1}{J(t_0 + \Delta t_0)} = \left( \frac{f_{cc}(t_e(t_0))}{f_{cc,28}} \right)^{\eta_E} \cdot E_{c,28} \quad (13)$$

where

$$\begin{aligned} \Delta t_0 &= \text{time span after loading employed as the definition of elastic modulus,} \\ &\quad \text{usually 0.001d is used, see [23], [d]} \\ f_{cc}^{ref}(t_e(t_0)) &= \text{compressive strength at time } t_0, \text{ calculated using Eq. 1 [Pa]} \\ t_e(t_0) &= \text{equivalent time at loading time } t_0 \text{ [d]} \\ \eta_E &= \text{connection parameter between the time development of elastic modulus and} \\ &\quad \text{compressive strength [-]} \\ E_{c,28} &= \text{elastic modulus at equivalent time} = 28\text{d [Pa]} \end{aligned}$$

The Linear Logarithmic Model (LLM) elaborated in the work in [21] is here used to evaluate the laboratory creep tests in order to determine the fitting parameters of the creep compliance, i.e. creep rate, described by

$$\Delta J(\Delta t_{load}, t_0) = \begin{cases} a_1(t_0) \cdot \log\left(\frac{\Delta t_{load}}{\Delta t_0}\right) & \text{for } \Delta t_0 \leq \Delta t_{load} \leq \Delta t_1 \\ a_1(t_0) \cdot \log\left(\frac{\Delta t_1}{\Delta t_0}\right) + a_2(t_0) \cdot \log\left(\frac{\Delta t_{load}}{\Delta t_1}\right) & \text{for } \Delta t_1 \leq \Delta t_{load} \end{cases} \quad (14)$$

where

$\Delta t_1$  = breakpoint in creep behaviour [d]

The total compliance then becomes

$$J(\Delta t_{load}, t_0) = \frac{1}{E(t_0)} + \begin{cases} a_1(t_0) \cdot \log\left(\frac{\Delta t_{load}}{\Delta t_0}\right) & \text{for } \Delta t_0 \leq \Delta t_{load} \leq \Delta t_1 \\ a_1(t_0) \cdot \log\left(\frac{\Delta t_1}{\Delta t_0}\right) + a_2(t_0) \cdot \log\left(\frac{\Delta t_{load}}{\Delta t_1}\right) & \text{for } \Delta t_1 < \Delta t_{load} \end{cases} \quad (15)$$

with  $a_1(t_0)$  and  $a_2(t_0)$  expressed as

$$\begin{aligned} a_1(t_0) &= a_1^{\min} + (a_1^{\max} - a_1^{\min}) \cdot \exp\left(-\left(\frac{t_0 - t_S}{t_{a1}}\right)^{\eta_{a1}}\right) \\ a_2(t_0) &= a_2^{\min} + (a_2^{\max} - a_2^{\min}) \cdot \exp\left(-\left(\frac{t_0 - t_S}{t_{a2}}\right)^{\eta_{a2}}\right) \end{aligned} \quad (16)$$

where

$a_i(t_0)$  = “logarithmic” creep rates for  $i = \{1, 2\}$  [ $\text{Pa}^{-12} / \log(\Delta t_{load})$ ]

$a_i(t_0)$  = “logarithmic” creep rates for  $i = \{1, 2\}$  [ $\text{Pa}^{-12} / \log(\Delta t_{load})$ ]

The values of  $a_i^{\min}$ ,  $a_i^{\max}$ ,  $\eta_{ai}$  [-] and  $t_{ai}$  [d] for  $i = \{1, 2\}$  are determined by regression analyses.

When a solution is found for the model Linear Logarithmic Model, i.e. creep values according to Eqs. 11-15, it is used as input to the program RELAX [22]. RELAX transforms the creep values to relaxation values, see e.g. Figure 10, which are parameters to a series of parallel Maxwell elements describing the viscoelastic behaviour of the concrete. This is done by solving the function for relaxation modulus  $R(t, t_0)$ , see [15], [21] and [23], from a compliance function  $J(t, t_0)$ , see [19]. Further information of how to prepare the input to RELAX is presented in Appendix A.1.

#### 4.5 Stresses in concrete at full restraint

With a temperature load corresponding to the mean temperature of a 700 mm thick wall, the stress at full restraint is measured. The free strain is hindered by the apparatus and the applied force is regulated to zero external strain, see e.g. [17] and [23].

The test set-up consists of a test frame (stress rig) and a concrete prism with rectangular cross-section. The concrete is cast into a form work which is sealed from drying shortly after casting. The concrete temperature is regulated with an air fan controlled by the temperature reference curve. Due to the volume change caused by the temperature change a positive or negative force is acting on a hydraulic servo-cylinder at one end of the concrete specimen. The servo-cylinder generates a counteracting force to simulate full restraint (100 % restraint), i.e. no external deformation is allowed. This force is directly proportional to the stress,  $\sigma$ , in the concrete specimen.

Calculations during the evaluation of the results from the stress rig can formally take place at a single point inside the concrete specimen, because it is considered to have a homogeneous state over its cross-section. The stress calculation is made as stepwise calculations in time. The stress variation from time =  $t_i$  to time  $t_{i+1}$  can be expressed by the constitutive equation by

$$\sigma_{i+1} = \sigma_i + \Delta\sigma_{i+1} \quad (17)$$

with

$$\Delta\sigma_{i+1} = E_{i+1}^{tot} \cdot (\Delta\varepsilon_{m,i+1} - \Delta\varepsilon_{i+1}^0) \quad (18)$$

Where

$\Delta E_{i+1}^{tot}$  = total fictive elasticity modulus including creep during the time step and the application of non-linear load-strain curve in Figure 1 [Pa]

$\Delta\varepsilon_{m,i+1}$  = change of the stress-related "material" strain during the time step [-]

$\Delta\varepsilon_{i+1}^0$  = total non-elastic deformation including relaxation during the time step [-]

The fictive E-modulus is described by

$$E_{i+1}^{tot} = E_{c,i+1} (1 + \gamma_d) \quad (19)$$

where

$E_{c,i+1}$  = effective modulus including creep effects calculated from RELAX [Pa]

$\gamma_d$  = correction factor for the non-linear application of the load-strain curve in Figure 1 [-]

At monotonic loading along the original curve for  $\sigma / f_{ct} > \alpha_{ct}$  the following applies

$$\gamma_d = \exp \left( - \frac{\frac{\varepsilon_{m,i+1} - \alpha_{ct}}{\varepsilon_0} - \alpha_{ct}}{1 - \alpha_{ct}} \right) - 1 \quad (20)$$

where  $\varepsilon_0 = f_{ct} / E_{c,i+1}$

$\varepsilon_{m,i+1}$  = average of the stress-related "material" strain during the time step [-]

- $\varepsilon_0 = f_{ct} / E_{c,i+1}$  = strain for an imaginary straight  $\sigma - \varepsilon$  curve reaches the tensile strength [-]  
 $f_{ct}$  = tensile strength of the concrete [Pa]  
 $\alpha_{ct}$  = the limit of the linear working curve of the concrete, see Figure 1, [-]

For all other cases of load changes  $\gamma_d = 0$ .

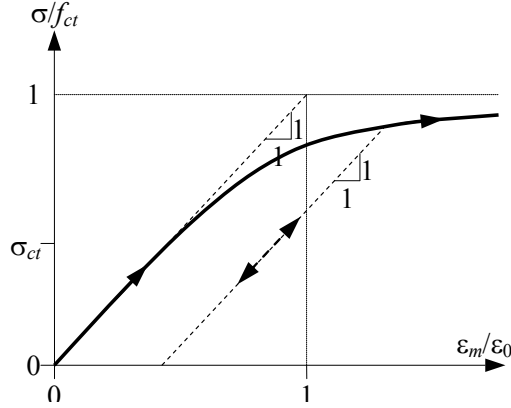


Figure 1 - Normalised adopted non-linear stress-strain behaviour (so-called working curve) for concrete.

The tensile strength of the concrete,  $f_{ct}$ , is related to the compressive strength as follows

$$f_{ct} = \left( \frac{f_{cc}}{f_{cc}^{ref}} \right)^{\beta_1} f_{ct}^{ref} \quad (21)$$

where

- $f_{ct}$  = current tensile strength [Pa]  
 $f_{cc}$  = current compression strength [Pa]  
 $\beta_1$  = 2/3, fitting parameter according to Eurocode 1992-1-1 [-]  
 $f_{cc}^{ref}$  = reference compressive strength [Pa]  
 $f_{ct}^{ref}$  = reference tensile strength [Pa]

The total non-elastic deformation during the time step can be expressed as

$$\Delta \varepsilon_{i+1}^0 = \Delta \varepsilon_{rel} + \Delta \varepsilon_T + \Delta \varepsilon_{sh} \quad (22)$$

where

- $\Delta \varepsilon_{rel}$  = non-linear strain calculated from the relaxation during the time step [-]  
 $\Delta \varepsilon_T$  = strain due to temperature change during the time step [-]  
 $\Delta \varepsilon_{sh}$  = strain due to change of basic shrinkage during the time step [-]

To be able to consider strain induced deformations, the so-called Picket effect, see [24] and [11], the strain dependent temperature and moist related strains may be adjusted by introduction of adjustment factors as follows

$$\Delta \varepsilon_T = \Delta \varepsilon_T^0 \cdot \left( 1 + \rho_T \cdot \frac{\sigma}{f_{ct}} \cdot \text{sign}(\Delta T) \right) \quad (23)$$

$$\Delta \varepsilon_{sh} = \Delta \varepsilon_{sh}^0 \cdot \left( 1 + \rho_{\varphi} \cdot \frac{\sigma}{f_{ct}} \cdot \text{sign}(\Delta T) \right) \quad (24)$$

where  $\rho_T$  and  $\rho_{\varphi}$  are adjustment factors describing the Pickett effect [-]

$\Delta \varepsilon_T^0$  = change of thermal dilation before adjustment due to Pickett effect [-]

$\Delta \varepsilon_{sh}^0$  = change of basic shrinkage before adjustment due to Pickett effect [-]

$\sigma$  = concrete stress during the time step [Pa]

$\Delta T$  = change of temperature during the time step [°C]

The key feature of the test is to make the concrete specimen to undergo tensile strength failure. This is done either spontaneously due to the constrained deformation or by increasing the force in the hydraulic servo-cylinder, see Figure 11. Out of this point the  $f_{ct}^{ref}$  can be determined, and to complete a full set of material parameters  $\alpha_{ct}$ ,  $\rho_T$  and  $\rho_{\varphi}$  need to be determined. This is done manually by using the measured concrete temperature to perform stress calculations with ConTeSt together with the evaluated parameters from the other tests. The calculated stress curve is compared to the measured stress curve in the evaluation process, and the calculated stress might be adjusted, if needed, by varying  $\alpha_{ct}$ ,  $\rho_T$  and  $\rho_{\varphi}$ .

## 5. LABORATORY RESULTS AND EVALUATION

### 5.1 General

The performed tests were used to examine the strength development, heat of hydration, basic creep, basic shrinkage and thermal dilation. Prior to the evaluation, the numerical data may need to be adjusted due to oddities caused by the measuring apparatus. Below the processes are described for each test. Figures show results from evaluations, however they are not always correlated.

### 5.2 Mix proportions

Fully tested and evaluated material parameters can be obtained for any commercially used concrete. To aid the demonstration of the evaluation process a concrete used in a by SBUF funded research project (Värme ett alternativ till kyla. Metodutveckling och ny teknik, see [3]) is used. This concrete is based on the Swedish cement type “Anläggningscement” and made fire resistant by adding Poly Propylene fibres. It is denoted as ANL PP C30/37 vct = 0.50, see Table 1.

Table 1 – Composition of the studied concrete

Composition	Amount
vct, [-]	0.50
CEM I 42.5 N MH/SR/LA ANL [kg/m <sup>3</sup> ]	365
Aggregate, 0/8 [kg/m <sup>3</sup> ]	968.1
Aggregate, 8/1, [kg/m <sup>3</sup> ]	803.9
Water, total [kg/m <sup>3</sup> ]	175.2
Poly Propylene fibres, [kg/m <sup>3</sup> ]	0.9
Air volume [%]	1.5

The air volume is the natural air content of the concrete and is obtained without the use of any air-entraining agents.

### 5.3 Strength development test procedure

In Figure 2 the recorded temperature development is shown in the centre of two specimens per water bath (three for the 20°C-bath), see also Appendix A.2.

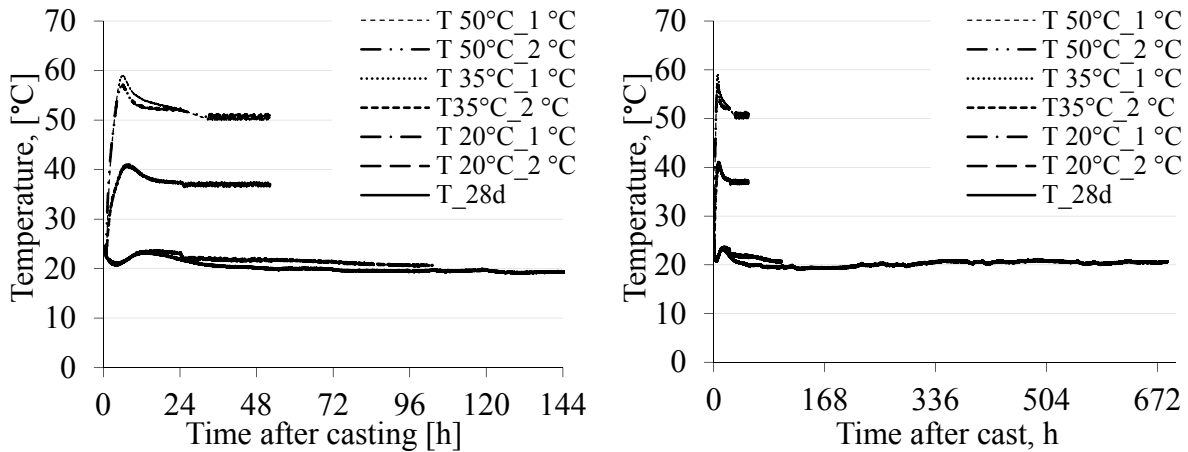


Figure 2 – Registered temperature in two (or three) concrete specimen in each water bath.

According to earlier description, evaluation of the strength at the different storage temperatures yields by regression the temperature factor,  $\beta_T$ , and strength development as a function of equivalent time,  $t_e$ , see Figures 3a and 3b. Measured strengths as a function of the equivalent time is shown in Figure 3b, where each point represents the average of all tested cubes at each occasion. The value for the compression strength at 28 days is used as a restraining point in the regression process. The fitted curve is forced to pass through this point.

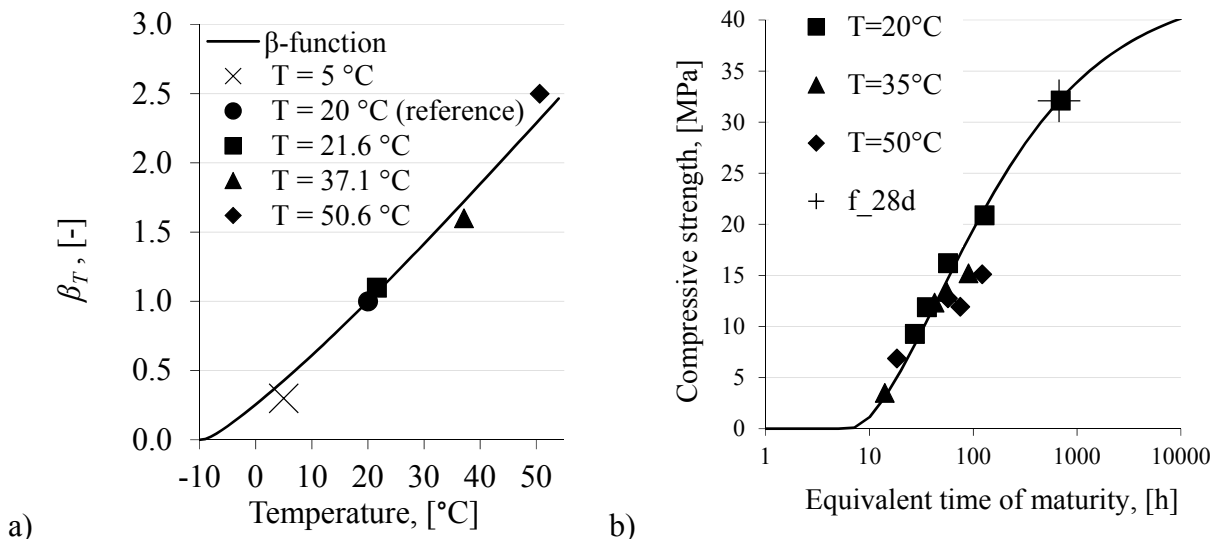


Figure 3 – a) Evaluated temperature factor  $\beta_T$ . For this example, the value at 5°C is given an approximate value by experience between 0,25-0,35 since no curing at this temperature was performed for this example concrete. b) Evaluated reference strength development. Each point is a mean value of three of all tested specimens at each equivalent time of maturity  $t_e$ .

The determined parameters of the reference strength development using Eq. 1 is listed in Appendix A.3. In Figure 3b it can be seen a small loss of strength for concrete temperatures higher than about 35 °C for maturity ages higher than about 90 h. This observation is, as mentioned earlier, not modelled here, and this is of minor importance for applications studying risk of temperature cracking for ordinary civil engineering structures, as these higher temperatures are in practice not maintained for long periods for these structures. For massive concrete structures, say foundations with the minimum size about several meters, there might be a significant loss of strength, and these structures will in the future be modelled with respect to possible strength loss.

#### *Semi-adiabatic calorimetric test procedure*

The documentation at the tests start with the logging of ambient air temperature by gauges placed near the top and bottom at each cellular plastic unit. As soon as the concrete is placed in the metal bucket the concrete temperature is measured by gauges placed in the two specimens, see Figure 4a.

Besides the natural temperature development measurements, the cooling evolution after a forced heating of the concrete is performed, see Figure 4b. After the temperature in the concrete has cooled down to the ambient temperature, a heating device attached to the metal bucket is activated. The heating proceeds until the concrete reaches about 50°C, and then the cooling is documented, see Figure 4b. Required level of heating is a concrete temperature of minimum 5°C above the natural peak temperature.

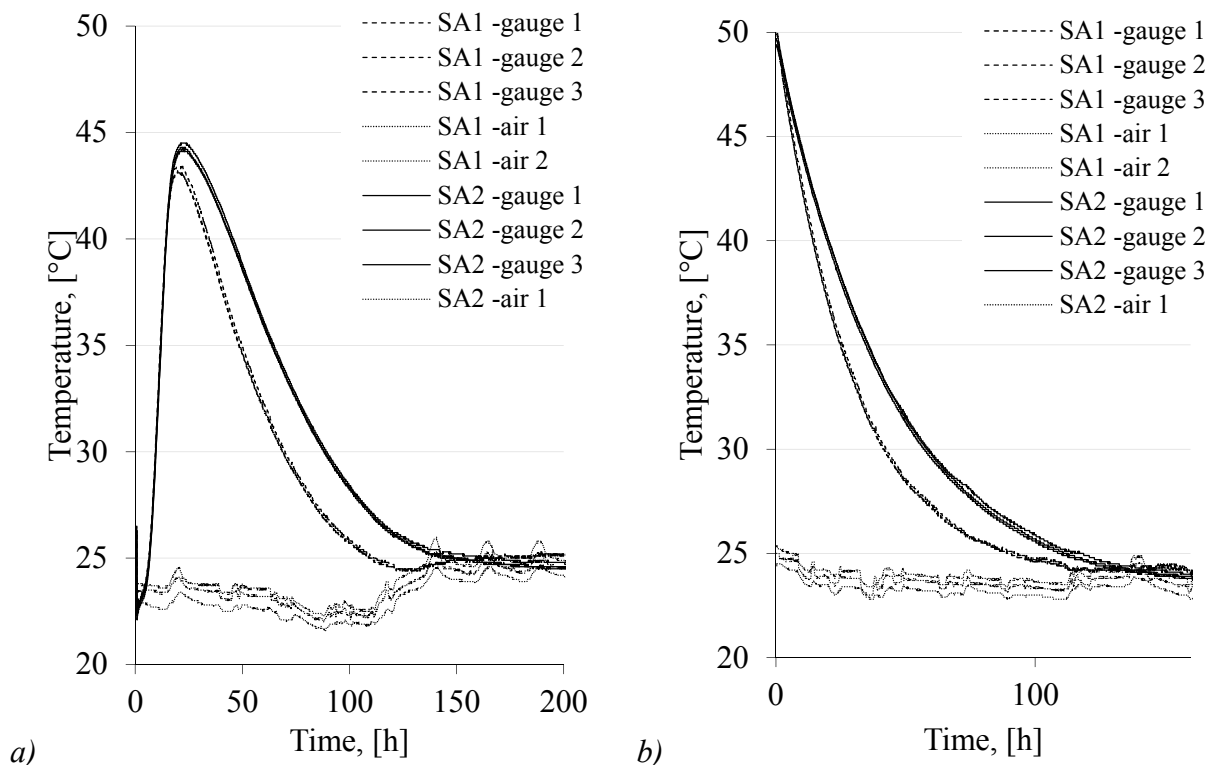


Figure 4 – a) Concrete and ambient temperature at semi-adiabatic calorimetric tests. b) Concrete and ambient temperature for the cooling evolution after forced heating. SA1 and SA2 denotes two tests.

With the help of the information given in Figure 4a and 4b the heat of hydration,  $q_{cem}$ , see Eqs. 6 and 8, can be calculated as a function of equivalent time of maturity, see Figure 5.

The determined parameters for the heat of hydration at any given time,  $q_u$ ,  $t_1$  and  $\kappa_1$ , are listed in Appendix A.3.

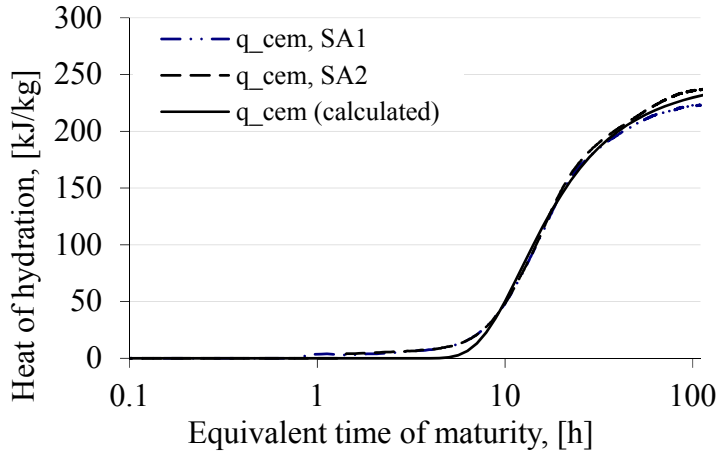


Figure 5 – Determination of heat of hydration, from two semi-adiabatic tests and calculated.

#### Basic shrinkage and free thermal dilation test procedure

As the specimens undergo volume changes, strain gauges register the change. In Figure 6 the result of both the measured strain and the by regression analysis calculated total strain is shown. The specimen stored in room temperature serve mainly for determination of the basic shrinkage parameters,  $t_{su}$  and  $\varepsilon_{su}$ , see Figure 6a. In Figure 6b the strains for the specimen stored in the temperate water bath are shown. The main purpose for this regression is the determination of thermal expansion coefficients,  $\alpha_T$ . The aim of the regression is to mimic the calculated total strain (thick line) to the measured strain (solid blue line). The strain caused by basic shrinkage (dashed line) and free thermal dilation (thin red line) is calculated individually and is also presented in the figures.

The determined parameters for the basic shrinkage and free thermal dilation is;  $\alpha_T$ ,  $\varepsilon_{su}$ ,  $t_{sh}$  and  $\eta_{sh}$  are listed in Appendix A.3.

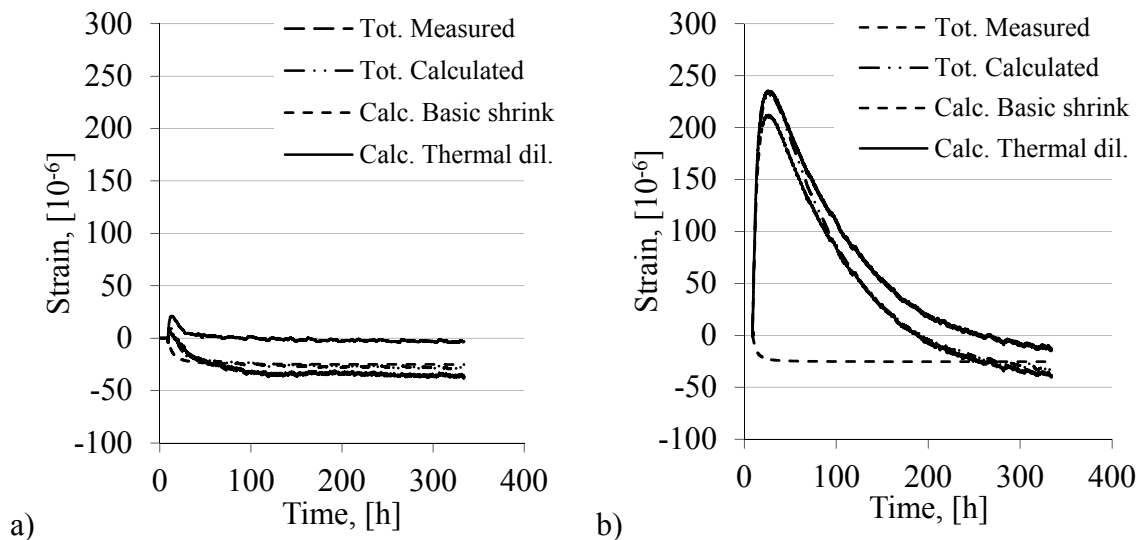


Figure 6 – a) Regression of strain at nearly constant temperature. b) Developed strains for a temperature curve of a 0.7 m thick wall.

#### Basic creep test

Two specimens are loaded roughly at five days after casting and two others are loaded after roughly 14 days. The time for the later loading may differ and at occasions 28 days is used. The remaining specimens are unloaded and are used to determine the basic shrinkage, which is deducted from the combined deformation during the evaluation period for the loaded specimens. Logged strain, and fitting with Linear Logarithmic Model in logarithmic time scale, is shown in Figure 7.

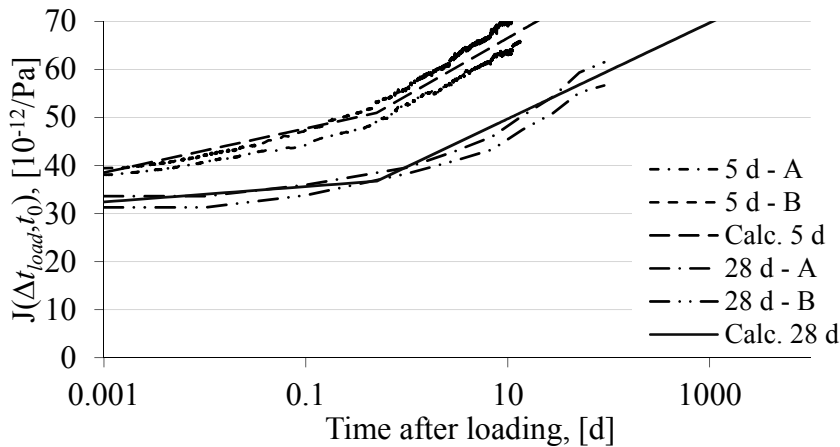


Figure 7 – Fitting of linear lines in logarithmic time scale to measured initial and basic creep strains. A and B denotes two specimens.

The E-modulus is obtained from the test for every loaded specimen at the elastic load duration of 0.001 d (ca. 1 min and 26 s). After this point the change in length of the specimens is considered to be caused by basic creep. Performed fitting of the E-modulus development towards obtained measurements is presented in Figure 8.

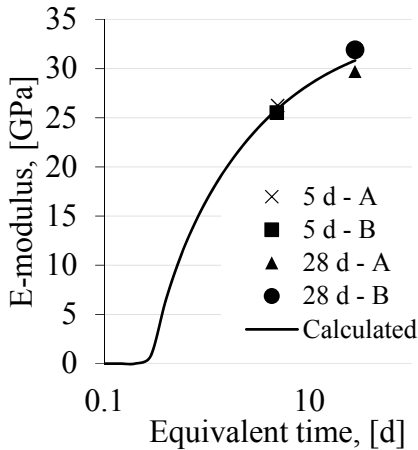


Figure 8 – Fitting of  $E(t_0)$ , “A” and “B” denotes two specimens.

From the fitting in Figures 7 and 8, general expressions for the total creep can be established for arbitrary time of loading ( $t_0$ ) and arbitrary time span of loading ( $\Delta t_{load}$ ) aided by the methodology given in [21]. The model parameter  $\Delta t_1$  and creep rate coefficients  $a_1(t_0)$  and  $a_2(t_0)$  need to be determined by means of regression, and the result is presented in Figure 9a. Thereafter a relaxation

spectrum is calculated with the computer program RELAX [22] to create input data to the ConTeSt software. RELAX uses the creep values to create a relaxation spectrum, see Figure 10. In case of negative relaxation values the limiting values  $(\Delta t_{load})_{age}$  and  $(\Delta t_0)_{age}$  in the input file to RELAX can be used to modify the transformation from creep to relaxation spectra. These set of calculated data makes it possible for ConTeSt to take the relaxation phenomena into the stress/strain calculation, using a rate type law by Maxwell chain model, see [19].

Instead of manipulating the creep values by using the limiting values to avoid negative relaxation, the estimation of the  $a_2$ -function may be done differently, see Figure 9b. By adopting a flatter behaviour in the early loading ages of the  $a_2$ -function for very young concrete, the same impact on the relaxation spectra can be achieved as using limiting values. The determined parameters for the  $E$ -modulus and basic creep in this process are:  $E_{c,28}$ ,  $\Delta t_1$ ,  $a_1(5d)$ ,  $a_2(5d)$ ,  $a_1(28d)$ , and  $a_2(28d)$ , and their numerical values are listed in Appendix A.3.

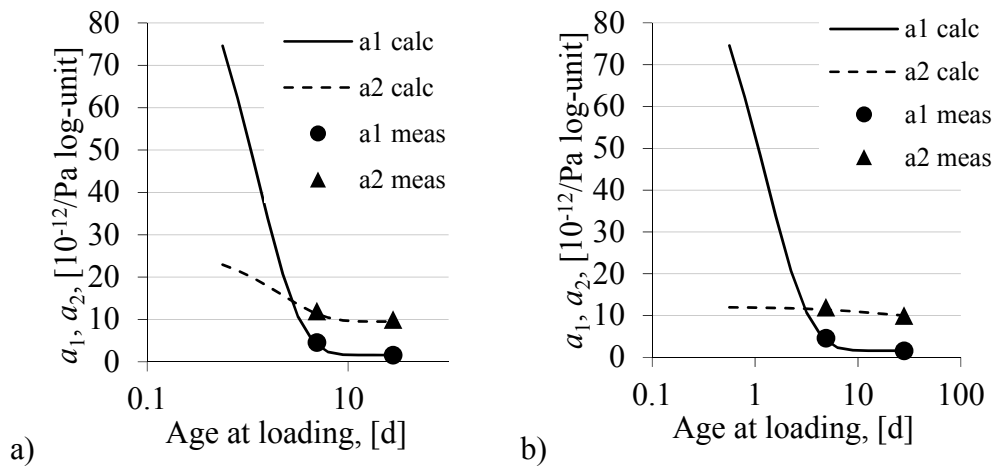


Figure 9 – Measured and calculated creep rate coefficients  $a_1(t_0)$  and  $a_2(t_0)$  of the Linear Logarithmic Model. a) Steeper behaviour of the  $a_2$ -function ( $a_2$  calc). Limiting values are needed to avoid negative relaxation. b) Flatter behaviour of the  $a_2$ -function ( $a_2$  calc). No limiting values are needed to avoid negative relaxation.

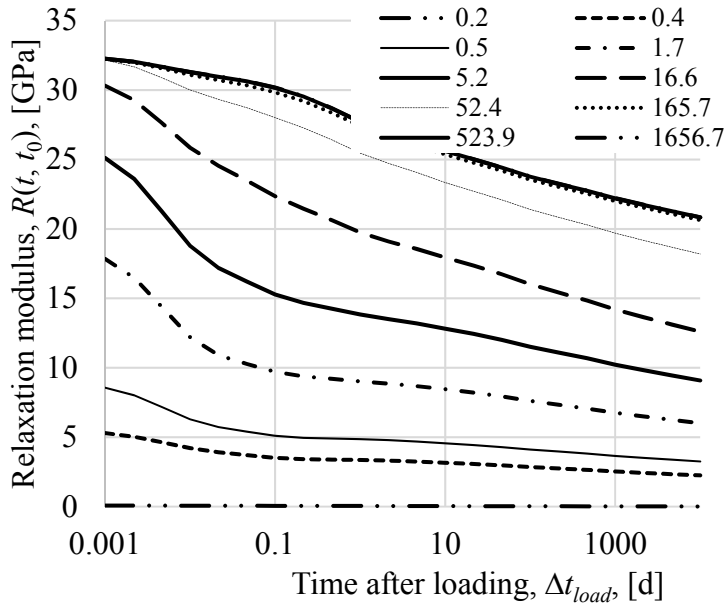


Figure 10 – Relaxation spectrum. The curves represent different equivalent time of maturity for the concrete,  $t_e$ , at the time of applied load,  $t_0$ , given in hours.

#### Stress development at full restraint

In Figure 11 the measured and calculated stress developments are presented. The calculated stress is adjusted, if needed, to resemble the measured curve by altering  $\rho_T$  and  $\rho_\phi$  (Pickett effect). If the agreement is not accepted a re-evaluation of the creep test and/or the free deformation test may be performed. The reason is that sometimes there is a tendency that these tests may give what can be described as “tentative unlogic” results. The reason for this is not known at present, but both areas are very complicated to perform. On the other hand, the measured stress at full restraint is the “final combined result” of the whole test series and represents a direct useful result comparing different recipes. Therefore, the calculated and measured stresses always have to coincide in an acceptable way.

However, for analysing the risk of through cracking it is more important that the calculated curve correspond well to the measured values from about reaching half the tensile strength and onwards. In this example, the obtained parameters are probably well suited for calculation of the risk of “through cracking”, at the cooling phase, for civil engineering structures.

Sometimes it can be observed that the calculated stress is lower compared to the measured, in the time span from casting to about 24 h after casting. This is probably a consequence of an implemented “smoothing” in ConTeSt to avoid program crashes caused by non-linear deformations when calculating the strain at the first time-period after casting.

The determined parameters for the calculation of stress development at full restraint is only  $\alpha_{ct}$ , as  $\rho_T = \rho_\phi = 0$  in this case, see Appendix A.3, where the parameter  $\beta_1$  is set to 0.667.

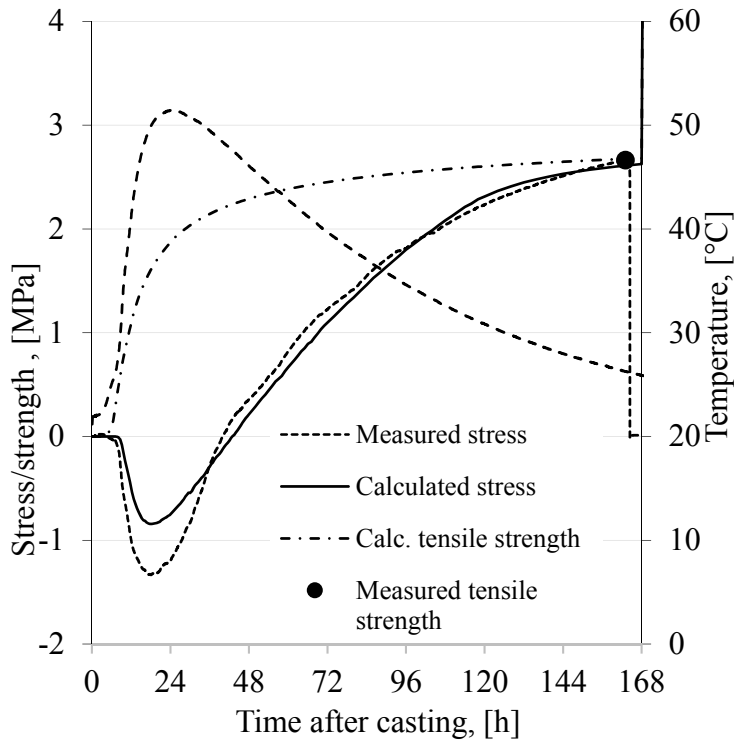


Figure 11 – Comparison between measured stresses at test and calculation. The test sample is loaded by a temperature curve corresponding to a 0.7 m thick wall.

To sum up, the overall material characteristics for the examined example concrete is presented as a collection of evaluated parameters in Appendix A.3. The underlying equations have been presented in Chapter 4.

## 6. SENSITIVITY OF INDIVIDUAL PARAMETERS

Sensitivity analyses varying some ingoing parameters in the ConTeSt software were performed to evaluate the impact on the calculated stress levels. The results are expressed as the stress ratio according to earlier description. The ratio is defined as the actual tensile stress in relation to the actual tensile strength value,  $\sigma / f_{ct}$ . The stress ratio can never exceed the value 1, but the strain ratio,  $\varepsilon_m / \varepsilon_0$ , see Figure 1, can formally exceed the value 1. In [25] the strain ratios at failure were in average in the size of order of 1.1 to 1.15 when evaluating strain ratios at failure in a real structure. Therefore, strain ratios are often used by designers to get relevant information near the failure situation. But, for stress and strain ratios up to  $\alpha_{ct}$ , these values are the same, which usually comprises the design situation.

In Table 3 it is described how the strain ratio varies with a change of some parameter affecting the evaluation of a typical wall on slab structure, see Figure 12. In the column “Explanation” it is listed the new value of the examined parameter(s), all the other parameters are kept constant as given in Appendix A.3.

To analyse the risk of through cracks an average was taken over the area in the construction where the maximum values of strain or stress ratio is calculated, which is the established method to estimate the risk of through cracking. When looking at a cross-section of the wall, the area (where

the average strain ratio is calculated) consists of a height that equals 15 % of the wall width and the width equals the width of the wall.

The stress/strain ratio of the young concrete has been estimated in the 2D FEM calculations by use of the following parameters:

- Geometry: see Figure 12.
- Concrete: C30/37, w/C = 0.50 and C = 365 kg/m<sup>3</sup>.
- Cement: CEM I 42.5 N MH/SR/LA.
- Wooden form, 21 mm thickness. Heat conductivity is 0.14 W/K m<sup>2</sup>.
- Ambient air, heat transfer coefficient is 500 W/K m<sup>2</sup>, wind speed is 2 m/s.
- Initial concrete temperature is 15°C and ambient air temperature is 5°C.
- Wall width: 700 mm.

Table 3 – Sensitivity test of some evaluated parameters. The table show how a change in the evaluated parameters effect a calculated strain ratio.

Parameter setup Thermal and mechanical parameters as in Appendix A.3. Wall width = 700 mm. If any parameter is changed, it is stated.	Temp max [°C]	Strain ratio (average) [-]	Explanation	Figure
<b>Original parameters</b>				
<i>Starting example.</i> Parameters as described above.	40.74	0.83	Temperature and average strain ratio at the location at maximum strain is calculated as a starting example.	
<b>Wall width</b>				
Wall width = 400 mm	31.36	0.65	Decreased wall width.	
Wall width = 1400 mm	47.17	0.99	Increased wall width.	
<b>Strength development</b>				
$\Theta_{ref} = 3760 \text{ K}, \kappa_3 = 0.635$	40.63	0.84	The sensitivity of the <i>maturity function</i> is tested with a change in the parameter set.	Figure 13
$\Theta_{ref} = 3760 \text{ K}, \kappa_3 = 0.635, t_S = 4.5 \text{ h}, t_A = 7 \text{ h}, s = 0.311$	40.63	0.84	The sensitivity of the <i>reference strength development</i> is tested with a change in the parameter set.	Figure 14
<b>Heat of hydration</b>				
$q_u = 251.9 \text{ kJ/kg}, t_1 = 7.820 \text{ h}, \kappa_1 = 2.468$ Wall width = 400 mm	31.10	0.64	The ambient was decreased 0.5°C, which effects the cooling factor, and a new parameter set is yielded.  The new parameter set is tested for three wall widths.	Figure 15
$q_u, t_1$ and $\kappa_1$ as above.	39.99	0.82		
$q_u, t_1$ and $\kappa_1$ as above. Wall width = 1400 mm	45.93	0.97		
<b>Basic shrinkage &amp; Free thermal dilation</b>				

$\alpha_T = 9.7 \text{ }^\circ\text{C}^{-1}$ , $\epsilon_{su} = -79 \cdot 10^{-6}$ $t_{su} = 3.16 \text{ h}$ , $\eta_{sh} = 1.30$	40.74	0.84	Estimated concrete temperature at cast is increased 1 °C prior to the evaluation, yielding a new parameter set.	Figure 16
<b>Basic creep</b>				
$a_1(5\text{d}) = 4.00$ , [see Eq. 16] $a_2(5\text{d}) = 9.70$ , $a_1(14\text{d}) = 1.00$ , $a_2(14\text{d}) = 6.58$	40.74	0.76	A change in creep rate coefficients is used.	Figure 17 a
$a_1(5\text{d})$ , $a_2(5\text{d})$ , $a_1(14\text{d})$ and $a_2(14\text{d})$ as above, $(\Delta t_{load})_{age} = 1 \text{ d}$ , $(\Delta t_0)_{age} = 22 \text{ d}$	40.74	0.78	The limiting parameters $(\Delta t_{load})_{age}$ and $(\Delta t_0)_{age}$ is used in the last two parameter set-ups.	Figure 17 b
$a_1(5\text{d})$ , $a_2(5\text{d})$ , $a_1(14\text{d})$ and $a_2(14\text{d})$ as above, $(\Delta t_{load})_{age} = 0.2 \text{ d}$ , $(\Delta t_0)_{age} = 35 \text{ d}$	40.74	0.84		Figure 17 c
$E_{28} = 32.72 \text{ GPa}$ , $\Delta t_1 = 0.2 \text{ d}$ , $a_1(5\text{d}) = 4.00$ , [see Eq. 16] $a_2(5\text{d}) = 11.11$ , $a_1(14\text{d}) = 1.00$ , $a_2(14\text{d}) = 6.22$	40.74	0.70	E-modulus for the measurement at 5 d is decreased by 1 GPa prior to the evaluation of $E_{c,28}$ and $a$ -values.	
$E_{c,28}$ , $\Delta t_1$ , $a_1(5\text{d})$ , $a_2(5\text{d})$ , $a_1(14\text{d})$ and $a_2(14\text{d})$ as above, $(\Delta t_{load})_{age} = 0.1 \text{ d}$ , $(\Delta t_0)_{age} = 40 \text{ d}$	40.74	0.90	The limiting parameters $(\Delta t_{load})_{age}$ and $(\Delta t_0)_{age}$ is used in the last parameter set-up.	

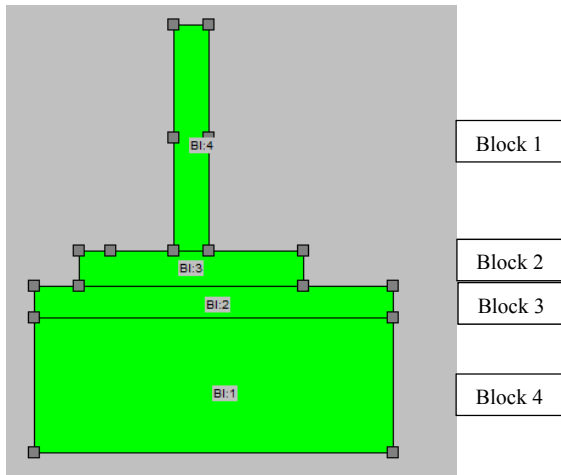


Figure 12 – Geometry of model used in the sensitivity test. Block 1 - 4 represents young concrete, mature concrete, gravel filling and soil, respectively. The width of block 1 (i.e. the wall) is varied according to Table 3.

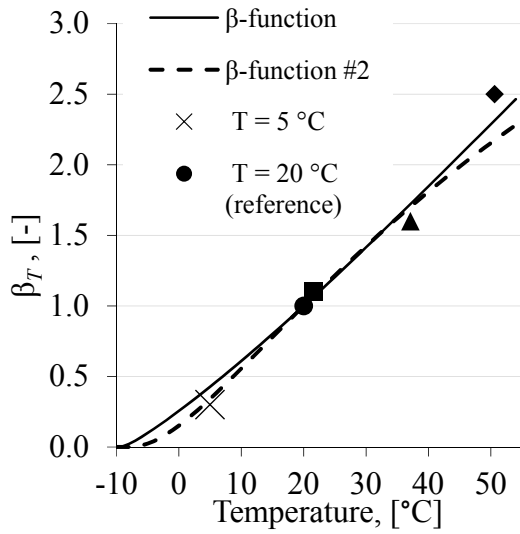


Figure 13 – Maturity function,  $\beta_T$ , is investigated with a variation of  $\Theta_{ref}$  and  $\kappa_3$ . “ $\beta$ -function” denotes original parameter. “ $\beta$ -function #2” denotes varied parameters.

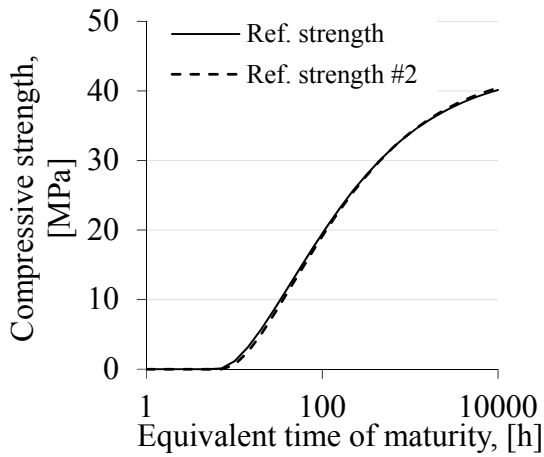


Figure 14 – Reference strength development is investigated with a variation of  $\Theta_{ref}$  and  $\kappa_3$ . “Ref. strength” denotes original parameter. “Ref. strength #2” denotes varied parameters.

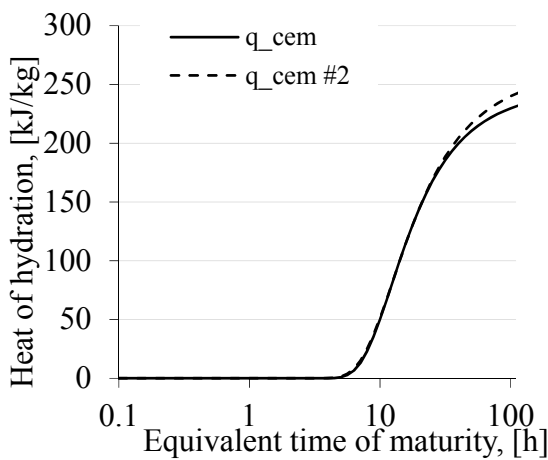


Figure 15 – The heat of hydration is investigated with a variation of  $q_u$ ,  $t_1$  and  $\kappa_1$ . “ $q_{cem}$ ” denotes original parameter. “#2” denotes regression with varied parameters.

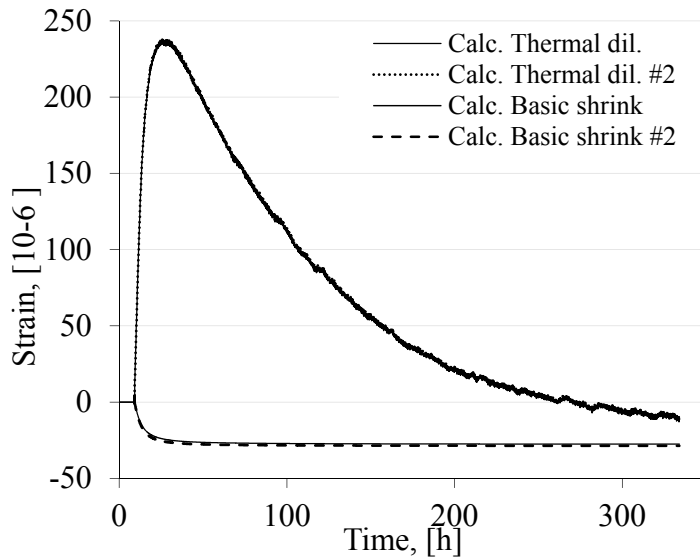
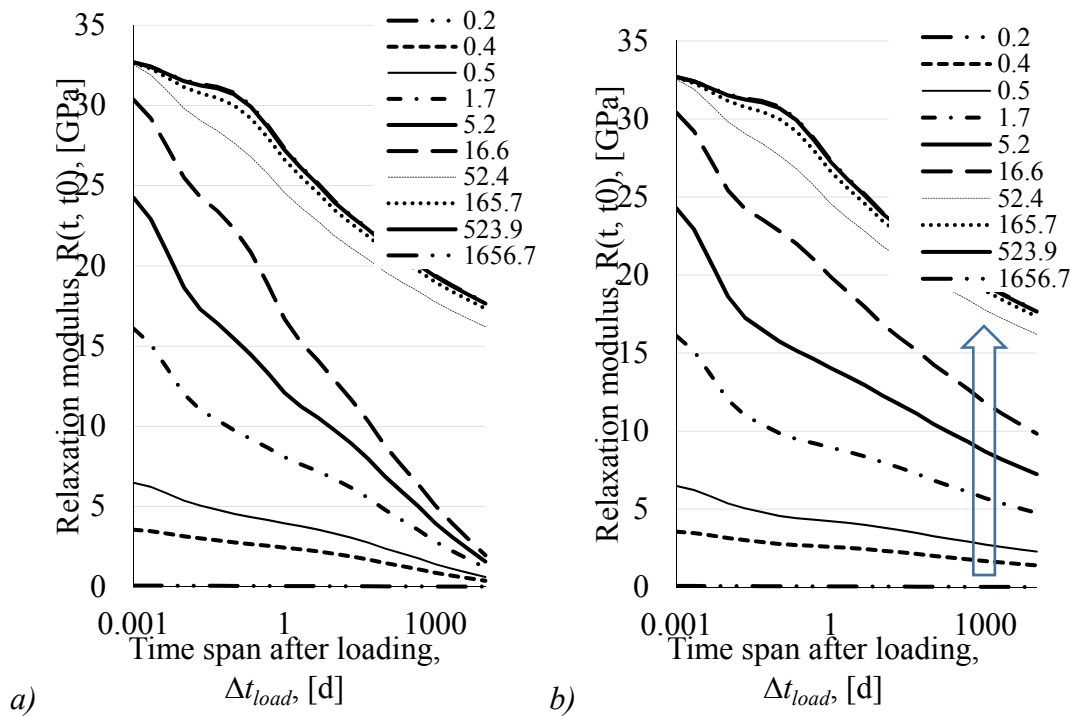
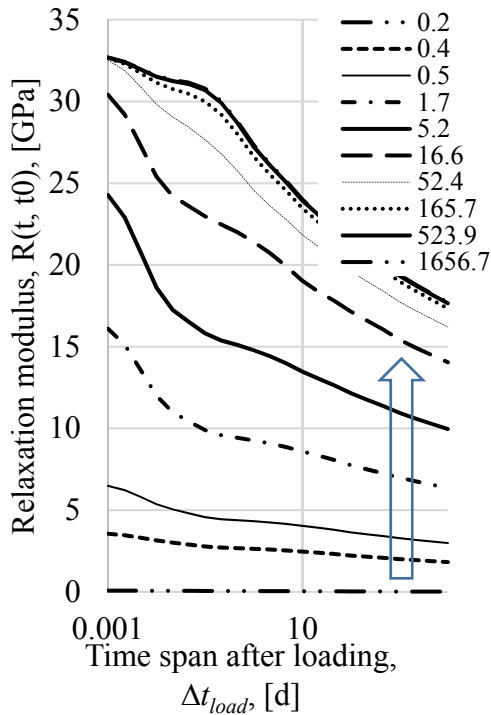


Figure 16 – The free thermal dilation and basic shrinkage is investigated with a variation of  $\alpha_T$ ,  $\varepsilon_{su}$ ,  $t_{sh}$  and  $\varepsilon_{sh}$ . “#2” denotes regression with varied parameters.

With the use of the limiting parameters, the doubtful creep spectra for really young concrete exposed for long load duration is truncated. This is performed prior to the transformation from creep to relaxation spectra, here done by RELAX. The effect is that the E-modulus is increased remarkably for concrete with equivalent maturity of less than about 17 days exposed for long load duration. The arrows visualize this effect in the figures. The curves represent different equivalent time of maturity for the concrete,  $t_e$  [d], at the time of applied load,  $t_0$ .





c)

Figure 17 a, b and c – Relaxation spectra obtained with the LLM at the evaluation of the creep data. a) Original spectra obtained with alternate creep rate coefficients. In b) and c) an adjustment of the original spectra is performed with the limiting values  $(\Delta t_{load})_{age}$  and  $(\Delta t_0)_{age}$ .

## 7. CONCLUSIONS

Evaluation of test results for young concrete is demonstrated. The obtained material parameter set, yielded from the evaluation, is used in thermal crack risk estimation. In this case, the obtained set of material parameters is suitable to be imported to the software ConTeSt. Furthermore, a sensitivity test of how a calculated strain ratio by ConTeSt was effected with an alternation of some of the evaluated parameters.

A slight change in ingoing parameters of the *maturity function* and *reference strength development* has a negligible effect on the calculated strain.

For the test of *heat of hydration*, a decreased temperature by  $0.5^\circ\text{C}$  of the air surround the test set-up effects the calculated strain by 1 percentage. It is therefore important to make a reliable estimation of the ambient air temperature, since a deviation of  $2^\circ\text{C}$  makes a significant impact of the calculated strain.

The calculated strain is only slightly effected by a deviated estimation of the initial concrete temperature by  $1^\circ\text{C}$  at the evaluation *basic shrinkage* and *free thermal dilation*.

The *basic creep* evaluation exhibits a high sensitivity on the calculated strain. It requires thoroughness and good portion of knowhow during the evaluation to estimate the relaxation to a satisfying degree.

An overall conclusion is that the fitting of the calculated strain development to the measured development during the evaluation of the *stress development at full restraint* tests more or less nullifies the direct effects described in the sensitivity test. For example, if the evaluated parameters

from the *basic creep* test to some extent were badly determined the effects make a direct impact of the calculated strain. If the calculated and measured strain development is deviating too much, the *basic creep* test is re-evaluated, and a new fit of the calculated and measured strain development is performed.

## 8. DISCUSSION

### 8.1. Relevance for the individual tests

Out of the five performed tests, three are of significant importance when it comes to provide an operational parameter set. These tests are the test of *strength development*, *heat of hydration* and *stress at full restraint*. As long as reliable measurements and a reasonable evaluation of these measurements can be provided there is room for errors in the measurements and evaluation for the remaining two test; *basic shrinkage and free thermal dilation* and *basic creep*. If one or both of these tests are unreliable in one way or another, the corresponding parameter values can be estimated based on previous experiences. Of course, a loss of accuracy for the estimated parameters is introduced, but this can to some extent be accounted for in the last evaluation step (mimic a calculated strain development to the measured). The measured strain development from the *stress development at full restraint* test can be considered as a checkpoint for the total parameter set. Since the calculated strain development is influenced by all evaluated parameters it is of great importance that it corresponds well to the empirical counterpart. This last evaluation step may be more time consuming if the parameters for the *basic shrinkage and free thermal dilation* and *basic creep* are estimated instead of properly evaluated. Furthermore, estimated parameters may also predict the strain development for other geometrically circumstances (i.e. thicker or thinner wall) with less precision. After all, the evaluated parameters describe the strain development of a 700 mm thick wall, and if the thickness deviates from this default, effects of size dependent origin may come into play.

### 8.2. Improvements

All of the individual tests may be improved to obtain a better accuracy.

The first and general improvement is to perform the tests on two mixes. Each mix of the concrete shows a natural variation due to the characters of the constituents of the concrete recipe. An effect may be that the test result may vary for the different mixes. The only way to account for this phenomenon is to perform tests to mixes prepared at different times, with renewed samples of aggregate and binders. However, that calls for a more expensive and long evaluation time before the parameter set can be established.

Below follow some suggestions to improve some of the individual tests.

#### *Strength development*

The curing of the used concrete specimens in this work was done at the temperatures of 20°C, 35°C and 50°C. An improvement would be to cure the specimens at 5°C to measure the strength development for lower temperatures. This is especially true for binder which is sensitive to low curing temperatures regarding their strength growth. Also, for concrete used in parts of the world which experiences a continental, polar or alpine climate the curing at 5°C would indeed be a significant improvement.

*Heat of hydration*

Since a small variation ( $0.5^{\circ}\text{C}$ ) in the ambient temperature around the test set-up effects the calculated strain development in a noticeable way, it is suggested that a thorough measurement around the set-up is performed. At least 6 temperature gauges, evenly distributed, around the set-up would be a good idea.

*Basic shrinkage & Free thermal dilation*

Even a small variation in the parameter set effects the calculated strain ratio. Therefore, well calibrated temperature and strain gauges of good quality are of significant importance. Advisably, a redundancy of gauges (one or two extra of each sort) could be of good use.

*Basic creep*

The determination of the creep rate coefficients ( $a_1(t_0)$  and  $a_2(t_0)$ ) is a tricky process. To aid the evaluation complementary measurements for other loading ages would improve the process significantly. Suggested is to test the basic creep also at a loading age of 2 days and 28 days.

*Stress development at full restraint*

To examine the effect on the stress development due to different temperature development an extra temperature reference curve could be used to control another concrete specimen. The temperature reference curve would represent another thickness of the fictive wall. Since the thickness per default is set to 700 mm, the other thickness could be determined by take the main building geometry into account. A suggestion for temperature reference curve is that it should represent a wall width that at least deviate 300 mm from the default (700 mm).

## 9. REFERENCES

1. Arizona Leisure: "Construction History of Hoover Dam – A Brief Overview of Hoover Dam Construction," *Webpage*, Available at: <http://www.arizona-leisure.com/hoover-dam-building.html>
2. JEJMS Concrete: "ConTeSt Pro – Users Manual - Program for Temperature and Stress Calculations in Concrete," *User's Manual*, Luleå, Sweden, April 2008, 198 pp.
3. SBUF project 13046, "Värme ett alternativ till kyla. Metodutveckling och ny teknik", *Webpage*, Available at: <http://www.sbuf.se/Projektsida/?id=f428827c-1372-4887-9a03-f6a7c80ba025>.
4. McDaniel A B: "Influence of Temperature on the Strength of Concrete," *Bulletin*, No. 81, University of Illinois, Engineering Experiment Station, July 1915.
5. McIntosh J D: "Electrical Curing of Concrete," *Magazine of concrete Research*, Vol. 1, No. 1, January 1949.
6. Nurse R W: "Steam Curing of Concrete," *Magazine of Concrete Research*, Vol. 1, No 2. June 1949.
7. Saul A G A: "Principals Underlying the Steam Curing of Concrete at Atmospheric Pressure," *Magazine of Concrete Research*, Vol. 2, No. 6, March 1951.
8. Bergström S G: "Curing Temperature, Age and Strength of Concrete," *Magazine of Concrete Research*, Vol. 5, No 14. December 1953.
9. Rastrup E: "Heat of Hydration in Concrete," *Magazine of Concrete Research*, Vol. 6, No. 17, September 1954.
10. Nykänen A: "Hardening of concrete at Different Temperatures, Especially Below the Freezing Point," *Proceedings*, RILEM Symposium on Winter Concreting – Theory and practice, Session BII, Danish Institute for Building Research, Copenhagen, Denmark, 1956.
11. Jonasson J-E: "Modelling of Temperature, Moisture and Stresses in Young Concrete," *Doctoral Thesis*, Dept. of Civil, Environmental and Natural Resources Engineering, Luleå University of Technology, Luleå, Sweden, 1994, 242 pp.
12. Fjellström P: "Measurement and Modelling of Young Concrete Properties," *Licentiate Thesis*, Dept. of Civil, Environmental and Natural Resources Engineering, Luleå University of Technology, Luleå, Sweden, 2013, 200 pp.
13. Svensk Byggtjänst: "Swedish Concrete handbook – Chapter 9 – Young and Hardening Concrete," *Handbook*, Svensk Byggtjänst, Stockholm, 2017 (In Swedish).
14. Jonasson J-E: "Slipform Construction – Calculations for Assessing Protection against Early Freezing," *Fo/Research Bulletin*, No. 4:84, Swedish Cement and Concrete Research Institute, Stockholm, 1984.
15. Emborg M: "Thermal Stresses in Concrete Structures at Early Ages," *Doctoral Thesis*, Dept. of Civil, Environmental and Natural Resources Engineering, Luleå University of Technology, Luleå, Sweden, 1989, 304 pp.
16. Hedlund H: "Hardening Concrete – Measurements and Evaluation of Non-Elastic Deformation and Associated Restraint Stresses", *Doctoral Thesis*, Dept. of Civil, Environmental and Natural Resources Engineering, Luleå University of Technology, Luleå, Sweden, 2000, 414 pp.
17. Hedlund H: "Stresses in High Performance Concrete due to Temperature and Moisture Variations at Early Ages", *Licentiate Thesis*, Dept. of Civil, Environmental and Natural Resources Engineering, Luleå University of Technology, Luleå, Sweden, 1996, 230 pp.
18. Bažant Z P, Ashgari A: "Computation of Age-dependent Relaxation Spectra," *Cem. Coner Res.*, No. 4, 1974.
19. Bažant Z P, Wu S T: "Rate-type Creep Law for Aging Concrete Based on Maxwell-Chain," *Materials and Structures*, Vol. 7, No. 37, 1974.

20. Jonasson J-E: "Computer Program for Non-linear Analyses of Concrete in View of Shrinkage, Creep and Temperature," *Fo/Research Bulletin*, No. 7:77, Swedish Cement and Concrete Research Institute, Stockholm, 1977 (In Swedish).
21. Larson M: "Thermal Crack Estimation in Early Age Concrete – Models and Methods for Practical Application," *Doctoral Thesis*, Dept. of Civil, Environmental and Natural Resources Engineering, Luleå University of Technology, Luleå, Sweden, 2003, 203 pp.
22. Jonasson J-E, Westman G: "Conversion of Creep Data to Relaxation Data by the Program RELAX," *IPACS Document*, TG 3.2/1, Dept. of Civil, Environmental and Natural Resources Engineering, Luleå University of Technology, Luleå, Sweden, 1999.
23. Westman G: "Concrete Creep and Thermal Stresses – New Creep Models and Their Effects on Stress Developments," *Doctoral Thesis*, Dept. of Civil, Environmental and Natural Resources Engineering, Luleå University of Technology, Luleå, Sweden, 1999, 319 pp.
24. Bažant Z P, Chern J: "Concrete Creep at Variable Humidity – Constitutive Law and Mechanisms," *Materials and Structures*, Vol. 18, 1985.
25. Larson M: "Estimation of Crack Risks in Early Age Concrete – Simplified Methods for Practical Use," *Licentiate Thesis*, Dept. of Civil, Environmental and Natural Resources Engineering, Luleå University of Technology, Luleå, Sweden, 2000.

## A. APPENDIX

### A.1.

As input to the RELAX program, both creep values and a file with general input is needed. This additional file states the shape of the output from the program, such as how many Maxwell elements the model should consist of. The outcome of the program is a relaxation spectrum which defines the relaxation for different maturity and loading ages.

The input file with creep values is made by six rows as follows;

KTYPE

$E_{ref}$  [GPa],  $t_{ref}$  [d],  $s$  [-],  $n_E$  [-],  $t_S$  [d]  
 $\Delta t_0$  [d],  $\Delta t_1$  [d],  
 $a_1^{min}$  [creep unit],  $a_1^{max}$  [creep unit],  $t_{a1}$  [d],  $n_{a1}$  [-],  
 $a_2^{min}$  [creep unit],  $a_2^{max}$  [creep unit],  $t_{a2}$  [d],  $n_{a2}$  [-],  
 $(\Delta t_{load})_{age}$  [d],  $(\Delta t_0)_{age}$  [d]

where

KTYPE is defining the used relaxation model within RELAX. Eight alternatives exist, and the showed input syntax is used for the eighth model (KTYPE = 8) which refers to the LLM.

$E_{ref}$  is the modulus of elasticity at equivalent age  $t_{ref}$ .

$n_E$  is set to 0.5, but can be varied, if necessary.

$(\Delta t_{load})_{age}$  [d] and  $(\Delta t_0)_{age}$  [d] = limit values for the load duration and loading ages to avoid "negative relaxation", see further [23].

### A.2.

Measured compressive strength ( $f_{cc}$ ) for three concrete specimens in each water bath at different time. Each temperature test is denoted as the typical temperature level.

Temp = 50°C						
Date	time, h	f_cc_1, MPa	f_cc_2, MPa	f_cc_3, MPa	f_cc average	
2015-06-13 08:57	0					
2015-06-13 17:20	8.38	6.3	6.9	7.4	6.9	
2015-06-14 09:20	24.38	11.6	11.8	12.1	11.8	

2015-06-14 17:02	32.08	14.4	11.8	12.3	12.9
2015-06-15 13:20	52.38	14.9	13.5	16.9	15.1

Temp=35°C					
Date	time, h	f_cc_1, MPa	f_cc_2, MPa	f_cc_3, MPa	f_cc average
2015-06-13 08:57	0				
2015-06-13 17:30	8.55	3.9	3.4	3.2	3.5
2015-06-14 09:30	24.55	11.7	13.1	12.0	12.3
2015-06-14 17:10	32.22	13.4	14.7	12.3	13.5
2015-06-15 13:14	52.28	14.4	15.4	15.8	15.2

Temp = 20°C					
Date	time, h	f_cc_1, MPa	f_cc_2, MPa	f_cc_3, MPa	f_cc average
2015-06-13 08:57	0				
2015-06-14 09:40	24.72	9.2	9.1	9.6	9.3
2015-06-14 17:18	32.35	12.3	10.7	12.7	11.9
2015-06-15 13:20	52.38	17.2	17.8	13.6	16.2
2015-06-18 09:45	120.80	20.6	20.7	21.4	20.9

f_cc_28d (ca 20°C)					
Date	time, h	f_cc_1, MPa	f_cc_2, MPa	f_cc_3, MPa	f_cc average
2015-07-11 08:57	672	31.1	33.1		32.1

### A.3.

Evaluated material parameters for ANL PP C30/37  $w/C$  (vct) = 0.50

Reference curve for compressive strength	$t_S$ [h]	$t_A$ [h]	$n_A$ [-]	$f_A$ [MPa]	$f_{cc,28}$ [MPa]	$s$ [-]	$n_{cc,28}$ [-]
	4.0	6.0	3.0	0.5	32.1	0.301	0.5

Maturity function	$\Theta_{ref}$ [K]	$\kappa_3$ [-]	$\Delta t_e^0$ [h]	$\beta_A$ [-]
	3473	0.412	0	1

Heat of hydration	$q_u$ [J/kg]	$t_1$ [h]	$\kappa_1$ [-]
	27088 1	8.2234 7	2.22877

Basic shrinkage and free thermal dilation	$\alpha_T$ [ $10^{-6}$ /°C]	$\epsilon_{su}$ [ $10^{-6}$ ]	$t_{sh}$ [h]	$\eta_{sh}$ [-]
	9.6	-100	2.11	1.14

E-modulus and basic creep	$E_{c,28}$ [GPa]	$\Delta t_1$ [d]	$a_1(5d)$ [ $10^{-12}$ /Pa $^{10}\log$ -unit]	$a_2(5d)$ [ $10^{-12}$ /Pa $^{10}\log$ -unit]	$a_1(28d)$ [ $10^{-12}$ /Pa $^{10}\log$ -unit]	$a_2(28d)$ [ $10^{-12}$ /Pa $^{10}\log$ -unit]
	32.33	1.0	3.48	9.79	1.0	6.73

Tensile strength and strain/stress calculations	$f_{ct,28}$ [MPa]	$\beta_1$ [-]	$\alpha_{ct}$ [-]	$\rho_T$ [-]	$\rho_\phi$ [-]
	2.72	0.667	0.9	0	0



## **Paper V:**

### **Thermal Crack Risk of Concrete Structures – Evaluation of Theoretical Models for Tunnels and Bridges.**

Nilimaa J, Emborg M, **Hösthagen A**, to be published.

## Thermal Crack Risk of Concrete Structures – Evaluation of Theoretical Models for Tunnels and Bridges



Jonny Nilimaa  
M.Sc., Ph.D., Ass. Sr. Lecturer  
Luleå University of Technology  
SE-971 87 Luleå  
E-mail: jonny.nilimaa@ltu.se



Anders Hösthagen  
M.Sc., Ph.D. student  
Luleå University of Technology  
SE-972 87 Luleå  
E-mail: anders.hosthagen@ltu.se



Mats Emborg  
M.Sc., Ph.D., Professor  
Luleå University of Technology  
SE-972 87 Luleå  
E-mail: mats.emborg@ltu.se

### ABSTRACT

An approach for thermal crack risk estimations was introduced in the Swedish design guidelines BRO 94. The cracking occurs during the early hardening process because of the exothermic reactions between water and cement and often result in high repair costs and delayed construction. This paper studies and validates the inherent safety levels for one typical case of construction. Three slab-frame structures were analysed and the original crack risk estimations were compared to the actual cracking and post-calculations were carried out, using actual parameters. This paper shows that walls with computed strain ratios over 70% were affected by thermal cracks.

**Key words:** Thermal cracking, Structural Design, Sustainability, Concrete Tunnels.

## 1. INTRODUCTION

Thermal cracking may occur during the early hardening process of concrete [1]. The exothermic reactions of the hydration process leads to increasing core temperatures in the structure and thereby inducing thermal expansion of the concrete. However, prohibited deformation due to different types of restraints leads to compressive strains in parts of the structure. As the hydration rate reduces, the core starts cooling, inducing shrinkage and tensile strains within the restrained structure. The tensile strains may also be associated to uneven expansion and contraction of the concrete due to differential temperatures in the inner core and the outer layers.

In some cases the tensile strains exceed the ultimate strain of the concrete and thermal and shrinkage cracks appear. Thermal cracks are usually identified as through cracks, emerged in the cooling phase, and supported by restraints. These types of cracks are generally associated with massive concrete infrastructure such as dams, foundations and tunnels, where the core temperature may become high and vary considerably internally. More slender structures may also be subjected to thermal cracks if e.g. high temperature differences arise between a newly cast wall and a previously cast slab. Thermal cracks may also emerge during the heating phase if the internal temperatures vary considerably and the cracks can be located both in the slab and the wall. Another type of cracks that usually emerge during the heating phase, are the surface cracks. These cracks are restricted to the concrete surface and thereby remain thin, with widths below 0,1 mm [2]. Surface cracks may also emerge due to rapid surface cooling associated with form removal or rapid shifts in the weather.

Factors influencing the heat of hydration and thereby the thermal crack risk of concrete, may, according to [2] be divided into internal and external factors as stated in Table 1.1. The internal factors are governed by the concrete recipe and the external factors are mainly governed by the casting procedure and other environmental factors.

Effects of restraint have been studied in e.g. [3-5]. The degree of restraint may vary between 0 – 100%, where the case of full restraint comprises casting on a completely rigid support, for example crack free bedrock or massive slabs, with full bond to adjoining structures, and no restraint represents casting on a bond-free surface. The main factors influencing the restraint of a concrete wall is the geometry of the wall, the adhesion between new and old members, the geometry and stiffness of the base slab, and the flexibility and stiffness of the ground.

*Table 1.1. Factors influencing the heat of hydration [2].*

<b>Internal factors</b>	<b>External factors</b>
Concrete recipe	Casting procedure and environment
Cement content and -type	Concrete temperature at casting, $T_c$
Aggregate content and -type	Air temperature, $T_{air}$
Aggregate size, $d_{max}$	Temperature of supporting structures, $T_{slab}$
Water-cement ratio	Heating/cooling
Additives	Formwork, insulation and hardening process
	Wind velocity, solar radiation, etc.

This paper considers two types of casting procedures: (1) Casting of a free wall on top of a slab and (2) Casting of a wall on top of a slab with one edge adjoining an existing wall while the other edge remains free. Figure 1.1 illustrates the restraint distribution for these two cases.

The risk of thermal cracking,  $\eta$ , may be calculated as the structural stress ratio, or alternatively the strain ratio:

$$\eta = \left( \frac{\sigma_t(t)}{f_{ct}(t)} \right)^{max} \approx \left( \frac{\varepsilon_t(t)}{\varepsilon_{ct}(t)} \right)^{max} \quad (1)$$

where  $\sigma_t(t)$  is the tensile stress at the time t  
 $f_{ct}(t)$  is the tensile strength at the time t  
 $\varepsilon_t(t)$  is the tensile strain at the time t  
 $\varepsilon_{ct}(t)$  is the ultimate tensile strain at the time t

The safety level for cracking,  $\Gamma$ , is defined as the inverse of  $\eta$ :

$$\Gamma = \frac{1}{\eta} \quad (2)$$

If the crack risk  $\eta$  is too high according to AMA Anläggning [6], measures are needed to mitigate the risk of cracking. Typical methods for such thermal crack prevention aim at reducing the temperature differences within a concrete casting, between different castings or between a concrete member and its surroundings. This can be accomplished by installing heating cables in the slab or cooling pipes in the wall. The degree of restraint may also be regulated by, for example, expansion joints or optimizing the casting order to avoid adjoining walls for critical members, and the concrete properties may be customized to alter the heat of hydration and reduce the risk of thermal cracking.

The prevailing concept for crack risk estimations was introduced in the Swedish construction standards BRO 94 [7], and can today be found in AMA Anläggning [6]. The concept aims at reducing the risk of thermal cracking of concrete structures by introducing different safety levels for different exposure classes (previously denoted environmental classes). Originally there were three major safety levels and today the design approach has expanded into five levels, as shown in Table 1.2. Unknown material parameters require higher safety levels, while tested parameters result in lower requirements for the safety level. The untested concrete has been divided into two levels depending on the cement content, where a higher heat of hydration and thereby higher safety factor is expected for the higher cement content, C.

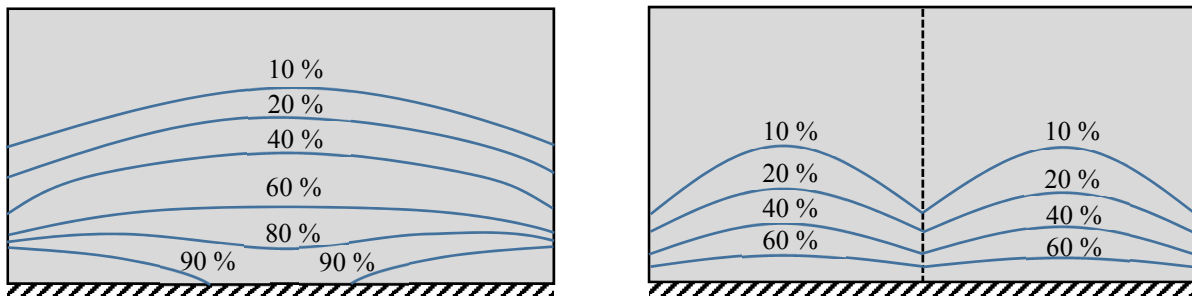


Figure 1.1. Restraint distribution for the two types of castings studied in this paper.

Table 1.2. Safety levels for thermal cracking of concrete structures [6].

Exposure class	Material parameters		
	Complete	$360 \leq C \leq 430 \text{ kg/m}^3$	$430 < C \leq 460 \text{ kg/m}^3$
XC2	1,05	1,18	1,33
XC4	1,11	1,25	1,42
XD1, XS2	1,18	1,33	1,54
XD3, XS3	1,25	1,42	1,67
Structures exposed to one sided water pressure			
All classes	1,42	1,67	2,0

The risk of thermal cracking should, according to AMA Anläggning, be reduced by applying one of the following three methods for crack prevention:

**Method 1:** Temperature requirements may be applied for the concrete and the surrounding air. Certain requirements for the geometry, cement content and structural restraints should also be fulfilled.

**Method 2:** Some typical design cases were studied in [2] and the most representative case, with associated design parameters and crack preventing actions, may be applied.

**Method 3:** Using sophisticated computer software to calculate the risk of thermal cracking and customize the crack preventing actions. The applied software should be thoroughly validated and the material parameters should be known.

The objective of this paper is to study the Swedish procedures for crack risk estimation and validate the accuracy of current safety levels for some concrete structures. The study is limited to Method 3 and the use of one commercial and widely applied 2D FE software ConTeSt Pro 5.0 [8]. The study is applied on frame structures where the crack prevention consists of pre-heating the slab before casting the walls.

## 2. METHOD

The method for this project can roughly be divided into six steps:

1. Identifying relevant structures with adequate documentation.
2. Studying construction documentation.
3. Checking original thermal crack risk estimations and suggested crack preventing measures based on expected parameters.
4. Carrying out post-project thermal crack risk estimations based on actual parameters.
5. Field inventory of emerging thermal cracks.
6. Analysis of the procedure and accuracy of crack risk estimations.

The most critical parameter for this project was identifying relevant structures with adequate documentation of the construction process, with construction drawings, material properties, crack preventing measures, concrete pouring rates and temperature logs. Three concrete structures were chosen for this project: a railway tunnel in Gamla Uppsala (2016) and two existing portal frame bridges in Ulriksdal (1990) and Antuna (1993). The geometry of the 2D FE-models are shown in Fig. 2.1 and structural parameters are found in Table 2.1. The structures were analyzed with

ConTeSt Pro, a commercial FEM software developed for purpose of temperature, strength and crack risk calculations in young concrete [8].

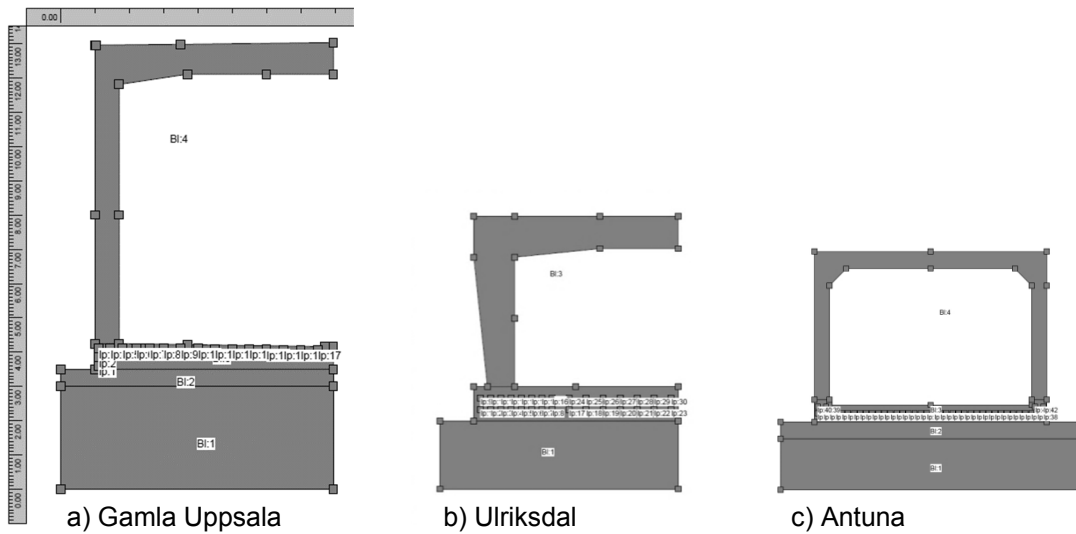


Figure 2.1. Geometry of the three slab-frame structures. a) Railway tunnel b-c) road tunnels.

Table 2.1. Structures analyzed in this paper.

Name of structure	Year of construction	Length	Cast length (walls)	Height	Wall thickness	References
Gamla Uppsala	2014-2016	610 m	10,0 m	9,5 m	0,7 m	[9-10]
Ulriksdal	1989-1990	41,6 m	10,4 m	6,0 m	0,8-1,2 m	[11]
Antuna	1993	35 m	35 m	5,0 m	0,45 m	[11]

Crack preventing measures were designed according to original crack risk estimations, carried out prior to casting. The crack preventing actions of the structures studied in this paper consisted of heating the slab with either internal heat cables or an external heat mat before and after the frame walls were casted. Construction fans were also used to increase the air temperature inside the tunnel for some castings. The original design was compared to the actual outcome of the project regarding temperatures and construction times. The recorded air- and concrete temperatures were thereafter used in ConTeSt Pro for the post-project thermal crack risk estimations.

The material properties are given in Table 2.2. The heat development within the concrete is highly influenced by the heat transfer coefficient along the boundaries of the structure. All free surfaces (air), formwork and expanded polyethylene (EPE) foam were modeled with heat transfer coefficients of 500; 4,7 and 3,6 W/m<sup>2</sup>·K, respectively. A frame wall had for example heat transfer coefficient of 4,667 until the formwork was removed, whereon the heat transfer coefficient increased to 500 W/m<sup>2</sup>·K as the boundary surface was exposed to air.

The structures were visually inspected and the presence of cracks was recorded. The railway tunnel in Gamla Uppsala was thoroughly inspected for all types of cracks and all smaller cracks (< 0,1 mm) were divided into 8 zones for each casting sequence as seen in Figure 2.2. Only cracks in the mid-part of the casting sequence with openings larger than 0,1 mm were considered as thermal cracks. The cracking was finally compared to the previous estimations.

Table 2.2. Material properties.

Structure	Parameter	Soil	Gravel	Slab	Frame
Uppsala	Material/strength class	Fine soil	coarse soil	C30/37	C30/37
	Density, kg/m <sup>3</sup>	1700	2200	2350	2350
	Thermal capacity, J/Kg K	1950	1400	1000	1000
	Thermal conductivity, W/m K	1,4	2,1	0-120 h: 1,7 120- h: 2,1	0-120 h: 1,7 120- h: 2,1
	Cement type	-	-	Anläggning*	Anläggning*
	Cement content, kg/m <sup>3</sup>	-	-	365	365
	Water/cement	-	-	0,48	0,48
Ulriksdal	Material/strength class	Not used	coarse soil	C32/40	C32/40
	Density, kg/m <sup>3</sup>	-	2200	2350	2350
	Thermal capacity, J/Kg K	-	1400	1000	1000
	Thermal conductivity, W/m K	-	2,1	1,7	0-24 h: 1,7 24- h: 2,1
	Cement type	-	-	Anläggning*	Anläggning*
	Cement content, kg/m <sup>3</sup>	-	-	390	390
	Water/cement	-	-	0,45	0,45
Antuna	Material/strength class	Fine soil	coarse soil	C32/40	C32/40
	Density, kg/m <sup>3</sup>	1700	2200	2350	2350
	Thermal capacity, J/Kg K	1950	1400	1000	1000
	Thermal conductivity, W/m K	1,4	2,1	1,7	0-24 h: 1,7 24- h: 2,1
	Cement type	-	-	Anläggning*	Anläggning*
	Cement content, kg/m <sup>3</sup>	-	-	390	390
	Water/cement	-	-	0,45	0,45

\*CEM I 42,5N – Anläggning Degerhamn, Cementa AB

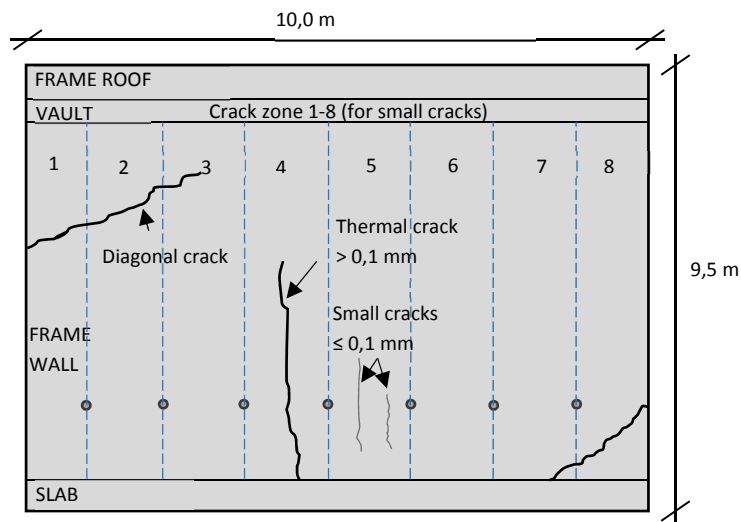


Figure 2.2. Example of visual crack inspection and crack types.

### 3. RESULTS

#### 3.1 Original design of thermal crack prevention

The original crack risk design was aimed at avoiding thermal cracks in the concrete members of Gamla Uppsala, Ulriksdal and Antuna. For Gamla Uppsala. Some typical cases were identified and the construction of each casting sequence was adjusted according to the prevailing conditions, basically depending on the type of casting, the concrete temperature at delivery,  $T_c$ , and the air temperature,  $T_{air}$ . The type of casting was either: a) casting of a free wall, without previously cast adjacent walls, or b) casting of a wall in direct contact to one adjacent wall. The crack preventing actions based on the original design were pre- and post-heating of the previously cast slab to avoid large strain differences between the slab and the wall. The original design cases of the Gamla Uppsala tunnel are presented in Table 3.1.

Figure 3.1 illustrates the typical crack preventive measures for wall casting in the Gamla Uppsala tunnel in cold weather, between  $-5^{\circ}\text{C}$  and  $+5^{\circ}\text{C}$ . The slab was pre-heated with heat cables of type 1 and 2 according to Fig 3.1. As the wall was casted, cables of type 1 were switched off and only the type 2 cables were used for post-heating. The slab was insulated with a 10 mm layer of EPE foam which was removed as the post-heating was terminated. For temperatures over  $5^{\circ}\text{C}$ , the type 2 cables furthest from the wall were removed and no heat cables on the bottom reinforcement were used for temperatures over  $10^{\circ}\text{C}$ .

Figure 3.2 illustrates an example of temperature evolution for the case of casting a wall in direct contact to an existing adjacent wall, with  $T_{air} = -5^{\circ}\text{C}$  and  $T_c = 15^{\circ}\text{C}$ . The horizontal axis represents the time after casting the slab, while the vertical axis represents the temperature to the left and the strain ratio to the right. Casting of the wall started at the relative time  $t = 0\text{h}$  with a concrete temperature of  $15^{\circ}\text{C}$ . The concrete temperature increased to a maximum of  $36^{\circ}\text{C}$  due to the exothermic reactions, and after the peak, the concrete started to cool off. The concrete exhibited a negative strain ratio (compression) of about  $\eta = 0,40$  relatively fast where after it was subjected to a strain ratio of maximally  $\eta = 0,77$ . The crack preventing actions can also be seen by the temperature development within the slab. The temperature of the slab was governed by the air temperature until the heating was started at  $t = -158\text{h}$  (the slab was covered/insulated 16 h later). The heating ended at  $t = 0$  and 24 h for the type 1 and 2 cables, respectively. The slab was also uncovered 24 h after the wall was cast. Note that the temperature gauge in the slab was located directly below the wall and the slab temperature was strongly influenced by the temperature development in the wall.

Table 3.1. Original design of the Gamla Uppsala tunnel.

Type of casting	$T_c$	$T_{air}$	Pre-/Post-heating	Form removal	$T_{max}$	Strain ratio (Analyzed in ConTeSt)	
						Design limit	Design value (average value)
	$^{\circ}\text{C}$	$^{\circ}\text{C}$	h/h	h	$^{\circ}\text{C}$		
Free seq.	15	-5	48/48	120	42,9	0,80	0,57
Free seq.	15	5	0/0	72	43,1	0,80	0,77
Adj. wall	15	-5	144/48	120	43,1	0,80	0,77
Adj. wall	15	5	96/24	120	43,1	0,80	0,77
Adj. wall	15	10	72/24	72	42,2	0,80	0,79
Adj. wall	25	20	72/24	72	58,0	0,80	0,80

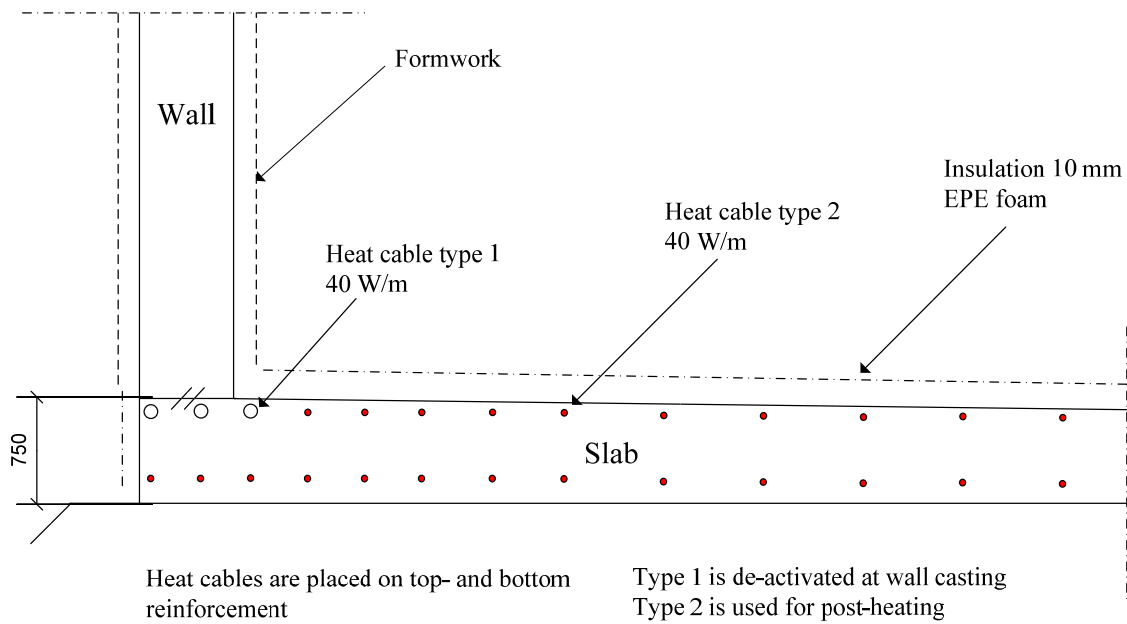


Figure 3.1 Typical approach for crack prevention with heating cables.

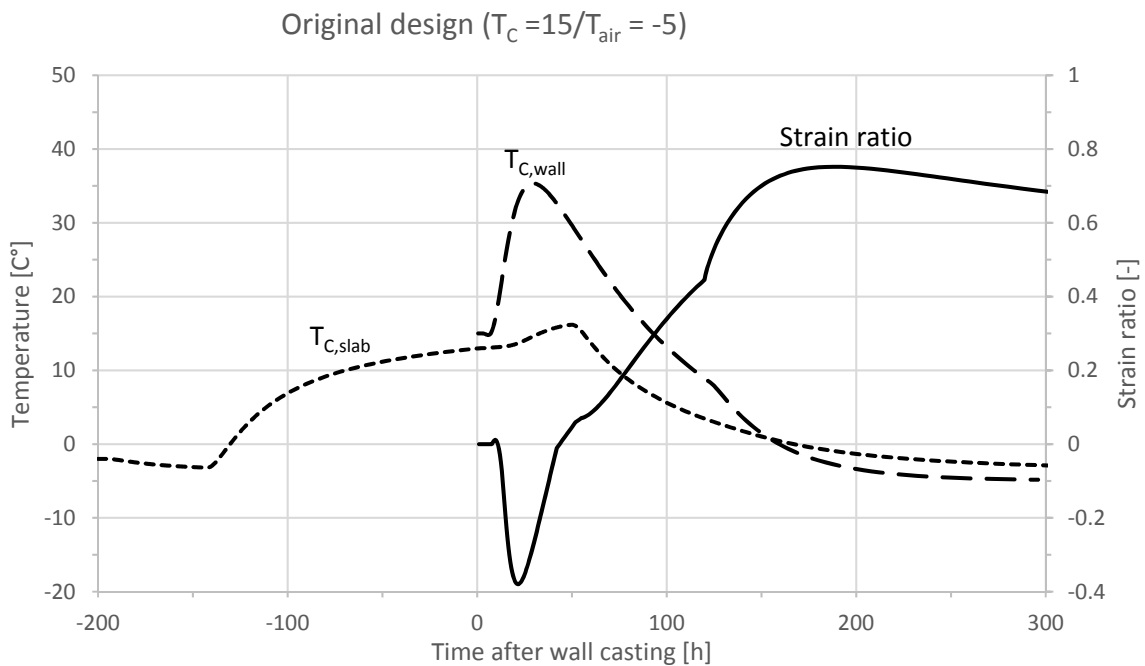


Figure 3.2. Example of temperature evolution for the original design case with  $T_{air} = 15^\circ\text{C}$  and  $T_c = -5^\circ\text{C}$ .

### 3.2 Post design of thermal crack prevention

Figure 3.3 presents the air- ( $T_{air}$ ), wall- ( $T_{wall}$ ) and slab ( $T_{slab}$ ) temperatures. Each temperature is given for the original- and post-design, as well as the actual measured values. The figure shows that the measured air temperature was much higher than assumed in the original design and the post-design was carried out according to a simplified temperature curve with straight lines

between temperature peaks. Due to the assumed lower temperatures in the original design, the maximum temperature in the wall, as well as the slab, was substantially underestimated. However, the post-design shows a relatively good adaption to the measured temperatures in the wall as well as the slab. The figure shows a common problem where the air temperature changes considerably after the crack preventing actions have already started. For this casting sequence, the typical case with an air temperature of +5°C would have been more suitable.

Figure 3.4 illustrates the strain distribution for casting sequence 5.1.2 of Gamla Uppsala at the time of maximum strain. Thermal cracks are assumed to develop as the average strain in a cross section exceed the ultimate strain of the concrete [12]. The strain ratio was calculated as an average value over a region of 0,7 x 0,2 m<sup>2</sup>, centered over the point of maximum strain, see the magnified part in Fig. 3.4. The maximum strain developed in the center of the wall, approximately 0,7 m over the slab. Previous research has shown that thermal cracks in wall-slab structures typically initiate at a height corresponding to the wall thickness above the joint [13-14]. The maximum strain ratio for sequence 5.1.2 was  $\eta = 1,02$  and the average strain for the shadowed region of Fig. 3.4 was  $\eta = 0,90$ . This value can be compared to the strain ratio  $\eta = 0,77$  from the original design and the strain limit of  $\eta = 0,90$  for exposure class XC4 and tested material parameters.

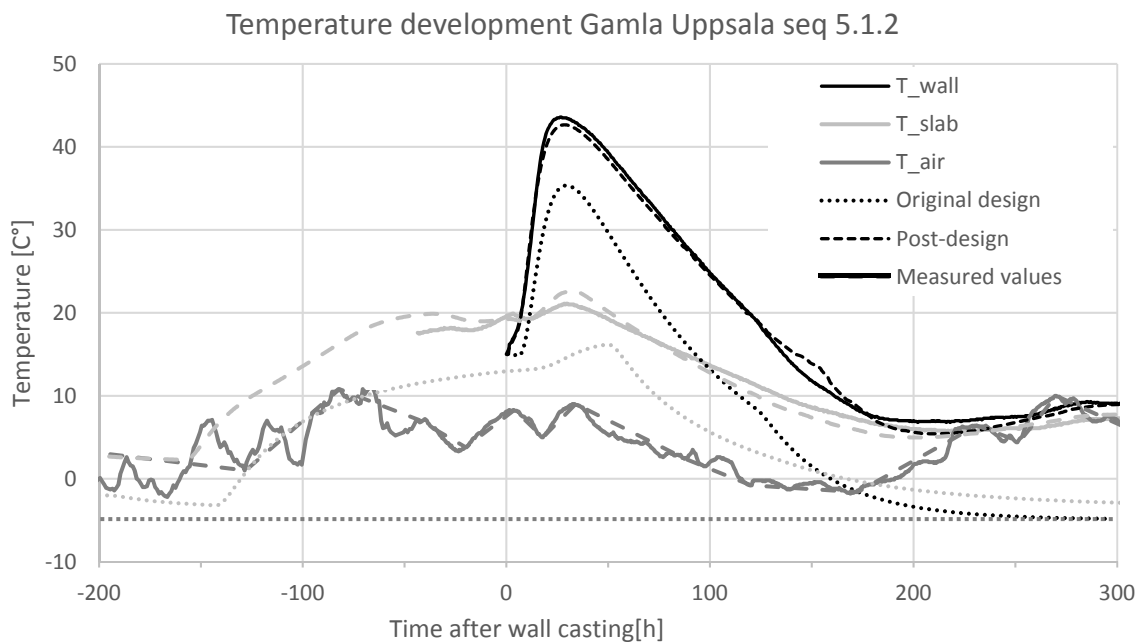


Figure 3.3. Measured, pre-calculated and post-calculated temperatures for the walls, slab and air for casting sequence 5.1.2 of the Gamla Uppsala tunnel.

### 3.3 Crack inventory

A summary of the original design, the post-design and the crack inventory is given in Table 3.2. Initially it is noted that no temperature cracks were supposed to be formed according to the original design for Gamla Uppsala, Ulriksdal or Antuna. Three casting sequences of the Gamla Uppsala tunnel exceeded their limiting strain ratio  $\eta = 0,90$  in their post-design. However, temperature cracks were found on 10 out of 14 analyzed sections. Small surface cracks, < 0,1 mm openings, were also studied and counted in the crack inspection. The compilation in Table 3.2

shows a large number of small cracks for all casting sequences of the Gamla Uppsala tunnel. The amount of small cracks ranged from 6 – 38 cracks for each casting.

For Ulriksdal, one out of four casting sequences exceeded the limiting strain ratio  $\eta = 0,70$  (based on exposure class XD3/XS3 and a cement content of  $390 \text{ kg/m}^3$ ) in the post-design and temperature cracks were found on two sections during the visual inspection. The single casting of Antuna was not supposed to crack according to neither the original design, nor the post-design, and no temperature cracks were actually detected.

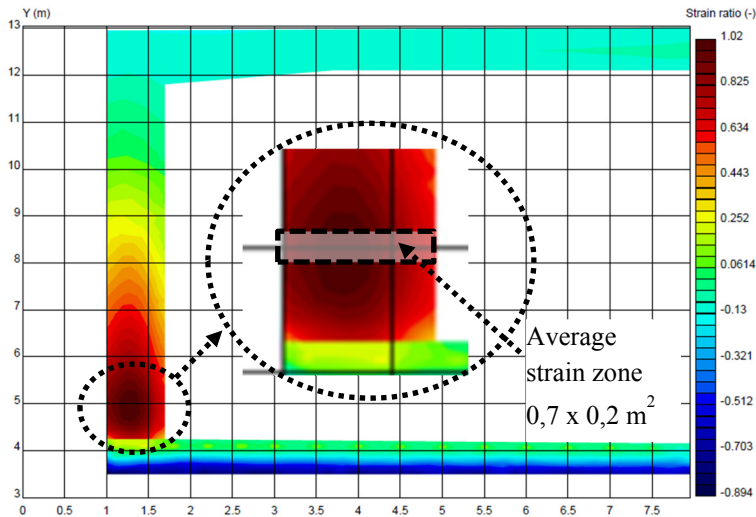


Figure 3.4. Strain distribution and average strain zone ( $0,7 \times 0,2 \text{ m}^2$ ) for the Gamla Uppsala tunnel, casting sequence 5.1.2.

Table 3.2. Summary of the original and post-designs for thermal crack risks.

Seq.	Exposure class	$\eta$ Limit	$\eta$ Original	$\eta$ Post	Temp. cracks >0,1 mm	Average crack width, mm	Small cracks $\leq 0,1 \text{ mm}$
<b>Gamla Uppsala</b>							
3.1.1	XC4/XF4 Tested material parameters	0,90	0,57	0,58	1	0,20	25
3.1.2			0,77	0,55	0	-	6
3.2.1			0,77	<b>0,97</b>	1	0,20	30
5.1.1			0,77	0,67	0	-	23
5.1.2			0,77	0,90	1	0,30	38
5.2.1			0,77	<b>1,01</b>	1	0,20	27
5.2.2			0,77	0,75	1	0,30	11
6.1.1			0,77	0,65	1	0,20	28
6.1.2			0,77	<b>1,04</b>	2	0,40	15
6.2.1			0,77	0,69	0	-	31
8.1.1			0,57	0,49	0	-	13
9.1.2			0,77	0,81	4	0,40	8
9.2.2			0,77	0,74	2	0,20	32
10.2.2			0,77	0,84	3	0,37	17
<b>Ulriksdal</b>							
1	XD3/XS3 360 < C < 430	0,70	0,70	0,693	1	0,4	-
2			0,70	0,461	0	-	-
3			0,70	0,438	0	-	-
4			0,70	<b>0,809</b>	3	0,27	-
<b>Antuna</b>							
1	XD3/XS3	0,70	0,70	0,55	0	-	-

#### 4. ANALYSIS AND DISCUSSION

Traditional crack preventing actions generally aims at reducing the tensile strains within the structure, typically by reducing the temperature differences within a massive concrete structure or between old and new concrete members. Existing slabs can for example be pre-heated before a new wall is cast to account for the thermal effects of the concrete hydration. Cooling pipes can also be installed in the new wall to avoid high temperatures and strains. All three structures within this study had their slabs pre-heated prior to casting the walls. The crack prevention was not always completely successful due to a number of factors and thermal cracks could be found in 12 of the 19 studied wall castings (63%).

Based on the results of this study it is observed that a correct weather forecast is crucial for an accurate original design, and can ultimately be the factor determining whether the structure remains crack-free or not. Under- or overestimated air temperatures in the original design leads to improper crack preventing actions, typically due to rapid temperature changes after the actions have started. Table 3.1 showed that six typical cases were used for the original design of the Gamla Uppsala tunnel. However, Fig.3.2 showed that a constant air temperature of  $-5^{\circ}\text{C}$  was chosen for the original design of casting sequence 5.1.2, but the measured temperature was in fact up to 15 degrees higher. This resulted in a higher wall temperature than anticipated in the original design. The construction process followed the original design restrictions and even though the formwork was removed later than planned, it was still a bit too early.

The concrete temperature was higher than planned at the point of form removal, resulting in a rapid cooling of the wall and accelerating tensile strains, see Figure 4.1. Instead of the originally anticipated strain ratio of 0,77, the strain ratio for this wall reached the limit  $\eta = 0,90$ . Other factors that may affect the accuracy of the crack risk estimation is the quality and function of the cooling/heating equipment, the workmanship, effects of sun exposed (locally heated) surfaces, etc. By using accurate quality controls, most functional errors may be avoided. However, the original design could be updated with a more reliable weather forecast and accordingly adjusted actions just before the wall casting starts. Another approach that may be used to reduce the risk of thermal cracks is more comprehensive monitoring of the concrete temperatures and avoiding unnecessary high tensile strains due to premature form removal.

The safety factor for thermal cracking of concrete infrastructure is given in the Swedish guidelines AMA Anläggning [6] and depends mainly on the structures exposure class, the cement content or whether the material parameters have been fully investigated. A summary of relevant safety factors is given in Table 4.1.

Table 3.2 showed a presence of thermal cracks for all walls with  $\eta > 0,70$  in the post-design and a few thermal cracks could also be seen on walls with even lower strain ratios. A more thorough analysis of the planned and executed crack preventive actions is presented in Table 4.2. The Table shows that the prescribed pre- and post-heating was relatively well complied, but there was still a high frequency of thermal cracks. Crack risk estimations according to the Swedish standards have probably reduced the amount of thermal cracks in the Swedish infrastructure, but there are still a large number of uncertainties involved in the design. Based on the results of this study, it seems relevant to question whether higher strain ratios than 0,70 should be allowed. However, the results of this study are based on a limited number of slab-frame structures where the only crack preventing action was pre-heating of the slab. Further studies of relevant structures with different crack prevention are required to validate these results.

Table 4.1. Safety factors (and corresponding strain ratios) for thermal cracking of concrete structures given in AMA Anläggning [6].

Exposure class	Material parameters		
	Complete	$360 \leq C \leq 430 \text{ kg/m}^3$	$430 < C \leq 460 \text{ kg/m}^3$
XC2	1,05 (0,95)	1,18 (0,85)	1,33 (0,75)
XC4	1,11 (0,90)	1,25 (0,80)	1,42 (0,70)
XD1, XS2	1,18 (0,85)	1,33 (0,75)	1,54 (0,65)
XD3, XS3	1,25 (0,80)	1,42 (0,70)	1,67 (0,60)
<b>Structures exposed to one sided water pressure</b>			
All	1,42 (0,70)	1,67 (0,60)	2,0 (0,50)

Table 4.2 Summary of planned and actual parameters for the Gamla Uppsala tunnel.

Seq.	T <sub>air</sub> Pre-design [°C]	T <sub>air</sub> Average [°C]	Planned heating Pre-/Post- [h/h]	Actual heating Pre-/Post- [h/h]	η Pre-design [-]	η Post-design [-]	η Limit [-]	Cracks > 0,1 mm [-]
3.1.1	-5	+4	48/48	100/50	0,57	0,58	0,90	Yes
3.1.2	-5	+6	144/48	150/40	0,77	0,55		-
3.2.1	+5	+10	96/24	150/30	0,77	<b>0,97</b>		Yes
5.1.1	+5	+5	96/24	45/35	0,77	0,67		-
5.1.2	-5	+5	144/48	160/25	0,77	0,90		Yes
5.2.1	-5	0	144/48	160/30	0,77	<b>1,01</b>		Yes
5.2.2	-5	-2	144/48	350/50	0,77	0,75		Yes
6.1.1	-5	+3	144/48	120/30	0,77	0,65		Yes
6.1.2	+5	+1	0/0	0/0	0,77	<b>1,04</b>		Yes
6.2.1	+5	+5	96/24	140/30	0,77	0,69		-
8.1.1	-5	0	48/48	110/50	0,57	0,49		-
9.1.2	-5	+2	144/48	110/40	0,77	0,81		Yes
9.2.2	-5	+4	144/48	160/25	0,77	0,74		Yes
10.2.2	+10	+12	72/24	25/60	0,79	0,84		Yes

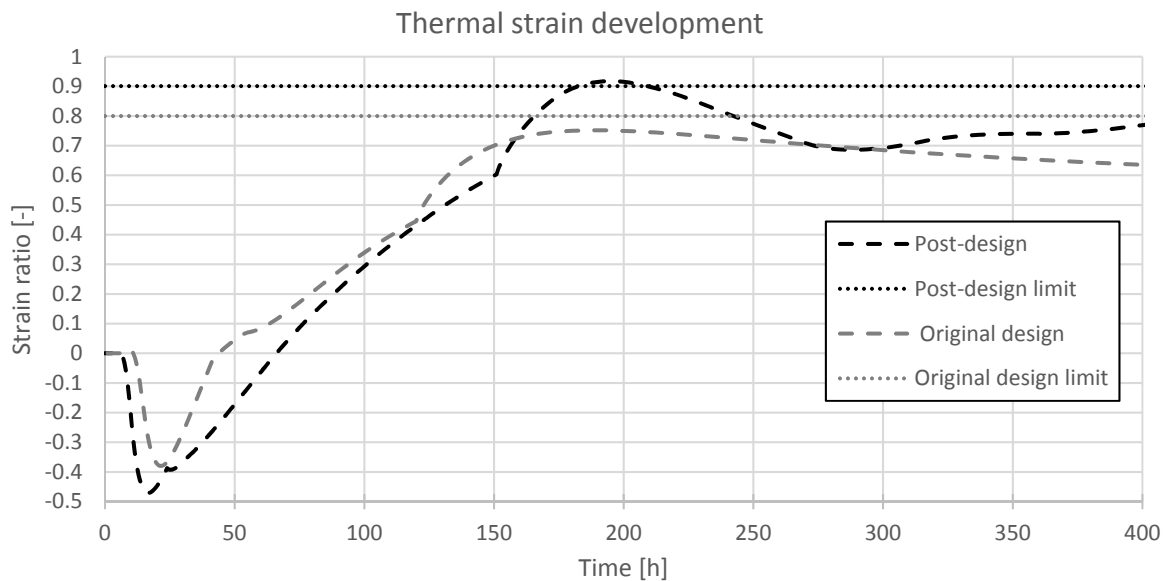


Figure 4.1. Comparison of average strain ratios in the original- and post-designs for casting sequence 5.1.2 of the Gamla Uppsala tunnel.

Finally, the visual crack inspection of the Gamla Uppsala tunnel showed that there was a strong correlation between the walls degree of restraint and the presence of surface cracks with crack widths  $< 0,1$  mm. A total of 144 frame-walls of the Gamla Uppsala tunnel were inspected and surface cracks were found on each one of them. According to theory [3], the restraint is supposed to be higher in the mid-part of the wall and decrease towards the wall-ends. Figure 4.2 shows a FE-analysis of the restraint situation for a wall casted in direct contact with an adjacent wall. The frequency of small cracks is plotted in front of the wall to illustrate the correlation between restraint and surface cracks.

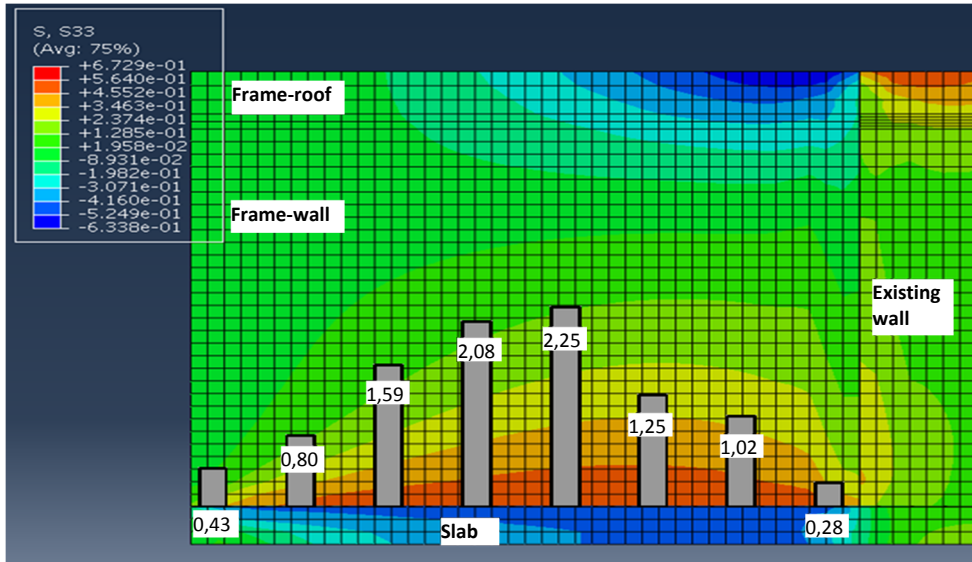


Figure 4.2. Illustration of the correlation between wall-restraint and the frequency of small surface cracks ( $< 0,1$  mm). The numbers represent the average number of small cracks in each of the eight crack zones (cracks/wall) and the colors represent the degree of restraint.

## 5. CONCLUSIONS

Thermal crack risk estimations were carried out for three concrete frame structures according to the directions in the Swedish design guidelines AMA Anläggning. The original crack risk estimations are influenced by a large number of uncertainties which may affect the outcome substantially. Typical uncertainties in thermal crack risk estimations include:

- Material properties of concrete, formwork and insulation.
- Environmental conditions, e.g. wind, temperatures, sun, etc.
- Structural properties, e.g. degree of restraint.
- Function and efficiency of heating and cooling equipment.
- Accomplishment of planned activities.

This paper demonstrates how thermal cracks have emerged in structures that were not supposed to crack according to their crack risk estimations, even if the estimations were post-processed using actual material- and environmental properties as well as work procedures. All structures that reached tensile strains higher than 70% of the concretes ultimate strain within the first weeks after casting were actually cracked. Further studies are needed to analyse other types of structures and crack preventing measures, and also to validate the results of this paper.

## ACKNOWLEDGEMENTS

The authors would like to express their appreciation for the financial support from Trafikverket, SBUF, Heidelberg cement, Cementsa, The Elsa & Sven Thysell Foundation and LTU. Those who have contributed with their knowledge in this project are Petter Eriksson and Jan-Erik Jonasson at LTU, Kjell Wallin at Betong & Stålteknik and Vilmer Andersson-Wass at PEAB.

## REFERENCES

1. De Schutter, G., Taerwe, L. "Degree of hydration-based description of mechanical properties of early age concrete," *Materials and Structures*, Vol. 29, No. 335, July 1996, doi:10.1007/BF02486341
2. Emborg M., Bernander S., Ekerfors K., Groth P., Hedlund H., "Temperatursprickor i betongkonstruktioner : beräkningsmetoder för hydrationsspänningar och diagram för några vanliga typfall. Del A, B och C," Dept. of Civil, Environmental and Natural Resources Engineering, Luleå University of Technology, Report No. 1997:02, 1997.
3. Knoppik-Wróbel, A., Klemczak, B., "Degree of restraint concept in analysis of early-age stresses in concrete walls," *Engineering Structures*, Vol. 102, Nov. 2015, pp 369–386
4. Nilsson, M., "Restraint factors and partial coefficients for crack risk analyses of early age concrete structures," Dept. of Civil, Environmental and Natural Resources Engineering, Luleå University of Technology, Doctoral Thesis, 2003.
5. Weiss, J., Yang, W., Shah, S.P., "Shrinkage Cracking of Restrained Concrete Slabs," *Journal of Engineering Mechanics*, Vol. 124, No. 7, July 1998.
6. Svensk Byggtjänst, "AMA Anläggning 13. Allmän material- och arbetsbeskrivning för anläggningsarbeten," Svensk Byggtjänst, Stockholm, 2014, ISBN 9789173336406
7. Vägverket, "BRO 94, Allmän teknisk beskrivning för broar," Vägverket, Borlänge, VV Publ 1999:20, March 1999.
8. JEJMS Concrete, "ConTeSt Pro Users manual: Program for temperature and stress calculations in concrete," Jejms Concrete, Luleå, 2008.
9. Vass-Andersson, V., "Temperatursprickor i betong- Metodutveckling för sprickbegränsning och uppföljning av uppsprickning i en tunnelkonstruktion," Dept. of Civil and Architectural Engineering, Stockholm, Master Thesis, Sept. 2015.
10. Eriksson, P., "Temperatursprickor i Ung Betong: Uppföljning av Den Svenska Sprickmodellen," Dept. of Civil, Environmental and Natural Resources Engineering, Luleå University of Technology, Master Thesis, Jan. 2017.
11. Wallin, K., Emborg, M., Jonasson, J.-E., "Värme ett alternativ till kyla," Dept. of Civil, Environmental and Natural Resources Engineering, Luleå University of Technology, Report No. 1997:15, 1997
12. Knoppik-Wróbel, A., "Analysis of early-age thermal–shrinkage stresses in reinforced concrete walls," Dept. of Structural Engineering, Silesian University of Technology, Doctoral Thesis, Jan. 2015.
13. A Al-Gburi, M., "Restraint Effects in Early Age Concrete Structures," Dept. of Civil, Environmental and Natural Resources Engineering, Luleå University of Technology, Doctoral Thesis, Sept. 2015.
14. Zhou, J., Xudong Chen, X., Zhang, J., "Early age temperature and strain in basement concrete walls: Field monitoring and numerical modelling," *Journal of Performance of Constructed Facilities*, Vol. 26, No. 6, Dec. 2012.

